

A dissertation submitted to the
FACULTY OF BIOLOGY, CHEMISTRY AND GEOSCIENCES
UNIVERSITY OF BAYREUTH

to obtain the academic degree of
DR. RER. NAT.

Eddy-covariance measurements as a tool for ecological and hydrological studies on the Tibetan Plateau

TOBIAS BIERMANN
Diplom Geoökologe

born 16 January, 1984
in Bochum, Germany

Bayreuth, July 2014

supervised by PROF. DR. THOMAS FOKEN

Eddy-covariance measurements as a tool for ecological and
hydrological studies on the Tibetan Plateau

supervised by PROF. DR. THOMAS FOKEN

Die vorliegende Arbeit wurde in der Zeit von März 2009 bis July 2014 in Bayreuth an der Abteilung Mikrometeorologie unter Betreuung von Herrn Prof. Dr. Thomas Foken angefertigt.

Vollständiger Abdruck der von der Fakultät für Biologie, Chemie und Geowissenschaften der Universität Bayreuth genehmigten Dissertation zur Erlangung des akademischen Grades eines Doktor der Naturwissenschaften (Dr. rer. nat.).

Dissertation eingereicht am: 18.07.2014

Zulassung durch die Prüfungskommission: 06.08.2014

Wissenschaftliches Kolloquium: 17.11.2014

Dekan:

Prof. Dr. Rett Kempe

Prüfungsausschuss:

Prof. Dr. Thomas Foken (Erstgutachter)

Prof. Dr. Christiane Werner Pinto (Zweitgutachterin)

Prof. Dr. Andreas Held (Vorsitz)

Prof. Dr. Anke Jentsch-Beierkuhnlein

Contents

List of manuscripts	v
List of additional publications	vi
Acknowledgements	viii
Summary	ix
Zusammenfassung	x
1. Introduction	1
1.1. Motivation	1
1.1.1. Ecosystems on the Tibetan Plateau	1
1.1.2. Estimation of energy, water and carbon fluxes on the Tibetan Plateau	2
1.2. Framework of this thesis	3
1.2.1. Main project objectives	4
1.2.2. Experiments	5
1.3. Objectives of this thesis	6
2. Material and Methods	9
2.1. Study sites	9
2.2. Methods	11
2.2.1. Eddy-covariance	11
2.2.2. $^{13}\text{CO}_2$ labeling	13
2.2.3. Coupling of eddy covariance and $^{13}\text{CO}_2$ labeling	14
2.2.4. Chamber based gas exchange measurements and micro-lysimeter	15
2.2.5. Land-surface atmosphere interaction and atmospheric Models	15
2.3. Experiment Setup	16
3. Results and Discussion	21
3.1. Turbulent fluxes on the Tibetan Plateau	21
3.1.1. Flux measurements over different surfaces	21
3.1.2. Accurate estimation of Q_E in Winter	24

3.2. Carbon Fluxes of <i>Kobresia pygmaea</i> pastures	26
3.2.1. Net Ecosystem Exchange	26
3.2.2. The role of the turf layer for carbon turnover	27
3.2.3. Effects of grazing cessation	29
3.2.4. Influence of degradation on C fluxes	30
3.3. Linking flux measurements and land surface modeling to estimate re- gional features	32
3.3.1. Lake fluxes and influence of the soil moisture	33
3.3.2. Coupling flux measurements to the ATHAM model	36
3.3.3. Influence of degradation on energy and C fluxes	36
4. Conclusions	39
References	43
A. Individual contributions to the joint publications	59
B. Biermann et al. (2014)	67
C. Gerken et al. (2014)	85
D. Babel et al. (2014)	105
E. Ingrisch et al. (2015)	131
F. Biermann et al. (subm)	145
Erklärung	165

List of manuscripts

This dissertation is presented in a cumulative form. It is based on the publications and manuscript as listed below.

Peer-reviewed publications

- Babel, W., Biermann, T., Coners, H., Falge, E., Seeber, E., Ingrisich, J., Schleuß, P.-M., Gerken, T., Leonbacher, J., Leipold, T., Willinghöfer, S., Schützenmeister, K., Shibistova, O., Becker, L., Hafner, S., Spielvogel, S., Li, X., Xu, X., Sun, Y., Zhang, L., Yang, Y., Ma, Y., Wesche, K., Graf, H.-F., Leuschner, C., Guggenberger, G., Kuzyakov, Y., Mieke, G., and Foken, T.: Pasture degradation modifies the water and carbon cycles of the Tibetan highlands, *Biogeosciences*, 11, 6633-6656, doi:10.5194/bg-11-6633-2014, 2014.
- Biermann, T., Babel, W., Ma, W., Chen, X., Thiem, E., Ma, Y., and Foken, T.: Turbulent flux observations and modelling over a shallow lake and a wet grassland in the Nam Co basin, Tibetan Plateau, *Theor. Appl. Climatol.*, 116(1-2), 301-316, doi:10.1007/s00704-013-0953-6, 2014.
- Gerken, T., Biermann, T., Babel, W., Herzog, M., Ma, Y., Foken, T., Graf, HF.: A modelling investigation into lake-breeze development and convection triggering in the Nam Co Lake basin, Tibetan Plateau, *Theor. Appl. Climatol.*, 117(1-2), 149-167 doi:10.1007/s00704-013-0987-9, 2014.
- Ingrisich, J., Biermann, T., Seeber, E., Leipold T., Li, M., Ma, Y., Xu, X., Mieke, G., Guggenberger, G., Foken, T., Kuzyakov Y.: Carbon pools and fluxes in a Tibetan alpine *Kobresia pygmaea* pasture partitioned by coupled eddy-covariance measurements and ¹³CO₂ pulse labeling, *Science of The Total Environment*, 505, 1213-1224, doi:10.1016/j.scitotenv.2014.10.082, 2015.

Non peer-reviewed publications

- Ingrisich, J., Biermann, T., Seeber, E., Leipold T., Li, M., Ma, Y., Xu, X., Mieke, G., Guggenberger, G., Foken, T., Kuzyakov Y.: Carbon pools and fluxes measured during a field campaign conducted in 2010 on the Tibetan Plateau at Kema. Dataset 833208, PANGAEA, doi:10.1594/PANGAEA.833208, 2014.

Manuscripts submitted

- Biermann, T., Pfab, D., Babel, W., Li, M., Wang, B., Ma, Y., and Foken, T.: Note: Measurements of latent heat flux and humidity on the Tibetan Plateau during winter conditions, submitted to *Atmos. Meas. Tech. Diss.*.

List of additional publications

The following list summarizes other publications with reference to the dissertation but not included. It consists of one peer-reviewed publication and three technical documentations of the experiments on the Tibetan Plateau. Furthermore the list contains three master theses initiated and supervised by myself.

Publications with reference to this thesis

Peer-reviewed publications

Gerken, T., Babel, W., Hoffmann, A., Biermann, T., Herzog, M., Friend, A. D., Li, M., Ma, Y., Foken, T., and Graf, H.-F.: Turbulent flux modelling with a simple 2-layer soil model and extrapolated surface temperature applied at Nam Co Lake basin on the Tibetan Plateau, *Hydrol. Earth Syst. Sci.*, 16, 1095-1110, doi:10.5194/hess-16-1095-2012, 2012.

Non peer-reviewed publications

Biermann, T., Babel, W., Olesch, J., and Foken, T.: Documentation of the Micrometeorological Experiment, Nam Tso, Tibet, 25th of June – 8th of August 2009, *Arbeitsergebn. Univ. Bayreuth Abt. Mikrometeorol.*, ISSN 1614-8916, 41, 38 pp., URL <https://epub.uni-bayreuth.de/450/>, 2009.

Biermann, T., and T. Leipold with contributions from Babel, W., Becker, L., Coners, H., Foken, T., Guggenberger, G., He, S., Ingrisich, J., Kuzyakov, Y., Leuschner, C., Mieke, G., Richards, K., Seeber, E., Wesche, K.: Tibet Plateau Atmosphere-Ecology-Glaciology Cluster Joint Kobresia Ecosystem Experiment: Documentation of the first Intensive Observation Period Summer 2010 in Kema, Tibet, *Arbeitsergebn. Univ. Bayreuth Abt. Mikrometeorol.*, ISSN 1614-8916, 44, 107pp., URL <https://epub.uni-bayreuth.de/356/2011>.

Biermann, T., E. Seeber, P. Schleuß, S. Willinghöfer, J. Leonbacher, K. Schützenmeister, L. Steingraber, W. Babel, H. Coners, T. Foken et al.: Tibet Plateau Atmosphere-Ecology-Glaciology Cluster Joint Kobresia Ecosystem Experiment: Documentation of the second Intensive Observation Period, Summer 2012 in KEMA, Tibet, *Arbeitsergebn. Univ. Bayreuth Abt. Mikrometeorol.*, ISSN 1614-8916, 54, 54pp., URL <https://epub.uni-bayreuth.de/145/>, 2013.

Gerken, T., Babel, W., Hoffmann, A., Biermann, T., Herzog, M., Friend, A. D., Li, M., Ma, Y., Foken, T., and Graf, H.-F.: Turbulent flux modelling with a simple 2-layer soil model and extrapolated surface temperature applied at Nam Co Lake basin on the Tibetan Plateau, *Hydrol. Earth Syst. Sci. Discuss.*, 8, 10 275–10 309, doi:10.5194/hessd-8-10275-2011, 2011.

Supervised Master theses

Leonbacher, J.: Chamber based carbon dioxide fluxes of three different vegetation treatments on the Tibetan Plateau, Master thesis, University of Bayreuth, 72pp., 2013.

Leipold, T.: Carbon dioxide exchange above *Kobresia* meadows, Master thesis, University of Bayreuth, 55pp., 2011.

Pfab, D.: Wasserdampfkonzentrationsmessungen in großen Höhen und bei niedrigen Temperaturen, Master thesis, University of Bayreuth, 73pp., 2011.

Acknowledgements

I am grateful to everybody who supported me during the completion of this thesis; in particular I want to thank:

- Prof. Thomas Foken for his guidance through all stages of this work, for his time spent during scientific discussions and the opportunity to learn from his experience within Micrometeorology
- Wolfgang Babel for the great time during all stages of the experiments on the Tibetan Plateau; the collaboration during data processing and manuscript writing and many hours of fruitful discussion and his support in many situations
- Kelly Hopping for her company during the first experiment in Tibet, many discussions and her help with language correction of manuscripts and this thesis
- All people who made the field campaigns in Tibet a special time as well as all co-authors for their contributions to the manuscript and discussions: Elke Seeber, Tobias Gerken, Elisabeth Thiem, Daniela Pfab, Johannes Ingrisch, Jürgen Leonbacher, Thomas Leipold, Heinz Coners, Sandra Willinghöfer, Per Schleuß, Klaus Schützenmeister, Benba and the people in Kema.
- All current and former staff members of the Department of Micrometeorology for their support and fruitful discussions, in particular Rafael Eigenmann, Jörg Hübner, Jo Olesch, Andrei Serafimovich, Johannes Lüers, Katharina Köck, Lukas Siebecke and Stefan Metzger
- The staff members of the ITP Nam Co Station & TU-ITPCAS Naqu Station and our Chinese project partners Li Maoshan, Ma Weiqiang, Chen Xuelong, Zhu Zhikun, Wang Binbin, Zhang Lang and Prof. Ma Yaoming for their work on the Tibetan Plateau
- My parents for their support and the freedom to let me follow my own way
- My friends who made the time in Bayreuth unforgettable, spent endless hours in the Alps, on Franconian rocks, around a campfire with me or just had time for a coffee and a good conversation! In particular Tibor, Rafael, Martina, Sevi, Andrea, Carsten, Maria, Sepp, Flo, Max, Steven, Karl, Tassilo, Anne, Steffen and Nancy and everyone from the DPSG Bayreuth.

This work has been financed by the German Research Foundation (DFG), Priority Programme 1372 "Tibetan Plateau: Formation, Climate, Ecosystems" (TiP) and by CEOP-AEGIS, a Collaborative Project/Small or medium-scale focused research project – Specific International Co-operation Action coordinated by the University of Strasbourg, France and funded by the European Commission under FP7 topic ENV.2007.4.1.4.2 "Improving observing systems for water resource management."

Summary

The environment of the Tibetan Plateau (TP) is regarded as one of the most sensitive ecosystems of the world. However, investigations on effects caused by global climate change or anthropogenic activities are rare due to its quite remote location. This thesis deals with various aspects of the carbon and water cycle within ecological and hydrological studies that can be assessed by measurements of turbulent fluxes with the eddy-covariance (EC) method. This includes flux measurements over the most common two vegetation types on the TP, *Kobresia pygmaea* pasture and alpine steppe. In particular these *in situ* measurements were used to investigate differences in the fluxes of grazed and ungrazed *Kobresia pygmaea* pasture at Kema in Naqu province and moist and dry alpine steppe within the Nam Co basin. Additionally for the first time on the TP direct flux measurements were conducted over a lake surface in the same basin. Furthermore, these flux measurements were used to adapt and validate land-surface models to be applied on the TP. Within the experiments a special focus were measurements of latent heat flux during winter conditions on the TP, involving side-by-side measurements with a LI-COR 7500 (LI-COR Biosciences) and a Krypton Hygrometer KH20 (Campbell Sci. Ltd.). This comparison revealed that in general an application of both sensors for an estimation of turbulent fluxes is possible but they can not be used for measurements of absolute humidity concentrations. Furthermore, this study showed the need for a thoroughly planned calibration procedure for gas analyzers at long-term stations. Carbon fluxes measured over the *Kobresia pygmaea* pastures were used for the estimation of short term effects of grazing cessation and to gain a detailed look into the carbon cycle of this unique ecosystem. For this purpose the EC derived fluxes were coupled with the results of a $^{13}\text{CO}_2$ pulse labeling experiment. With this quite novel approach it is possible to on the one hand estimate a more suitable timing for the pulse labeling experiment and on the other hand to estimate absolute C turnover in different compartments of the soil-plant-atmosphere continuum. These results identified the unique root layer of *Kobresia pygmaea* as the most important part of the pasture ecosystem. This is of great importance for the further conducted study which estimated the effect of degradation on the carbon and water cycle within these pastures with an interdisciplinary approach, which combined plot- and ecosystem scale *in situ* measurements with land-surface-atmosphere models. A simulation of different stages of degradation of the *Kobresia pygmaea* pastures and also a vegetation shift to alpine steppe, showed that only an intact *Kobresia pygmaea* pastures acts as C sink for the observation period within the main vegetation growing season. Although evapotranspiration in general is not affected as strong as carbon exchange, a shift in the ratio between evaporation and transpiration has a feedback on convection development and precipitation which could be also shown with an atmospheric model.

Zusammenfassung

Das Hochland von Tibet zählt zu den empfindlichsten Ökosystemen der Erde. Trotz eines gesteigerten Interesse in den letzten Jahren ist es in Hinblick auf die möglichen Veränderungen durch den globalen Klimawandel und zunehmende menschliche Aktivität aufgrund seiner abgeschiedenen Lage ein immer noch relativ wenig erforschtes Gebiet. Aus diesem Grund wurden turbulente Flüsse (Kohlenstoffaustausch und Verdunstung) mit der Eddy Kovarianz Methode über unterschiedlichen Oberflächen auf dem Hochplateau gemessen und so verschiedene Aspekten des Kohlenstoff- und Wasserkreislaufes untersucht. Im Besonderen wurden hier die zwei dominanten Vegetationsformen, alpine Steppe und *Kobresia pygmaea*-Weiden sowie zu ersten Mal auf dem Hochplateau ein See untersucht. Im Nam Co Einzugsgebiet wurde der Einfluss von unterschiedlicher Bodenfeuchte auf die Flüsse über alpiner Steppe gemessen und auch ein Vergleich zwischen den Flüssen über Land und See angestellt. Die Messungen über den *Kobresia pygmaea*-Weiden wurden genutzt, um den Effekt unterschiedlicher Beweidungensintensität und Degradation zu untersuchen. Alle Messungen haben dazu beigetragen, Modelle, welche die Austauschprozesse zwischen dem Ökosystem und der Atmosphäre simulieren, an die Bedingungen des Hochplateaus anzupassen und deren Ergebnisse zu validieren. Insbesondere wurde bei den Messungen ein Augenmerk auf die Bestimmung des latenten Wärmestroms unter Winterbedingungen gelegt. Zu diesem Zweck wurde eine Vergleichsmessung zwischen einem LI-COR 7500 (LI-COR Biosciences) und einem Krypton Hygrometer KH20 (Campbell Sci. Ltd.) durchgeführt, mit dem Ergebnis, dass beide Geräte zwar für den Einsatz zur Bestimmung von turbulenten Flüssen geeignet sind, nicht jedoch für die Bestimmung des absoluten Feuchtegehalts der Atmosphäre. Die Abweichung zwischen den Geräten macht außerdem deutlich, dass eine geeignete Kalibrierprozedur nötig ist um eine fehlerfreie Bestimmung von Langzeit-Messreihen zu gewährleisten. Neben diesen Untersuchungen über der alpinen Steppe wurden die Messungen des Kohlenstoffaustausches in Kema dazu genutzt den Einfluss von Umzäunungen und dem damit verbundene Beweidungsausschluss zu untersuchen. Jedoch konnte auf der relativ kurzen Zeitskala seit Errichtung der Zäune kein Unterschied zwischen den Flächen auf der Ökosystemskala festgestellt werden. Eine detailliertere Betrachtung des Kohlenstoffumsatzes durch die Kopplung der EC Messungen mit einem $^{13}\text{CO}_2$ Markierungsexperiments zeigte auch keinen Unterschied, jedoch konnten so zum ersten Mal absolute Umsatzraten zwischen Boden, Pflanze und Atmosphäre gemessen werden. Eine wichtige Erkenntnis hierbei war die Identifizierung des markanten Wurzelfilzes der *Kobresia pygmaea*-Weiden als wichtigster Teil für den gesamten Kohlenstoffumsatz im Ökosystem. Vor allem vor dem Hintergrund der Degradierung der Weiden, der damit einhergehenden Zerstörung des Wurzelfilzes und der Funktion des Graslands als potentieller Kohlenstoffspeicher ist dies von großer Bedeutung. Der Effekt dieser Degradierung, und auch ein möglicher Wechsel der Vegetationsstruktur, wurde mit Hilfe der zuvor angepassten Modelle simuliert. Diese Simulation zeigt, dass in der untersuchten Vegetationsperiode nur eine intakte *Kobresia pygmaea*-Weide als Kohlen-

stoffspeicher dient, die Degradationsstufen sowie die alpine Steppe müssen jedoch als neutral oder leichte Quellen angesehen werden. Während der Kohlenstoffaustausch stark verändert wird ist bei der Verdunstung im Gesamten keine grosse Veränderung zu beobachten, jedoch verschiebt sich das Verhältnis von Evaporations und Transpiration stark. Dies hat wiederum hat, zusammen mit sich verändernden Oberflächen Eigenschaften durch die Degradation, einen erheblichen Einfluss auf die Bildung von Konvektion und Niederschlag, wie in einer Modellstudie gezeigt werden konnte.

1. Introduction

1.1. Motivation

In recent years the Tibetan Plateau (TP) has been referred to as the “third pole”, reflecting the importance of the highlands as the water tower of Asia and taking into account the high sensitivity of this ecosystem to external disturbances such as climatic change or anthropogenic land use changes (Yao et al., 2012; Qiu, 2008; Immerzeel et al., 2010; Cui and Graf, 2009; Mieke et al., 2011; Yang et al., 2014). Additionally the plateau is a unique geological feature, with its landmass covering 2.5 million km² and an average altitude over 4000 m, which plays an important role in the modulation of atmospheric circulations in Asia such as the East-Asian monsoon (e.g. Hsu and Liu, 2003; Molnar et al., 2010; Boos and Kuang, 2010).

Changes in surface properties therefore may have a major influence on the regional and also global hydrological cycles. The importance of evaporation for the hydrological cycle under the influence of climate change has been highlighted by Yang et al. (2011). Furthermore these changes will also influence the carbon cycle, as 52 % of the highlands are covered with grassland (Sheehy et al., 2006) and its soils have a disproportional high share on global soil C storage, at 2.5% (Wang et al., 2002) while the plateau’s area only accounts for approximate 1.0% of the global terrestrial land area (Fang et al., 2010). Traditionally grasslands on the TP are used for pastoral nomadism. However since the 1950s changes in grazing practice and livestock husbandry by the local Tibetan population have been observed (Du et al., 2004; Goldstein and Beall, 1991; Harris, 2010; Lu et al., 2009; Sheehy et al., 2006). These changes significantly affect the state of the ecosystems in the highlands (Mieke et al., 2014), with a strong feedback on the interaction between the land surface and the atmosphere (Cui and Graf, 2009; Cui et al., 2006). To understand the feedbacks between changes in surface properties and the water and C cycles on the TP is therefore necessary to evaluate the influence of climate and anthropogenically induces changes on energy and matter exchange within this unique environment.

1.1.1. Ecosystems on the Tibetan Plateau

Although grassland comprise most of the landscape, the Tibetan Highland is fairly heterogeneous, including alpine steppe, *Kobresia pygmea* mats, wetlands and open water surfaces of various sizes. This grassland is dominated by alpine steppe and *Kobresia*

pygmaea pastures, forming the of the world's highest and largest alpine ecosystems. Roughly speaking, alpine steppe is more frequently found in the arid north-western part of the Plateau, while the *Kobresia pygmaea* pastures can be found mainly in the in the more humid south-eastern part. The alpine steppe, covering 600.000 km², is a central Asian short-grass steppe with alpine cushions and a east-to-west plant cover gradient from 40% to 10%. (Miehe et al., 2011). The distribution of the Cyperaceae species, *Kobresia pygmaea*, extends approximately 450.000 km² along an altitudinal range between 3000 to nearly 6000 m, with a 98% cover in its core region (Miehe et al., 2008b). *Kobresia pygmaea* does not usually grow more than a few centimeter tall, but it develops a very extensive rooting system. This leads to a very dense turf layer, which consists of roots, root remains, amorphous humus and minerogenic matter that protects the soil from erosion as well as trampling damage by large herbivores (Kaiser, 2004; Miehe et al., 2011). Furthermore it is assumed that the vegetation composition and structure of the *Kobresia pygmaea* ecosystem depends strongly on grazing by herbivores (Miehe et al., 2008b; Wu et al., 2009).

The distribution of alpine steppe and *Kobresia* pastures on the plateau is changing due to climatic change (Zhao et al., 2011; Cui and Graf, 2009; Ni, 2011; Klein et al., 2004). Furthermore the surface properties on the plateau are strongly affected by anthropogenically induces land use change and resulting degradation. The level of degradation reported for the Tibetan grassland varies between studies depending on the underlying definition of degradation stages. According to Niu (1999) 30 % of the *Kobresia* grassland should be regarded as degraded. A study by Holzner and Kriebbaum (2000) reports that 20 % show complete degradation, 20 % is heavily overgrazed, and only 30 % is in optimal condition while the remaining 30 % are under increasing grazing pressure. As a reaction to this degradation caused by overgrazing, rangeland policies in recent years included the regulation of livestock numbers and the implementation of grazing exclosures (Han et al., 2008). Although this had the purpose to either control pasture quality or even restore degraded pastures, the outcome of such measures is still debated (Davidson et al., 2008; Foggin, 2008; Gao et al., 2007; Harris, 2010). Aside from grassland, lakes also make up a great portion of the surface of the highland, covering approximately 45.000 km² with an increasing area in recent years as a result of thawing permafrost and glacial melt due to rising mean annual temperatures (Xu et al., 2009; Liu et al., 2010).

1.1.2. Estimation of energy, water and carbon fluxes on the Tibetan Plateau

Most parts of the Plateau are sparsely inhabited and infrastructure is missing in wide regions, thus observations of energy and matter exchange and in situ measurements of C cycling are sparsely distributed over a wide distance on the Plateau (Frauenfeld et al., 2005; Kang et al., 2010; Maussion et al., 2011; Chen et al., 2013; Hafner et al., 2012;

Wang et al., 2002; Wu et al., 2010). Besides international campaigns like GAME/Tibet and CAMP (GEWEX- Global Energy and Water cycle Experiment Asian Monsoon Experiment and Coordinated Enhanced Observing Period Asia-Australia Monsoon Project, Xu and Haginoya, 2001; Ma et al., 2003), permanent measurements of the energy balance and turbulent flux are conducted by the Institute of Tibetan Plateau Research (ITP) within the framework "Tibetan Observation and Research Platform" (TORP) (Ma et al., 2009). However, especially long term stations measure fluxes only over one dominant surface type, causing a certain degree of uncertainty in representativeness when this data is used to ground truth gridded data sets from remote sensing applications or in model studies (Ma et al., 2009). Furthermore changes within the ecosystem might be overlooked or not resolved at all. Due to the great contribution of lakes to the regional energy balance and water cycle in different catchments around the world (Rouse et al., 2005; Nordbo et al., 2011), fluxes over lake surfaces on the Tibetan Plateau should not be neglected. However no direct measurements of turbulent fluxes over a lake surface on the Tibetan Plateau have been conducted so far; estimations of evaporation over lake surfaces have only been modeled using remote sensing or land surface observations as forcing (Xu et al., 2009; Haginoya et al., 2009). From these model-based estimations it is known that evaporation over lake surfaces differs from evapotranspiration over land throughout the year due to the heat storage capacity of the lakes (Haginoya et al., 2009).

The majority of studies concerning the C cycle on the TP are found within the north-east part of the Plateau between 3000-4000 m a.s.l.. These *Kobresia humilis/pygmaea* pastures act neutral or represent a weak C sink but show a high uncertainty and great inter-annual variability (Kato et al., 2004a,b, 2006; Zhao et al., 2005). Additionally, more process orientated studies are found in this region using chamber-based measurements to investigate the response of CO₂ fluxes to grazing or changes in climate (Saito et al., 2009; Cao et al., 2004; Hirota et al., 2009; Zhang et al., 2009). Above- and belowground C budgets and C allocation within the plant-soil-system was estimated by ¹³CO₂ labeling (Cao et al., 2004; Wu et al., 2010, 2011; Hafner et al., 2012; Unteregelsbacher et al., 2012).

C fluxes have been estimated for *Kobresia pygmaea* pastures in the southern highlands in an elevation above 4000 m with eddy covariance by Fu et al. (2009) and with chamber measurements by Fu et al. (2013). Within the Nam Co Basin over alpine steppe and in an approximate altitude of 4700 m Wei et al. (2012) estimated grazing effects on CO₂ emissions and Hu et al. (2013) the influence of changes in air temperature and snowfall on CO₂ fluxes by using chamber measurements.

1.2. Framework of this thesis

The work of this thesis was embedded in the Project "Mesoscale circulations and energy and Gas exchange over the Tibetan Plateau" (MESO-TiP) and "Atmosphere-Ecology-

Glaciology Cluster" (TiP-AEG) of the DFG (Deutsche Forschungs-Gemeinschaft) Priority Programme 1372 "Tibetan Plateau; Formation, Climate, Ecosystems" (TiP).

1.2.1. Main project objectives

The TiP project investigates the interaction of the main forcing mechanisms on the plateau, its formation, climate evolution, human impact, and their effects on ecosystems. This is done on three different time scales; the plateau formation through the uplift dynamics and related climate change during the last millions to several tens of millions of years, late Cenozoic climate evolution and environmental response during the last tens of thousands to hundreds of thousands of years, as well as the phase of human impact and global change focusing on the present stage, the past 8000 years, and perspectives for the future. The MESO-TiP project and the TiP-AEG Cluster are part of the branch "Phase of human impact and Global Change" within TiP. Its main goal is to investigate the plateau's regional climatic features and its feedbacks with changes in surface properties induced by anthropogenic land use change or other global change impacts. Within this context, the TiP-AEG Cluster deals with the following aspects of the TiP Project:

- How will global change, especially climate and human activity, impact the Tibetan ecosystems and how does this feed back to the global climate?
- What are the consequences for humans on the Tibetan Plateau?

This was achieved within the TiP-AEG Cluster by linking process-orientated studies with the help of *in situ* eddy-covariance measurements and land surface modeling to meso scale modeling. The main focus was on the question how changes in grazing intensity and resulting degradation affect the water and carbon cycling of *Kobresia pygmaea* pastures.

This involved the following work carried out as part of the MESO-TiP project:

- Eddy-covariance measurements to estimate the energy and heat budget including estimation of evapotranspiration and carbon fluxes for the main Tibetan ecotypes: *Kobresia pygmaea* pastures and alpine steppe. These flux estimates represent the link between the ecosystem and the atmosphere.
- Quality control, including estimation and closure of the energy balance and footprint analysis of these flux measurement with respect to specific problems arising on the plateau.
- Adaptation of SVAT models to the specific conditions found on the plateau and validation of the model output with the *in situ* flux measurements. Incorporation of changes within evapotranspiration and carbon exchange observed at plot and ecosystem scale to evaluate effects at a landscape scale

- Meso scale modeling to estimate the impact of these effects on a greater spatial scale and investigate the consequences for atmospheric processes like convection.

1.2.2. Experiments

The work of the TiP-AEG Cluster in Tibet involved several field campaigns to the highlands. The original plan involved concentrating the field work to sites close to the village Kema in the Naqu Prefecture for the ecological studies and the Nam Co Basin for the glaciology, hydrology and also the atmospheric modeling part. Furthermore it was planned to set up a permanent eddy-covariance station in Kema. Due to unforeseen logistical reasons, this station could not be set and only short field campaigns could be conducted. Additionally these logistical and also political reasons caused changes within the original plan for the field campaigns, sometimes involving splitting of the research group and changes of locations. The experiments, their goals and brief summaries are described below:

Nam Co 2009 The purpose of the experiment at Nam Co in 2009 was to measure turbulent fluxes over different typical land cover types on the TP, including alpine steppe and a lake surface. Within this first experiment on the TP the applicability of the eddy-covariance method under the conditions of the highland was tested. Furthermore important parameters needed for the adaptation of the land surface and meso scale atmospheric models used within the project were estimated. The data from this experiment was used in Biermann et al. (2014a, Appendix B), Gerken et al. (2014, Appendix C), Gerken et al. (2012) and Babel et al. (2014, Appendix D).

Xinghai 2009 Research in Xinghai in 2009 focused on long-term effects of grazing on vegetation biomass and composition as well as on carbon cycling in the plant-soil system of the upper montane belt on the Tibetan Plateau. Field measurements focused on analyzing vegetation biomass, composition and regrowth, as well C and N turnover in plant and soil within grazing exclosure plots and on adjacent grazed areas between 3000-3600 m a.s.l. and along a precipitation gradient of 375-505 mm. Results are presented in Hafner et al. (2012), Unteregelsbacher et al. (2012) and Babel et al. (2014, Appendix D).

Nam Co 2010 The winter experiment in February 2010 at Nam Co was conducted to determine the accuracy of the latent heat flux Q_E measurements under situations with low temperatures and water vapor concentrations. More about this experiment can be read in Biermann et al. (2014b, Appendix F).

Kema 2010 The experiment at Kema in 2010 was mainly conducted to estimate the effect of grazing cessation on C and water fluxes within *Kobresia pygmaea* pastures. This experiment involved measurements at ecosystem and plot scale, to

provide a better insight into the water and C cycle of the *Kobresia pygmaea* pastures and especially the characteristic root turf. The results of this experiment are presented in Ingrisch et al. (2015, Appendix E), and the CO₂ flux data is available via ?. Furthermore the measured fluxes are used in Babel et al. (2014, Appendix D).

Kema 2012 The experiment at Kema in 2012 concentrated on the effect of different degradation stages found within the *Kobresia pygmaea* pasture on the C and water cycle. For this purpose three degradation classes were defined and investigated: dense vegetation with an intact turf layer, patches with a turf layer and Cryptogam crusts and areas without the characteristic turf layer. The experiment involved plot scale measurements of C and water exchange, standard meteorological forcing data and needed parameters were determined for use in a model study. This field campaign served as basis for Babel et al. (2014, Appendix D).

Nam Co 2012 The main goal of the 2012 experiment at Nam Co was to investigate the vertical structure of the atmosphere in the Basin in order to link local/mesoscale atmospheric circulation and local convection to the surface. The experiment is a continuation of the 2009 experiment and serves to initialize the ATHAM (Active Tracer High-resolution Atmospheric Model) model with *in situ* atmospheric profiles measured with radiosounding. The results are presented in Gerken et al. (2013).

1.3. Objectives of this thesis

The main goal of this thesis is to investigate the influence of different surfaces found within the heterogeneous landscape of the Tibetan Plateau on C fluxes and turbulent exchange between the ecosystem and the lower atmosphere. In particular this thesis is based on the following research questions and objectives:

- Are measurements of turbulent exchange with eddy-covariance limited due to the special conditions on the Tibetan Plateau, especially under winter conditions?
- How does available soil moisture and a lake surface influence turbulent fluxes? What consequences does this possible effect have for representativeness of a single flux station?
- How important is the root turf for C turnover and storage within *Kobresia pygmaea* pastures?
- How do changes in grazing habits and consequent changes in surface properties such as degradation or vegetation shifts affect processes within the ecosystem and its exchange with the atmosphere?

- EC derives fluxes to link plot scale measurements with landscape scale modeling

The direct measurements of turbulent fluxes and energy balance components were conducted with special focus on differences in available soil moisture within alpine steppe, fluxes over open water bodies, winter conditions and *Kobresia pygmaea* pastures.

To our knowledge this included the first direct estimation of turbulent exchange over a lake surface on the TP with EC measurements which is presented in Biermann et al. (2014a, Appendix B). Although not within the main focus of this study the applied quality control of the measured data represents an implicit checkup on the applicability of EC measurements on the TP. Furthermore flux measurements were attributed to a specific target land surface using footprint analysis which was a prerequisite for the use of the measured turbulent fluxes to validate and adapt land surface models as presented in Gerken et al. (2014, Appendix C), Biermann et al. (2014a, Appendix B) and Babel et al. (2014, Appendix D).

The applicability of standard configured EC stations within longterm measurement networks on the TP was tested through an investigation of the influence of winter conditions on the estimation of Q_E , presented in Biermann et al. (2014b, Appendix F). This included a direct comparison of a KH20 Krypton Hygrometer and a LI-COR 7500 Infrared gas analyzer under winter conditions on the TP for the first time. Furthermore a novel calibration unit was tested under *insitu* field conditions.

Within the core region of *Kobresia pygmaea* pastures the influence of grazing and degradation, as most pronounced human induced changes, on C fluxes and evaporation was investigated. This included a study (Ingrisch et al., 2015, Appendix E) on grazing and the role of the characteristic turf layer of *Kobresia pygmaea*. In order to gain a detailed insight, $^{13}\text{CO}_2$ pulse labeling was coupled with continuous EC measurements in which is a relative novel approach and was so far not applied to the TP yet. While the above mentioned study focusses on an intact *Kobresia pygmaea* turf, Babel et al. (2014, Appendix D) focuses on degradation and its consequence for the water and C cycle in a more general way. It incorporates the findings of the different field campaigns and three field sites, the findings were incorporated into a widespread overview. In addition to the direct findings for the C and water balance it can be seen in Babel et al. (2014, Appendix D) that *in situ* measurements are of great importance for the adaptation of models to the TP, which is a necessary step to bridge from process oriented small scale measurements to a ecosystem or even broader regional scale.

2. Material and Methods

2.1. Study sites

The experiments within the TiP-AEG Cluster were carried out at three locations on the Tibetan Plateau. Characteristic properties of the sites are summarized in Table 2.1. A map of the Plateau with the experimental sites indicated is shown in Figure 2.1:

Nam Co The Nam Co site is located in Xizang province at the Nam Co Monitoring and Research Station for Multisphere Interactions (NAMORS) of the Institute of Tibetan Plateau Research of the Chinese Academy of Sciences (Ma et al., 2008). The station is located in the Nam Co Basin at the foot of the Nyainqentanglha mountain range, 220 km north of Lhasa. It represents alpine steppe pastures and a lake. For more details refer to Biermann et al. (2009).

Kema The study site at Kema is located in the within the core distribution area of *Kobresia pygmaea* (Miehe et al., 2008b), adjacent to the village Kema (Naqu prefecture, Xizang province) and the Naqu Ecological and Environmental Observation and Research Station and represents a typical alpine *Kobresia pygmaea* pasture. For more details refer to Biermann et al. (2011, 2013)

Xinghai The experimental site at Xinghai is located in Qinghai province in the north-eastern Tibetan Plateau, approximately 200 km southwest of Xining, and about 15 km south of Xinghai city. The montane grassland has developed on a loess-covered (1.2 m) terrace of the Huang He River. The grassland is used as a winter pasture for yaks and sheep for 6 to 7 months of the year, and about 20% of the pasture at the experiment site is completely covered with blue-green algae and crustose-lichens. A detailed site description can be found in Miehe et al. (2008a), Unteregelsbacher et al. (2012) and Hafner et al. (2012).

2. Material and Methods

Table 2.1. Characteristic properties of the three study sites, Nam Co, Kema and Xinghai on the Tibetan Plateau, modified after Babel et al. (2014, Appendix D)

	Nam Co	Kema	Xinghai
Coordinates	30°46'22"N 90°57'47"E	31°16'56"N 92°6'18"E	35°42'0"N 99°51'0"E
Altitude	4745 m	4410 m	3440 m
land cover	Alpine steppe pastures with mosaic <i>Kobresia</i> turf	Alpine <i>Kobresia pygmaea</i> pastures	Montane <i>Kobresia/Stipa</i> winter pastures
soil (IUSS-ISRIC-FAO 2006)	Stagnic Cambisols, Arenosol	stagnic (molic) Cambisol	haplic Kastanozems
vegetation composition	<i>Stipa</i> , <i>Carex</i> , <i>Kobresia</i> and <i>Oxytropis</i>	<i>Kobresia pygmaea</i> , <i>Carex</i> spec., <i>Festuca</i> spec., <i>Kobresia humilis</i> , <i>Poa</i> spec., <i>Stipa purpurea</i> , <i>Trisetum</i> spec.	<i>Kobresia</i> spp., <i>Stipa</i> spp.
References to soil and vegetation data	Kaiser et al. (2008), Miehe et al. (2014), Mügler et al. (2010)	Kaiser et al. (2008), Miehe et al. (2011), Biermann et al. (2011, 2013), Babel et al. (2014)	Kaiser et al. (2008), Miehe et al. (2008a), Unteregelsbacher et al. (2012), Hafner et al. (2012)
Nearest Climate Station (1971-2000)	Bangoin 4700 m 31°23'N, 90°01'E & Damxung 4200 m 30°29'N, 91°06'E	Naqu 4507 m 31°29'N, 92°04'E	Xinghai 3323 m 35°35'N, 99°59'E
Annual precipitation ¹	322 mm & 460 mm	430 mm	353 mm
Annual mean temperature	-0.8 °C & 1.7 °C	-1.2 °C	1.4 °C
Mean temperature in July	8.7 °C & 10.9 °C	9.0 °C	12.3 °C
Source of climate data		http://cdc.cma.gov.cn/	

¹ precipitation falls mainly during the summer monsoon months due to the influence of the East Asian

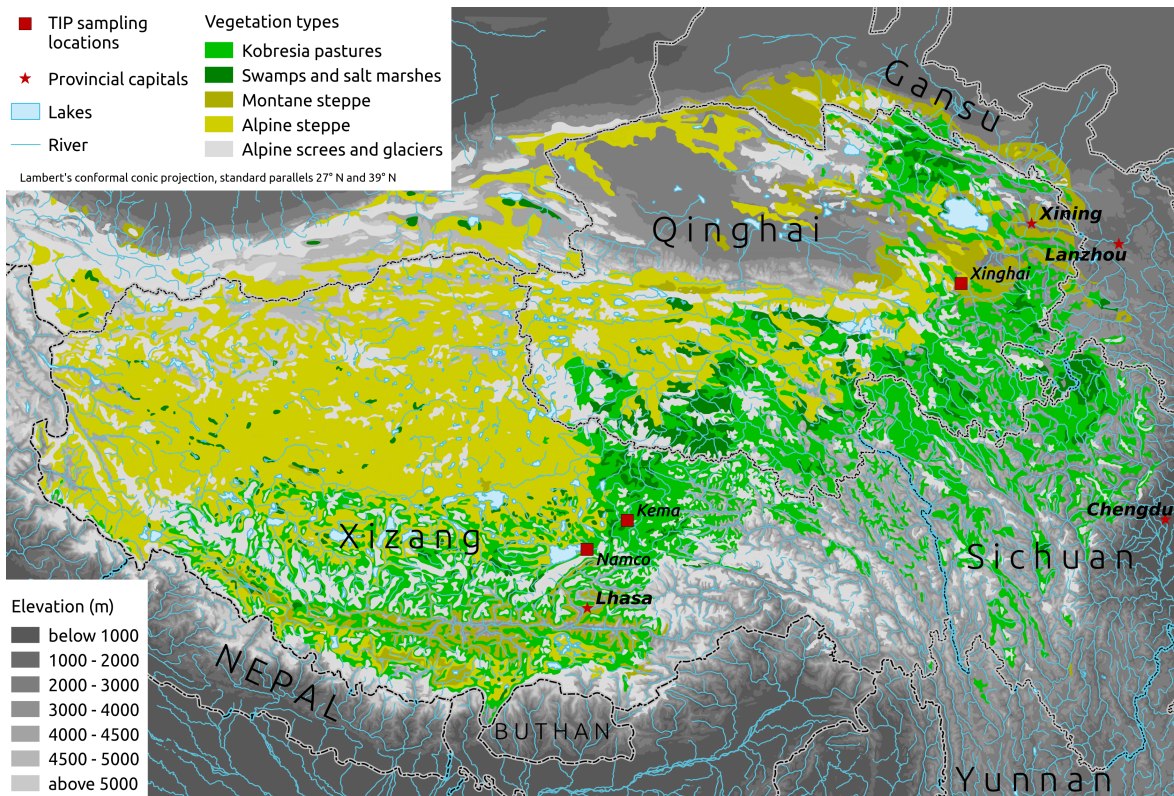


Figure 2.1. Map of the Tibetan Plateau, showing the distribution of the main vegetation types. Experimental sites of the TiP-AEG Cluster are marked by red squares. The map was created by the Faculty of Geography, Univ. Marburg and taken from Babel et al. (2014, Appendix D).

2.2. Methods

2.2.1. Eddy-covariance

Turbulent flux measurements with the eddy covariance (EC) method is a direct micrometeorological approach to estimate turbulent exchange of energy and matter between the atmosphere and the underlying surface (Aubinet et al., 2012). It is also a commonly used approach to estimate the C budget on the ecosystem scale, the net ecosystem exchange (NEE) (Baldocchi, 2003; Wohlfahrt et al., 2012). For the determination of turbulent fluxes with the EC method the wind vector is measured at 20 Hz with an ultrasonic anemometer. Further concentrations of trace gases, like water vapor or CO_2 are measured simultaneous with a gas analyzer, in close vicinity to the anemometer. The calculation, post processing of the turbulent fluxes is described in the following paragraph.

Post-processing of turbulent data and quality control

For all experiments, 30 min averages of turbulent fluxes were calculated from the high frequent raw data with the well tested software package TK2/TK3 (Department of Micrometeorology, University of Bayreuth; Mauder and Foken, 2004, 2011). The internationally compared software (Mauder et al., 2008) includes all necessary data correction. Its implemented data quality control tool considers sources of errors. Calculated fluxes match up to date micrometeorological standards (Foken et al., 2012; Rebmann et al., 2012). A quality flagging scheme ranging from 1 to 9, after Foken and Wichura (1996), accounts for the development of turbulence as well as stationarity and enables to distinguish data with high quality (flags 1-3), intermediate quality (flag 4-6) and poor quality (flag 7-9) (Foken et al., 2004).

Flux measurements in complex terrain

Eddy-covariance measurements require a mostly homogeneous flow field as a prerequisite. Since this requirement is hard to fulfill for most *in situ* measurements, the resulting terrain effects on the wind measurements are normally considered by rotation of the data according to the planar-fit rotation method (Wilczak et al., 2001). This was also applied to the data measured on the TP. A special case appeared at one of the EC stations during the 2009 experiment in the Nam Co basin due to its position at the shoreline of a small lake. Measurements were influenced by the transition from the plane of the lake surface to the gently sloping grassland with a steep step in between. Paw U et al. (2000) and Finnigan et al. (2003) suggest that such terrain structures should be considered by using the rotation procedure on the eddy-covariance data. Therefore the planar-fit rotation was applied for four different sectors taking terrain into account. This procedure accounts for two planes with different slopes and two transition areas. Most of the vertical wind speed disappears after the rotation; 95% of the vertical wind speed data for the lake and for the land surface remain within $\pm 0.1 \text{ m s}^{-1}$ and $\pm 0.07 \text{ m s}^{-1}$, respectively. For wind sectors parallel to the shoreline, 95% of the residual mean vertical wind velocity stays within $\pm 0.12 \text{ m s}^{-1}$. These values stay inside acceptable limits, compared to a multi-site quality analysis by Göckede et al. (2008).

Representativeness of flux measurements

To ensure that the EC measurements are representative for the selected target land cover, the distribution of the measured flux data in the context of the underlying land surface was analyzed (Göckede et al., 2006). The footprint analysis is based on a Lagrangian stochastic forward model, providing a two-dimensional contributions of source areas (Rannik et al., 2000). This analysis also ensures the comparability between plot-scale measurements and the EC, as recommended in Reth et al. (2005).

Energy balance closure

Heterogeneity within the roughness or thermal properties of the underlying surface might result in large-scale turbulent structures, not measured with EC, causing a gap in the energy balance closure (EBC) (Foken, 2008b). Two methods to correct the turbulent fluxes for the missing energy were applied. The first method distributes the residual of the energy balance according to the Bowen ratio Bo to the latent and sensible heat flux, further referred to as EBC- Bo (Twine et al., 2000). In the second correction method the residual of the energy balance is attributed to the sensible and latent heat flux according to their contribution to the buoyancy flux. This fraction depends mainly on the Bowen ratio Bo and to a lesser extent on air temperature; therefore more than 90% are attributed to the sensible heat flux in the case of $Bo=1$ and approximately 60% in the case of $Bo=0.1$. This method follows Charuchittipan et al. (2014) and is named EBC-HB, and it is based on suggestions made by recent studies, such as Mauder et al. (2006); Ingwersen et al. (2011); Brötz et al. (2014). It takes into account that secondary circulations may cause the unclosed energy balance as hypothesized by Foken et al. (2010, 2011). While the latent and sensible heat flux were corrected, this is not applicable for NEE measurements (Foken et al., 2011). While the data from the Nam Co 2009 experiment were corrected with the EBC- Bo method, the EBC-HB method was used to correct all fluxes from later experiments.

Gap filling and partitioning of turbulent C fluxes

Time series of EC-derived turbulent fluxes will inevitably have gaps due to malfunctioning of the measurements devices or rejection of data with poor quality. To ensure a continuous time series of NEE, which is necessary for the estimation of C budgets, the data gaps were filled with a widely used technique (Desai et al., 2008; Falge et al., 2002; Lasslop et al., 2010; Reichstein et al., 2012). The utilized approach is described in detail in Ruppert et al. (2006) which follows Falge et al. (2001) and uses a light response function following Michaelis and Menten (1913) to estimate assimilation (GEE, Gross Ecosystem Exchange) and respiration (*Reco*, Ecosystem Respiration) and is parameterized from in situ measured night-time NEE and temperature measurements following Lloyd and Taylor (1994). The composite NEE from the models is reinserted into the data gaps of the original time series. By using the modeled fluxes it is furthermore possible to partition the measured NEE into assimilation and respiration.

2.2.2. $^{13}\text{CO}_2$ labeling

Pulse labeling with ^{13}C or ^{14}C enriched CO_2 (Kuzyakov and Domanski, 2000; Kuzyakov, 2001) is one of the most commonly used methods in C studies. It enables the allocation of assimilated C to be tracked to the various pools within the plant-soil continuum, since labeled assimilates are used for metabolism by shoots, roots and rhizosphere

microorganisms or become incorporated into soil organic matter. This distribution is of great importance because it affects how long the assimilated C will be stored in the ecosystem before returning to the atmosphere via root and microbial respiration (Carbone and Trumbore, 2007), which may vary from minutes to hundreds of years (Kuzyakov, 2006).

The $^{13}\text{CO}_2$ pulse labeling was conducted with sealed chambers with dimensions of 60 cm \times 60 cm \times 10 cm and build from transparent plastic foil. The label was released at noon into the chamber atmosphere by injecting an excess of 5 M sulphuric acid with a syringe into a vial with 2 g of ^{13}C enriched (99 atom-%) Na_2CO_3 dissolved in water. Chambers were opened after four hours of labeling, and the first sampling was conducted. Sampled pools are above- and belowground biomass, soil and CO_2 efflux. The labeling and sampling procedure is presented in detail by Hafner et al. (2012) and Ingrisch et al. (2015, Appendix E).

2.2.3. Coupling of eddy covariance and $^{13}\text{CO}_2$ labeling

The use of either EC or $^{13}\text{CO}_2$ pulse labeling alone involves a number of limitations when trying to fully understand the C cycling of an ecosystem, and so coupling of both methods will provide a deeper insight. Pulse labeling with $^{13}\text{CO}_2$ only provides a relative distribution, although mass units and absolute fluxes are important in *in situ* studies related to C balance and turnover (Kuzyakov and Domanski, 2000), and EC measurements do not reveal processes within single compartments of the ecosystem due to the footprint of EC measurements, which integrates over a large portion of the ecosystem Leclerc and Foken (2014).

By coupling a mean daily assimilation derived from eddy-covariance measurements with the relative distribution of the C estimated within the $^{13}\text{CO}_2$ pulse labeling after a defined allocation period, absolute C fluxes into the different pools of the plant-soil compartments can be derived following Riederer (2014):

$$n(C)_i = GEE \cdot R(^{13}\text{C}_i)_t \quad (2.1)$$

with $n(C)_i$ being the absolute flux into a specific pool i , GEE being the mean daily C input estimated with EC during the allocation period and $R(^{13}\text{C}_i)_t$ the percentage of recovered ^{13}C within pool i at the end of the defined allocation period.

Allocation of ^{13}C to the various pools in the plant-soil-microorganism system is considered to be completed when the metabolic plant components are depleted of ^{13}C (Saggar et al., 1997). However, the length of this allocation period, not to be confused with the end of the observation period (also called chase period), is difficult to identify, yet is critical for the interpretation of the distribution of the assimilated tracer (Wang et al., 2007). Numerous studies report that allocation is finished within 3-4 weeks (Hafner et al., 2012; Keith et al., 1986; Riederer, 2014; Swinnen et al., 1994; Wu et al., 2010).

One advantage of coupling both methods is finding a suitable timing for the labeling experiment through continuous *in situ* observations of the C exchange regime with EC measurements. This is important as the partitioning of the assimilates can vary greatly, depending on the climatic conditions (Meharg and Killham, 1989; Palta and Gregory, 1997) as well as during the course of the growing season (Swinnen et al., 1994), a crucial fact in an environment such as the TP with a very short vegetation growing period.

2.2.4. Chamber based gas exchange measurements and micro-lysimeter

Plot-scale CO₂ flux measurements were conducted with a long term chamber system from LI-COR Biosciences (Lincoln, NE, USA). The LI-COR long-term chamber system contains a LI-8100 Infrared Gas Analyser (LI-COR Lincoln, NE, USA), which is linked with an automated multiplexing system (LI-8150) and two fully automatically rotating chambers, one opaque for respiration and the other transparent for NEE measurements. The applied LI-COR chambers were compared against eddy-covariance measurements by Riederer et al. (2014). Besides differences mainly under stable atmospheric stratification, the comparison was satisfactory. The small micro-lysimeters used to investigate plot-scale hydrological properties are near-natural soil monoliths with a dimension of 15 cm × 30 cm within an inner and outer plexiglass tube reinserted in their natural place. To prevent artificially high water saturation through disruption of the flow paths to the lower soil horizons (Ben-Gal and Shani, 2002; Gee et al., 2009), a constant drainage with a suction of 10 hPa of a hanging water column was applied. Water content was estimated by weighing the lysimeter with a portable scale.

2.2.5. Land-surface atmosphere interaction and atmospheric Models

The investigations on the TP within the project also involved modeling with different models. The selection of the models was based on the target land surface or the flux and process of interest. For land surfaces the following soil - vegetation - atmosphere transfer models were utilized; SEWAB (Mengelkamp et al., 1999, 2001) for turbulent fluxes, SVAT-CN (Reichstein, 2001; Falge et al., 2005) for C fluxes. Furthermore Hybrid, a vegetation dynamics and biosphere model (Friend et al., 1997; Friend and Kiang, 2005), was used to estimate for turbulent fluxes in connection with the cloud-resolving Active Tracer High-resolution Atmospheric Model (ATHAM, Oberhuber et al., 1998; Herzog et al., 2003), allowing simulation of feedbacks of land surface exchange to the atmosphere. While the first two models use measured standard meteorological as forcing data, the latter is fully coupled to the atmosphere. The utilized models were adapted to the Tibetan Plateau and individual parameter sets have been elaborated from field measurements for Nam Co and Kema (Gerken et al., 2012, Biermann et al. (2014a,

Appendix B), Babel et al. (2014, Appendix D)). The models are therefore capable of dealing with the TP's specific problems such as a strong diurnal cycle of the surface temperature (Yang et al., 2009; Hong and Kim, 2010), a diurnal variation of the thermal roughness length observed on the Tibetan Plateau (Yang et al., 2003; Ma et al., 2002), and high, bare soil evaporation in semiarid areas (e.g. Agam et al., 2004; Balsamo et al., 2011). For the lake surface a hydrodynamic multilayer model (HM) by Foken (1979, 1984) was utilized. Turbulent fluxes are parameterized with a bulk approach. However HM uses an integrated profile coefficient accounting for the molecular boundary layer, the viscous buffer layer and the turbulent layer within the surface layer instead of a bulk coefficient. Therefore near-surface exchange conditions are reflected according to hydrodynamic theory. The model is originally designed for simulating the exchange over the ocean, and Panin and Foken (2005) added a correction term for shallow water which increased turbulent fluxes due to an enhanced mixing by higher waves in shallow water. The model has been successfully applied to simulate fluxes above ocean and lake surfaces as well as over arctic snow fields (Foken, 1986; Panin et al., 2006; Lüers and Bareiss, 2010; Biermann et al., 2014a, Appendix A).

2.3. Experiment Setup

The two experiments At Nam Co were carried out in summer 2009 and February 2010. Experiments in Kema were conducted in summer 2010 and 2012. The following section will briefly summarize the goals of the experiments and introduce the methods. The detailed setup of the experiments is presented in Table 2.2.

Xinghai 2009 In Xinghai five grazing enclosure plots were established in 1995 along an altitudinal gradient from 3000-3600 m a.s.l.. Three sites were dominated by *Kobresia* spp. and the two others in the drier region were dominated by grasses, mainly *Stipa* spp., the common vegetation types of the upper montane belt on the Tibetan Plateau. Vegetation and soil samples were taken from fenced and unfenced plots in five replicates and used for laboratory analysis which included DNA analyses of the plant species, changes in the belowground biomass, C and N contents in plants, bulk soil and different density fractions representing soil organic matter (SOM) with different turnover time, and biomarker analyses (lignin, suberin and cutin). The pulse labeling experiments with ^{13}C and ^{15}N were carried out only at one key site.

Nam Co 2009 The purpose of the experiment at Nam Co in 2009 was to measure turbulent fluxes over different typical land cover types on the TP, including alpine steppe and a lake surface. Therefore atmospheric fluxes were observed with two eddy-covariance and energy balance stations at Nam Co. One station was the permanently operating eddy-covariance complex (NamITP) within NAMORS, measuring fluxes over a sparse and dry alpine steppe. The second station was

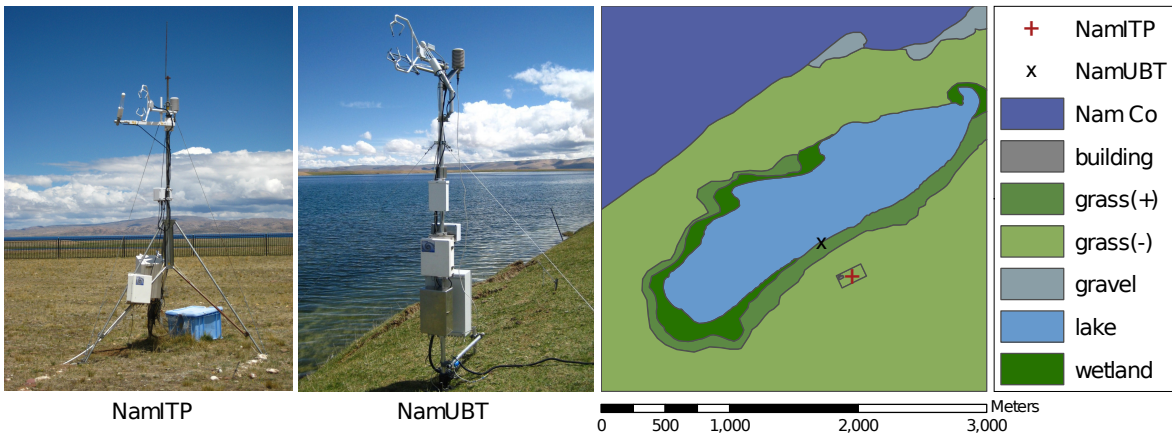


Figure 2.2. Measurement setup of the 2009 campaign in the Nam Co Basin showing the eddy-covariance stations NamITP and NamUBT (left Photo and red +; right Photo, black x in the schematic drawing). Additionally a land use classification is given: wetland (dark green), moist (+, medium green), dry (–, light green) grassland, partly flooded gravel (grey), the small lake (light blue) and Nam Co (dark blue). NamITP was also used during the winter experiment in 2010. Figure from Biermann et al. (2014a, Appendix B)

temporarily set up by the University of Bayreuth (NamUBT) at a shallow lake at the SE side of Nam Co Lake, measuring over the lake surface and the surrounding grassland depending on the instantaneous wind direction (2.2). To account for the effect of different moisture supply on the vegetation at the stations, we have classified the grassland into (grass⁺) for denser and moister vegetation at NamUBT and (grass[–]) for comparatively drier and sparser vegetation at NamITP. A detailed map of the field site and pictures of the two stations can be seen in Biermann et al. (2014a, Appendix B). Both eddy-covariance stations measured turbulent fluxes and all necessary components for the estimation of the energy balance. Furthermore standard meteorological measurements are available. For more specific information on the setup refer to Biermann et al. (2014a, Appendix B) or Biermann et al. (2009).

Nam Co 2010 The winter experiment in February 2010 at Nam Co was conducted to check the accuracy of the estimation of the latent heat flux Q_E under situations with low temperatures and water vapor concentrations. For this purpose, site by site measurements with a Li7500 and a KH20 were conducted. Additionally a new calibration device for the KH20 was tested under *in situ* conditions.

Kema 2010 The experiment at Kema in 2010 was mainly conducted to estimate the effect of grazing cessation on C and water fluxes within *Kobresia pygmaea* pastures. Therefore in 2009 an area of 100 x 250 m was fenced for a grazing manip-

2. Material and Methods

ulation at the research site, excluding grazing livestock such as yak, sheep and goat. In addition, four subplots (15 x 15 m) that also exclude the Plateau Pika (*Ochotona curzoniae*) were established inside the livestock enclosure. Water and C fluxes under three grazing treatments, normal grazing (G), a partial enclosure, with exclusion of livestock but pika grazing (P) and no grazing (U) were investigated with micro-lysimeter and $^{13}\text{CO}_2$ labelling. Turbulent atmospheric fluxes were observed over G and P. Thus, effects of livestock grazing correspond to the difference between G and P, whereas the combined grazing effects of livestock and pikas are reflected by the difference between U and G. Further setup information is given in Ingrisch et al. (2015, Appendix E) and Biermann et al. (2011). The $^{13}\text{CO}_2$ pulse labeling was conducted on the 1st July 2010 with four replicates of each of the three treatments (G, P, U). In order to assess hydrological properties small weighing micro-lysimeters were set up in June 2010 on four subplots inside the fenced area of the Kema site at a distance of 20 to 50 m from the eddy covariance station, with one micro-lysimeter within vegetation and one in bare soil with a maximum distance of 1 m within each subplot. All micro-lysimeters were weighed every 2 to 10 days with a precision hanging balance from June till September.

Kema 2012 The experiment at Kema in 2012 concentrated on different degradation stages found within the *Kobresia pygmaea* pasture. For this purpose three degradation classes were defined: dense vegetation with an intact turf layer (Intact Root Mat, IM), patches with Cryptogam crusts (Unteregelsbacher et al., 2012) and a turf layer cover (Degraded Root Mat, DM) and areas without the characteristic turf layer (Bare soil, BS). Photos of the surface types are shown in Figure 2.3. A survey of the distribution of these classes revealed that IM covers 64.7% , DM 16.6% and BS 18.7% of the research area. Carbon exchange of these treatments



Figure 2.3. The three defined degradation levels at Kema; Intact Root Mat, IM: dense vegetation with an intact turf layer, Degraded Root Mat, DM: patches with Cryptogams and a turf layer cover and Bare soil, BS: areas without the characteristic turf layer (Bare soil, BS). Figure from Babel et al. (2014, Appendix D).

was observed with an automated long-term chamber system, Li8100, on a rotational base. Hydrological properties of the degradation classes were investigated with micro-lysimeters again from June till September. More information on the experiment setup can be found in Babel et al. (2014, Appendix D) or Biermann et al. (2013).

2. Material and Methods

Table 2.2. Devices used for the experiments at Nam Co and Kema on the Tibetan Plateau, including manufacturer and measurement heights.

Device	Nam Co 2009	Nam Co 2010	Kema 2010	Kema 2012
Wind velocity and direction	CSat-3 ^a : 3.0 ¹ , 3.1m ²	CSat-3 ^a : 3.0m	CSat-3 ^a : 2.20 ³ , 2.21m ⁴	WindSonic 1 ^b : 2.0m
CO ₂ measurements	Li7500 ^c : 2.9 ¹ , 3.0m ²	Li7500 ^c : 3.0m	Li7500 ^c : 2.19 ³ , 2.16m ⁴	Li8100 ^c : Soil chambers
H ₂ O measurements	Li7500 ^c : 2.9 ¹ , 3.0m ²	Li7500 ^c ; KH20 ^a : 3.0m	Li7500 ^c : 2.19 ³ , 2.16m ⁴	—
Solar radiation	CNR1 ^d : 2.0m ¹ , CM3+CG3 ^d : 1.5m ²	CM3+CG3 ^d 1.5m	CNR1 ^d : 1.88 ³ , 1.90 ⁴	Pyranometer SP 110 ^e ; NR Lite ^d ; LI 190 SB ^c ; CNR1 ^d : 2m
Temperature and humidity	HMP45 ^f : 3.0 ¹ , 3.1m ²	HMP45 ^f : 3.1m	HMP45 ^f : 2.19 ³ , 2.16m ⁴	CS 215 ^a : 2m
Precipitation	Tipping bucket 1m	Tipping bucket 1m	Tipping bucket 1m	Tipping bucket 1m
Soil moisture	TDR ^g : -0.1,- 0.15,-0.2m ¹ ;-0.1,-0.2,-0.4,- 0.8,-1.6m ²	TDR ^g : -0.1,-0.2,-0.4,- 0.8,-1.6m	TDR ^g : -0.1 ³ , 0.15 ⁴ ,0.2m ³	Campbell CS 616 ^a : -0.05,- 0.125,-0.25m TDR ^g : -0.1,-0.2m
Soil temperature	Pt 100: -0.025,-0.075,- 0.125,-0.2m ¹ ; -0.1,-0.2,-0.4,- 0.8,-1.6m ²	Pt 100: -0.1,-0.2,-0.4,- 0.8,-1.6m	Pt 100: -0.025,-0.075,- 0.125,-0.2m ³	Pt 100: -0.025,-0.075,- 0.125,-0.175,- 0.25m
Soil heat flux	-0.15 m ^h	-0.15m ^h	-0.15m ^h	-0.2m ^{h,i}
Logger	Cr3000 ^{a,1} Cr5000 ^{a,2}	Cr5000 ^a	Cr3000 ^a	Cr1000 ^a

¹ NamUBT

² NamITP

³ EC-P

⁴ EC-G

^a Campbell Sci. Ltd.

^b Gill

^c LI-COR Biosciences

^d Kipp & Zonen

^e Apogee

^f Vaisala

^g Imko

^h HP3

ⁱ Hukseflux

3. Results and Discussion

3.1. Turbulent fluxes on the Tibetan Plateau

3.1.1. Flux measurements over different surfaces

Measured and modeled energy fluxes on the TP exhibit distinct spatial heterogeneity corresponding to different surface types. Differences in energy and matter fluxes can be triggered through variations in available soil moisture and different vegetation or surface characteristics, as can be seen in Figure 3.1. Mean diurnal turbulent fluxes for a dry (grass⁻, NamITP) and a wet (grass⁺, NamUBT) alpine steppe and *Kobresia pygmaea* show the typical behavior as expected for the monsoon season on the TP with a greater latent heat flux than sensible heat flux. This observation is in agreement with e.g. Gu et al. (2005) and Ma and Ma (2006). Although measured in consecutive year and at different sites, the mean diurnal cycle of the energy fluxes measured over *Kobresia pygmaea* pastures at Kema in 2010 show a similar magnitude and diurnal cycle as over the alpine steppe in the Nam Co basin measured in 2009. However it needs to be considered that absolute values are not directly comparable.

The mean diurnal cycles of surface and air temperature also show typical dynamics, with unstable stratification during the daytime. Surface temperatures are the highest over alpine steppe grass⁻, followed by *Kobresia pygmaea* and alpine steppe grass⁺. Ground heat flux and sensible heat flux are in the same order of magnitude for each land surface, again with higher values for alpine steppe grass⁻ and *Kobresia pygmaea*. In consequence, the latent heat flux is lower over these two land surfaces than over alpine steppe grass⁺, although there are not big differences overall. The similarity between the measurements over alpine steppe in 2009 and the *Kobresia pygmaea* in 2010 can be explained through relatively dry conditions during the experiment in 2010. More pronounced is the difference between energy fluxes measured over the land surfaces in comparison to fluxes measured over a lake surface, which show differences in magnitude and dynamics. The daytime net radiation is substantially higher over the lake surface, caused by a lower albedo and decreased upwelling long wave radiation due to dampened surface temperatures over the lake. Turbulent fluxes over the lake do not show a diurnal cycle, but remain constant over the day as the energy input from radiation is stored in the lake body and is available at any time throughout the day. Due to its small extent and the shallow water close to the shoreline, the lakes surface temperature is high, leading to unstable stratification even during the daytime. Turbulent exchange

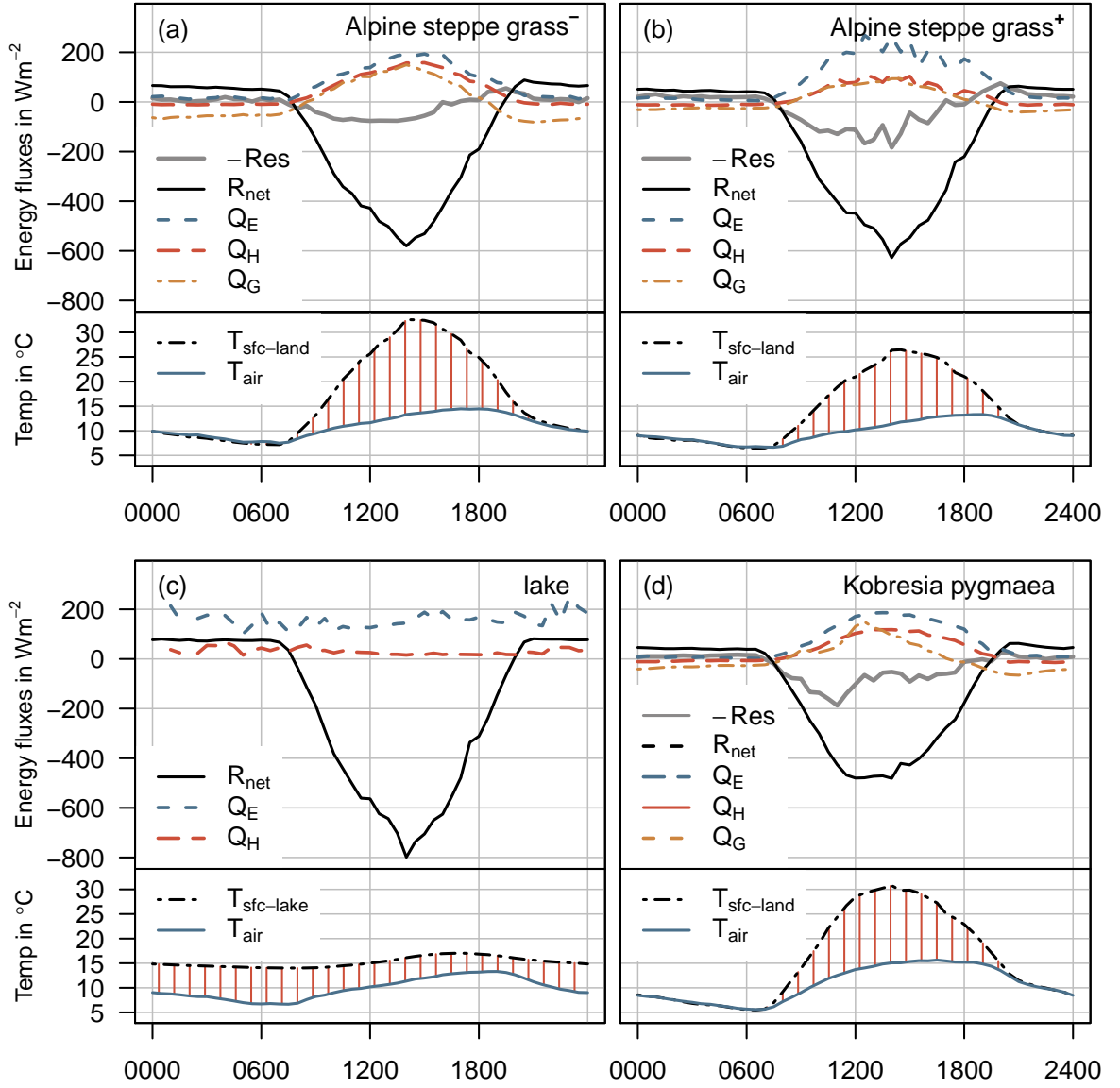


Figure 3.1. Mean diurnal energy fluxes, diurnal surface and air temperature for the Nam Co 2009 (a, b, c) and Kema 2010 (d) experiment, separated for a: Alpine steppe grass⁻, b: Alpine steppe grass⁺, c: lake and d: *Kobresia pygmaea*; all components are measured for land fluxes (a, b, d); for lake fluxes (c), the net radiation is calculated from measured down welling radiation, an albedo of 0.06, lake surface temperature and an emissivity of 0.96. (Time axis in Beijing standard time (CST), mean local solar noon at 1400). Modified and extended after Biermann et al. (2014a, Appendix B)

is consequently enhanced compared to stable stratification typically found over lake surfaces during the daytime (Beyrich et al., 2006; Nordbo et al., 2011). Furthermore high wind velocities of 4 m s^{-1} on average lead to enhanced evaporation in this case. Since no measurements exist for the heat storage in the water body and heat fluxes into the sediment, it was not possible to determine a complete energy balance over the lake surface. The results of the energy balance analysis over the land surfaces revealed a closure of 73% at NamUBT and 80 % at NamITP. The results at Kema were 73% at EC-P and 71% at EC-G. These values of the EBC are all within a range typical for stations in heterogeneous landscapes Foken (2008a).

3.1.2. Accurate estimation of Q_E in Winter

A direct comparison of the latent heat fluxes measured with the Li7500 and the KH20 during a side by side experiment in February 2010 reveals 20% greater fluxes measured by the KH20. Apart from this offset only a little scatter exists between both fluxes (Figure 3.2). The comparison also shows that the deviation is greatest for high latent heat fluxes above $150 \text{ W m}^{-2} \text{ s}^{-1}$ which occur rarely. Furthermore it needs to be considered that the calibration of the KH20 has an error range of up to 10%. It can therefore not be determined whether the difference is related to the temperature sensitivity of absolute humidity measurements by the Li7500 or a calibration error of the KH20. A comparison of continuous measurements of absolute humidity with the Li7500 and the HMP45 for 2009 and 2010 are shown in Figure 3.3, and also included is the maximum absolute humidity at saturation and air temperature. It is clearly visible

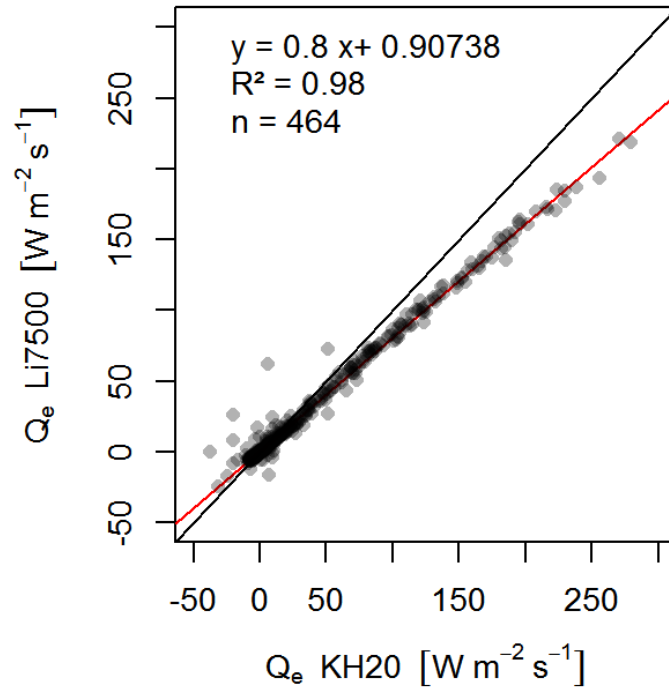


Figure 3.2. Comparison of the observed latent heat flux with both gas analyzers, Li7500 and KH20, during the side by side measurements in February 2010 at NAMORS. Geometric mean regression calculated after Dunn (2004) From Biermann et al. (2014b, Appendix F)

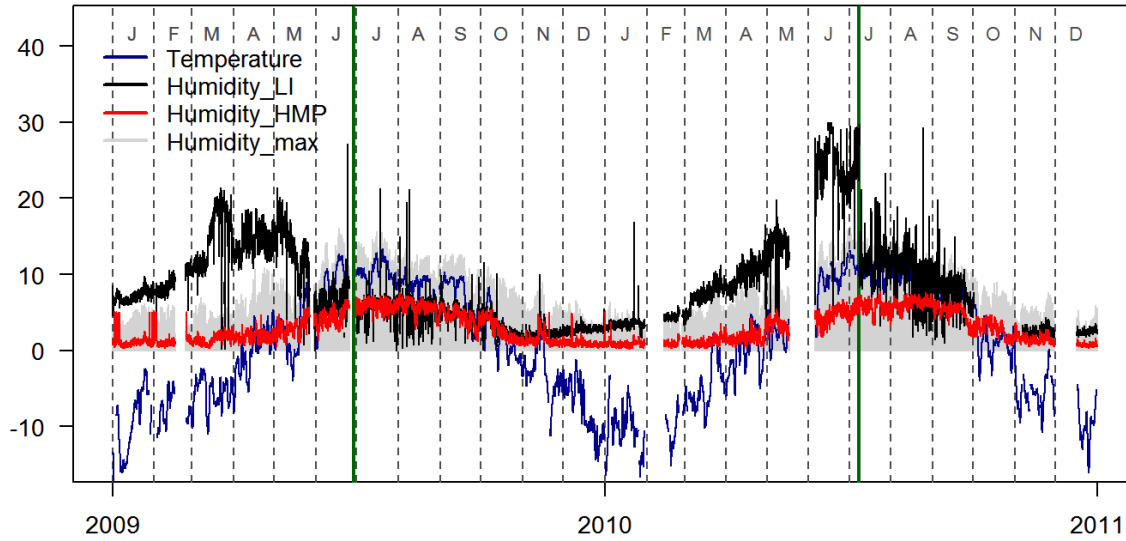


Figure 3.3. Timeline of absolute humidity measurements conducted with the LiCOR 7500 (black) and the HMP 45 (red) at NAMORS from 2008 to 2011. The grey shaded area indicates the amount of water in the air when 100% relative humidity is reached; the blue line represents air temperature. Vertical green lines mark the field calibration dates for the LiCOR 7500 on 30.06.2009 and 08.07.2010. From Biermann et al. (2014b, Appendix F)

that the humidity measurements by the Li7500 exceed the physical limit of 100% humidity regularly during the winter months, while for summer months this is only true occasionally. The effect of a recent field calibration is also visible in this figure. After the calibration on 30th June, 2009 the measurements from the LI-7500 fit well with the measurements from the HMP45, until the air temperature starts to fall below 0°C in October again. While in 2009 the absolute humidity measurements by the Li-7500 start to decrease again with the rise of the air temperature above freezing in April and May, in 2010 such an effect is not visible. However the effect of the calibration on 8th July, 2010 is again visible. Together with the data gap in May this indicates a malfunction of the sensor in June 2010. Overall this investigation showed that either of the two devices can be used for a correct estimation of Q_E in winter as long as great emphasis is laid upon a correct calibration routine.

3.2. Carbon Fluxes of *Kobresia pygmaea* pastures

3.2.1. Net Ecosystem Exchange

The observed net ecosystem exchange (NEE) flux during the Kema 2010 experiment, 8th June till 3rd August (Figure 3.4 upper panel) enables us to characterize the overall C exchange conditions between the atmosphere and the *Kobresia pygmaea* ecosystem. In general, the dynamics of the C fluxes measured at both EC stations are very similar (therefore only EC-P is shown), and the observations can be divided into three periods with different characteristics. At the beginning of the observation period the NEE did not show a clear daily cycle.

With the onset of rain in June (Figure 3.5) and rising temperatures, assimilation became more dominant on 27th June, followed by a period characterized by constant fluxes until 23th July. Within this period the strongest assimilation was observed, whereas when averaged over the whole period the NEE is quite small at both stations. This is due to the C fluxes prior to 27th June and after 23th July, which are characterized by a weaker assimilation during overall drier conditions, visible in the Bowen ratio for these periods which has a greater value than 1 when the sensible heat flux dominates over the latent heat flux (Figure 3.4 lower panel).

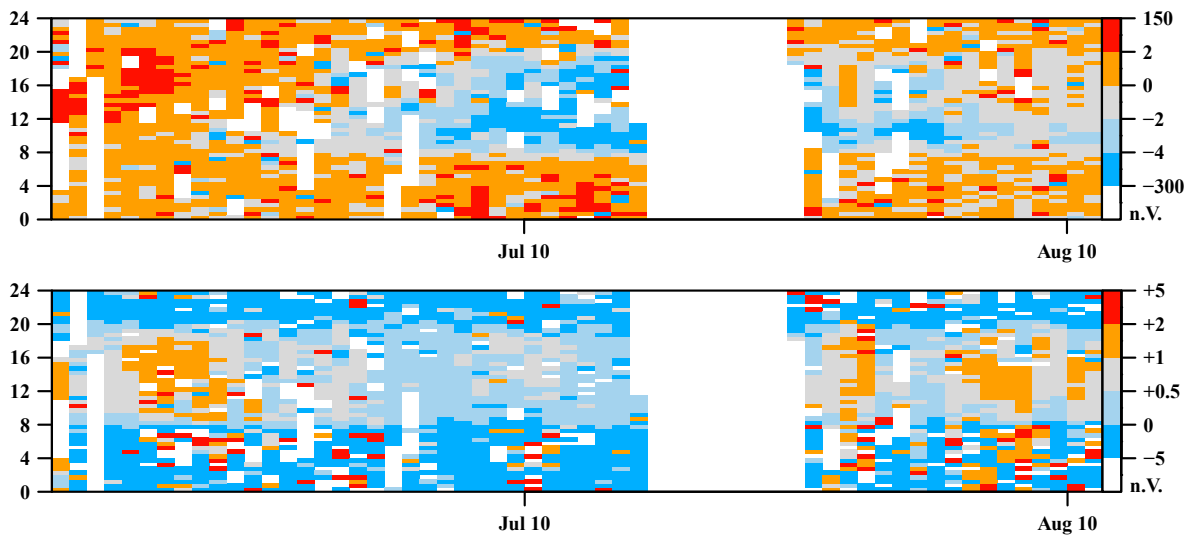


Figure 3.4. Hovmöller diagrams of NEE (upper panel) and the bowen ratio (lower panel), measured at EC-P in Kema from 8th July till 3rd August. Colors indicate the mean half hour values, the x axis the period and the y axis the time of day.

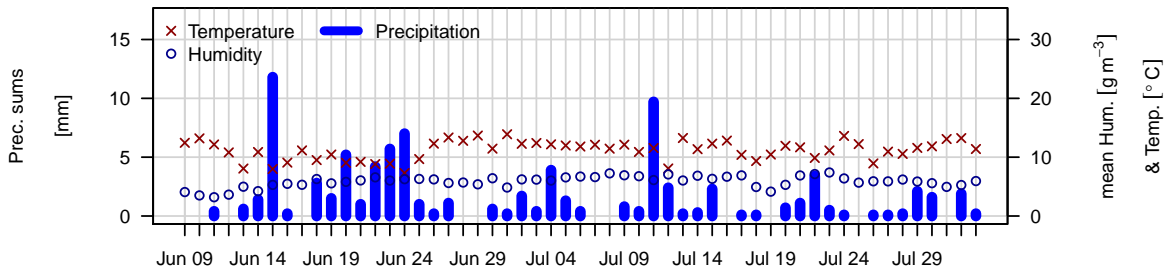


Figure 3.5. Precipitation, Humidity, Temperature. From Ingrisich et al. (2015, Appendix E)

3.2.2. The role of the turf layer for carbon turnover

In order to investigate the importance of the unique turf layer within the *Kobresia pygmaea* pastures it is necessary to couple a $^{13}\text{CO}_2$ pulse labeling experiment with continuous NEE measurements with the eddy covariance method Riederer (2014). This approach provides detailed information about the C turnover within the soil-plant-atmosphere continuum. Based on the knowledge about C dynamics (Figure 3.6) from the EC measurements, the start of the $^{13}\text{CO}_2$ pulse labeling experiment was scheduled on 1st July. Furthermore, the results show no restriction for the $^{13}\text{CO}_2$ pulse labeling experiment from its start till 23th July, and thus a coupling with of both methods was possible.

In general, the distribution of C revealed by the $^{13}\text{CO}_2$ pulse labeling is assumed to be valid for the day of labeling, and therefore extrapolating the results over a longer period needs caution or is not possible at all. Changes in the partitioning patterns over a growing season usually make it impossible to relate a single $^{13}\text{CO}_2$ pulse labeling experiment to the whole growth period (Kuzyakov and Domanski, 2000; Swinnen et al., 1994). However, combining labeling with EC measurements enables us to judge whether C fluxes undergo strong changes within the allocation period. With constant assimilation and respiration, as shown by the EC measurements, and with low variability in the partitioning within this period, the fraction of partitioning from the labeling experiment can be considered to be representative for the whole allocation period.

In the investigated alpine *Kobresia pygmaea* ecosystem, the majority of assimilated C is allocated to belowground pools which have the largest contribution to C turnover within *Kobresia pygmaea* pastures. The results of the $^{13}\text{CO}_2$ pulse labeling experiment show that 93.7 % of recovered ^{13}C after 15 days is either found in belowground pools and in soil CO_2 efflux, as displayed in Figure 3.7. Coupled with the EC fluxes this corresponds to $1.87 \text{ gCm}^{-2} \text{ d}^{-1}$ which is also shown in the same figure. This is more than the 59% reported for a montane *Kobresia humilis* meadow (Wu et al., 2010)

3. Results and Discussion

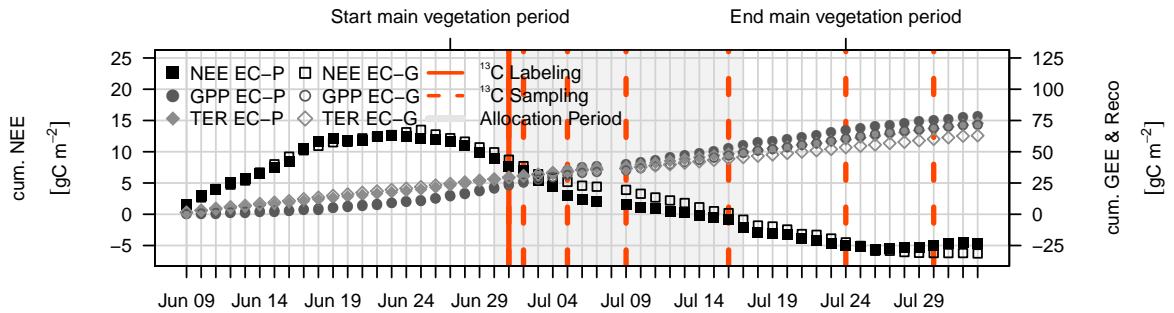


Figure 3.6. Cumulative C fluxes, NEE (squares), GPP (circles) and TER (diamonds) from the 2010 experiment in Kema, for the two EC stations EC-P (solid symbols) and EC-G (hollow symbols). NEE is measured while GPP and TER are partitioned from the NEE with a model. The main dates of the ¹³C labeling experiment are indicated by red lines, the grey shaded area marks the allocation period of 15 days. Modified from Ingrisich et al. (2015, Appendix E).

and the observed 40% for a montane *Kobresia* pasture found by Hafner et al. (2012) and also displayed in Figure 3.7. This emphasizes the importance of belowground C allocation and cycling in these alpine *Kobresia pygmaea* pastures. During the Kema 2010 experiment 23.6% of the ¹³CO₂ allocated belowground was recovered as CO₂ efflux from soil (root exudates and root-derived CO₂), which is well in accordance with values reviewed by Kuzyakov and Domanski (2000). The high incorporation of C in the roots can be related to the very large rooting system maintained by *Kobresia pygmaea*. The high storage of C in roots is also expressed in the root to shoot ratio (R:S) of 90 for the alpine *Kobresia* pasture which is higher than the reported 52 by Fan et al. (2008) and the 35.7 by Yang et al. (2009) for alpine pastures of the TP.

The high ¹³C recovery in roots and the low recovery in SOC is in contrast to the results observed for a montane *Kobresia* meadow in Qinghai by Hafner et al. (2012), who report only minor ¹³C allocation to roots, but very high amounts in the soil organic carbon (SOC) only one day after the labeling. However their ¹³C pulse labeling was conducted later in the growing season. They argue that the rooting system was already developed and assimilates were invested mainly aboveground in vegetative and generative organs and shoot tissue and belowground into root exudation.

It can be stated that the roots within the turf layer acted as the greatest sink for recently assimilated C which is in good agreement with Fan et al. (2008) who found the highest C density in the uppermost centimeter of alpine soils on the QTP. For the allocation period of the ¹³C labeling experiment, which was also the period with the greatest C uptake during the observation period, this sums up to 28 gCm⁻².

3.2. Carbon Fluxes of *Kobresia pygmaea* pastures

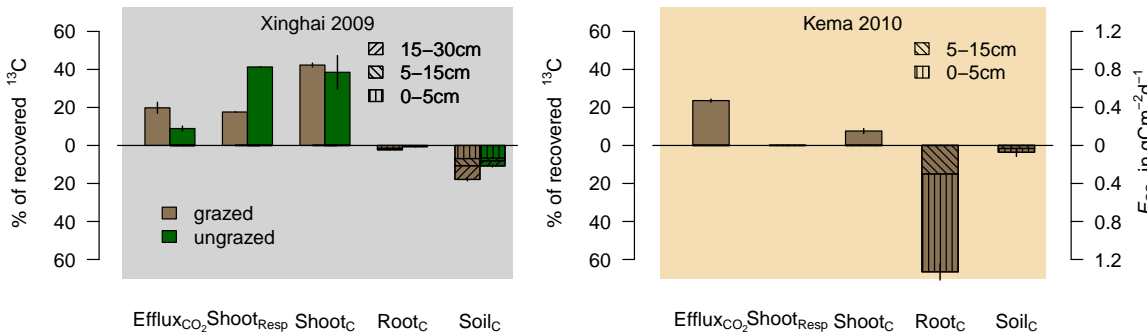


Figure 3.7. ^{13}C partitioning of montane and alpine *Kobresia* pastures determined at the end of a 27- and 15- day allocation period in Xinghai (2009) and Kema (2010), respectively. ^{13}C distribution and C fluxes are shown for CO_2 efflux, shoots and roots and SOC in two depth (0-5, 5-15cm). In Xinghai grazing-induced differences can be seen and therefore the results from two treatments are shown. Since no grazing effects could be observed only pooled results are shown for Kema. The additionally absolute C fluxes shown for Kema were estimated by the coupling of the pulse labeling with eddy-covariance measurements. From Babel et al. (2014, Appendix D)

3.2.3. Effects of grazing cessation

The EC derived NEE measurements from Kema in 2010 were used to test the hypothesis that even within one growing season grazing cessation would affect the C balance of the *Kobresia pygmaea* pastures. However a comparison of the measured NEE fluxes from the two stations, EC-P and EC-G using the geometric mean regression (Dunn, 2004), the method of choice when expecting an error in both time series, shows only a 3% difference (Figure 3.8). The absolute difference between the fluxes measured in the yak grazing enclosure P and the grazed site G throughout the whole period of the experiment in 2010 was only $0.027 \pm 0.028 \mu\text{mol m}^{-2} \text{s}^{-1}$. As this difference in ecosystem scale is not pronounced, it cannot be attributed to any differences in grazing. Existing differences between individual half hour values of the two EC stations are rather related to differences in the distribution of vegetation and bare soil within the actual footprint of these flux estimates or free convection events which are not captured with the EC measurements. As these differences in the short timescale propagate also through the cumulative and mean daily fluxes, it explains the small divergence within the dynamics of the fluxes from the two sites (Figure 3.6). This result is not surprising due to the short grazing enclosure time in Kema.

As no difference were noticeable at the ecosystem scale, a closer look into the plant-soil-atmosphere continuum is necessary. The $^{13}\text{CO}_2$ pulse labeling results from the montane pastures in Xinghai (Hafner et al., 2012, Figure 3.7) showed that a smaller amount of C is allocated to belowground pools in pastures where grazing was excluded

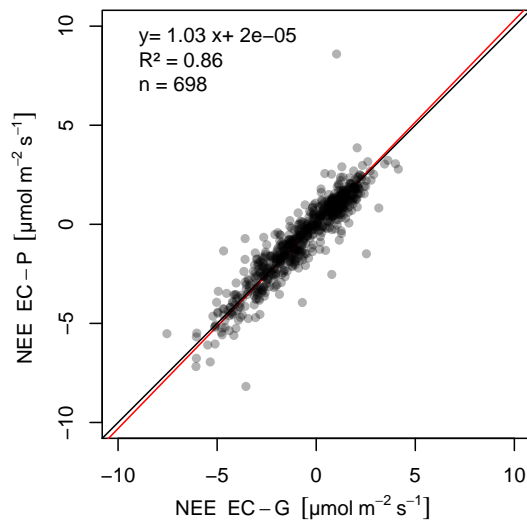


Figure 3.8. Comparison of eddy covariance NEE measurements from EC-G and EC-P at Kema. Geometric mean regression calculated after Dunn (2004).

for 7 years and vegetation had changed from Cyperaceae to Poaceae dominance. The $^{13}\text{CO}_2$ pulse labeling in the alpine pastures in Kema, however, did not show that grazing cessation caused such a reduction in the belowground pools, though a slightly higher amount of ^{13}C was recovered in aboveground biomass in P relative to G. The greatest effect was found within plots which additionally excluded small mammals as well.

3.2.4. Influence of degradation on C fluxes

The chamber-based C flux measurements during the Kema 2012 experiment over the three defined degradation classes IM, DM and BS show large differences especially in NEE (Figure 3.9). Ecosystem respiration (Reco) also differs from class to class but only the values over BS show a great difference as values are about half of the values found over IM and DM. However a direct comparison of the different degradation classes is not possible, due to the consecutive measurements and changing meteorological parameters and a proceeding of the growing season. The changing meteorological conditions are visible in the vapour pressure deficit (VPD) which decreases rapidly as soon as moisture is available after rainfall. Since continuous EC measurements as in the case of the pulse labeling in 2010 were not available, the SVAT-CN model was utilized to provide continuous time series for each degradation class for direct comparison. The model output was validated against the measured fluxes with the chambers for 2012 and the EC measurements in 2010. The mean simulated C fluxes with SVAT-CN for the whole vegetation growing period 2012 show once more the importance of an intact

3.2. Carbon Fluxes of *Kobresia pygmaea* pastures

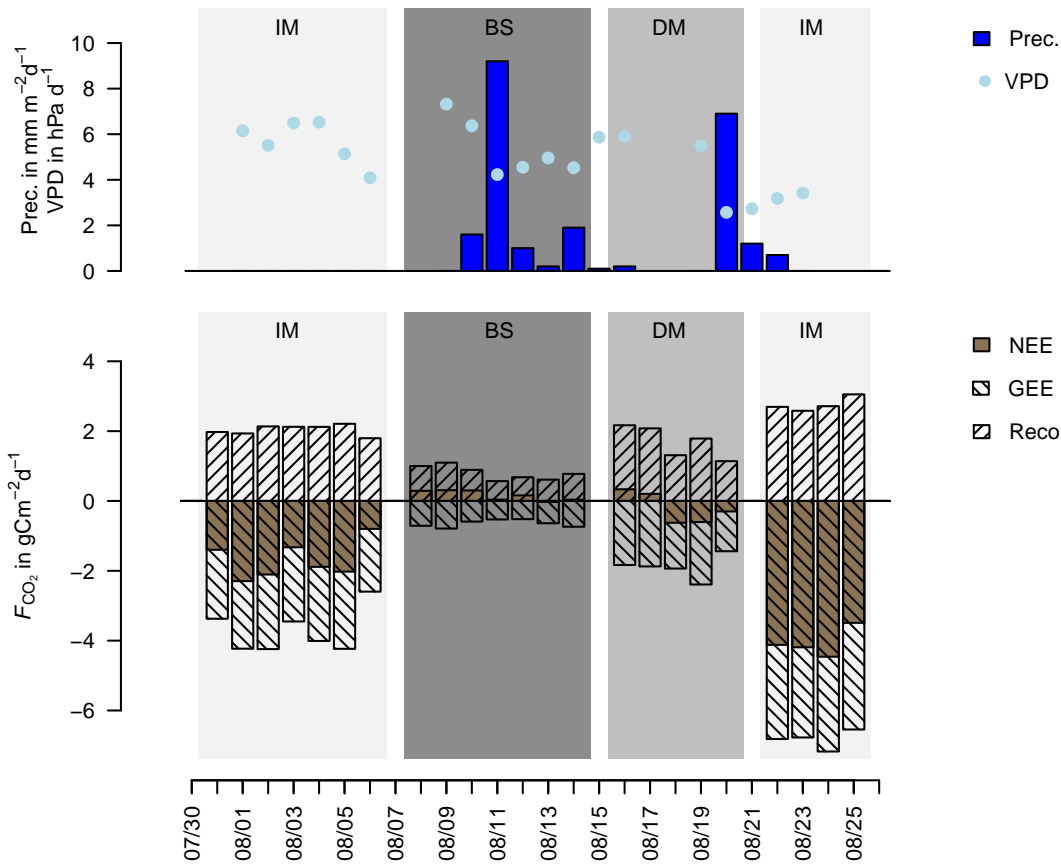


Figure 3.9. C fluxes of the three degradation classes IM, DM and BS. NEE (brown) and Reco (hashed upward) measured with a LiCOR Chamber, GEE (hashed downward) is estimated as the difference from these two fluxes. Measurements were conducted consecutively with the same chambers: IM (31.07. - 06.08.), BS (08.08. - 14.08.), DM (16.08. - 20.08.), IM (22.08. - 25.08.). The upper panel shows precipitation (dark blue) and the vapour pressure deficit (VPD, light blue). Modified after Leonbacher (2013).

Kobresia pygmaea with its turf layer for the C balance of this ecosystem (Figure 3.10). Respiration over IM and DM are nearly equal while the C uptake over IM is more than double that of DM. IM acts as a C sink while DM and BS show no noticeable NEE.

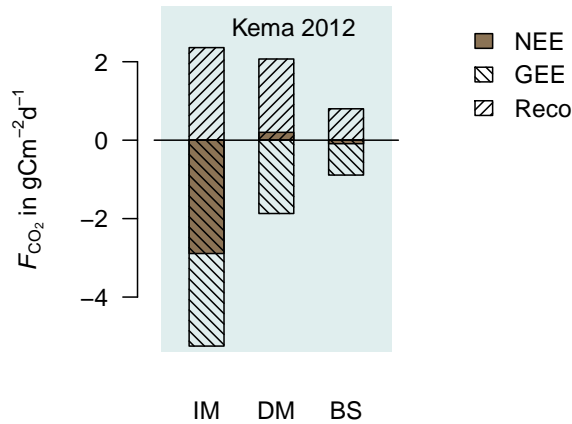


Figure 3.10. Mean simulated C fluxes for a 46-day period in 2012 for the three degradation classes IM,DM and BS. NEE(brown), GEE (hashed downward) and Reco(hashed upward).From Babel et al. (2014, Appendix D)

3.3. Linking flux measurements and land surface modeling to estimate regional features

Since most *in situ* measurements are limited to a comparably small spatial scale it is often necessary to utilize simulations in order to link the knowledge gained from the observations to a broader scale. In this section, three cases of linking models and measurements are described. The first case study describes linking the EC measurements from Nam Co experiment in 2009 to the models SEWAB and HM to investigate turbulent fluxes over an alpine steppe, influenced by different soil moistures, as well as over a lake surface (Biermann et al., 2014a, Appendix B). Besides estimating fluxes for a direct comparison this approach enabled to explicitly resolve fluxes over certain land surface types, a prerequisite for the second case study, which shows how an *in situ* observed lake-breeze during the experiment in 2009 at Nam Co was reproduced with the ATHAM model (Gerken et al., 2014, Appendix C). Using *in situ* parameters and measurements from the field campaigns as input and for validation of models, as shown in Gerken et al. (2012) and Biermann et al. (2014a, Appendix B), enabled than the use of SEWAB and ATHAM in a third study to investigate the influence of degradation on C fluxes, evapotranspiration and eventually convection and circulation on the TP (Babel et al., 2014, Appendix D). In this study the SVAT-CN model was utilized, in addition to the models mentioned above, to model CO₂ exchange.

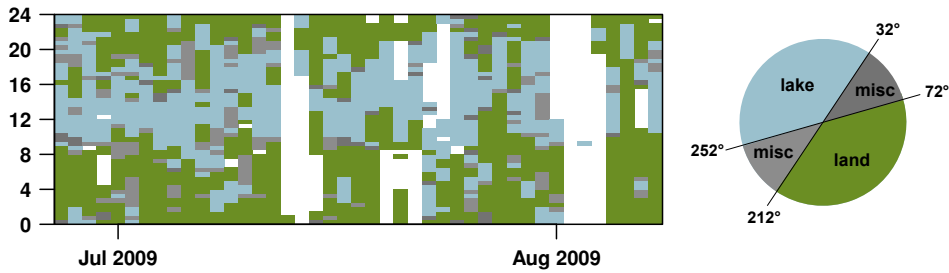


Figure 3.11. Diurnal distribution of the wind direction for for the Nam Co 2009 experiment and corresponding land cover in the upwind direction, classified according to the sectors shown on the right. From Biermann et al. (2014a, Appendix B)

3.3.1. Lake fluxes and influence of the soil moisture

It is well known that heterogeneous surfaces affect landscape-scale fluxes. The measurements presented above (Section 3.1.1) have shown that the fluxes over land and lake surfaces behave differently, as do the fluxes over wet and dry alpine steppe. Within the Nam Co 2009 experiment turbulent fluxes were observed with two stations. While the EC station NamITP always measured fluxes over land surface grass^- , the measurements of Nam UBT originated from different surface types. Within the footprint of this station the surfaces grass^+ , grass^- and lake could be found, with a strong diurnal variation within contribution of the underlying surfaces to the measured flux due to a land – lake circulation system (Figure 3.11). During midday wind was coming predominantly from the direction of the lake while in the morning, evening and night-time hours wind from the land surface dominated. Therefore NamUBT provided flux measurements over the land and water surface only for certain periods of the day. The land surface furthermore was made up of grass^+ and grass^- . However, as the influence of grass^- was comparatively small during neutral and unstable stratification and only larger during stable conditions which occur mostly at night, when flux differences between the two surface types were small, the influence can be regarded as negligible. Therefore it is reasonable to relate the observations and parameter over the land surface at NamUBT to the wetter grass^+ surface and to discriminate between grass^+ at NamUBT, grass^- at NamITP and the lake only. Although it was possible to attribute the measured fluxes to the a specific surface type due to the footprint analyzes a direct comparison of the fluxes was nearly impossible since the strict pattern of the lake breeze was causing gaps in one or the other time series at NamUBT. In order to fill the gaps and to complete the flux time series for grass^+ and lake a model was applied for each surface type and validated with the existing data. The model SEWAB was used in the case of the land surfaces and the model HM in the case of the lake surface (model descriptions: Chapter 2.2.5).

The validation of the model was done by attributing measured fluxes to a single surface type with footprint modeling, a tool that relates measurements to specific sur-

faces. For each time step, the footprint approach provides the relative contribution of all involved surfaces to the measured fluxes. Fluxes can therefore be selected to their underlying surface. Obviously the investigated surface types have differences in characteristics, especially the land and the lake surface. It is therefore not surprising to see this reflected in the observation-based simulated mean fluxes for the whole period (Figure 3.12). The close combination of turbulent flux observations and land surface modeling could show that the mean latent heat flux became more dominant with increasing soil moisture for the land surfaces, showing a mean differences in latent heat flux between grass^+ and grass^- of -33.5 W m^{-2} . The evaporation over the small lake is even higher, due to its shallow water table resulting in comparatively high surface temperatures, the resulting difference between grass^+ and lake is -27.3 W m^{-2} . The difference in sensible heat flux between the surfaces is smaller with 24.0 W m^{-2} .

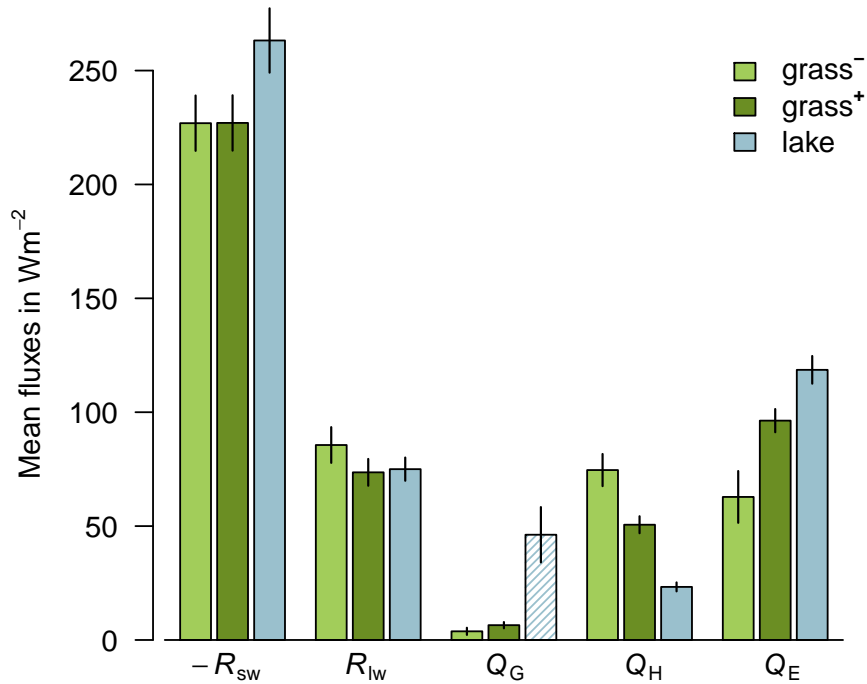


Figure 3.12. Mean fluxes for the three surface types (grass^- , grass^+ , lake) from observation-based simulations. (Land surfaces: SEWAB, Lake: HM). Net shortwave radiation (R_{sw}) and net longwave radiation (R_{lw}) for the lake surface are calculated as explained in Fig. 3.1. For land surface fluxes, Q_g represents the ground heat flux. For the lake energy balance it sums up the energy fluxes not accounted for, e.g. storage change in the water body and flux into the sediment. Error bars indicate 1.96 times the standard error of the mean, based on daily mean fluxes; assuming normal distribution and statistical independence of daily mean fluxes, the bars would correspond to the 95 % confidence interval. From Biermann et al. (2014a, Appendix B).

3.3. Linking flux measurements and land surface modeling to estimate regional features

difference between grass⁺ and grass⁻ and 22.3 W m⁻² difference between grass⁺ and lake.

Using foot analysis to resolve relative contribution of the involved surfaces, gives a great advantage when observations originate from more than one land use type. This enables simulations to be connected to the observations by calculating a weighted mean from the model output according to the actual land cover contribution, as is shown with the footprint integrated simulations for lake and grass⁺ together with the EC observations at NamUBT in Figure 3.13 for 17th July. For all wind directions the eddy-covariance measurements can be closely modeled by the footprint integrated simulation. This also holds for measurements with contributions from both surfaces,

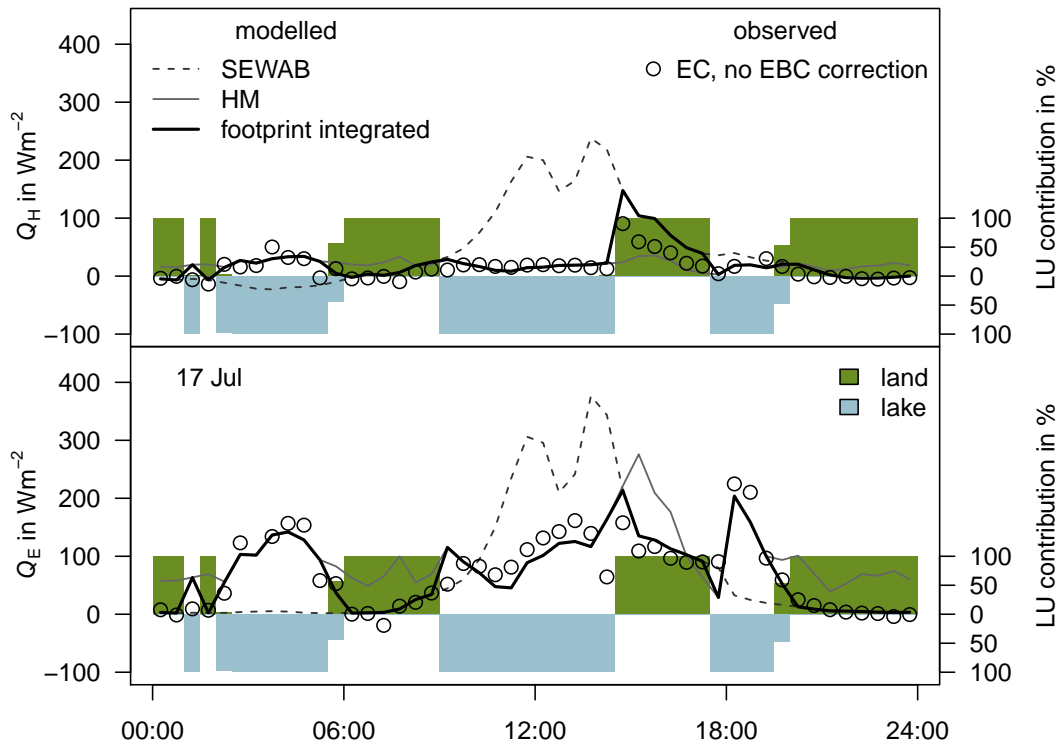


Figure 3.13. Source weight integrated modeled fluxes at NamUBT exemplarily shown on 17th July. Displayed are simulated fluxes with SEWAB (dashed line) and HM (solid grey line) and integrated simulations (solid black line) according to contributions of lake or land within the footprint. Observations (not energy balance corrected) are shown as black circles. The land use contribution in % is indicated by bar plot, with upwind situations from the land in green and upwind situations from the lake in blue. The time axis is displayed in Beijing standard time (CST), and mean local solar noon during the observation period is at 1400 CST. Modified after Biermann et al. (2014a, Appendix B).

seen in some events on this selected day. As this approach enables to resolve fluxes explicitly to the underlying surface it improves the possibility to use these fluxes to validate model output of special circulation patterns, compared to a tile approach which would resolve fluxes originating from different surfaces according to their percentage of occurrence within a grid cell.

3.3.2. Coupling flux measurements to the ATHAM model

In order to estimate the feedback of surface fluxes and mesoscale circulations Gerken et al. (2012) adapted the Hybrid model to the TP by an inter-comparison of the model output with *in situ* eddy-covariance flux measurements and also the above mentioned SWEAB model (Subsection 3.3.1). Hybrid was then coupled to the ATHAM model (Subsection 2.2.5) for further studies on local circulations and convection. Such as the land – lake circulation system, with strong diurnal pattern in wind direction, was observed at Nam Co during the 2009 experiment (Figure 3.11). Gerken et al. (2014, Appendix C) aimed to reproduce the development of this lake breeze and furthermore to investigate how this lake breeze would effect development of convection within the Nam Co Basin. This 2D model approach showed that the lake breeze can be modeled reasonably. Additionally the study showed the interaction between the lake breeze and convection triggering, identifying two different mechanisms. These are a triggering of convection over topography in situations when the background wind and the lake breeze have the same flow direction and a triggering caused by convergence between the lake-breeze front and the background wind.

3.3.3. Influence of degradation on energy and C fluxes

In order to estimate the effect of degradation on an ecosystem scale on the TP it was necessary to utilize models to extend the gained knowledge from the measurements of water and carbon fluxes on the defined surface classes, intact *Kobresia* root mat (IM), degraded root mat (DM), bare soil (BS) and alpine Steppe (AS). IM, DM and BS are seen as degradation stages within a *Kobresia pygmaea* pasture and AS represents the second main type of vegetation cover on the TP. As reference site for the *Kobresia pygmaea* Kema was picked while Nam Co represents AS. within Babel et al. (2014, Appendix D) following 1D Soil - vegetation - atmosphere transfer models were adapted to the TP to examine, (i) evapotranspiration: SEWAB (ii) carbon fluxes: SVAT-CN (iii) surface feedbacks: Hybrid model and ATHAM (Subsection 2.2.5 and Babel et al. (2014, Appendix D)). Adaptation of the models to the special conditions of the TP was done through implementation of *in situ* measured parameter. The model output was validated with *in situ* measurements. Modeled results for IM, DM and BS were compared to the chamber measurements from 2012 and EC measurements from 2010 at Kema and for AS at Nam Co in the case of C fluxes and against the EC measurements only in case of evapotranspiration.

3.3. Linking flux measurements and land surface modeling to estimate regional features

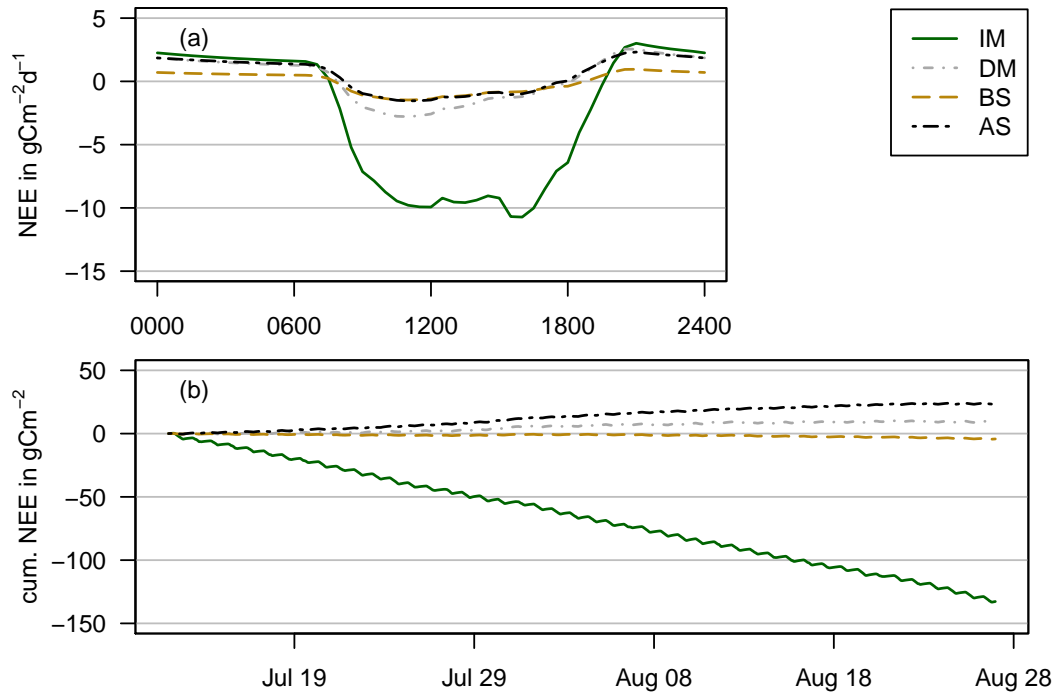


Figure 3.14. Modeled carbon fluxes of the three degradation stages IM, DM and BS, displayed as mean daily cycle and as cumulative curve for the vegetation growing period. From Babel et al. (2014, Appendix D)

While total evapotranspiration of the different degradation stages did not differ much, although the ratio of evaporation and transpiration changed, C fluxes are strongly affected (Figure 3.14). The strong difference in NEE between IM and all other stages can be seen in the modeled mean daily cycle as well as in the cumulative budget of the modeled values for the vegetation period in July and August 2012. While IM represents a C sink and BS behaves neutral it is interesting to note that DM and also AS represent a C source over the defined vegetation period.

Although evapotranspiration was not altered significantly the above mentioned change in the ratio of evaporation and transpiration had an effect in the simulations by the ATHAM model over different vegetation fractions. The model was run for a wet and dry scenario with 25% and 75% vegetation cover. In both scenarios the lower vegetation cover would result in more convection and higher cloud cover at an earlier stage of the day. This leads to reduced surface temperatures and consequently lower surface fluxes.

4. Conclusions

The integration of turbulent fluxes estimated with the eddy-covariance method within ecological and hydrological studies on the Tibetan Plateau showed that these fluxes can serve as a useful and necessary tool to bridge different spatial scales. An important aspect when either differences in surface properties only occur on a small scale or in process-oriented experiments need to be extrapolated to the whole ecosystem.

Furthermore this thesis showed that an estimation of latent heat flux on the TP with the standard setup of a eddy-covariance complex with a LI-7500 for the measurements of latent heat flux is suitable also for harsh winter conditions, which is of great importance for long-term observations. However side-by-side measurements of a LI-7500 and a KH20 revealed a flux difference between these two different sensor types. Although this difference can be regarded as acceptable, it shows that a careful calibration of the devices is necessary, and special arrangements for the winter months are needed to assure accurate flux estimations. In addition the campaign showed that an estimation of absolute humidity concentrations is not possible with both sensors.

The 2009 measurements at Nam Co, over wet grassland and for the first time on the TP also over a shallow lake, showed that it is possible to measure turbulent fluxes accurately over different surfaces on the TP by using only a single eddy-covariance complex. This is of great importance in areas where access is limited but heterogeneity and different surfaces need to be still taken into account. Further it can be concluded that theoretical requirements for eddy-covariance are not substantially violated on the TP and even complex topography, as found along the shoreline of a lake, has no negative effect on the quality of the flux estimates when a careful coordinate rotation is performed with a sector-wise application of the planar-fit method. The study furthermore showed that by combing measurements, selected for the target surface lake by footprint analysis, with a suitable model the challenging task of conducting eddy-covariance measurements over lake surfaces and the adjacent land surface can be realized on the TP. It was shown that the for this purpose utilized HM model a HM model is able to estimate lake evaporation at a high standard of quality and temporal resolution, even resolving the diurnal course so that gap-free time series can be derived. As this method offers the possibility to directly measure evaporation over lake surfaces on the TP, this will be a great advantage for the estimation of water budgets in hydrological studies.

When a larger spatial scale is of interest, as in remote sensing applications or modeling studies, it needs to be considered that a comparison of turbulent fluxes from the three dominant land cover types found in the Nam Co basin, moist and dry grassland and the lake, revealed sharp differences in characteristics of these fluxes. A single flux

4. Conclusions

station with only one surface type within the footprint might therefore not be representative for a grid cell. Since it could be shown that for spatial integration the tile approach is valid it is recommended to account for these differences when using eddy-covariance derived fluxes for the validation. This can be done by using model derived simulations of adjacent surfaces and upscale these according to the fraction of surfaces within the grid cell. On the other hand it is also possible to derive fluxes on an explicit spatial and temporal scale to special model applications, considering the specific characteristics of the underlying surface and therefore improving the link between the model and conditions found at a measurement site.

Overall, the high alpine *Kobresia pygmaea* pasture acted as a weak sink for C over the two-month observation period in 2010 at Kema. It could be shown that a short-term response to grazing cessation was only visible within the C stocks of the aboveground plant biomass while recent C fluxes did not show any response. The study showed that the living roots of the turf layer represent the most active part in terms of C cycling of the *Kobresia pygmaea* pasture and the turf layer is the main ecosystem compartment for the turnover of recent assimilates. The root turf plays a key role for the overall C cycling, C storage and function of the *Kobresia pygmaea* ecosystem. The coupling of the two commonly used methods, pulse labeling and EC, represents a new and more powerful approach to the understanding of C cycling in the plant-soil-atmosphere system compared to singular plot- or ecosystem scale approaches. It proved to be helpful for estimating absolute C fluxes in various pools of the *Kobresia pygmaea* pastures and for identifying C dynamics at various spatial scales. The C stocks in the soil and the entire ecosystem need to be regarded as very vulnerable to environmental and anthropogenic factors destroying this characteristic *Kobresia* root turf. Destruction of this layer, caused by overgrazing-induced degradation as well as a change in vegetation and supersession of *Kobresia pygmaea* through long-term cessation of grazing, will consequently lead to a great release of CO₂ to the atmosphere. This could be shown in an estimation of a degradation effect on C and water fluxes in the Tibetan highlands. Comparing C fluxes of a typical *Kobresia pygmaea* pasture with the frequently found degradation stages of a decaying root turf and the so called black beaches which resemble mainly bare soil shows a strong reduction in C uptake. Therefore, degradation of the turf significantly limits the function of *Kobresia* pastures as a carbon sink. Furthermore a change in vegetation structure from Cyperaceae to Poaceae has a great influence on the ratio of belowground to aboveground allocation of C as shown in Xingahi. Furthermore this is also visible in the comparison of the simulated C fluxes for alpine steppe and *Kobresia pygmaea* pastures. In terms of the hydrological cycle, degradation did not show a large affect on the magnitude of the evapotranspiration but on the variability and ratio of evaporation to transpiration. This fact, coupled with a change in surface temperature, leads to a change in convection development as shown as shown with the ATHAM simulations comparing different fractions of vegetation cover. Due to the size of the grassland and the high percentage of area which shows strong signs of degradation, these just described changes might

even show an effect at greater, possibly global, scale.

References

- Agam, N., Berliner, P. R., Zangvil, A., and Ben-Dor, E.: Soil water evaporation during the dry season in an arid zone, *J Geophys Res*, 109, D16 103, 2004.
- Aubinet, M., Vesala, T., and Papale, D., eds.: *Eddy Covariance: A Practical Guide to Measurement and Data Analysis*, Springer, Dordrecht, 2012.
- Babel, W., Biermann, T., Coners, H., Falge, E., Seeber, E., Ingrisch, J., Schleuß, P.-M., Gerken, T., Leonbacher, J., Leipold, T., Willinghöfer, S., Schützenmeister, K., Shibistova, O., Becker, L., Hafner, S., Spielvogel, S., Li, X., Xu, X., Sun, Y., Zhang, L., Yang, Y., Ma, Y., Wesche, K., Graf, H.-F., Leuschner, C., Guggenberger, G., Kuzyakov, Y., Miehe, G., and Foken, T.: Pasture degradation modifies the water and carbon cycles of the Tibetan highlands, *Biogeosciences*, 11, 6633–6656, doi:10.5194/bg-11-6633-2014, 2014.
- Baldocchi, D.: Assessing the eddy covariance technique for evaluating carbon dioxide exchange rates of ecosystems: past, present and future, *Global Change Biol*, 9, 479–492, doi:10.1046/j.1365-2486.2003.00629.x, 2003.
- Balsamo, G., Boussetta, S., Dutra, E., Beljaars, A., Viterbo, P., and van den Hurk, B.: Evolution of land surface processes in the IFS, *ECMWF Newsletter*, 127, 17–22, 2011.
- Ben-Gal, A. and Shani, U.: A highly conductive drainage extension to control the lower boundary condition of lysimeters, *Plant and Soil*, 239, 9–17, doi:10.1023/A:1014942024573, 2002.
- Beyrich, F., Leps, J.-P., Mauder, M., Bange, J., Foken, T., Huneke, S., Lohse, H., Lüdi, A., Meijninger, W. M. L., Mironov, D., Weisensee, U., and Zittel, P.: Area-Averaged Surface Fluxes Over the Litfass Region Based on Eddy-Covariance Measurements, *Bound-Lay Meteorol*, 121, 33–65, doi:10.1007/s10546-006-9052-x, 2006.
- Biermann, T., Babel, W., Olesch, J., and Foken, T.: Mesoscale Circulations and Energy and Gas Exchange Over the Tibetan Plateau Documentation of the Micrometeorological Experiment, Nam Tso, Tibet, *Arbeitsergebn, Univ Bayreuth, Abt Mikrometeorol*, ISSN 1614-89166, 41, 41, 38, <https://epub.uni-bayreuth.de/450/>, 2009.

- Biermann, T., Leipold, T., Babel, W., Becker, L., Coners, H., Foken, T., Guggenberger, G., He, S., Ingrisch, J., Kuzyakov, Y., Leuschner, C., Miehe, G., Richards, K., Seeber, E., and Wesche, K.: Tibet Plateau Atmosphere-Ecology-Glaciology Cluster Joint Kobresia Ecosystem Experiment: Documentation of the first Intensive Observation Period Summer 2010 in Kema, Tibet, Arbeitsergebn, Univ Bayreuth, Abt Mikrometeorol, ISSN 1614-89166, 44, 44, 107, <https://epub.uni-bayreuth.de/356/>, 2011.
- Biermann, T., Seeber, E., Schleuß, P., Willinghöfer, S., Leonbacher, J., Schützenmeister, K., Steingraber, L., Babel, W., Coners, H., Foken, T., Guggenberger, G., Kuzyakov, Y., Leuschner, C., Miehe, G., and Wesche, K.: Tibet Plateau Atmosphere-Ecology-Glaciology Cluster Joint Kobresia Ecosystem Experiment: Documentation of the second Intensive Observation Period, Summer 2012 in KEMA, Tibet, Arbeitsergebn, Univ Bayreuth, Abt Mikrometeorol, ISSN 1614-89166, 54, 54, 54, <https://epub.uni-bayreuth.de/145/>, 2013.
- Biermann, T., Babel, W., Ma, W., Chen, X., Thiem, E., Ma, Y., and Foken, T.: Turbulent flux observations and modelling over a shallow lake and a wet grassland in the Nam Co basin, Tibetan Plateau, *Theor Appl Climatol*, 116, 301–316, doi:10.1007/s00704-013-0953-6, 2014a.
- Biermann, T., Pfab, D., Babel, W., Li, M., Wang, B., Ma, Y., and Foken, T.: Note: Measurements of latent heat flux and humidity on the Tibetan Plateau, submitted to *Atmos Meas Tech Discuss*, 2014b.
- Boos, W. R. and Kuang, Z.: Dominant control of the South Asian monsoon by orographic insulation versus plateau heating, *Nature*, 463, 218–222, doi:10.1038/nature08707, 2010.
- Brötz, B., Eigenmann, R., Dörnbrack, A., Foken, T., and Wirth, V.: Early-Morning Flow Transition in a Valley in Low-Mountain Terrain Under Clear-Sky Conditions, *Bound-Lay Meteorol*, 152, 45–63, doi:10.1007/s10546-014-9921-7, 2014.
- Cao, G.-M., Tang, Y., Mo, W. H., Wang, Y. A., Li, Y. N., and Zhao, X.: Grazing intensity alters soil respiration in an alpine meadow on the Tibetan plateau, *Soil Biol and Biochem*, 36, 237–243, doi:10.1016/j.soilbio.2003.09.010, 2004.
- Carbone, M. S. and Trumbore, S. E.: Contribution of new photosynthetic assimilates to respiration by perennial grasses and shrubs: residence times and allocation patterns, *New Phytol*, 176, 124–135, doi:10.1111/j.1469-8137.2007.02153.x, 2007.
- Charuchittipan, D., Babel, W., Mauder, M., Beyrich, F., Leps, J.-P., and Foken, T.: Extension of the averaging time of eddy-covariance measurements and its effect on the energy balance closure, *Bound-Lay Meteorol*, p. in print, doi:10.1007/s10546-014-9922-6, 2014.

- Chen, H., Zhu, Q., Peng, C., Wu, N., Wang, Y., Fang, X., Gao, Y., Zhu, D., Yang, G., Tian, J., Kang, X., Piao, S., Ouyang, H., Xiang, W., Luo, Z., Jiang, H., Song, X., Zhang, Y., Yu, G., Zhao, X., Gong, P., Yao, T., and Wu, J.: The impacts of climate change and human activities on biogeochemical cycles on the Qinghai-Tibetan Plateau, *Global Change Biol*, 19, 2940–2955, doi:10.1111/gcb.12277, 2013.
- Cui, X. and Graf, H.-F.: Recent land cover changes on the Tibetan Plateau: a review, *Climatic Change*, 94, 47–61, doi:10.1007/s10584-009-9556-8, 2009.
- Cui, X., Graf, H.-F., Langmann, B., Chen, W., and Huang, R.: Climate impacts of anthropogenic land use changes on the Tibetan Plateau, *Global Planet Change*, 54, 33–56, doi:10.1016/j.gloplacha.2005.07.006, 2006.
- Davidson, G., Behnkde, R., and Kerven C.: Implications of Rangeland Enclosure Policy on the Tibetan Plateau, *IDHP Update*, pp. 59–62, 2008.
- Desai, A. R., Richardson, A. D., Moffat, A. M., Kattge, J., Hollinger, D. Y., Barr, A. G., Falge, E., Noormets, A., Papale, D., Reichstein, M., and Stauch, V. J.: Cross-site evaluation of eddy covariance GPP and RE decomposition techniques, *Agr Forest Meteorol*, 148, 821–838, doi:10.1016/j.agrformet.2007.11.012, 2008.
- Du, M., Kawashima, S., Yonemura, S., Zhang, X., and Chen, S.: Mutual influence between human activities and climate change in the Tibetan Plateau during recent years, *Human Dim Natural Proc Environ Change*, 41, 241–249, doi:10.1016/j.gloplacha.2004.01.010, 2004.
- Dunn, G.: Statistical evaluation of measurement errors, *Design and analysis of reliability studies*, Arnold, London, 2 edn., 2004.
- Falge, E., Baldocchi, D., Olson, R., Anthoni, P., Aubinet, M., Bernhofer, C., Burba, G., Ceulemans, R., Clement, R., Dolman, H., Granier, A., Gross, P., Grünwald, T., Hollinger, D. Y., Jensen, N.-O., Katul, G., Keronen, P., Kowalski, A., Lai, C. T., Law, B. E., Meyers, T., Moncrieff, J., Moors, E., Munger, J. W., Pilegaard, K., Rannik, I., Rebmann, C., Suyker, A., Tenhunen, J., Tu, K., Verma, S., Vesala, T., Wilson, K., and Wofsy, S.: Gap filling strategies for defensible annual sums of net ecosystem exchange, *Agr Forest Meteorol*, 107, 43–69, doi:10.1016/S0168-1923(00)00225-2, 2001.
- Falge, E., Baldocchi, D., Tenhunen, J., Aubinet, M., Bakwin, P., Bernhofer, C., Burba, G., Clement, R., Davis, K. J., Elbers, J. A., Goldstein, A. H., Grelle, A., Granier, A., Guðmundsson, J., Hollinger, D. Y., Kowalski, A. S., Katul, G., Law, B. E., Malhi, Y., Meyers, T., Monson, R. K., Munger, J. W., Oechel, W., Paw U, K. T., Pilegaard, K., Rannik, I., Rebmann, C., Suyker, A., Valentini, R., Wilson, K., and Wofsy, S.: Seasonality of ecosystem respiration and gross primary

References

- production as derived from FLUXNET measurements, *Agr Forest Meteorol*, 113, 53–74, doi:10.1016/S0168-1923(02)00102-8, 2002.
- Falge, E., Reth, S., Brüggemann, N., Butterbach-Bahl, K., Goldberg, V., Oltchev, A., Schaaf, S., Spindler, G., Stiller, B., Queck, R., Köstner, B., and Bernhofer, C.: Comparison of surface energy exchange models with eddy flux data in forest and grassland ecosystems of Germany, *Ecol Model*, 188, 174–216, doi:10.1016/j.ecolmodel.2005.01.057, 2005.
- Fan, J., Zhong, H., Harris, W., Yu, G., Wang, S., Hu, Z., and Yue, Y.: Carbon storage in the grasslands of China based on field measurements of above- and below-ground biomass, *Climatic Change*, 86, 375–396, doi:10.1007/s10584-007-9316-6, 2008.
- Fang, J., Tang, Y., and Son, Y.: Why are East Asian ecosystems important for carbon cycle research?, *Sci China Life Sci*, 53, 753–756, doi:10.1007/s11427-010-4032-2, 2010.
- Finnigan, J., Clement, R., Malhi, Y., Leuning, R., and Cleugh, H.: A Re-Evaluation of Long-Term Flux Measurement Techniques Part I: Averaging and Coordinate Rotation, *Bound-Lay Meteorol*, 107, 1–48, doi:10.1023/A:1021554900225, 2003.
- Foggin, J. M.: Depopulating the Tibetan Grasslands, *Mt Res Dev*, 28, 26–31, doi:10.1659/mrd.0972, 2008.
- Foken, T.: Vorschlag eines verbesserten Energieaustauschmodells mit Berücksichtigung der molekularen Grenzschicht der Atmosphäre, *Z Meteorol*, 29, 32–39, 1979.
- Foken, T.: The parameterisation of the energy exchange across the air-sea interface, *Dynam Atmos Oceans*, 8, 297–305, doi:10.1016/0377-0265(84)90014-9, 1984.
- Foken, T.: An operational model of the energy exchange across the air-sea interface, *Z Meteorol*, 36, 345–359, 1986.
- Foken, T.: *Micrometeorology*, Springer, Berlin, 2008a.
- Foken, T.: The Energy Balance Closure Problem: An Overview, *Ecol Appl*, 18, 1351–1367, doi:10.2307/40062260, 2008b.
- Foken, T. and Wichura, B.: Tools for quality assessment of surface-based flux measurements, *Agr Forest Meteorol*, 78, 83–105, doi:10.1016/0168-1923(95)02248-1, 1996.
- Foken, T., Göckede, M., Mauder, M., Mahrt, L., Amiro, B., and Munger, J.: Post-field data quality control, in: *Handbook of Micrometeorology: A Guide for Surface Flux Measurement and Analysis*, edited by Lee, X., Massman, W. J., and Law, B., vol. 29 of *Atmospheric and Oceanographic Sciences Library*, pp. 181–208, Kluwer Academic Publishers, Dordrecht, doi:10.1007/1-4020-2265-4_9, 2004.

- Foken, T., Mauder, M., Liebethal, C., Wimmer, F., Beyrich, F., Leps, J.-P., Raasch, S., DeBruin, H. A. R., Meijninger, W. M. L., and Bange, J.: Energy balance closure for the LITFASS-2003 experiment, *Theor Appl Climatol*, 101, 149–160, doi:10.1007/s00704-009-0216-8, 2010.
- Foken, T., Aubinet, M., Finnigan, J. J., Leclerc, M. Y., Mauder, M., and Paw U, K. T.: Results Of A Panel Discussion About The Energy Balance Closure Correction For Trace Gases, *Bull Amer Meteor Soc*, 92, ES13–ES18, doi:10.1175/2011BAMS3130.1, 2011.
- Foken, T., Leuning, R., Oncley, S. P., Mauder, M., and Aubinet, M.: Corrections and data quality, in: *Eddy Covariance: A Practical Guide to Measurement and Data Analysis*, edited by Aubinet, M., Vesala, T., and Papale, D., pp. 85–131, Springer, Dordrecht, Heidelberg, London, New York, 2012.
- Frauenfeld, O. W., Zhang, T., and Serreze, M. C.: Climate change and variability using European Centre for Medium-Range Weather Forecasts reanalysis (ERA-40) temperatures on the Tibetan Plateau, *J Geophys Res*, 110, D02101, doi:10.1029/2004JD005230, 2005.
- Friend, A. and Kiang, N.: Land surface model development for the GISS GCM, *J Climate*, 18, 2883–2902, 2005.
- Friend, A. D., Stevens, Knox, R. G., and Cannell, M. G. R.: A process-based, terrestrial biosphere model of ecosystem dynamics (Hybrid v3.0), *Ecol Model*, 95, 249–287, 1997.
- Fu, G., Zhang, Y.-J., Zhang, X.-Z., Shi, P.-L., Zhou, Y.-T., Li, Y.-L., and Shen, Z.-X.: Response of ecosystem respiration to experimental warming and clipping in Tibetan alpine meadow at three elevations, *Biogeosciences Discuss*, 10, 13 015–13 047, doi:10.5194/bgd-10-13015-2013, 2013.
- Fu, Y., Zheng, Z., Yu, G., Hu, Z., Sun, X., Shi, P., Wang, Y., and Zhao, X.: Environmental influences on carbon dioxide fluxes over three grassland ecosystems in China, *Biogeosciences*, 6, 2879–2893, doi:10.5194/bg-6-2879-2009, 2009.
- Gao, Y. L. P., Wu, N., Chen, H., and Wang, G.: Grazing Intensity Impacts on Carbon Sequestration in an Alpine Meadow on the Eastern Tibetan Plateau, *Res J Agr Biol Sc*, pp. 642–647, 2007.
- Göckede, M., Markkanen, T., Hasager, C., and Foken, T.: Update of a Footprint-Based Approach for the Characterisation of Complex Measurement Sites, *Bound-Lay Meteorol*, 118, 635–655, doi:10.1007/s10546-005-6435-3, 2006.

References

- Göckede, M., Foken, T., Aubinet, M., Aurela, M., Banza, J., Bernhofer, C., Bonnefond, J. M., Brunet, Y., Carrara, A., Clement, R., Dellwik, E., Elbers, J., Eugster, W., Fuhrer, J., Granier, A., Grünwald, T., Heinesch, B., Janssens, I. A., Knohl, A., Koble, R., Laurila, T., Longdoz, B., Manca, G., Marek, M., Markkanen, T., Mateus, J., Matteucci, G., Mauder, M., Migliavacca, M., Minerbi, S., Moncrieff, J., Montagnani, L., Moors, E., Ourcival, J.-M., Papale, D., Pereira, J., Pilegaard, K., Pita, G., Rambal, S., Rebmann, C., Rodrigues, A., Rotenberg, E., Sanz, M. J., Sedlak, P., Seufert, G., Siebicke, L., Soussana, J. F., Valentini, R., Vesala, T., Verbeeck, H., and Yakir, D.: Quality control of CarboEurope flux data – Part 1: Coupling footprint analyses with flux data quality assessment to evaluate sites in forest ecosystems, *Biogeosciences*, 5, 433–450, doi:10.5194/bg-5-433-2008, 2008.
- Gee, G. W., Newman, B. D., Green, S. R., Meissner, R., Rupp, H., Zhang, Z. F., Keller, J. M., Waugh, W. J., van der Velde, M., and Salazar, J.: Passive wick fluxmeters, *Water Resour Res*, 45, W04420, doi:10.1029/2008WR007088, 2009.
- Gerken, T., Babel, W., Hoffmann, A., Biermann, T., Herzog, M., Friend, A. D., Li, M., Ma, Y., Foken, T., and Graf, H.-F.: Turbulent flux modelling with a simple 2-layer soil model and extrapolated surface temperature applied at Nam Co Lake basin on the Tibetan Plateau, *Hydrol Earth Syst Sci*, 16, 1095–1110, doi:10.5194/hess-16-1095-2012, 2012.
- Gerken, T., Babel, W., Sun, F., Herzog, M., Ma, Y., Foken, T., and Graf, H.-F.: Uncertainty in atmospheric profiles and its impact on modeled convection development at Nam Co Lake, Tibetan Plateau, *J Geophys Res*, 118, 12,317–12,331, doi:10.1002/2013JD020647, 2013.
- Gerken, T., Biermann, T., Babel, W., Herzog, M., Ma, Y., Foken, T., and Graf, H.-F.: A modelling investigation into lake-breeze development and convection triggering in the Nam Co Lake basin, Tibetan Plateau, *Theor Appl Climatol*, 117, 149–167, doi:10.1007/s00704-013-0987-9, 2014.
- Goldstein, M. C. and Beall, C. M.: Change and continuity in Nomadic Pastoralism on the Western Tibetan Plateau, *Nomadic Peoples*, pp. 105–122, 1991.
- Gu, S., Tang, Y., Cui, X., Kato, T., Du, M., Li, Y., and Zhao, X.: Energy exchange between the atmosphere and a meadow ecosystem on the Qinghai–Tibetan Plateau, *Agr Forest Meteorol*, 129, 175–185, doi:10.1016/j.agrformet.2004.12.002, 2005.
- Hafner, S., Unteregelsbacher, S., Seeber, E., Lena, B., Xu, X., Li, X., Guggenberger, G., Miehe, G., and Kuzyakov, Y.: Effect of grazing on carbon stocks and assimilate partitioning in a Tibetan montane pasture revealed by $^{13}\text{CO}_2$ pulse labeling, *Global Change Biol*, 18, 528–538, doi:10.1111/j.1365-2486.2011.02557.x, 2012.

- Haginoya, S., Fujii, H., Kuwagata, T., Xu, J., Ishigooka, Y., Kang, S., and Zhang, Y.: Air-Lake Interaction Features Found in Heat and Water Exchanges over Nam Co on the Tibetan Plateau, *SOLA*, 5, 172–175, doi:10.2151/sola.2009-044, 2009.
- Han, J. G., Zhang, Y. J., Wang, C. J., Bai, W. M., Wang, Y. R., Han, G. D., and Li, L. H.: Rangeland degradation and restoration management in China, *Rangeland J*, 30, 233–239, doi:10.1071/RJ08009, 2008.
- Harris, R. B.: Rangeland degradation on the Qinghai-Tibetan plateau: A review of the evidence of its magnitude and causes, *J Arid Environ*, 74, 1–12, doi:10.1016/j.jaridenv.2009.06.014, 2010.
- Herzog, M., Oberhuber, J. M., and Graf, H. F.: A prognostic turbulence scheme for the nonhydrostatic plume model ATHAM, *J Atmos Sci*, 60, 2783–2796, 2003.
- Hirota, M., Zhang, P., Gu, S., Du, M., Shimono, A., Shen, H., Li, Y., and Tang, Y.: Altitudinal variation of ecosystem CO₂ fluxes in an alpine grassland from 3600 to 4200 m, *J Plant Ecol*, 2, 197–205, doi:10.1093/jpe/rtp024, 2009.
- Holzner, W. and Kriechbaum, M.: Pastures in South and Central Tibet (China), I. Methods for a rapid assessment of pasture conditions, *Bodenkultur*, 51, 259–266, 2000.
- Hong, J. and Kim, J.: Numerical study of surface energy partitioning on the Tibetan plateau: comparative analysis of two biosphere models, *Biogeosciences*, 7, 557–568, doi:10.5194/bg-7-557-2010, 2010.
- Hsu, H.-H. and Liu, X.: Relationship between the Tibetan Plateau heating and East Asian summer monsoon rainfall, *Geophys. Res. Lett.*, 30, 2066, doi:10.1029/2003GL017909, 2003.
- Hu, J., Hopping, K. A., Bump, J. K., Kang, S., and Klein, J. A.: Climate Change and Water Use Partitioning by Different Plant Functional Groups in a Grassland on the Tibetan Plateau, *PLoS ONE*, 8, e75 503, doi:10.1371/journal.pone.0075503, 2013.
- Immerzeel, W. W., van Beek, L. P. H., and Bierkens, M. F. P.: Climate Change Will Affect the Asian Water Towers, *Science*, 328, 1382–1385, doi:10.1126/science.1183188, 2010.
- Ingrisch, J., Biermann, T., Seeber, E., Leipold, T., Li, M., Ma, Y., Xu, X., Mieke, G., Guggenberger, G., Foken, T., and Kuzyakov, Y.: Carbon pools and fluxes results from a field campaign conducted in 2010 on the Tibetan Plateau at Kema. Dataset #833208, PANGAEA, doi:10.1594/PANGAEA.833208, 2014.

References

- Ingrisch, J., Biermann, T., Seeber, E., Leipold, T., Li, M., Ma, Y., Xu, X., Mieke, G., Guggenberger, G., Foken, T., and Kuzyakov, Y.: Carbon pools and fluxes in a Tibetan alpine *Kobresia pygmaea* pasture partitioned by coupled eddy-covariance measurements and ^{13}C pulse labeling, *Science of The Total Environment*, 505, 1213–1224, doi:10.1016/j.scitotenv.2014.10.082, 2015
- Ingwersen, J., Steffens, K., Högy, P., Warrach-Sagi, K., Zhunusbayeva, D., Poltoradnev, M., Gäbler, R., Wizemann, H.-D., Fangmeier, A., Wulfmeyer, V., and Streck, T.: Comparison of Noah simulations with eddy covariance and soil water measurements at a winter wheat stand, *Agr Forest Meteorol*, 151, 345–355, 2011.
- Kaiser, K.: Pedogeomorphological transect studies in Tibet: Implications for landscape history and present-day dynamics, *Prace Geograficzne*, pp. 147–165, 2004.
- Kaiser, K., Mieke, G., Barthelmes, A., Ehrmann, O., Scharf, A., Schult, M., Schlütz, F., Adamczyk, S., and Frenzel, B.: Turf-bearing topsoils on the central Tibetan Plateau, China: Pedology, botany, geochronology, *Catena*, 73, 300–311, doi:10.1016/j.catena.2007.12.001, 2008.
- Kang, S., Xu, Y., You, Q., Flügel, W.-A., Pepin, N., and Yao, T.: Review of climate and cryospheric change in the Tibetan Plateau, *Environ Res Lett*, 5, 015101, doi:10.1088/1748-9326/5/1/015101, 2010.
- Kato, T., Tang, Y., Gu, S., Cui, X., Hirota, M., Du, M., Li, Y., Zhao, X., and Oikawa, T.: Carbon dioxide exchange between the atmosphere and an alpine meadow ecosystem on the Qinghai–Tibetan Plateau, China, *Agr Forest Meteorol*, 124, 121–134, doi:10.1016/j.agrformet.2003.12.008, 2004a.
- Kato, T., Tang, Y., Gu, S., Hirota, M., Cui, X., Du, M., Li, Y., Zhao, X., and Oikawa, T.: Seasonal patterns of gross primary production and ecosystem respiration in an alpine meadow ecosystem on the Qinghai-Tibetan Plateau, *J Geophys Res*, 109, D12109, doi:10.1029/2003JD003951, 2004b.
- Kato, T., Tang, Y., Gu, S., Hirota, M., Du, M., Li, Y., and Zhao, X.: Temperature and biomass influences on interannual changes in CO_2 exchange in an alpine meadow on the Qinghai-Tibetan Plateau, *Global Change Biol*, 12, 1285–1298, doi:10.1111/j.1365-2486.2006.01153.x, 2006.
- Keith, H., Oades, J. M., and Martin, J. K.: Input of carbon to soil from wheat plants, *Soil Biol and Biochem*, 18, 445–449, doi:10.1016/0038-0717(86)90051-9, 1986.
- Klein, J. A., Harte, J., and Zhao, X.: Experimental warming causes large and rapid species loss, dampened by simulated grazing, on the Tibetan Plateau, *Ecol Lett*, 7, 1170–1179, doi:10.1111/j.1461-0248.2004.00677.x, 2004.

- Kuzyakov, Y.: Tracer studies of carbon translocation by plants from the atmosphere into the soil (A review), *Eurasian Soil Sci.*, 34, 28–42, 2001.
- Kuzyakov, Y.: Sources of CO₂ efflux from soil and review of partitioning methods, *Soil Biol and Biochem*, 38, 425–448, doi:10.1016/j.soilbio.2005.08.020, 2006.
- Kuzyakov, Y. and Domanski, G.: Carbon input by plants into the soil. Review, *J Plant Nutr Soil Sc*, 163, 421–431, doi:10.1002/1522-2624(200008)163:4<421::AID-JPLN421>3.0.CO;2-R, 2000.
- Lasslop, G., Reichstein, M., Papale, D., Richardson, A. D., Arneeth, A., Barr, A. G., Stoy, P., and Wohlfahrt, G.: Separation of net ecosystem exchange into assimilation and respiration using a light response curve approach: critical issues and global evaluation, *Global Change Biol*, 16, 187–208, doi:10.1111/j.1365-2486.2009.02041.x, 2010.
- Leclerc, M. and Foken, T.: *Footprints in Micrometeorology and Ecology*, Springer, Berlin, Heidelberg, 2014.
- Leonbacher, J.: Chamber based carbon dioxide fluxes of three different vegetation treatments on the Tibetan Plateau, MSc thesis, University of Bayreuth, Bayreuth, 2013.
- Lüers, J. and Bareiss, J.: The effect of misleading surface temperature estimations on the sensible heat fluxes at a high Arctic site – the Arctic Turbulence Experiment 2006 on Svalbard (ARCTEX-2006), *Atmos Chem Phys*, 10, 157–168, doi:10.5194/acp-10-157-2010, 2010.
- Liu, J., Kang, S., Gong, T., and Lu, A.: Growth of a high-elevation large inland lake, associated with climate change and permafrost degradation in Tibet, *Hydrol Earth Syst Sci*, 14, 481–489, doi:10.5194/hess-14-481-2010, 2010.
- Lloyd, J. and Taylor, J.: On the temperature dependence of soil respiration, *Funct Ecol*, 8, 315–323, doi:10.2307/2389824, 1994.
- Lu, T., Wu, N., and Luo, P.: Sedentarization of Tibetan Nomads, *Conserv Biol*, 23, 1074, doi:10.1111/j.1523-1739.2009.01312.x, 2009.
- Ma, W. and Ma, Y.: The annual variations on land surface energy in the northern Tibetan Plateau, *Environ Geol*, 50, 645–650, doi:10.1007/s00254-006-0238-9, 2006.
- Ma, Y., Tsukamoto, O., Wang, J., Ishikawa, H., and Tamagawa, I.: Analysis of aerodynamic and thermodynamic parameters on the grassy marshland surface of Tibetan Plateau, *Prog Nat Sci*, 12, 36–40, 2002.

References

- Ma, Y., Su, Z., Koike, T., Yao, T., Ishikawa, H., Ueno, K., and Menenti, M.: On measuring and remote sensing surface energy partitioning over the Tibetan Plateau—from GAME/Tibet to CAMP/Tibet, *Physics and Chemistry of the Earth, Parts A/B/C*, 28, 63–74, doi:10.1016/S1474-7065(03)00008-1, 2003.
- Ma, Y., Menenti, M., Feddes, R., and Wang, J.: Analysis of the land surface heterogeneity and its impact on atmospheric variables and the aerodynamic and thermodynamic roughness lengths, *J Geophys Res*, 113, doi:10.1029/2007JD009124, 2008.
- Ma, Y., Wang, Y., Wu, R., Hu, Z., Yang, K., and Li, M.: Recent advances on the study of atmosphere-land interaction observations on the Tibetan Plateau, *Hydrol Earth Syst Sci*, 13, 1103–1111, doi:10.5194/hess-13-1103-2009, 2009.
- Mauder, M. and Foken, T.: Documentation and Instruction Manual of the Eddy Covariance Software Package TK2, *Arbeitsergebn, Univ Bayreuth, Abt Mikrometeorol*, ISSN 1614-89166, 26, 26, 42, URL <http://nbn-resolving.de/urn/resolver.pl?urn:nbn:de:bvb:703-opus-8000>, 2004.
- Mauder, M. and Foken, T.: Documentation and Instruction Manual of the Eddy-Covariance Software Package TK3, *Arbeitsergebn, Univ Bayreuth, Abt Mikrometeorol*, ISSN 1614-89166, 46, 46, 60, URL <http://nbn-resolving.de/urn/resolver.pl?urn:nbn:de:bvb:703-opus-8665>, 2011.
- Mauder, M., Liebethal, C., Göckede, M., Leps, J.-P., Beyrich, F., and Foken, T.: Processing and quality control of flux data during LITFASS-2003, *Bound-Lay Meteorol*, 121, 67–88, doi:10.1007/s10546-006-9094-0, 2006.
- Mauder, M., Foken, T., Clement, R., Elbers, J. A., Eugster, W., Grünwald, T., Heusinkveld, B., and Kolle, O.: Quality control of CarboEurope flux data – Part 2: Inter-comparison of eddy-covariance software, *Biogeosciences*, 5, 451–462, doi:10.5194/bg-5-451-2008, 2008.
- Maussion, F., Scherer, D., Finkelnburg, R., Richters, J., Yang, W., and Yao, T.: WRF simulation of a precipitation event over the Tibetan Plateau, China – an assessment using remote sensing and ground observations, *Hydrol Earth Syst Sci*, 15, 1795–1817, doi:10.5194/hess-15-1795-2011, 2011.
- Meharg, A. and Killham, K.: Distribution of assimilated carbon within the plant and rhizosphere of *Lolium perenne*: Influence of temperature, *Soil Biol and Biochem*, 21, 487–489, doi:10.1016/0038-0717(89)90119-3, 1989.
- Mengelkamp, H.-T., Warrach, K., and Raschke, E.: SEWAB a parameterization of the surface energy and water balance for atmospheric and hydrologic models, *Adv Water Resour*, 23, 165–175, 1999.

- Mengelkamp, H. T., Kiely, G., and Warrach, K.: Evaluation of the hydrological components added to an atmospheric land-surface scheme, *Theor Appl Climatol*, 69, 199–212, 2001.
- Mügler, I., Gleixner, G., Günther, F., Mäusbacher, R., Daut, G., Schütt, B., Berking, J., Schwalb, A., Schwark, L., Xu, B., Yao, T., Zhu, L., and Yi, C.: A multi-proxy approach to reconstruct hydrological changes and Holocene climate development of Nam Co, Central Tibet, *J Paleolimnol*, 43, 625–648, doi:10.1007/s10933-009-9357-0, 2010.
- Michaelis, L. and Menten, M. L.: Die Kinetik der Invertinwirkung, *Kinetics of the invertin reaction.*, *Biochem Z*, 49, 333–369, 1913.
- Miehe, G., Kaiser, K., Co, S., Zhao, X., and Liu, J.: Geo-ecological transect studies in northeast Tibet (Qinghai, China) reveal human-made mid- Holocene environmental changes in the upper Yellow River catchment changing forest to grassland, *erdkunde*, 62, 187–199, doi:10.3112/erdkunde.2008.03.01, 2008a.
- Miehe, G., Miehe, S., Kaiser, K., Liu, J., and Zhao, X.: Status and dynamics of *Kobresia pygmaea* ecosystem on the Tibetan plateau, *Ambio*, 37, 272–279, doi:10.1579/0044-7447(2008)37[272:SADOTK]2.0.CO;2, 2008b.
- Miehe, G., Bach, K., Miehe, S., Kluge, J., Yongping, Y., Duo, L., Co, S., and Wesche, K.: Alpine steppe plant communities of the Tibetan highlands, *Appl Veg Sci*, 14, 547–560, doi:10.1111/j.1654-109X.2011.01147.x, 2011.
- Miehe, G., Miehe, S., Böhner, J., Kaiser, K., Hensen, I., Madsen, D., Liu, J., and Opgenoorth, L.: How old is the human footprint in the world’s largest alpine ecosystem? A review of multiproxy records from the Tibetan Plateau from the ecologists’ viewpoint, *Quat Sci Rev*, 86, 190–209, doi:10.1016/j.quascirev.2013.12.004, 2014.
- Molnar, P., Boos, W. R., and Battisti, D. S.: Orographic Controls on Climate and Paleoclimate of Asia: Thermal and Mechanical Roles for the Tibetan Plateau, *Annu. Rev. Earth Planet. Sci.*, 38, 77–102, doi:10.1146/annurev-earth-040809-152456, 2010.
- Ni, J.: Impacts of climate change on Chinese ecosystems: key vulnerable regions and potential thresholds, *Reg Environ Change*, 11, 49–64, doi:10.1007/s10113-010-0170-0, 2011.
- Niu, Y.: The study of environment in the Plateau of Qin-Tibet (In Chinese with English abstract), *Prog Geography*, 18, 163–171, 1999.
- Nordbo, A., Launiainen, S., Mammarella, I., Leppäranta, M., Huotari, J., Ojala, A., and Vesala, T.: Long-term energy flux measurements and energy balance over a small boreal lake using eddy covariance technique, *J Geophys Res*, 116, D02119, doi:10.1029/2010JD014542, 2011.

References

- Oberhuber, J. M., Herzog, M., Graf, H. F., and Schwanke, K.: Volcanic Plume Simulation on Large Scales, *Journal of Volcanology and Geothermal Research*, 87, 29–53, doi:10.1016/S0377-0273(98)00099-7, 1998.
- Palta, J. A. and Gregory, P. J.: Drought affects the fluxes of carbon to roots and soil in ^{13}C pulse-labelled plants of wheat, *Soil Biol and Biochem*, 29, 1395–1403, doi:10.1016/S0038-0717(97)00050-3, 1997.
- Panin, G. N. and Foken, T.: Air–sea interaction including a shallow and coastal zone, *J Atmos Ocean Sci*, 10, 289–305, doi:10.1080/17417530600787227, 2005.
- Panin, G. N., Nasonov, A. E., and Foken, T.: Evaporation and heat exchange of a body of water with the atmosphere in a shallow zone, *Izv Atmos Ocean Phys*, 42, 337–352, doi:10.1134/S0001433806030078, 2006.
- Paw U, K., Baldocchi, D., Meyers, T., and Wilson, K.: Correction Of Eddy-Covariance Measurements Incorporating Both Advective Effects And Density Fluxes, *Bound-Lay Meteorol*, 97, 487–511, doi:10.1023/A:1002786702909, 2000.
- Qiu, J.: China: The third pole, *Nature*, 454, 393–396, doi:10.1038/454393a, 2008.
- Rannik, I., Aubinet, M., Kurbanmuradov, O., Sabelfeld, K. K., Markkanen, T., and Vesala, T.: Footprint Analysis For Measurements Over A Heterogeneous Forest, *Bound-Lay Meteorol*, 97, 137–166, doi:10.1023/A:1002702810929, 2000.
- Rebmann, C., Kolle, O., Heinesch, B., Queck, R., Ibrom, A., and Aubinet, M.: Data Acquisition and Flux Calculations, in: *Eddy Covariance: A Practical Guide to Measurement and Data Analysis*, edited by Aubinet, M., Vesala, T., and Papale, D., pp. 59–83, Springer, Dordrecht, doi:10.1007/978-94-007-2351-1_3, 2012.
- Reichstein, M.: Drought effects on ecosystem carbon anwater exchange in three Mediterranean forest ecosystems-a combined top-down and bottom-up analysis, *Bayreuther Forum Ökologie*, 89, 1–150, 2001.
- Reichstein, M., Stoy, P. C., Desai, A. R., Lasslop, G., and Richardson, A. D.: Partitioning of Net Fluxes, in: *Eddy Covariance: A Practical Guide to Measurement and Data Analysis*, edited by Aubinet, M., Vesala, T., and Papale, D., pp. 263–289, Springer, Dordrecht, 2012.
- Reth, S., Reichstein, M., and Falge, E.: The effect of soil water content, soil temperature, soil pH-value and the root mass on soil CO_2 efflux - A modified model, *Plant and Soil*, 268, 21–33, 2005.
- Riederer, M.: Carbon fluxes of an extensive meadow and attempts for flux partitioning, PhD thesis, University of Bayreuth, Bayreuth, 2014.

- Riederer, M., Serafimovich, A., and Foken, T.: Net ecosystem CO₂ exchange measurements by the closed chamber method and the eddy covariance technique and their dependence on atmospheric conditions, *Atmospheric Measurement Techniques*, 7, 1057–1064, doi:10.5194/amt-7-1057-2014, 2014.
- Rouse, W. R., Oswald, C. J., Binyamin, J., Spence, C., Schertzer, W. M., Blanken, P. D., Bussi eres, N., and Duguay, C. R.: The Role of Northern Lakes in a Regional Energy Balance, *J Hydrometeor*, 6, 291–305, doi:10.1175/JHM421.1, 2005.
- Ruppert, J., Mauder, M., THOMAS, C., and L uers, J.: Innovative gap-filling strategy for annual sums of CO₂ net ecosystem exchange, *Agr Forest Meteorol*, 138, 5–18, doi:10.1016/j.agrformet.2006.03.003, 2006.
- Saggar, S., Hedley, C., and Mackay, A. D.: Partitioning and translocation of photosynthetically fixed ¹⁴C in grazed hill pastures, *Biol Fert Soils*, 25, 152–158, doi:10.1007/s003740050296, 1997.
- Saito, M., Kato, T., and Tang, Y.: Temperature controls ecosystem CO₂ exchange of an alpine meadow on the northeastern Tibetan Plateau, *Global Change Biol*, 15, 221–228, doi:10.1111/j.1365-2486.2008.01713.x, 2009.
- Sheehy, D. P., Miller, D., and Johanson, D. A.: Transformatopn of traditional pastoral livestock systems on the Tibetan steppe, *S echeresse*, 17, 142–151, 2006.
- Swinnen, J., Vanveen, J. A., and Merckx, R.: C-14 Pulse labeling of field-grown spring whean - an evaluation of its use in rhizosphere Carbon budget estimations, *Soil Biol and Biochem*, 26, 161–170, 1994.
- Twine, T., Kustas, W., Norman, J., Cook, D., Houser, P., Meyers, T., Prueger, J., Starks, P., and Wesely, M.: Correcting eddy-covariance flux underestimates over a grassland, *Agr Forest Meteorol*, 103, 279–300, doi:10.1016/S0168-1923(00)00123-4, 2000.
- Unteregelsbacher, S., Hafner, S., Guggenberger, G., Miede, G., Xu, X., Liu, J., and Kuzyakov, Y.: Response of long-, medium- and short-term processes of the carbon budget to overgrazing-induced crusts in the Tibetan Plateau, *Biogeochemistry*, 111, 187–201, doi:10.1007/s10533-011-9632-9, 2012.
- Wang, G., Qian, J., Cheng, G., and Lai, Y.: Soil organic carbon pool of grassland soils on the Qinghai-Tibetan Plateau and its global implication, *Sci Total Environ*, 291, 207–217, doi:10.1016/S0048-9697(01)01100-7, 2002.
- Wang, Z., Li, L.-H., Han, X.-G., Li, Z., and Chen, Q.-S.: Dynamics and allocation of recently photo-assimilated carbon in an Inner Mongolia temperate steppe, *Environ Exp Bot*, 59, 1–10, doi:10.1016/j.envexpbot.2005.09.011, 2007.

References

- Wei, D., Ri, X., Wang, Y., Wang, Y., Liu, Y., and Yao, T.: Responses of CO₂, CH₄ and N₂O fluxes to livestock enclosure in an alpine steppe on the Tibetan Plateau, China, *Plant Soil*, 359, 45–55, doi:10.1007/s11104-011-1105-3, 2012.
- Wilczak, J., Oncley, S. P., and Stage, S.: Sonic Anemometer Tilt Correction Algorithms, *Bound-Lay Meteorol*, 99, 127–150, doi:10.1023/A:1018966204465, 2001.
- Wohlfahrt, G., Klumpp, K., and Soussana, J.-F.: Eddy Covariance Measurements over Grasslands, in: *Eddy Covariance: A Practical Guide to Measurement and Data Analysis*, edited by Aubinet, M., Vesala, T., and Papale, D., pp. 333–344, Springer, Dordrecht, 2012.
- Wu, G.-L., Du, G.-Z., Liu, Z.-H., and Thirgood, S.: Effect of fencing and grazing on a Kobresia-dominated meadow in the Qinghai-Tibetan Plateau, *Plant Soil*, 319, 115–126, doi:10.1007/s11104-008-9854-3, 2009.
- Wu, Y., Tan, H., Deng, Y., Wu, J., Xu, X., Wang, Y., Tang, Y., Higashi, T., and Cui, X.: Partitioning pattern of carbon flux in a Kobresia grassland on the Qinghai-Tibetan Plateau revealed by field ¹³C pulse-labeling, *Global Change Biol*, 16, 2322–2333, doi:10.1111/j.1365-2486.2009.02069.x, 2010.
- Wu, Y., Wu, J., Deng, Y., Tan, H., Du, Y., Gu, S., Tang, Y., and Cui, X.: Comprehensive assessments of root biomass and production in a Kobresia humilis meadow on the Qinghai-Tibetan Plateau, *Plant Soil*, 338, 497–510, doi:10.1007/s11104-010-0562-4, 2011.
- Xu, J. and Haginoya, S.: An Estimation of Heat and Water Balances in the Tibetan Plateau, *J Meteorol Soc Jap*, 79, 485–504, 2001.
- Xu, J., Yu, S., Liu, J., Haginoya, S., Ishigooka, Y., Kuwagata, T., Hara, M., and Yasunari, T.: The Implication of Heat and Water Balance Changes in a Lake Basin on the Tibetan Plateau, *Hydrol Res Lett*, 3, 1–5, doi:10.3178/hrl.3.1, 2009.
- Yang, K., Koike, T., and Yang, D.: Surface Flux Parameterization in the Tibetan Plateau, *Bound-Lay Meteorol*, 116, 245–262, doi:10.1023/A:1021152407334, 2003.
- Yang, K., Ye, B., Zhou, D., Wu, B., Foken, T., Qin, J., and Zhou, Z.: Response of hydrological cycle to recent climate changes in the Tibetan Plateau, *Climatic Change*, 109, 517–534, doi:10.1007/s10584-011-0099-4, 2011.
- Yang, K., Wu, H., Qin, J., Lin, C., Tang, W., and Chen, Y.: Recent climate changes over the Tibetan Plateau and their impacts on energy and water cycle: A review, *Global Planet Change*, 112, 79–91, doi:10.1016/j.gloplacha.2013.12.001, 2014.

- Yang, Y., Fang, J., Ji, C., and Han, W.: Above- and belowground biomass allocation in Tibetan grasslands, *J Veg Sci*, 20, 177–184, doi:10.1111/j.1654-1103.2009.05566.x, 2009.
- Yao, T., Thompson, L. G., Mosbrugger, V., Zhang, F., Ma, Y., Luo, T., Xu, B., Yang, X., Joswiak, D. R., Wang, W., Joswiak, M. E., Devkota, L. P., Tayal, S., Jilani, R., and Fayziev, R.: Third Pole Environment (TPE), *Environ Develop*, 3, 52–64, doi:10.1016/j.envdev.2012.04.002, 2012.
- Zhang, P., Tang, Y., Hirota, M., Yamamoto, A., and Mariko, S.: Use of a regression method to partition sources of ecosystem respiration in an alpine meadow, *Soil Biol and Biochem*, 41, 663–670, doi:10.1016/j.soilbio.2008.12.026, 2009.
- Zhao, D., Wu, S., Yin, Y., and Yin, Z.-Y.: Vegetation distribution on Tibetan Plateau under climate change scenario, *Reg Environ Change*, 11, 905–915, doi:10.1007/s10113-011-0228-7, 2011.
- Zhao, L., Li, Y.-N., Gu, S., Zhao, X.-Q., Xu, S.-X., and Yu, G.-R.: Carbon Dioxide Exchange Between the Atmosphere and an Alpine Shrubland Meadow During the Growing Season on the Qinghai-Tibetan Plateau, *J Integr Plant Biol*, 47, 271–282, doi:10.1111/j.1744-7909.2005.00066.x, 2005.

A. Individual contributions to the joint publications

This cumulative thesis consists of publications and manuscripts listed hereafter. Since other authors contributed to these papers as well, my own contribution to the individual manuscripts is specified in this section. As the following publications are based on the experiments on the TP (described in section 1.2.2) individual contributions to the experiments are listed as well. The experiments 2009 in Xinghai and 2012 at Nam Co are not included since although I was partially involved in the organization prior to the experiments I did not participate in the experiments.

Nam Co experiment 2009 and data preparation

Together with Wolfgang Babel I was responsible for the realization of the experiment. The setup and design were planned and prepared together with Wolfgang Babel in equal shares. We both assembled the measurement complex at the site, while for the campaign I was responsible for data collection and maintenance.

The data measured during the Nam Co experiment at our own EC station (NamUBT) as well as data provided from the permanent station of the ITP (NamITP) were post-processed as follows: I conducted the quality checks on low-frequency data and turbulent flux processing with the TK2/TK3 software package, including sector-wise planar-fit and quality control. Wolfgang Babel elaborated the actual land cover distribution and contributed with the footprint analysis as well as the calculation of the ground heat flux and energy balance, including the EBC correction methods.

Nam Co experiment 2010 and data preparation

The winter experiment in 2010 at Nam Co was organized and realized by myself with the support of Daniela Pfab, during her master thesis. Furthermore Wolfgang Babel, Johannes Olesch and Thomas Foken provided support during the preparation and also from Germany during the experiment itself. Calibration of the KH₂O was conducted in the field by Daniela and myself. The calculation of the turbulent fluxes and quality control of the data was done by myself during the experiment. Further evaluation of the data was done by Daniela within her master thesis under my supervision.

Kema experiments 2010/12 and data preparation

I was responsible for the organization and realization of the two experiments with the support of two master students, Thomas Leipold in 2010 and Jürgen Leonbacher in 2012, prior to and during the experiments. Both helped with the preparation of the eddy-covariance stations and all additionally devices in Bayreuth and also during their installation and maintenance in the field. We were also supported by Wolfgang Babel during the preparation in Bayreuth for both experiments. Due to logistical problems in 2012 Jürgen Leonbacher and I could only use the long-term LI-COR chamber system in the field and were not able to install the prepared EC stations, as it was originally planned. The data from both experiments were post-processed and quality checked within the masters theses of Thomas Leipold and Jürgen Leonbacher under my supervision. The $^{13}\text{CO}_2$ pulse labeling in 2010 was conducted by Johannes Ingrisich during his master thesis.

Appendix B

Biermann, T., Babel, W., Ma, W., Chen, X., Thiem, E., Ma, Y., and Foken, T.: Turbulent flux observations and modelling over a shallow lake and a wet grassland in the Nam Co basin, Tibetan Plateau, *Theor. Appl. Climatol.*, 116(1-2), 301-316, doi:10.1007/s00704-013-0953-6, 2014.

- The idea of this manuscript was developed in equal parts by Wolfgang Babel and myself. We both realized the Nam Co experiment (p. 59), conducted data preparation and wrote the text in equal shares. While Wolfgang Babel focused on the modeling parts and its inter-comparison with the measured data, I put my emphasis more on literature and scope of the manuscript as well as on the experimental parts, including data preparation and analysis of the measured fluxes in respect to special conditions on the Tibetan Plateau. I also acted as corresponding author.
- Ma Yaoming, Chen Xuelong and Ma Weiqiang supported us during the field trip in 2009 and gave access to data from the ITP station
- Elisabeth Thiem contributed to the manuscript within her master thesis under the supervision of Wolfgang Babel and Thomas Foken. Thereby she filled gaps in the model forcing data, implemented the shallow water term in the lake model HM, and conducted a preliminary sensitivity analysis for the lake model.
- Thomas Foken acted as supervisor and liberally shared his experience in encouraging and fruitful discussions.

Appendix C

Gerken, T., Biermann, T., Babel, W., Herzog, M., Ma, Y., Foken, T., Graf, H.F.: A modelling investigation into lake-breeze development and convection triggering in the Nam Co Lake basin, Tibetan Plateau, *Theor. Appl. Climatol.*, 117(1-2), 149-167 doi:10.1007/s00704-013-0987-9, 2014.

- Tobias Gerken developed the idea of the manuscript and coordinated individual contributions. He conducted the ATHAM modeling and the analysis. He wrote the whole publication and acted as corresponding author.
- Wolfgang Babel and I provided the NamUBT data set from the Nam Co experiment (see p. 59).
- Michael Herzog contributed with technical advice for the ATHAM model and the modeling setup.
- Ma Yaoming provided data from the ITP station and supported the field trip.
- Thomas Foken and Hans-F. Graf contributed to the manuscript at various stages with fruitful discussions.

Appendix D

Babel, W., Biermann, T., Coners, H., Falge, E., Seeber, E., Ingrisich, J., Schleuß, P.-M., Gerken, T., Leonbacher, J., Leipold, T., Willinghöfer, S., Schützenmeister, K., Shibistova, O., Becker, L., Hafner, S., Spielvogel, S., Li, X., Xu, X., Sun, Y., Zhang, L., Yang, Y., Ma, Y., Wesche, K., Graf, H.-F., Leuschner, C., Guggenberger, G., Kuzyakov, Y., Miede, G., and Foken, T.: Pasture degradation modifies the water and carbon cycles of the Tibetan highlands, *Biogeosciences*, 11, 6633-6656, doi:10.5194/bg-11-6633-2014, 2014.

- The idea of this manuscript was developed mainly in Bayreuth by Thomas Foken, Wolfgang Babel and myself. The manuscript was further discussed and refined by all authors in group meetings in Göttingen..
- Wolfgang Babel was responsible for the modeling of turbulent fluxes with the SEWAB model and coordinated the contributions concerning the land surface modeling, writing most of the text.
- I was responsible for the measurements of turbulent fluxes in 2009 and 2010 and the chamber measurements in 2012. I further contributed to the manuscript by providing a literature background on C studies on the TP and writing the part about the setup of the EC measurements and the parts about the chamber measurements as well as the pulse labeling experiments.

A. Individual contributions to the joint publications

- Heinz Coners was responsible for establishing the micro-lysimeter measurements and contributed to the manuscript with the description of this experiment and the data analysis.
- Eva Falge was responsible for modeling C fluxes with the SVAT-CN model.
- Elke Seeber was involved in the field work in the Kema 2010 and 2012. She furthermore contributed to the manuscript with her expertise on the vegetation of the Tibetan Highlands and was involved in the writing and discussion process of the manuscript.
- Johannes Ingrisch contributed with the pulse labeling experiment 2010 in Kema.
- Per Schleuß contributed with soil parameter measurements in 2012 at Kema and was involved in the writing and discussion process of the manuscript.
- Tobias Gerken was responsible for simulations with the ATHAM model.
- Jürgen Leonbacher contributed to the manuscript's workload within a master thesis under the supervision of me and Thomas Foken. Thereby he calculated and analyzed C fluxes from the chamber measurements.
- Thomas Leipold contributed to the manuscript's workload within a master thesis under the supervision of me and Thomas Foken. Thereby he calculated turbulent fluxes from the eddy-covariance measurements of the 2010 experiment.
- Sandra Willinghöfer contributed with vegetation parameters used within the modeling approach and was involved in the writing and discussion process of the manuscript.
- Klaus Schützenmeister, Olga Shibostova, Lena Becker participated in the field campaign 2010 and 2012.
- Silke Hafner contributed with the pulse labeling experiment in 2009 at Xinghai.
- Sandra Spielvogel helped during the writing process of the manuscript in fruitful discussions.
- Li X., Sun Y., Zhang L., Yang Y. Ma Y, Xu supported us during the field trip in 2010 and 2012.
- Karsten Wesche advised the work of his PhD student Elke Seeber and contributed to the manuscript within the discussions.
- Hans F. Graf advised the work of his PhD student Tobias Gerken and contributed to the manuscript within the discussions.

-
- Christoph Leuschner advised the work of his PhD student Sandra Willinghöfer and contributed to the manuscript within the discussions.
 - Georg Guggenberger provided soil parameters needed within the models and helped during the writing process of the manuscript and in fruitful discussions.
 - Yakov Kuzyakov coordinated the pulse labeling experiments, advised the work of his PhD student Per Schleuß and the master students Silke Hafner, Sebastian Unteregelsbacher, Johannes Ingrisch and was involved during the writing process of the manuscript and discussions.
 - Georg Mieke initiated the investigation of the *Kobresia pygmaea* pastures and provided the framework for this manuscript
 - Thomas Foken coordinated and implemented the individual contributions to the manuscript.

Appendix E

Ingrisch, J., Biermann, T., Seeber, E., Leipold T., Li, M., Ma, Y., Xu, X., Mieke, G., Guggenberger, G., Foken, T., Kuzyakov Y.: Carbon pools and fluxes in a Tibetan alpine *Kobresia pygmaea* pasture partitioned by coupled eddy-covariance measurements and $^{13}\text{CO}_2$ pulse labeling, *Science of The Total Environment*, 505, 1213–1224, doi:10.1016/j.scitotenv.2014.10.082, 2015.

Supplementary data:

Ingrisch, J., Biermann, T., Seeber, E., Leipold T., Li, M., Ma, Y., Xu, X., Mieke, G., Guggenberger, G., Foken, T., Kuzyakov Y.: Carbon pools and fluxes measured during a field campaign conducted in 2010 on the Tibetan Plateau at Kema. Dataset 833208, PANGAEA, doi:10.1594/PANGAEA.833208, 2014.

- The idea of this manuscript was developed in equal parts by Johannes Ingrisch and me, and the text was also written in equal shares. Within the Kema 2010 experiment Johannes Ingrisch realized the $^{13}\text{CO}_2$ pulse labeling and I focused on the eddy-covariance measurements (p. 59). While the specific data analyses for the two methods were conducted individually, both authors were equally involved in the coupling of the two methods and the interpretation of the results with respect to the carbon cycle of the *Kobresia pygmaea* pastures. Johannes Ingrisch is the corresponding author for the submitted manuscript. I was responsible for the upload of the data to the data-archive PANGAEA.

A. Individual contributions to the joint publications

- Elke Seeber helped during the field work of the Kema 2010 experiment. She and I were mainly responsible for the logistical part of the field campaign making the whole experiment possible. She furthermore contributed to the manuscript with her expertise on the vegetation of the Tibetan Highlands and in numerous discussions.
- Thomas Leipold contributed to the manuscript within his master thesis under the supervision of Thomas Foken and myself. Thereby he calculated turbulent fluxes from the eddy-covariance measurements and analyzed the impact of the different grazing treatments at Kema on these fluxes, especially on net ecosystem exchange of carbon.
- Ma Yaoming, Xu Xingliang and Li Maoshan supported us during the field trip in 2010.
- Georg Miehe initiated the investigation of the *Kobresia pygmaea* pastures and helped with his expertise on this unique ecosystem.
- Georg Guggenberger helped during the writing process of the manuscript in fruitful discussions.
- Yakov Kuzyakov and Thomas Foken acted as supervisor and liberally shared their experience during discussions during the writing process of the manuscript.

Appendix F

Biermann, T., Pfab, D., Babel, W., Li, M., Wang, B., Ma, Y., and Foken, T.: Note: Measurements of latent heat flux and humidity on the Tibetan Plateau during winter conditions, submitted to Atmos. Meas. Tech. Diss..

- The Paper was written by myself on the basis of the master thesis of Daniela Pfab. Both of us conducted the Nam Co winter experiment (p. 59) together. While her task was mainly the calibration of the KH₂O and the inter-comparison of measured data by the different sensors, I was responsible for the organization of the experiment as well as the calculation and quality checking of the turbulent flux data with respect to special conditions on the Tibetan Plateau. Main data analysis was conducted within Daniela Pfab's master thesis under my supervision. I act as the corresponding author for the submitted manuscript.
- Wolfgang Babel helped during the experiment preparation and the data analysis.
- Li Maoshan, Wang Binbin and Ma Yaoming supported us during the field trip in 2010 and gave access to data from the ITP station

-
- Thomas Foken acted as supervisor and liberally shared his experience in encouraging and fruitful discussions.

B. Biermann et al. (2014)

Biermann, T., Babel, W., Ma, W., Chen, X., Thiem, E., Ma, Y., and Foken, T.: Turbulent flux observations and modelling over a shallow lake and a wet grassland in the Nam Co basin, Tibetan Plateau, *Theor. Appl. Climatol.*, 116(1-2), 301-316, doi:10.1007/s00704-013-0953-6, 2014.

Turbulent flux observations and modelling over a shallow lake and a wet grassland in the Nam Co basin, Tibetan Plateau

Tobias Biermann · Wolfgang Babel · Weiqiang Ma ·
Xuelong Chen · Elisabeth Thiem · Yaoming Ma ·
Thomas Foken

Received: 7 March 2013 / Accepted: 11 June 2013 / Published online: 5 July 2013
© The Author(s) 2013. This article is published with open access at Springerlink.com

Abstract The Tibetan Plateau plays an important role in the global water cycle and is strongly influenced by climate change. While energy and matter fluxes have been more intensely studied over land surfaces, a large proportion of lakes have either been neglected or parameterised with simple bulk approaches. Therefore, turbulent fluxes were measured over wet grassland and a shallow lake with a single eddy-covariance complex at the shoreline in the Nam Co basin in summer 2009. Footprint analysis was used to split observations according to the underlying surface, and two sophisticated surface models were utilised to derive gap-free time series. Results were then compared with observations and simulations from a nearby eddy-covariance station over dry grassland, yielding pronounced differences. Observations and footprint integrated simulations compared

well, even for situations with flux contributions including grassland and lake. The accessibility problem for EC measurements on lakes can be overcome by combining standard meteorological measurements at the shoreline with model simulations, only requiring representative estimates of lake surface temperature.

1 Introduction

The role of the Tibetan Plateau in the global water cycle and its reaction to climate change has become a topic of strong scientific interest (e.g. Immerzeel et al. 2010; Ni 2011). Representing a unique geological formation, the Tibetan Plateau is considered the largest and highest plateau on earth, with an average elevation greater than 4,000 m a.s.l.. Furthermore, the Tibetan Plateau is the source of a large number of major rivers in Asia. Its role in the modulation of the Asian Monsoon and the climate for large parts of Asia, because of its heat budget caused by its elevation in conjunction with the bordering Himalayan mountain range, has been of major research interest (Molnar et al. 2010; Boos and Kuang 2010).

To understand the role of the Tibetan Plateau for the global heat and water budget, much effort has been put into the estimation of energy balance and turbulent flux measurements within international campaigns like GAME/Tibet (Global Energy and Water cycle Experiment Asian Monsoon Experiment) and CAME (Coordinated Enhanced Observing Period Asia-Australia Monsoon Project) (Xu and Haginoya 2001; Ma et al. 2003; Ma et al. 2005) and in the framework of the Tibetan Observation and Research Platform (Ma et al. 2009).

Despite these efforts, observations on the Tibetan Plateau are sparse because of its remote location (Frauenfeld et al. 2005; Kang et al. 2010; Maussion et al. 2011). The importance of evaporation for the hydrological cycle under the

T. Biermann (✉) · W. Babel · T. Foken
Department of Micrometeorology, University of Bayreuth,
Universitätsstr. 30, 95440 Bayreuth, Germany
e-mail: tobias.biermann@uni-bayreuth.de

W. Ma
Cold and Arid Regions Environment and Engineering Research
Institute, Chinese Academy of Sciences, Lanzhou, China

X. Chen
Faculty of Geo-Information Science and Earth Observation,
University of Twente, Enschede, The Netherlands

E. Thiem
Department of Geography, Ludwig-Maximilian University,
Munich, Germany

Y. Ma
Laboratory of Tibetan Environment Changes and Land Surface
Processes, Institute of Tibetan Plateau Research, Chinese Academy
of Sciences, Beijing, China

T. Foken
Member of Bayreuth Center of Ecology and Ecosystem Research
(BayCEER), Bayreuth, Germany

influence of climate change has been highlighted by Yang et al. (2011).

Most long-term observation stations focus on the major land cover types such as alpine steppe, *Kobresia* pastures and wetlands (Zhao et al. 2010), however approximately 45,000 km² of the plateau are covered by lakes (Xu et al. 2009). This lake area has been subject to changes in the last decades; the reasons are not well understood due to lack of observational data (Xu et al. 2009). Although Huang et al. (2008) report a general decrease of lake volume in Qinghai-Tibet Plateau, the Nam Co lake area has been increasing (Liu et al. 2010; Wu and Zhu 2008; Zhu et al. 2010). They attribute this change to increasing precipitation as well as thawing permafrost and glacial melt due to rising mean annual temperatures, nevertheless the relative contribution of the balance components, especially the role of evaporation, is discussed controversially. Consequently, fluxes over lake surfaces on the Tibetan Plateau should not be neglected since various studies have shown the contribution of lakes to the regional energy balance and water cycle in different catchments around the world (Rouse et al. 2005; Nordbo et al. 2011). Until now, estimations of evaporation over lake surfaces on the Tibetan Plateau have been modelled using remote sensing or land surface observations as forcing (Xu et al. 2009; Haginoya et al. 2009), whereas no direct measurements of turbulent fluxes over a lake surface have been conducted so far. The installation of a flux station in a lake on the Tibetan Plateau is nearly impossible, due to problems of accessibility, strong winds and waves during the summer, as well as ice cover during winter.

Nevertheless, it is known from model estimations that evaporation over lake surfaces differs from evapotranspiration over land throughout the year due to the heat storage capacity of the lakes and has a strong effect on convection and thus on local climates (Haginoya et al. 2009). The landscape on the Tibetan Plateau is fairly heterogeneous, including alpine steppe, *Kobresia pygmaea* mats, wetlands and open water surfaces in various sizes. Therefore high quality evaporation measurements over water surfaces on the Tibetan Plateau need to be considered when data based on satellites or estimated with models is validated with ground-based flux measurements. Lakes differ strongly in their temperature regimes and exchange coefficients due to extent and depth (Rouse et al. 2005; Panin et al. 2006a; Nordbo et al. 2011). Evaporation estimation with simple bulk approaches on daily or monthly timescales (Haginoya et al. 2009; Xu et al. 2009; Krause et al. 2010; Yu et al. 2011) are not appropriate for resolving such differences. These specific characteristics of each lake, such as a diurnal course of atmospheric stratification over the lake surface, can only be captured by eddy measurements and more sophisticated models.

For this study, we selected the area around Nam Co, the largest and deepest lake in the Tibet Autonomous Region

(Xu et al. 2009; Liu et al. 2010). The Nam Co basin is considered one of the key areas of interest on the Tibetan Plateau due to its location influenced by the Westerlies, the South West Asian Monsoon and the East Asian Monsoon (Haginoya et al. 2009; Keil et al. 2010).

In order to measure fluxes over lake and land surfaces, we set up an eddy-covariance station at the shoreline of a shallow lake next to Nam Co.

Measured fluxes were utilised to validate simulations of two different surface models in order to estimate turbulent fluxes over the lake and adjacent grassland surface. For the lake surface, a validated hydrodynamic multilayer model (HM; Foken 1979, 1984) with an extension for shallow lakes (Panin and Foken 2005) and for the land surface, a SVAT model (SEWAB; Mengelkamp et al. 1999, 2001) were used to generate a complete time series for each surface. The simulated data set was then used to characterise the exchange for these surfaces and to link the simulations with spatial heterogeneity on footprint scale.

2 Material and methods

2.1 Site description and setup of the EC stations

The experiment was carried out during the 2009 summer monsoon season. The observation site was located in the Nam Co Basin, 220 km north of Lhasa, at 4,730 m a.s.l. on the Tibetan Plateau. The basin is dominated by Nam Co Lake and the Nyainqentanglha mountain range which stretches along the lake's SE side at approximately 5–10 km distance and reaches up to 7270 m a.s.l. with an average height of 5230 m (Liu et al. 2010). In the year 2000 the great lake had an area of 1,980 km² (Wu and Zhu 2008).

Atmospheric fluxes were observed with two eddy-covariance and energy balance stations. One station was set up by the University of Bayreuth (NamUBT) at a shallow lake of approximately 1 km² in area located at the SE side of Nam Co Lake. It was installed adjacent to the southern shoreline of the lake to ensure that measurements from the lake and land surface were identifiable according to the instantaneous wind direction. The other station at roughly 300 m distance is the permanently operating eddy-covariance complex (NamITP) within the Nam Co Monitoring and Research Station for Multisphere Interactions, NAMORS (30°46'22"N, 90°57'47"E) operated by the Institute of Tibetan Plateau Research (ITP), Chinese Academy of Sciences (CAS) (Ma et al. 2009). A detailed map of the field site and pictures of the two stations can be seen in Fig. 1.

The soil is moister at NamUBT than at NamITP due to the influence of the water table around the small lake. To account for the effect of higher moisture supply on the vegetation, we

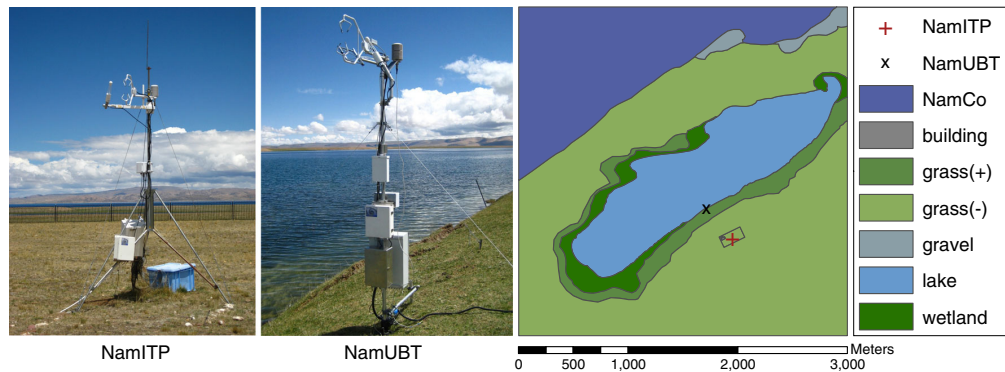


Fig. 1 Measurement site in Nam Co Basin, showing the small lake, the land use, the EC Stations NamITP (left) and NamUBT (right). NamITP is marked with a red cross and NamUBT with a black error mark. Land use is classified as wetland (dark green), moist (positive, medium green)

and dry (negative, light green) grassland; the small lake (light blue); and Nam Co (dark blue). In addition, at the shore line of Nam Co, partly flooded gravel bars are shown in light grey. The Nam Co Station buildings are marked in dark grey (Illustration from Gerken et al. 2012)

have classified the grassland into grass⁺ for denser and moister vegetation and grass⁻ for comparatively drier and sparser vegetation. From NamUBT the terrain rises gently in three terraces to the level of NamITP, with an average slope of approximately 8°. The shoreline of the small lake in the vicinity of NamUBT is fairly steep, with the lake starting out quite shallow and reaching a maximum depth of 12 m at the centre. Soils and vegetation around both stations are typical for a semi-arid to semi-humid climate at this altitude. Soil types range from alpine steppe to desert soils and the vegetation is dominated by alpine meadow and steppe grasses including species of *Stipa*, *Carex*, *Kobresia* and *Oxytropis* (Mügler et al. 2010).

Both eddy-covariance stations were equipped with an ultrasonic anemometer and an infrared gas analyser. Standard meteorological measurements are available for both stations and, additionally, all necessary components for the estimation of the energy balance were measured.

For specifications of the two stations, see Table 1 or Biermann et al. (2009) for NamUBT, and Zhou et al. (2011) for NamITP.

2.2 Analysis of observed data

2.2.1 EC data processing

The measurements of both eddy-covariance stations were post-processed using the TK2/3 software package, developed at the Department of Micrometeorology, University of Bayreuth (Mauder and Foken 2004, 2011) and evaluated in an international comparison study by Mauder et al. (2008). The software applies all necessary flux corrections and post-processing steps for turbulence measurements as recommended in Foken et al. (2012) and Rebmann et al. (2012).

Further data processing included quality filtering according to Foken and Wichura (1996), using the quality

Table 1 Specifications of the eddy-covariance stations NamUBT and NamITP

	Instrument	NamUBT	NamITP
Surface		Lake, grass ⁺ and grass ⁻	Grass ⁻
Ultrasonic anemometer	CSAT3 (Campbell Scientific Ltd.)	3.0 m	3.1 m
Gas analyser	LI-COR7500 (LI-COR Biosciences)	2.9 m	3.1 m
Temperature-humidity sensor	HMP 45 (Vaisalla)	3.0 m	3.1 m
Net radiometer	CNR1 (Kipp & Zonen)	2.0 m	–
Net radiometer	CM3 and CG3 (Kipp & Zonen)	–	1.5 m
Rain gauge	Tipping bucket	1 m	1 m
Soil moisture	Imko-TDR	–0.1, –0.3 and –0.5	–0.1, –0.2, –0.4, –0.8 and –1.60
Soil temperature	Pt100	–0.025, –0.05, –0.1, –0.15, –0.2, –0.3 and –0.5	–0.2, –0.4, –0.8 and –1.60
Soil heat flux	HP3	–0.15	–
Water temperature	Pt100	–0.3	–
Logger	(Campbell Scientific Ltd.)	CR3000	CR5000

flagging scheme as recommended by Foken et al. (2004). For displaying diurnal cycles, we used best to intermediate quality flagged data (Flag 1–6 out of 9 classes) and for model performance evaluation, we used best quality flagged data (Flag 1–3).

2.2.2 Coordinate rotation and footprint analysis

In this section, we describe the coordinate rotation and footprint analysis which was conducted for both EC stations. We focus mainly on the analysis for NamUBT, since for NamITP detailed studies of footprint and data quality can be found for other data sets in Zhou et al. (2011) and Metzger et al. (2006).

The wind direction exhibits a strong diurnal pattern due to a land – lake circulation system, which can be seen in NamUBT data (Fig. 2).

During midday, the wind came predominantly from the direction of the lake while in the morning, evening and night-time hours wind from the land surface dominated. Therefore NamUBT provides flux measurements over the land and water surface only for certain periods of the day, while NamITP always represents fluxes from the land surface.

For the necessary coordinate rotation, we chose the planar-fit method according to Wilczak et al. (2001) which rotates the coordinate system into the mean streamlines by fitting a plane to individual half-hourly mean wind velocity components. While the mean vertical wind for the whole period is set to zero by this method, the individual half-hourly values do not vanish completely. Eddy-covariance measurements require a homogeneous flow field as a prerequisite. In our study this is not the case at NamUBT due to the transition from the plane lake surface to the gently sloping grassland. Paw et al. (2000) and Finnigan et al. (2003) suggest considering such terrain structures in the rotation procedure of the eddy-covariance data. Therefore the planar-fit rotation was applied for four different sectors according to Fig. 2. This procedure accounts for two planes with different slopes and two transition areas. Most of the vertical wind speed disappears after the rotation; 95 % of the vertical wind speed data for the lake and for the land surface remain within ± 0.1 and ± 0.07 ms^{-1} , respectively. For wind sectors parallel to the shoreline, 95 % of the residual mean vertical wind velocity stays within ± 0.12 ms^{-1} . These values

stay within acceptable limits, compared to a multi-site quality analysis by Göckede et al. (2008).

The footprint analysis was conducted following Göckede et al. (2004, 2008). The approach is based on a Lagrangian stochastic forward model providing two dimensional contributions of source areas (Rannik et al. 2000). The resulting footprint for NamUBT (Fig. 3) shows that flux contributions from the lake are not found under stable conditions, which are typical for night times, while they can be found during unstable and neutral stratification. These findings match well with the distribution of wind directions mentioned above.

The footprint analysis includes not only the calculation of the footprint, but also the spatial distribution of flux quality according to Göckede et al. (2008), which enables the user to identify spatial patterns such as obstacles or heterogeneities contributing to the quality of the measured fluxes. In our study no such patterns could be identified for either station.

The average land use contribution to the measured signal for unstable and neutral stratification depending on the wind direction is shown in Fig. 4. The differentiation between stability classes were defined by the stability parameter z/L^{-1} with the measurement height z and L as the Obukhov length. The contribution from grass^+ dominates the influence of the land surface in the respective wind sector. Influence of wetland and buildings are close to zero, even for stable conditions (not shown). The influence of grass^- is comparatively small. During stable conditions, it is larger but these occur mostly at night, when flux differences between grass^- and grass^+ are negligible. Therefore, it is reasonable to relate land surface parameters to the wetter grass^+ surface and we continue with a simplified land use scheme, discriminating only between land (grass^+) and lake for NamUBT. The footprint analysis of NamITP confirmed the representativeness of this station for grass^- .

2.2.3 Energy balance correction

Investigation of the energy balance closure (Foken 2008) at NamUBT shows that 70 % of the energy balance is closed for the measurement period, a typical value for flux stations in heterogeneous landscapes. The energy balance closure correction (EBC) for the land surface fluxes was calculated after Twine et al. (2000), distributing the residual of the energy balance according to the Bowen ratio to the latent and

Fig. 2 Temporal distribution of the wind direction for the measuring period 27 June to 8 August and corresponding land use in upwind direction, classified according to the sectors shown on the right

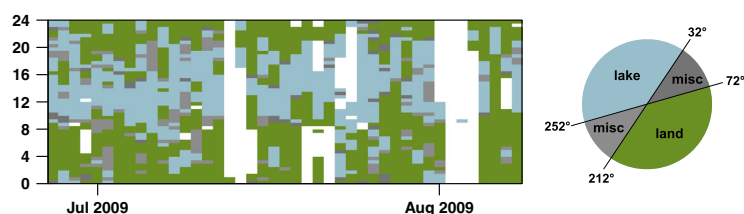
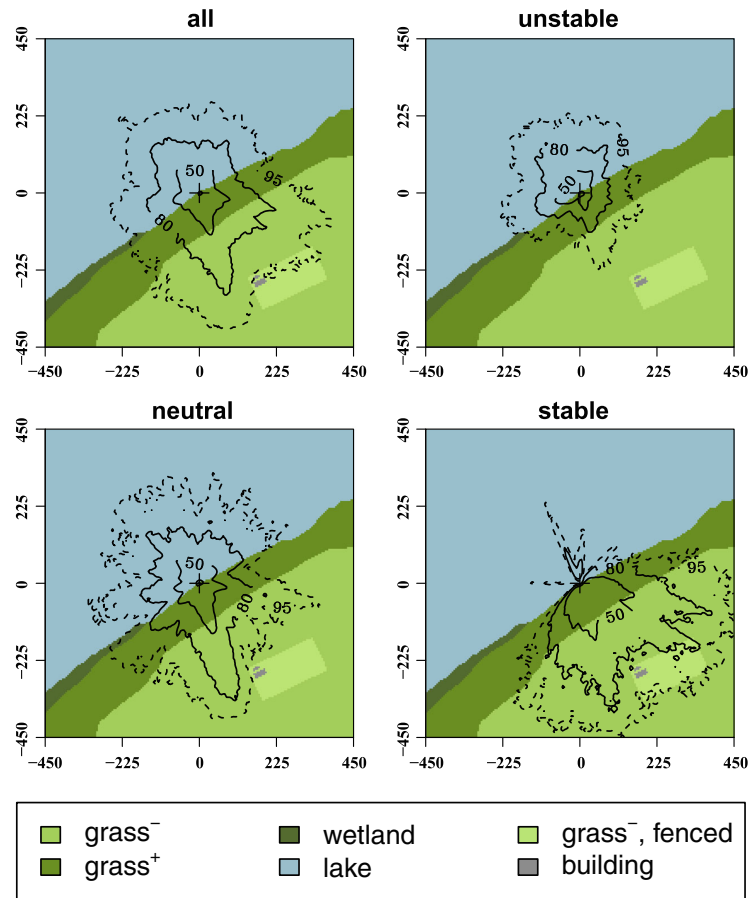


Fig. 3 Footprint climatology of NamUBT for the measuring period 27 June to 8 August. The figures show a combined footprint as well as footprints under unstable ($z L^{-1} \leq -0.0625$), neutral ($-0.0625 \leq z L^{-1} \leq 0.0625$) and stable stratification ($z L^{-1} > 0.0625$) of the atmosphere



sensible heat flux. We subsequently refer to this correction as EBC-Bo. Since Kracher et al. (2009) show with another data set that the land surface model SEWAB, which is used in this study (see Section 2.3.1), roughly preserves the Bowen ratio

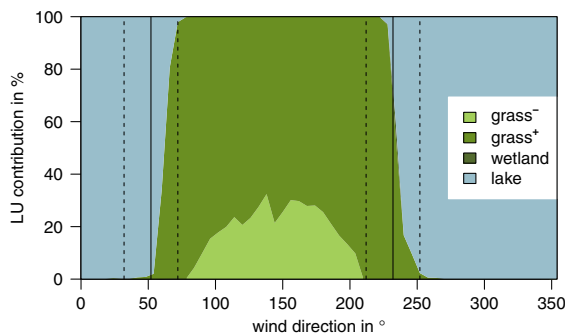


Fig. 4 Average land use contribution of NamUBT under unstable and neutral conditions ($z L^{-1} \leq 0.0625$) for all wind directions. *Solid lines* represent the shoreline; *dashed lines* represent the borders of the sectors classified as land, lake and miscellaneous (*misc*) in Fig. 2

measured by eddy covariance, we regard EBC-Bo as a suitable correction for comparing the observations with SEWAB.

Nevertheless, recent studies suggest that a predominant fraction of the residual should be attributed to the sensible heat flux (Mauder and Foken 2006; Ingwersen et al. 2011; Foken et al. 2012). In case the reason for the unclosed energy balance is the existence of secondary circulations due to convection, as hypothesized by Foken et al. (2010, 2011), a physically meaningful correction would be related to buoyancy. The buoyancy flux Q_{HB} is driven by differences in air density and thus can be decomposed into a fraction governed by sensible heat (density differences because of temperature) and a fraction governed by latent heat (density differences due to moisture). The findings mentioned above suggest a correction where the residual of the energy balance is distributed to the sensible and latent heat flux according to their contribution to the buoyancy flux. This fraction depends on the Bowen ratio Bo and (to a small extent) on air temperature, and more than 90 % are attributed to the sensible heat flux in the case of Bo=1 and approximately 60 % in the case

of $Bo=0.1$. We applied this correction, here named EBC-HB, for comparison with the more common EBC-Bo.

The EBC for the lake surface could not be estimated since only one sensor was used to measure the water temperature and no measurements of the storage flux within the lake or the sediment were conducted.

2.3 Modelling of the turbulent fluxes

Because of the location of NamUBT at the shore line, the wind direction determined whether turbulent fluxes over the land or the lake surface were measured, resulting in gaps of one or the other time series. Therefore, a model was applied for each surface type and validated with the existing data. The results then complete the flux time series for the land and lake surface.

In addition, fluxes for grass⁻ at NamITP were modelled using the same land surface model.

2.3.1 Description of the models used

For the lake surface, a HM by Foken (1979, 1984) was utilised. In order to account for multiple layers within the surface layer, turbulent fluxes are parameterised in HM using an integrated profile coefficient. As opposed to a single bulk coefficient, the integrated profile coefficient resolves the molecular boundary layer, the viscous buffer layer and the

turbulent layer. Therefore, near-surface exchange conditions are reflected according to hydrodynamic theory. Originally designed for exchange over the ocean, a correction term for shallow water (Panin and Foken 2005) was added, resulting in increased turbulent fluxes due to an enhanced mixing by higher waves in shallow water. The model has been successfully applied to simulate fluxes above ocean surfaces and lakes with a large fetch as well as over arctic snow fields (Panin et al. 2006b; Foken 1986; Lüers and Bareiss 2010). Details of the governing equations can be found in Table 2.

Turbulent fluxes over the land surface were simulated with the one-dimensional SEWAB scheme (Mengelkamp et al. 1999, 2001), a soil-vegetation-atmosphere-transfer model. All energy balance components are given separately. Turbulent fluxes are formulated with bulk approaches, atmospheric stability is considered. The main features are summarized in Table 3. The energy balance is then closed by iteration of the surface temperature. Evapotranspiration from vegetation is calculated with a single leaf concept in a Jarvis-type scheme after Noilhan and Planton (1989). Emphasis is placed on the description of soil processes. Soil temperature distribution and vertical soil water movement are described by the diffusion equation and the Richards equation, respectively. Soil moisture characteristics are inter-related following Clapp and Hornberger (1978).

Both models were forced with standard meteorological in-situ measurements. In order to provide gap-free input data,

Table 2 Governing equations for the HM (Foken 1979, 1984) with shallow water extension (Panin and Foken 2005)

Variable/component	Equation
Sensible heat flux	$Q_H^{\text{ocean}} = I(T_{\text{stc}} - T_z)$ with $\Gamma = \kappa \cdot u_* \cdot \left[(\kappa \cdot \text{Pr} - \frac{1}{6}) \cdot \delta_T^+ + 5 + \ln \frac{u_* z}{30\nu} \right]^{-1}$
Latent heat flux	Analog to Q_H^{ocean} , assuming $\delta_T^+ \approx \delta_q^+$, $\Delta T^+ \approx \Delta q^+$ and replacing Pr with Sc
Stability dependence	Monin–Obukhov Similarity Theory, universal function after Foken and Skeib (1983)
Shallow water term	$Q_{H,E}^{\text{SW}} = Q_{H,E}^{\text{ocean}} \cdot (1 + k_{H,E}^{\text{SW}} \cdot h H^{-1})$ with mean square wave height $h \approx 0.07 u_*^2 (gH \cdot (u_*^{-2}))^{0.6} \cdot g^{-1}$ (Davidan et al. 1985) and $k_{H,E}^{\text{SW}} \approx 2$ (Panin et al. 2006b)
Symbols	
g gravity acceleration (ms^{-2})	T temperature (K)
H lake depth (m)	T^+ dimensionless temperature (-)
h mean square wave height (m)	u_* friction velocity (ms^{-1})
$k_{H,E}^{\text{SW}}$ empirical correction factor (-)	u_z wind velocity in height z (ms^{-1})
Pr Prandtl number (-)	z measurement height (m)
$Q_{H,E}^{\text{ocean}}$ sensible (H) and latent (L) heat flux without shallow water correction (W m^{-2})	Γ profile coefficient (ms^{-1})
$Q_{H,E}^{\text{SW}}$ sensible (H) and latent (L) heat flux with shallow water correction (W m^{-2})	δ_T^+ dimensionless thickness of the molecular temperature boundary layer (-)
q specific humidity (-)	κ von Kármán constant (-)
Sc Schmid number (-)	ν kinematic viscosity (m^2s^{-1})

Table 3 Governing equations for SEWAB (Mengelkamp et al. 1999, 2001) and adaptations to the Tibetan Plateau as used in Babel et al. (2013)

Variable/component	Equation
Net radiation	$R_{\text{net}} = -R_{\text{swd}}(1-a) - R_{\text{lwd}} + \varepsilon \sigma T_{\text{sfc}}^4$ R_{swd} and R_{lwd} in forcing data set
Ground heat flux	$Q_G = \lambda_s (T_{\text{sfc}} - T_{S1}) \cdot \Delta z_{S1}^{-1}$
Sensible heat flux	$Q_H = C_H \rho c_p u(z) (T_{\text{sfc}} - T(z))$
Latent heat flux	Composed of bare soil E_s , wet foliage E_f and plant transpiration E_{tr} , after Noilhan and Planton (1989) $E_s = C_E \rho u(z) (\alpha q_s (T_{\text{sfc}}) - q(z))$ $E_f = C_E \rho u(z) (q_s (T_{\text{sfc}}) - q(z))$ $E_{tr} = (R_a - R_s)^{-1} \rho (q_s (T_{\text{sfc}}) - q(z))$
Stability dependence	C_H after Louis (1979), $C_E = C_H$
Adaptations to TP	
Soil thermal conductivity	$\lambda_s(\Theta) = \lambda_{\text{dry}} + (\lambda_{\text{sat}} - \lambda_{\text{dry}}) \exp[k_T(1 - \Theta_{\text{sat}}/\Theta)]$, $k_T = 0.36$ (Yang et al. 2005)
Thermal roughness length	$z_{0h} = 70 \nu \cdot u_*^{-1} \cdot \exp(-\beta u_*^{0.5} T_* ^{0.25})$ $\beta = 7.2 \text{ s}^{0.5} \text{ m}^{-0.5} \text{ K}^{-0.25}$ (Yang et al. 2008)
Bare soil evaporation	$\alpha = \begin{cases} 1 - \left(1 - \frac{\Theta}{\Theta_{\text{FC}}}\right)^2, & \Theta \leq \Theta_{\text{FC}} \\ 1, & \Theta > \Theta_{\text{FC}} \end{cases}$ (Mihailović et al. 1993)
Symbols	
a albedo (-)	α dependence factor of soil air humidity to soil water content (-)
C_H Stanton number (-)	ε emissivity (-)
C_E Dalton number (-)	Θ volumetric soil water content (-)
c_p air heat capacity ($\text{J kg}^{-1} \text{K}^{-1}$)	Θ_{sat} volumetric soil water content at saturation, porosity (-)
q specific humidity (-)	Θ_{FC} volumetric soil water content at field capacity (-)
q_s saturation specific humidity (-)	λ_s soil thermal conductivity ($\text{W m}^{-1} \text{K}^{-1}$)
R_a turbulent atmospheric resistance (s m^{-1})	λ_{dry} soil thermal conductivity for dry soil ($\text{W m}^{-1} \text{K}^{-1}$)
R_s stomata resistance (s m^{-1})	λ_{sat} soil thermal conductivity, soil moisture at saturation ($\text{W m}^{-1} \text{K}^{-1}$)
R_{lwd} long-wave downward radiation (W m^{-2})	ρ air density (kg m^{-3})
R_{swd} short-wave downward radiation (W m^{-2})	σ Stefan Boltzmann constant ($\text{W m}^{-2} \text{K}^{-4}$)
T temperature (K)	ν kinematic viscosity ($\text{m}^2 \text{s}^{-1}$)
T_* dynamic temperature scale (K)	
T_{sfc} surface temperature (K)	
T_{S1} temperature in first soil layer (K)	
u_* friction velocity (ms^{-1})	
z measurement height (m)	
Δz_{S1} thickness of first soil layer (m)	

the small gaps within the forcing data from NamUBT were filled by linear interpolation while larger gaps were filled by linear regression using the data from NAMORS.

2.3.2 Application of the HM model to a shallow lake

The forcing data set for the HM model includes the standard meteorological parameters wind velocity, air temperature,

humidity and air pressure. Radiation measurements are not required for the HM model, instead water surface temperature has to be supplied instead. In this study we used the measured water temperature (Table 1) as an estimate for the water surface temperature.

Wendisch and Foken (1989) investigated the relative error contribution of model parameter, amongst others water temperature, air temperature, air humidity and wind velocity, to

the model output with a sensitivity analysis (Fourier Amplitude Sensitivity Test by Cukier et al. 1978). Assuming typical measurement errors for the initial parameter distribution they estimated that water temperature contributed up to 50 % of the overall error while the influence of wind velocity, air temperature and humidity are comparatively small, each contributing 10–20 % to the error. Since the temperature probe was only shielded against direct (downward) radiation, the effect of diffuse radiation on the accuracy of the water temperature measurements was evaluated. The radiation error has been estimated with a graphical analysis of short term temperature perturbations as related to rapid changes in downward shortwave radiation. Caused by the small fraction of diffuse radiation in the low air density of the Tibetan Plateau and sudden cloud cover changes, the shortwave radiation observations occasionally drop from 1,000 to 150 W m⁻² (or increase in reverse) within a few minutes. The corresponding shifts in water temperature suggest a possible radiation error of approximately 0.2 K. Therefore, water temperature measurements have been accepted for model forcing without correction.

The shallow water parameterisation included in the current version of the HM model accounts for an enhanced turbulent exchange due to increased wave heights in shallow water. Consequently, the turbulent fluxes increase with the mean square wave height (Table 2). Together with the wave height parameterisation after Davidan et al. (1985), additional parameters influence the model results. These are the wind velocity, lake depth and an empirical coefficient, which was set to 2 in this study following Panin et al. (2006b). In this study, the water depth has been estimated as 1.5 m within the average footprint area of the measurement period.

The influence of the shallow water term becomes dominant with increasing wind velocity and decreasing water depth. Calculation of the shallow water equations described in Table 2 with the estimated water depth of 1.5 m and the average wind velocity of 4 ms⁻¹ yields an increase in turbulent fluxes of 14.5 % compared with deep water conditions. Consideration of small changes in wind velocity and water depth yields local sensitivities of roughly 2.9 %/ms⁻¹ of the deep water fluxes/m⁻¹ and -3.9 %/m⁻¹ water depth, respectively. For high wind velocities (10 ms⁻¹) the shallow water extension causes an increase of 30.1 % with sensitivities of 2.4 %/ms⁻¹ and -8.0 %/m water depth. Assuming a typical error of 0.3 ms⁻¹ for wind velocity and variability of the lake depth up to 1 m within the footprint leads to flux uncertainties of 1 and 4 %, respectively. These errors, although not negligible, are within the uncertainty range of the EC flux measurements.

2.3.3 Adaptation of SEWAB

On the Tibetan Plateau, a strong diurnal cycle of the surface temperature during dry periods over bare soil and short

grassland have been observed, which typically leads to an overestimation of surface sensible heat flux (Yang et al. 2009; Hong and Kim 2010). To account for these conditions, SEWAB has been adapted for the Tibetan Plateau by (1) a revised calculation of the soil thermal conductivity as used in Yang et al. (2005), (2) a different formulation of the thermal roughness length after Yang et al. (2008) and (3) by changing the parameterisation of bare soil evaporation according to Mihailović et al. (1993). The formulations can be seen in Table 3.

These changes have been implemented using flux data from NamITP station and flux data from NamUBT corresponding to land surface (Babel et al. 2013), who evaluated this adaptation as an improvement compared with the original version.

SEWAB has been run offline, forced by measurements of precipitation, air temperature, wind velocity, air pressure, relative humidity and downwelling shortwave and longwave radiation. The respective parameters for both land surface types were estimated by a combination from the in-situ measurements and laboratory investigation of soil characteristics (Chen et al. 2012). Surface emissivity, leaf area index and minimum stomatal resistance have been derived from various sources (Yang et al. 2009; Hu et al. 2009; Alapaty et al. 1997)

2.4 Statistics

For evaluation of model performance, simple comparisons were carried out using the bias $B = N^{-1} \sum_{i=1}^N (P_i - O_i)$ and the mean absolute error MAE = $N^{-1} \sum_{i=1}^N |P_i - O_i|$, with O as the observations and P the model predictions.

In equivalence to the MAE, the differences between two time series of predictions can be quantified and we define the desired measure as

$$\delta_{\text{sim}} = N^{-1} \sum_{i=1}^N |P_{1,i} - P_{2,i}| \quad (1)$$

with P_1 and P_2 as predictions from the respective land use types 1 and 2. The Nash–Sutcliffe coefficient (NS) serves as a goodness-of-fit measure

$$\text{NS} = 1 - \frac{\sum_{i=1}^N (P_i - O_i)^2}{\sum_{i=1}^N (O_i - \bar{O})^2} \quad (2)$$

with \bar{O} as the mean of the observations.

3 Results

3.1 Flux measurements

The measured energy fluxes over the lake surface and land (grass^+) show pronounced differences in their magnitude and dynamics. The daytime net radiation is substantially higher over the lake surface, caused by a lower albedo and decreased upwelling longwave radiation due to damped surface temperatures over the lake (Fig. 5c). However, upward radiation components were only measured over the land surface; for the lake surface they were parameterised using an albedo of 0.06 and the lake surface temperature with an emissivity of 0.96.

As expected for the monsoon season on the Tibetan Plateau, the latent heat flux over the land surface was larger than the sensible heat flux (Fig. 5a, b). This observation is in agreement with, e.g. Gu et al. (2005) and Ma and Ma (2006). The mean diurnal cycles of surface and air temperature also show the typical dynamics above land surface, with unstable stratification during daytime but higher surface temperatures are observed over grass^- . Ground heat flux and sensible heat flux are in the same order of magnitude for each land surface again with higher values for grass^- . In consequence, the latent heat flux is lower over this land surface.

The turbulent fluxes over the lake, however, do not show a diurnal cycle, but remain constant over the day. The energy input from radiation is stored in the lake body and is available at any time as indicated by the lake surface temperature in Fig. 5c. No complete energy balance could be estimated over the lake surface, as no measurements exist for the heat storage in the water body and heat fluxes into the sediment.

Evaporation is comparably high for lake surfaces due to high wind velocities of 4 ms^{-1} on average. In addition, high lake surface temperatures, caused by the shallow water table and the small extent of this lake, lead to unstable stratification even during daytime (Fig. 5c). Therefore turbulent exchange is enhanced compared with stable stratification typically found over lake surfaces during daytime (e.g. Beyrich et al. 2006; Nordbo et al. 2011).

3.2 Model performance

Different measures for model performance are summarised in Table 4. The results from grass^+ simulations show reasonable performance, although there are only few observations left after filtering, separation and energy balance closure correction (Fig. 6). In case of the EBC-Bo-corrected observations, the latent heat flux is slightly underestimated while the simulation of the sensible heat flux resembles the measurements quite well. The opposite is true when using the buoyancy flux method for energy balance closure correction (EBC-HB). The correlation is affected in a similar way. Good R^2 values are achieved for the sensible heat flux corrected using EBC-Bo and latent heat flux corrected using EBC-HB, and they decrease for the other two cases. Lake surface modelling yields reasonable coherence to the EC observations within the footprint of the measurements, with a bias of -23.3 and -2.7 W m^{-2} for the latent heat flux Q_E and the sensible heat flux Q_H , respectively.

For grass^- at NamITP, mean absolute errors for sensible heat flux are larger, mainly caused by the bias, although a good correlation is obtained in the case of EBC-Bo corrected observations. Aside from model deficiencies, the reason for

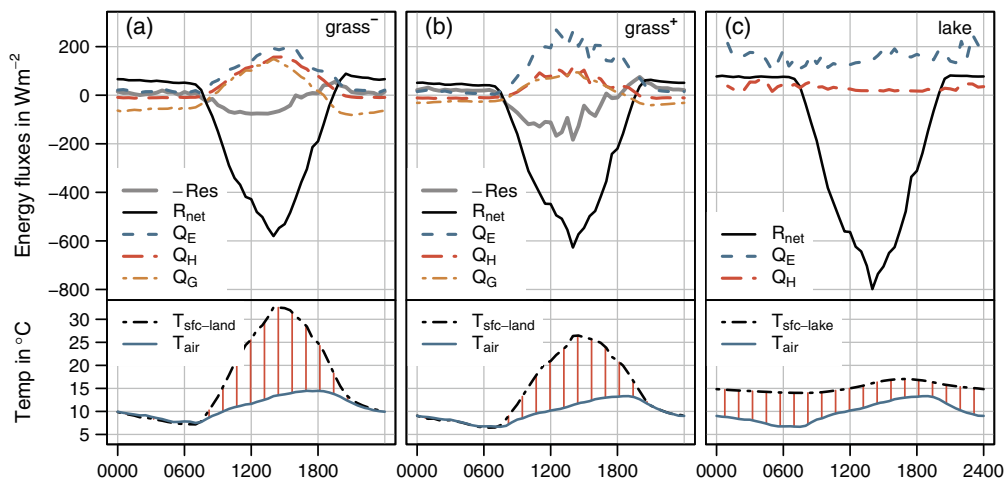


Fig. 5 Mean diurnal energy fluxes for the whole measurement period, separated for **a** grass^- , **b** grass^+ and **c** lake; for land surfaces, all components are measured; lake fluxes, the net radiation is calculated from measured downwelling radiation and using an albedo of 0.06 and

the lake surface temperature with an emissivity of 0.96; the lower panel shows diurnal surface and air temperature. The time axis is displayed in Beijing standard time (CST), mean local solar noon during the observation period is at 1400 CST

Table 4 Model performance of turbulent fluxes for the three land use types and two energy balance correction methods for the land observations: number of observations, bias, mean absolute error (MAE), offset

Flux	Land use	EBC	Number of observations	Bias (W m^{-2})	MAE (W m^{-2})	Offset (W m^{-2})	Slope (-)	NS (-)	R^2 (-)
Q_H	Grass ⁻	Bo	627	52.2	55.5	36.8	1.13	0.26	0.80
		HB	572	38.3	55.5	36.9	1.01	0.36	0.62
	Grass ⁺	Bo	81	18.5	23.8	17.2	1.02	0.61	0.78
		HB	71	-24.4	40.5	12.9	0.7	0.38	0.52
Q_E	Lake	-	327	-2.7	7.6	5.3	0.72	0.75	0.79
		Grass ⁻	Bo	627	-10.8	45.3	-8.6	0.99	0.70
	Grass ⁻	HB	572	-0.4	42.0	-14.3	1.1	0.68	0.74
		Grass ⁺	Bo	81	-28.6	50.8	13.5	0.77	0.60
	Grass ⁺	HB	71	1.7	23.4	5.4	0.98	0.82	0.82
		Lake	-	392	-23.3	30.3	-8.5	0.9	0.50

and slope from linear regression (mean geometric regression) as well as Nash–Sutcliffe coefficient (NS) and R^2

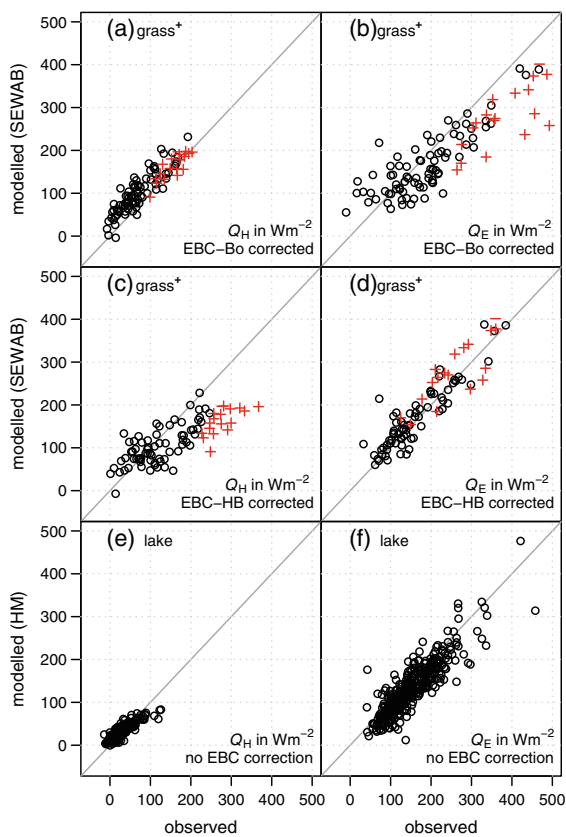


Fig. 6 Scatterplots of modelled and observed turbulent fluxes. For land surface flux observations (grass⁺) vs. SEWAB model simulations, observations are energy balance corrected with the Bowen ratio method (a, b) and with the buoyancy method (c, d). Turbulent fluxes without EBC correction over lake vs. HM model runs (e, f). Model performance is indicated with the Nash–Sutcliffe coefficient, bias and the squared Pearson correlation coefficient. Red crosses indicated data excluded because of residuals $-\text{Res} > 150 \text{ W m}^{-2}$

the remaining bias can be attributed to uncertainties in estimation of the observed ground heat flux due to high gravel content in the soil and a lack of temperature measurements in the topmost soil layer.

3.3 Footprint and spatial integration

In the previous section, we have shown that eddy-covariance measurements, selected according to their footprint as pure fluxes from each surface type, can be represented by SEWAB in case of grassland and by the HM model in case of the lake surface. However, a part of the measurements show contributions from more than one land use type as well. The footprint concept enables us to link the simulations even with such observations. For each time step, the footprint approach provides the relative contribution of all involved surfaces to the measured fluxes. The simulations are then related to the observations by calculating a weighted mean from the output of both models according to the actual land use contribution. This is shown with the footprint integrated simulations for lake and grass⁺ together with the EC observations at NamUBT in Fig. 7 for three different situations: 17 July—changing conditions under moderate wind velocities, 5 August—typical day with land–lake circulation and moderate winds of about $2\text{--}6 \text{ ms}^{-1}$ and 6 August—situation with larger than average wind speeds of about 6 ms^{-1} . In all selected situations the eddy-covariance measurements can be closely modelled by the footprint integrated simulation. This also holds for measurements with contributions from both surfaces, seen in some events on 17 July and 5 August. Instantaneous turbulent fluxes can show differences of up to 200 W m^{-2} because of the different exchange of each surface with its atmosphere over the course of the day. The performance of the footprint-integrated simulation is displayed in Fig. 8 for the whole period. Situations with contributions from both surface types larger than 20 %

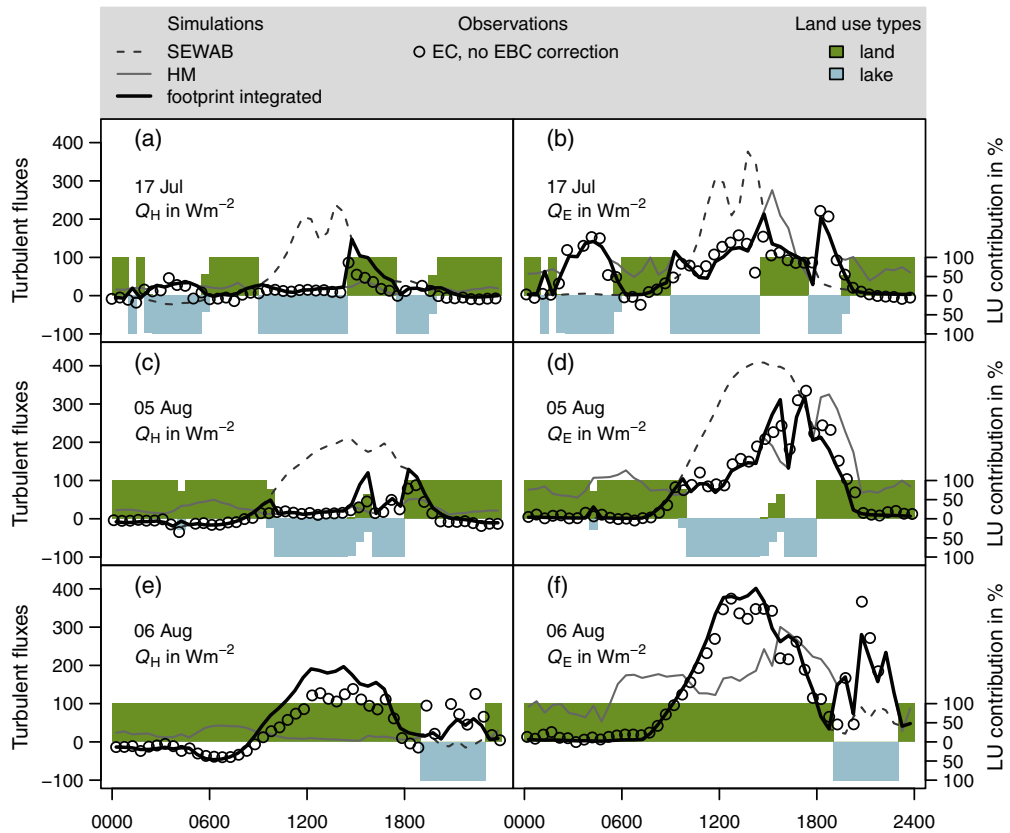


Fig. 7 Source weight integrated modelled fluxes at NamUBT, 17 July (a, b), 5 August (c, d) and 6 August (e, f). Displayed are simulated fluxes with SEWAB (dashed line) and HM (solid grey line) and integrated simulations (solid black line) according to contributions of lake or land within the footprint. Observations (not energy balance

corrected) are shown as black circles. The land use contribution in percent is indicated as bar plot, with upwind situations from the land in green and upwind situations from lake in blue. The time axis is displayed in Beijing standard time (CST); mean local solar noon during the observation period is at 1400 CST

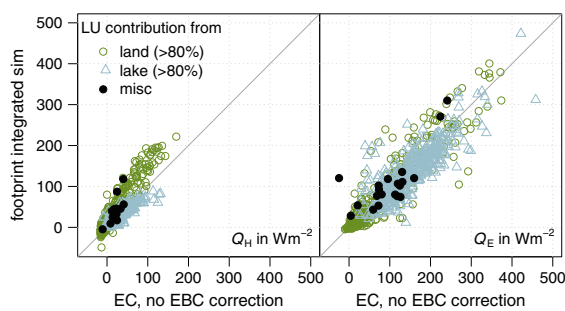


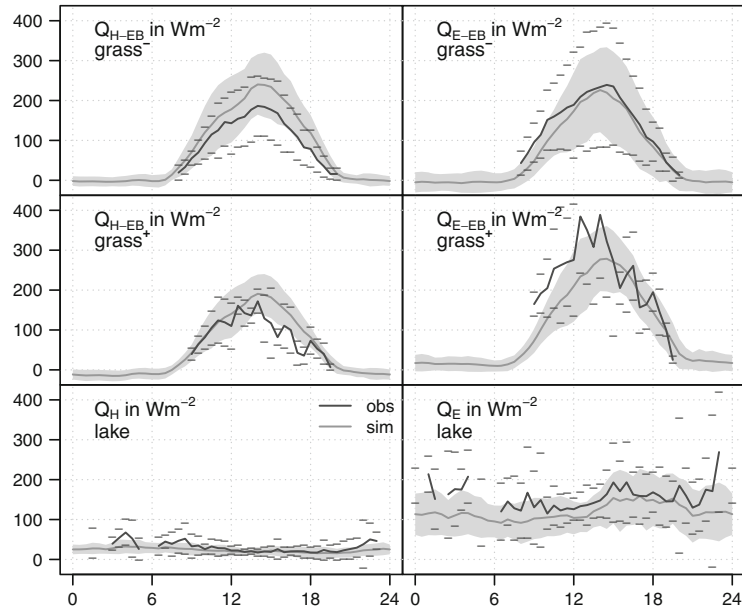
Fig. 8 Observations vs. footprint integrated model simulations at NamUBT. Three classes of data are presented, cases with a greater contribution than 80 % of one land use type are considered as representative. The misc cases contain all fluxes with a contribution less than 80 % for both land use types. Since no EBC correction could be performed for the lake data, all data are shown without correction for better inter comparison

(misc) are highlighted. The simulations for such situations follow the same pattern as simulations for the pure surface types (contribution of a single surface greater than 80 %). Miscellaneous footprints, however, did not occur for situations with very high fluxes.

3.4 Flux heterogeneity at Nam Co

It is well known that heterogeneous surfaces affect the landscape scale fluxes. The presented measurements have shown that the fluxes over land and lake surfaces behave differently. To consider the most abundant surfaces near Nam Co station, grass⁻ at NamITP has also been included in addition to the observations and simulations of grass⁺ and lake at NamUBT. Figure 9 shows the mean diurnal cycles of measured fluxes, corrected with EBC-Bo for land surfaces, and modelled fluxes. The model simulations resemble the observed characteristics of the different surfaces in a reasonable sense.

Fig. 9 Mean diurnal cycles for the whole measurement period. Observed fluxes (corrected with EBC-Bo) are denoted by *black solid lines*, the *horizontal bars* indicate the respective standard deviation; *grey lines* show the modelled fluxes with standard deviations given by the *grey shaded area*. The time axis is displayed in Beijing standard time (CST); mean local solar noon during the observation period is at 1400 CST



Since simulations overestimated the sensible heat flux for both land surfaces, the differences between land use types were maintained.

The obvious differences in characteristics of the investigated surfaces, especially between land and lake, are also reflected in mean fluxes for the whole period (Fig. 10). The two land surface types already differ in the longwave radiation balance. As expected, the mean latent heat flux became

more dominant with increasing soil moisture for the land surfaces. The evaporation over the small lake is even higher, due to its shallow water table resulting in comparatively high surface temperatures. Mean differences of sensible and latent heat flux between grass⁺ and grass⁻ are 24.0 and -33.5 W m⁻², respectively, and between grass⁺ and lake are -27.3 and 22.3 W m⁻², respectively.

Furthermore, we investigated whether these mean differences were substantial with respect to the performance of the simulation. Table 5 displays the mean absolute differences δ_{sim} between grass⁺ and the other two surface types. As δ_{sim} is calculated for the data subset used to evaluate the model performance at grass⁺ ($n=81$ for EBC-Bo and $n=71$ for EBC-HB), it can be compared directly to the respective MAE for grass⁺. When comparing the sensible heat flux of the two land surfaces, mean differences between simulations slightly exceed the respective MAE, and it is substantially higher in the other cases, especially between the lake surface and grass⁺. Obviously, this also holds true when comparing grass⁻ with lake (not shown). This suggests that the differences in fluxes between land use types exceed the uncertainty with respect to model simulation.

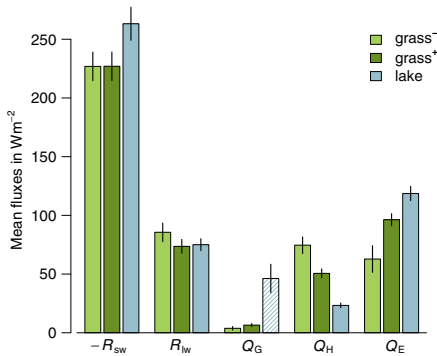


Fig. 10 Mean fluxes for the three surface types (grass⁻, grass⁺ and lake) from observation-based simulations. Land surfaces fluxes are SEWAB output. Net shortwave radiation (R_{sw}) and net longwave radiation (R_{lw}) for the lake surface are calculated as explained in Fig. 5. The residual of the lake energy balance is shown as hatched bar (Q_g); it sums up the energy fluxes not accounted for, e.g. storage change in the water body and flux into the sediment. For land surface fluxes, Q_g represents the ground heat flux. *Error bars* indicate 1.96 times the standard error of the mean, based on daily mean fluxes; assuming normal distribution and statistical independence of daily mean fluxes, the *bars* would correspond to the 95 % confidence interval

4 Conclusions

Turbulent fluxes over wet grassland and a shallow lake were measured with a single eddy-covariance complex at a shallow lake in the Nam Co basin during the monsoon season in 2009. The measurements were split up according to the underlying surface by footprint analysis, and the coordinate

Table 5 Mean absolute differences (δ_{sim}) between simulations of grass⁺ and the other two land use types: grass⁻ and lake

	Q_H	Q_E
Grass ⁺ –grass ⁻	43.3 (81)	59.5 (81)
	45.9 (71)	59.1 (71)
Grass ⁺ –lake	76.1 (81)	68.1 (81)
	83.5 (71)	57.8 (71)

Numbers in parentheses are the number of data points used, corresponding to the number of observations used to calculate the MAE for grass⁺ in Table 4

rotation for this non-flat terrain has been successfully performed with a sector-wise application of the planar-fit method. Energy balance closure algorithms were deployed, and gap-free time series were derived by surface modelling. We showed that the modelled time series can be linked to the measurements by integration according to the contribution of each surface type. Finally, this data set was compared with observed and modelled fluxes from the nearby ITP station with a target land use of dry grassland. Sharp differences in characteristics of turbulent fluxes from the three dominant land use types found in close vicinity to the lake were revealed.

Both models we used, HM and SEWAB, are able to reproduce the characteristics, magnitude and dynamics reasonably well without deploying optimisation algorithms. There are no parameters which need to be tuned for the HM model except the lake depth. The sensitivity and error analysis for the HM model suggests that expected errors do not exceed the measurement uncertainty of eddy-covariance fluxes. The model parameters for SEWAB have been constrained by measurements. However, a bias remains, in particular at the grass⁻ site. This depends not only on model deficiencies, but on the method applied for the energy balance closure correction as well. As long as the underlying mechanism causing the gap is not specified clearly (Foken et al. 2011), this error cannot be exactly determined. On the other hand, measurements of available energy are prone to errors as well, especially in the estimation of the ground heat flux. Nonetheless, it was shown that the differences among land use types of dry grassland, wet grassland and lake exceed the simulation errors. We therefore assume that the simulated time series are able to resolve the differences between the land use types involved here.

The footprint (source weight) integrated modelled fluxes resemble the observations at NamUBT reasonably well, even for conditions where both lake and grass⁺ contribute to the measured flux. With the tile approach, a grid cell with edge lengths of 1–5 km can be directly linked to the simulation as long as the relative contribution of each land use type is known for this cell. Our finding shows that the tile approach is valid in this terrain for spatial integration. Therefore, representative flux simulations can be given for each time step for comparison with remote sensing data.

The measurements over dry grassland at NAMORS are considered to be a reference for the land surface exchange in the Nam Co region. However, in regional estimates the pronounced differences in the fluxes from the three investigated surface types make it obvious that the fluxes above the lake and moist grassland should be taken into account as well. Daytime turbulent fluxes over the lake surface can differ from the land surface fluxes up to 200 W m⁻². Therefore the land use distribution within a remote sensing pixel or grid cell for mesoscale modelling has to be carefully determined before validating with the dry grassland station. This potential representation error can be reduced by integrating the simulated fluxes of adjacent land use types according to their contribution to the respective grid cell.

The conducting of eddy covariance measurements over lake surfaces on the Tibetan Plateau poses a rarely met challenge. Nevertheless, more accurate flux estimates will be necessary since a significant fraction of the Tibetan Plateau is covered with lakes of various sizes and therefore different characteristics. Based on this study, we can conclude that theoretical requirements for eddy covariance are not substantially violated by the topography at the shoreline station and that the data can be accepted for the HM model validation. Unfortunately, data from the lake surface was only available for unstable and neutral stratification. We showed that the HM model can be used to estimate lake evaporation for these conditions at a high-quality standard and a temporal resolution, even resolving the diurnal course. This can be derived from standard land-based meteorological measurements, and a representative surface temperature being the only measurement required directly from the lake. Lake surface exchange under stable conditions, however, could not be validated, but the results from Panin et al. (2006b) indicate reasonable performance also for stable conditions. On the other hand, due to the prevailing high wind velocities, strong stable stratification above lake surfaces on the Tibetan Plateau is unlikely. However, temperature profile measurements at different locations in the lake (and sediment, where indicated) would be a costly but valuable addition to estimate necessary storage terms and thereby the observed energy balance closure. Especially for large lakes like the Nam Co, the estimation of water temperature requires more efforts since multiple locations within the lake should be sampled.

Acknowledgements This work was funded by the German Research Foundation (Deutsche Forschungsgemeinschaft (DFG)) Priority Programme 1372 “Tibetan Plateau: Formation, Climate, Ecosystems”(TiP) and CEOP-AEGIS, a Collaborative Project/Small or medium-scale focused research project—Specific International Co-operation Action coordinated by the University of Strasbourg, France and funded by the European Commission under FP7 topic ENV.2007.4.1.4.2 “Improving observing systems for water resource management”. The authors would like to thank everybody who participated in the collection of the data on the Tibetan Plateau, especially the colleagues from the ITP for logistical support during the field campaign. Furthermore, the authors acknowledge H.T. Mengelkamp for providing the source code of SEWAB. The publication costs including open access was funded by the German Research Foundation.

Open Access This article is distributed under the terms of the Creative Commons Attribution License which permits any use, distribution, and reproduction in any medium, provided the original author(s) and the source are credited.

References

- Alapaty K, Pleim JE, Raman S, Niyogi DS, Byun DW (1997) Simulation of atmospheric boundary layer processes using local- and nonlocal-closure schemes. *J Appl Meteorol* 36(3):214–233. doi:10.1175/1520-0450(1997)036<0214:SOABLP>2.0.CO;2
- Babel W, Chen Y, Biermann T, Yang K, Ma Y, Foken T (2013) Adaptation of a land surface scheme for modeling turbulent fluxes on the Tibetan Plateau under different soil moisture conditions. *J Geophys Res* (in press)
- Beyrich F, Leps J, Mauder M, Bange J, Foken T, Huneke S, Lohse H, Lüdi A, Meijninger WML, Mironov D, Weissenböck U, Zittel P (2006) Area-averaged surface fluxes over the LITFASS region based on eddy-covariance measurements. *Boundary-Layer Meteorol* 121(1):33–65. doi:10.1007/s10546-006-9052-x
- Biermann T, Babel W, Olesch J, Foken T (2009) Documentation of the micrometeorological experiment, Nam Tso, Tibet, 25th of June–8th of August 2009. Work Report University of Bayreuth, Dept. of Micrometeorology. ISSN 1614-8916, 41, 38 pp., URL <http://opus.uni-bayreuth.de/opus4-ubbayreuth/frontdoor/index/index/docId/626>
- Boos WR, Kuang Z (2010) Dominant control of the South Asian monsoon by orographic insulation versus plateau heating. *Nature* 463(7278):218–222. doi:10.1038/nature08707
- Chen Y, Yang K, Tang W, Qin J, Zhao L (2012) Parameterizing soil organic carbon's impacts on soil porosity and thermal parameters for Eastern Tibet grasslands. *Sci China Earth Sci* 55:1001–1011. doi:10.1007/s11430-012-4433-0
- Clapp RB, Hornberger GM (1978) Empirical equations for some soil hydraulic properties. *Water Resour Res* 14(4):601–604
- Cukier R, Levine H, Shuler K (1978) Nonlinear sensitivity analysis of multi-parameter model systems. *J Comput Phys* 26(1):1–42. doi:10.1016/0021-9991(78)90097-9
- Davidan I, Lopatuhin L, Rogkov V (1985) *Volny v okeane* (waves in the ocean). Gidrometeoizdat, Leningrad, 256 pp
- Finnigan J, Clement R, Malhi Y, Leuning R, Cleugh H (2003) A re-evaluation of long-term flux measurement techniques, part I: averaging and coordinate rotation. *Bound-Lay Meteorol* 107:1–48. doi:10.1023/A:1021554900225
- Foken T (1979) Vorschlag eines verbesserten Energieaustauschmodells mit Berücksichtigung der molekularen Grenzschicht der Atmosphäre. *Z Meteorol* 29:32–39
- Foken T (1984) The parameterisation of the energy exchange across the air–sea interface. *Dynam Atmos Oceans* 8(3–4):297–305. doi:10.1016/0377-0265(84)90014-9
- Foken T (1986) An operational model of the energy exchange across the air–sea interface. *Z Meteorol* 36:354–359
- Foken T (2008) The energy balance closure problem: an overview. *Ecol Appl* 18(6):1351–1367, URL <http://www.jstor.org/stable/40062260>
- Foken T, Skeib G (1983) Profile measurements in the atmospheric near-surface layer and the use of suitable universal functions for the determination of the turbulent energy exchange. *Bound-Lay Meteorol* 25:55–62. doi:10.1007/BF00122097
- Foken T, Wichura B (1996) Tools for quality assessment of surface-based flux measurements. *Agr Forest Meteorol* 78(1–2):83–105
- Foken T, Göckede M, Mauder M, Mahrt L, Amiro B, Munger W (2004) Post-field data quality control. In: Lee X, Massman W, Law B (eds) *Handbook of micrometeorology*. Kluwer, Dordrecht, pp 181–208
- Foken T, Mauder M, Liebethal C, Wimmer F, Beyrich F, Leps JP, Raasch S, DeBruin H, Meijninger W, Bange J (2010) Energy balance closure for the LITFASS-2003 experiment. *Theor Appl Climatol* 101:149–160. doi:10.1007/s00704-009-0216-8
- Foken T, Aubinet M, Finnigan JJ, Leclerc MY, Mauder M, Paw UKT (2011) Results of a panel discussion about the energy balance closure correction for trace gases. *B Am Meteorol Soc* 92(4):ES13–ES18. doi:10.1175/2011BAMS3130.1
- Foken T, Leuning R, Oncley SR, Mauder M, Aubinet M (2012) Corrections and data quality control. In: Aubinet M, Vesala T, Papale D (eds) *Eddy covariance: a practical guide to measurement and data analysis*. Springer, Dordrecht, pp 85–131. doi:10.1007/978-94-007-2351-1_4
- Frauenfeld OW, Zhang T, Serreze MC (2005) Climate change and variability using European Centre for Medium-Range Weather Forecasts reanalysis (ERA-40) temperatures on the Tibetan Plateau. *J Geophys Res* 110(D2):D02101. doi:10.1029/2004JD005230
- Gerken T, Babel W, Hoffmann A, Biermann T, Herzog M, Friend AD, Li M, Ma Y, Foken T, Graf HF (2012) Turbulent flux modelling with a simple 2-layer soil model and extrapolated surface temperature applied at Nam Co lake basin on the Tibetan Plateau. *Hydrol Earth Syst Sci* 16(4):1095–1110. doi:10.5194/hess-16-1095-2012
- Göckede M, Rebmann C, Foken T (2004) A combination of quality assessment tools for eddy covariance measurements with footprint modelling for the characterisation of complex sites. *Agr Forest Meteorol* 127(3–4):175–188. doi:10.1016/j.agrformet.2004.07.012
- Göckede M, Foken T, Aubinet M, Aurela M, Banza J, Bernhofer C, Bonnefond JM, Brunet Y, Carrara A, Clement R, Dellwik E, Elbers J, Eugster W, Fuhrer J, Granier A, Grunwald T, Heinesch B, Janssens IA, Knohl A, Koeble R, Laurila T, Longdoz B, Manca G, Marek M, Markkanen T, Mateus J, Matteucci G, Mauder M, Migliavacca M, Minerbi S, Moncrieff J, Montagnani L, Moors E, Ourcival JM, Papale D, Pereira J, Pilegaard K, Pita G, Rambal S, Rebmann C, Rodrigues A, Rotenberg E, Sanz MJ, Sedlak P, Seufert G, Siebicke L, Soussana JF, Valentini R, Vesala T, Verbeeck H, Yakir D (2008) Quality control of carboEurope flux data—part 1: coupling footprint analyses with flux data quality assessment to evaluate sites in forest ecosystems. *Biogeosciences* 5(2):433–450. doi:10.5194/bg-5-433-2008
- Gu S, Tang Y, Cui X, Kato T, Du M, Li Y, Zhao X (2005) Energy exchange between the atmosphere and a meadow ecosystem on the Qinghai–Tibetan Plateau. *Agr and Forest Meteorol* 129(3–4):175–185. doi:10.1016/j.agrformet.2004.12.002
- Haginoya S, Fujii H, Kuwagata T, Xu J, Ishigooka Y, Kang S, Zhang Y (2009) Air-lake interaction features found in heat and water exchanges over Nam Co on the Tibetan Plateau. *Sola* 5:172–175. doi:10.2151/sola.2009-044
- Hong J, Kim J (2010) Numerical study of surface energy partitioning on the Tibetan Plateau: comparative analysis of two biosphere models. *Biogeosciences* 7(2):557–568. doi:10.5194/bg-7-557-2010
- Hu Z, Yu G, Zhou Y, Sun X, Li Y, Shi P, Wang Y, Song X, Zheng Z, Zhang L, Li S (2009) Partitioning of evapotranspiration and its controls in four grassland ecosystems: application of a two-source model. *Agr Forest Meteorol* 149(9):1410–1420. doi:10.1016/j.agrformet.2009.03.014
- Huang Z, Xue B, Yao S, Pang Y (2008) Lake evolution and its implication for environmental changes in China during 1950–2000. *J Geogr Sci* 18(2):131–141. doi:10.1007/s11442-008-0131-4
- Immerzeel WW, van Beek LPH, Bierkens MFP (2010) Climate change will affect the Asian water towers. *Science* 328(5984):1382–1385. doi:10.1126/science.1183188
- Ingwersen J, Steffens K, Högy P, Warrach-Sagi K, Zhunusbayeva D, Poltoradnev M, Gäbler M, Wizeemann HD, Fangmeier A, Wulfmeyer V, Streck T (2011) Comparison of Noah simulations

- with eddy covariance and soil water measurements at a winter wheat stand. *Agr Forest Meteorol* 151(3):345–355. doi:10.1016/j.agrformet.2010.11.010
- Kang S, Xu Y, You Q, Flügel W, Pepin N, Yao T (2010) Review of climate and cryospheric change in the Tibetan Plateau. *Environ Res Lett* 5(1):15101
- Keil A, Berking J, Mügler I, Schütt B, Schwalb A, Steeb P (2010) Hydrological and geomorphological basin and catchment characteristics of Lake Nam Co, South-Central Tibet. *Quat Int* 218(1–2):118–130. doi:10.1016/j.quaint.2009.02.022
- Kracher D, Mengelkamp HT, Foken T (2009) The residual of the energy balance closure and its influence on the results of three SVAT models. *Meteorol Z* 18(6):1–15. doi:10.1127/0941-2948/2009/0412
- Krause P, Biskop S, Helmschrot J, Flügel W, Kang S, Gao T (2010) Hydrological system analysis and modelling of the Nam Co basin in Tibet. *Adv Geosci* 27:29–36. doi:10.5194/adgeo-27-29-2010
- Liu J, Kang S, Gong T, Lu A (2010) Growth of a high-elevation large inland lake, associated with climate change and permafrost degradation in Tibet. *Hydrol Earth Syst Sci* 14(3):481–489. doi:10.5194/hess-14-481-2010
- Louis J (1979) A parametric model of vertical eddy fluxes in the atmosphere. *Bound-Lay Meteorol* 17:187–202. doi:10.1007/BF00117978
- Lüers J, Bareiss J (2010) The effect of misleading surface temperature estimations on the sensible heat fluxes at a high arctic site—the arctic turbulence experiment 2006 on Svalbard (ARCTEX-2006). *Atmos Chem Phys* 10(1):157–168. doi:10.5194/acp-10-157-2010
- Ma W, Ma Y (2006) The annual variations on land surface energy in the northern Tibetan Plateau. *Environ Geol* 50(5):645–650. doi:10.1007/s00254-006-0238-9
- Ma Y, Su Z, Koike T, Yao T, Ishikawa H, Ueno K, Menenti M (2003) On measuring and remote sensing surface energy partitioning over the Tibetan Plateau—from GAME/Tibet to CAMP/Tibet. *Appl Quant Remote Sensing Hydrol* 28(1–3):63–74. doi:10.1016/S1474-7065(03)00008-1
- Ma Y, Fan S, Ishikawa H, Tsukamoto O, Yao T, Koike T, Zuo H, Hu Z, Su Z (2005) Diurnal and inter-monthly variation of land surface heat fluxes over the central Tibetan Plateau area. *Theor Appl Climatol* 80(2–4):259–273. doi:10.1007/s00704-004-0104-1
- Ma Y, Wang Y, Wu R, Hu Z, Yang K, Li M (2009) Recent advances on the study of atmosphere-land interaction observations on the Tibetan Plateau. *Hydrol Earth Syst Sci* 13(7): 1103–1111
- Mauder M, Foken T (2004) Documentation and instruction manual of the eddy covariance software package TK2. Work Report University of Bayreuth, Dept. of Micrometeorology, ISSN 1614–8916, 26, 42 pp., URL <http://opus.ub.uni-bayreuth.de/opus4-ubbayreuth/frontdoor/index/index/docId/639>
- Mauder M, Foken T (2006) Impact of post-field data processing on eddy covariance flux estimates and energy balance closure. *Meteorol Z* 15(13):597–609. doi:10.1127/0941-2948/2006/0167
- Mauder M, Foken T (2011) Documentation and instruction manual of the eddy-covariance software package TK3. Work Report University of Bayreuth, Dept. of Micrometeorology, ISSN 1614–8916, 46, 58 pp., URL <http://opus.ub.uni-bayreuth.de/opus4-ubbayreuth/frontdoor/index/index/docId/681>
- Mauder M, Foken T, Clement R, Elbers JA, Eugster W, Grünwald T, Heusinkveld B, Kolle O (2008) Quality control of CarboEurope flux data—part 2: inter-comparison of eddy-covariance software. *Biogeosciences* 5(2):451–462. doi:10.5194/bg-5-451-2008
- Mausson F, Scherer D, Finkelnburg R, Richters J, Yang W, Yao T (2011) WRF simulation of a precipitation event over the Tibetan Plateau, China—an assessment using remote sensing and ground observations. *Hydrol Earth Syst Sci* 15(6):1795–1817. doi:10.5194/hess-15-1795-2011
- Mengelkamp HT, Warrach K, Raschke E (1999) SEWAB—a parameterization of the surface energy and water balance for atmospheric and hydrologic models. *Adv Water Resour* 23(2):165–175. doi:10.1016/S0309-1708(99)00020-2
- Mengelkamp HT, Kiely G, Warrach K (2001) Evaluation of the hydrological components added to an atmospheric land-surface scheme. *Theor Appl Climatol* 69(3–4):199–212. doi:10.1007/s007040170025
- Metzger S, Ma Y, Markkanen T, Göckede M, Li M, Foken T (2006) Quality assessment of Tibetan Plateau eddy covariance measurements utilizing footprint modeling. *Adv Earth Sci* 21(12):1260–1267
- Mihailović DT, Pielke RA, Rajković B, Lee TJ, Jeftić M (1993) A resistance representation of schemes for evaporation from bare and partly plant-covered surfaces for use in atmospheric models. *J Appl Meteorol* 32(6):1038–1054. doi:10.1175/1520-0450(1993)032<1038:ARROSF>2.0.CO;2
- Molnar P, Boos WR, Battisti DS (2010) Orographic controls on climate and Paleoclimate of Asia: thermal and mechanical roles for the Tibetan Plateau. *Annu Rev Earth Planet Sci* 38(1):77–102. doi:10.1146/annurev-earth-040809-152456
- Mügler I, Gleixner G, Günther F, Mäusbacher R, Daut G, Schütt B, Berking J, Schwalb A, Schwark L, Xu B, Yao T, Zhu L, Yi C (2010) A multi-proxy approach to reconstruct hydrological changes and Holocene climate development of Nam Co, Central Tibet. *J Paleolimnol* 43(4):625–648. doi:10.1007/s10933-009-9357-0
- Ni J (2011) Impacts of climate change on Chinese ecosystems: key vulnerable regions and potential thresholds. *Reg Environ Chang* 11(1):49–64. doi:10.1007/s10113-010-0170-0
- Noilhan J, Planton S (1989) A simple parameterization of land surface processes for meteorological models. *Mon Weather Rev* 117(3):536–549. doi:10.1175/1520-0493(1989)117<0536:ASPOLS>2.0.CO;2
- Nordbo A, Launiainen S, Mammarella I, Lepparanta M, Huotari J, Ojala A, Vesala T (2011) Long-term energy flux measurements and energy balance over a small boreal lake using eddy covariance technique. *J Geophys Res* 116(D2):D02119
- Panin GN, Foken T (2005) Air–sea interaction including a shallow and coastal zone. *J Atmos Ocean Sci* 10(3):289–305. doi:10.1080/17417530600787227
- Panin GN, Nasonov AE, Foken T (2006a) Evaporation and heat exchange of a body of water with the atmosphere in a shallow zone. *Izv Atmos Ocean Phys* 42(3):337–352. doi:10.1134/S0001433806030078
- Panin GN, Nasonov AE, Foken T, Lohse H (2006b) On the parameterization of evaporation and sensible heat exchange for shallow lakes. *Theor Appl Climatol* 85:123–129. doi:10.1007/s00704-005-0185-5
- Paw UK, Baldocchi D, Meyers T, Wilson K (2000) Correction of eddy-covariance measurements incorporating both advective effects and density fluxes. *Bound-Lay Meteorol* 97:487–511. doi:10.1023/A:1002786702909
- Rannik U, Aubinet M, Kurbanmuradov O, Sabelfeld KK, Markkanen T, Vesala T (2000) Footprint analysis for measurements over a heterogeneous forest. *Bound-Lay Meteorol* 97(1):137–166. doi:10.1023/A:1002702810929
- Rebmann C, Kolle O, Heinesch B, Queck R, Ibrom A, Aubinet M, Vesala T, Papale D (eds) Eddy covariance. Springer, Amsterdam, pp 59–83
- Rouse WR, Oswald CJ, Binyamin J, Spence C, Schertzer WM, Blanken PD, Bussi eres N, Duguay CR (2005) The role of Northern Lakes in a regional energy balance. *J Hydrometeorol* 6(3):291–305. doi:10.1175/JHM421.1
- Twine TE, Kustas WP, Norman JM, Cook DR, Houser PR, Meyers TP, Prueger JH, Starks PJ, Wesely ML (2000) Correcting eddy-covariance flux underestimates over a grassland. *Agr Forest Meteorol* 103(3):279–300. doi:10.1016/S0168-1923(00)00123-4

- Wendisch M, Foken T (1989) Sensitivity test of a multilayer energy exchange model. *Z Meteorol* 39:36–39
- Wilczak J, Oncley S, Stage S (2001) Sonic anemometer tilt correction algorithms. *Bound-Lay Meteorol* 99:127–150. doi:10.1023/A:1018966204465
- Wu Y, Zhu L (2008) The response of lake-glacier variations to climate change in Nam Co Catchment, central Tibetan Plateau, during 1970–2000. *J Geogr Sci* 18(2):177–189. doi:10.1007/s11442-008-0177-3
- Xu J, Haginoya S (2001) An estimation of heat and water balances in the Tibetan Plateau. *J Meteorol Soc Jpn* 79(1B):485–504. doi:10.2151/jmsj.79.485
- Xu J, Yu S, Liu J, Haginoya S, Ishigooka Y, Kuwagata T, Hara M, Yasunari T (2009) The implication of heat and water balance changes in a lake basin on the Tibetan Plateau. *Hydrol Res Lett* 3:1–5. doi:10.3178/hrl.3.1
- Yang K, Koike T, Ye B, Bastidas L (2005) Inverse analysis of the role of soil vertical heterogeneity in controlling surface soil state and energy partition. *J Geophys Res* 110(D8):D08101. doi:10.1029/2004JD005500
- Yang K, Chen YY, Qin J (2009) Some practical notes on the land surface modeling in the Tibetan Plateau. *Hydrol Earth Syst Sci* 13(5):687–701. doi:10.5194/hess-13-687-2009
- Yang K, Koike T, Ishikawa H, Kim J, Li X, Liu H, Wang J, Liu S, Ma Y (2008) Turbulent flux transfer over bare-soil surfaces: characteristics and parameterization. *J Appl Meteorol Clim* 47:276–290. doi:10.1175/2007JAMC1547.1
- Yang K, Ye B, Zhou D, Wu B, Foken T, Qin J, Zhou Z (2011) Response of hydrological cycle to recent climate changes in the Tibetan Plateau. *Clim Chang* 109(3–4):517–534. doi:10.1007/s10584-011-0099-4
- Yu S, Liu J, Xu J, Wang H (2011) Evaporation and energy balance estimates over a large inland lake in the Tibet–Himalaya. *Environ Earth Sci* 64(4):1169–1176. doi:10.1007/s12665-011-0933-z
- Zhao L, Li J, Xu S, Zhou H, Li Y, Gu S, Zhao X (2010) Seasonal variations in carbon dioxide exchange in an alpine wetland meadow on the Qinghai-Tibetan Plateau. *Biogeosciences* 7(4):1207–1221. doi:10.5194/bg-7-1207-2010
- Zhou D, Eigenmann R, Babel W, Foken T, Ma Y (2011) The study of near-ground free convection conditions at Nam Co station on the Tibetan Plateau. *Theor Appl Climatol* 105(1–2):217–228. doi:10.1007/s00704-010-0393-5
- Zhu L, Xie M, Wu Y (2010) Quantitative analysis of lake area variations and the influence factors from 1971 to 2004 in the Nam Co basin of the Tibetan Plateau. *Chin Sci Bull* 55(13):1294–1303. doi:10.1007/s11434-010-0015-8

C. Gerken et al. (2014)

Gerken, T., Biermann, T., Babel, W., Herzog, M., Ma, Y., Foken, T., Graf, HF.: A modelling investigation into lake-breeze development and convection triggering in the Nam Co Lake basin, Tibetan Plateau, *Theor. Appl. Climatol.*, 117(1-2), 149-167 doi:10.1007/s00704-013-0987-9, 2014. ¹

¹published with kind permission of (C) Springer Science and Business Media

A modelling investigation into lake-breeze development and convection triggering in the Nam Co Lake basin, Tibetan Plateau

Tobias Gerken · Tobias Biermann · Wolfgang Babel · Michael Herzog · Yaoming Ma · Thomas Foken · Hans-F. Graf

Received: 3 April 2013 / Accepted: 25 July 2013 / Published online: 25 August 2013
© Springer-Verlag Wien 2013

Abstract This paper uses the cloud resolving Active Tracer High-resolution Atmospheric Model coupled to the interactive surface model Hybrid in order to investigate the diurnal development of a lake-breeze system at the Nam Co Lake on the Tibetan Plateau. Simulations with several background wind speeds are conducted, and the interaction of the lake breeze with topography and background wind in triggering moist and deep convection is studied. The model is able to adequately simulate the systems most important dynamical features such as turbulent surface fluxes and the development of a lake breeze for the different wind conditions. We identify two different mechanisms for convection triggering that are dependent on the direction of the background wind: triggering over topography, when the background wind and the lake breeze have the same flow direction, and triggering due to convergence between the lake-breeze front and the background wind. Our research also suggests that precipitation measure-

ments at the centre of the basins on the Tibetan Plateau are not representative for the basin as a whole as precipitation is expected to occur mainly in the vicinity of the topography.

1 Introduction

The Tibetan Plateau (TP) and its role within the Asian Monsoon system have recently come into focus of atmospheric research. Land-use change, pasture degradation (Cui and Graf 2009) and a changing climate have an impact on regional circulation, precipitation patterns, cloud cover and hydrological resources (i.e. Cui et al. 2007a, b, 2006; Immerzeel et al. 2010; Yang et al. 2011). Subsequently, these changes will also be seen on the local scale. While temperatures rise on the whole TP, changes in precipitation are more complex and may be a key for understanding future climate changes. Precipitation is a relatively small-scale process that is strongly influenced by topography, and there are diverging trends for precipitation on TP (Xu et al. 2008) with an increase in precipitation in eastern and a decrease on western TP. At the same time, there are no permanent weather stations on the TP above 4,800 m (Maussion et al. 2011), and gridded precipitation products such as Tropical Rainfall Measuring Mission or reanalysis data sets have large errors due to terrain effects (i.e. Yin et al. 2008). Gaining a better understanding on the interactions and feedbacks in TP's circulation system is crucial, and we believe that modelling studies will be an important part of this effort. This includes the modelling of the interactions between the surface, complex topography and the atmosphere in the generation of mesoscale circulation systems, the organisation of cloud cover and the surface energy balance.

T. Gerken (✉) · T. Biermann · W. Babel · T. Foken
Department of Micrometeorology, University of Bayreuth,
95440 Bayreuth, Germany
e-mail: tobias.gerken@uni-bayreuth.de

T. Gerken · M. Herzog · H.-F. Graf
Department of Geography, Centre for Atmospheric Science,
University of Cambridge, Cambridge CB2 3EN, UK

Y. Ma
Key Laboratory of Tibetan Environment Changes and Land
Surface Processes, Institute of Tibetan Plateau Research,
Chinese Academy of Sciences, Beijing 100101, China

T. Foken
Center of Ecology and Environmental Research (BayCEER),
Bayreuth, Germany

Due to the high elevation of the Tibetan Plateau and its low-pressure environment, the surface receives strong solar radiation input, and surface heating leads to large diurnal surface temperature cycles (Gao et al. 1981). The fraction of diffuse to total radiation is very small so that clouds and shadows blocking out direct radiation have a profound impact on surface temperatures. This is illustrated by previously unpublished downward shortwave radiation measurements conducted in 1996 (Fig. 1a; 10 August 1996, Sereng Co Lake). Surface–atmosphere interactions through turbulent latent and sensible heat fluxes (Q_E and Q_H , respectively) as well as the complex topography of the plateau are of great importance, but not fully understood (e.g. Ma et al. 2009; Tanaka et al. 2003). Deep convection triggered by topography is a major source of precipitation in semi-arid mountainous environments (e.g. Banta and Barker Schaaf 1987; Gochis et al. 2004). In the context of TP, thermal valley circulation systems are an important factor in the diurnal organisation of cloud development and convection (Yatagai 2001; Kuwagata et al. 2001; Kurosaki and Kimura 2002). Valley scales of 160–240 km were determined to be most effective for this process through modelling (Kuwagata et al. 2001) and satellite observations (Yatagai 2001). Similarly, Yang et al. (2004) have investigated secondary triggering of convection within Tibetan valleys as a result of cold pool fronts caused by convective events that were triggered over the mountains.

Isotopic analysis of precipitation conducted by Tian et al. (2001a, b) show the influence of the monsoon as a water source declining as one proceeds north, with a strong monsoonal influence on the central TP, while a more recent analysis by Kurita and Yamada (2008) for the central TP highlights the importance of local moisture recycling: More than half of the rain events in their 14-day study period were locally generated, and a large fraction of the total precipitation was water recycled from the region. An important factor in the development of deep convection on TP is the availability of moisture. During the monsoon season, a conditionally unstable atmosphere is prevalent over central TP, and precipitation events are facilitated by atmospheric moisture contents (Taniguchi and Koike 2008). The two potential sources are local moisture from evapotranspiration or mid-tropospheric water vapour advection associated with monsoonal fronts. It is very perceivable that the initial moistening of the profile occurs through monsoonal transport and that subsequently the convective system remains active through local recycling. Therefore, the transport of moisture and the generation of convection that leads to recycling of water are important processes in the surface–atmosphere system, yet remain poorly understood.

Lake breezes are a subcategory of sea-breeze systems and form due to the thermal contrast between land and

water surfaces. Two recent reviews have summarised the current state of research on sea-breeze structure (Miller et al. 2003) and their numerical modelling (Crosman and Horel 2010): The role of topography onto sea-breeze development is highly dependent on the slope of terrain. Steep slopes act as an obstacle to flow, while thermal hill–valley circulations can assist in the development of mesoscale circulation system. The onset of sea breezes has been studied by Antonelli and Rotunno (2007). Additionally, the role of mountains in thermal circulations is discussed in Rampanelli et al. (2004). The work described here investigates the combination of both mesoscale processes. Kuwagata et al. (1994) have found that a substantial amount of energy relative to turbulent fluxes is advected within sea breezes. Additionally, daytime convergence on mountain tops results in the transport of air to the free troposphere (e.g. Banta 1990).

Our research focuses on surface–atmosphere interactions, the development of mesoscale circulations such as a lake-breeze system and its interaction with local topography in the development of moist convection in the Nam Co Lake basin. In Gerken et al. (2012), we stated that such research needs both (1) a surface model that can reproduce the system’s turbulent flux dynamics and (2) an atmospheric model with a resolution, high enough to resolve the scales that are significant for boundary-layer processes and convection. Typical resolutions of mesoscale models are on the kilometre scale, whereas the triggering of single convective plumes, simulation of local circulations driven by surface features and the surface shadowing of clouds require high-resolution approaches with resolutions in the order of 200 m assumed to be sufficient (Petch 2004, 2006). As convection development is highly dependent on moisture, it is of large importance for any modelling approach to get a good estimate of the initial atmospheric moisture contents. The sparseness of observations in remote regions, the coarse representation of topography as well as the limited number of model levels prevent the availability of good-quality atmospheric profiles on TP, a problem we address here by using a Global Forecasting System–Final analysis (GFS-FNL) profile downscaled after Maussion et al. (2011) using the Weather Research and Forecasting model (WRF).

The simulations conducted in this study are designed to explore the interaction between the lake breeze system, the background wind and topography on the development of moist convection. We show that the model is able to (1) simulate the development of the characteristic land–lake circulation system, (2) investigate the sensitivity of the system to different wind speeds and (3) show that the interaction of the lake-breeze, topography and background wind leads to the triggering of deep convection at the Nam Co Lake.

2 Model setup and methodology

The non-hydrostatic, cloud resolving Active Tracer High-resolution Atmospheric Model (ATHAM) (Oberhuber et al. 1998; Herzog et al. 2003) was first developed for the study of volcanic plume development (Graf et al. 1999) and then subsequently extended for biomass-burning plumes (e.g. Trentmann et al. 2006) and cloud studies (Guo et al. 2004). ATHAM consists of a dynamic core solving the Navier–Stokes equations in two or three dimensions with an implicit time stepping scheme on a Cartesian grid with a z -vertical coordinate. Incorporated tracers are active in the sense that they influence heat capacity and density of the mixture at each grid point (Oberhuber et al. 1998). In the present study, all classes of hydrometeors are treated

as active tracers. The turbulence scheme is based on a 1.5-order turbulence closure predicting horizontal and vertical turbulent kinetic energy as well as turbulent length scale (Herzog et al. 2003). ATHAM's modular structure allows for the incorporation of several physical processes. In this study, short- and longwave radiation (Langmann et al. 1998; Mlawer et al. 1997); bulk microphysics treating the conversion between water vapour, cloud water, cloud ice, graupel and rain (Herzog et al. 1998); a land surface (Friend and Kiang 2005; Friend et al. 1997) and a water surface (Fairall et al. 1996a, b) scheme supplying turbulent energy fluxes are used. The process-based terrestrial ecosystem model Hybrid (v6) (Friend and Kiang 2005; Friend et al. 1997) was modified for the use on the TP and was able to capture flux dynamics at the Nam Co lake for observed forcing

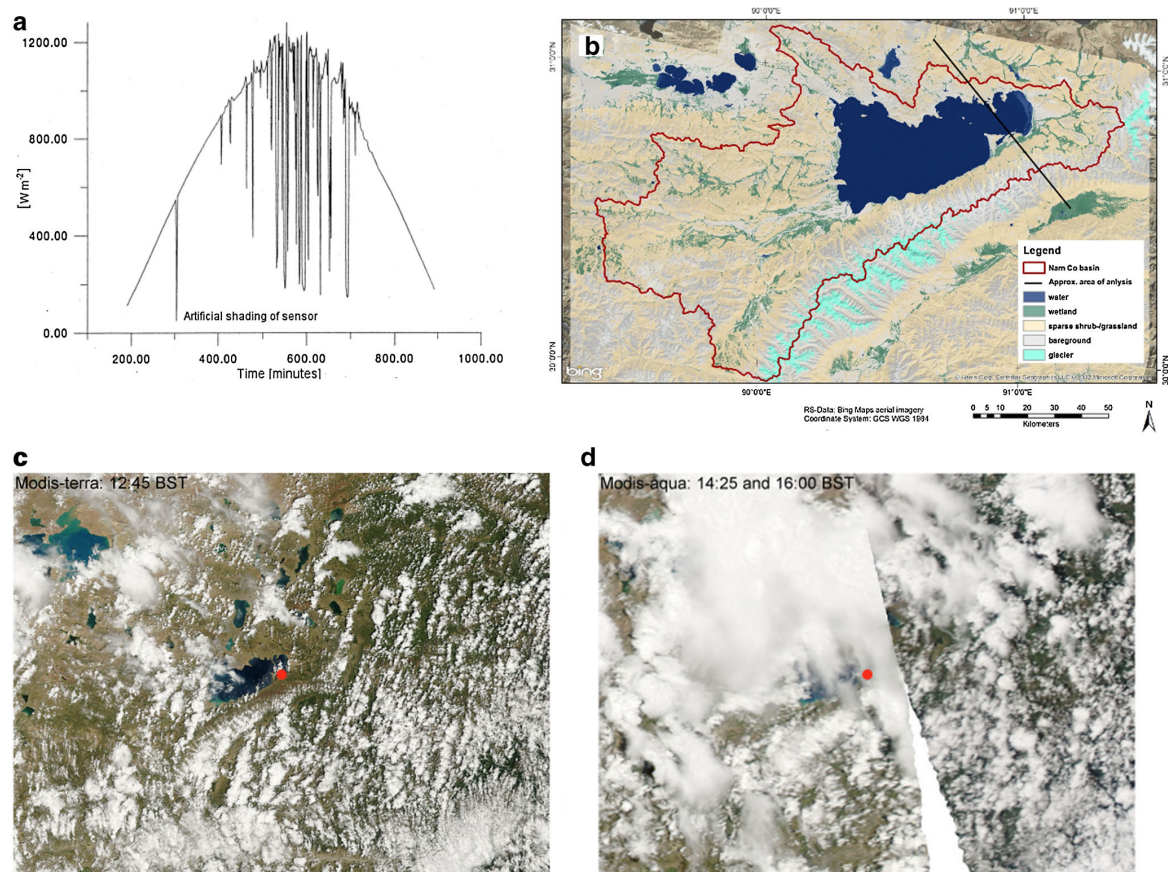


Fig. 1 **a** Downwelling solar radiation (SWD, in watt per square metre) measured with high temporal resolution on the Tibetan Plateau at the Sereng Co Lake on 10 August 1996. At approx. 300 min, the radiation sensor was artificially shaded in order to show the strong difference between total and diffuse radiation. Later decreases in radiation are due to passing boundary-layer clouds. **b** Land use map of the Nam Co Lake basin created from Landsat data. **c** MODIS–Terra composite

of the Nam Co Lake captured at 1245 hours BST on 6 August 2009. **d** MODIS–Aqua composite for the same day and region as in panel c, but at 1420 and 1600 hours BST. The red circles indicate the location of the Nam Co Lake research station. Microsoft bing map used with permission from Microsoft Corporation. ©2012 The Microsoft Corporation, ©Harris Corp, Earthstar Geographics LLC

data (Gerken et al. 2012). The Coupled Ocean-Atmosphere Response Experiment algorithm v2 (Fairall et al. 1996a, b) is a bulk flux algorithm based on the framework of Liu et al. (1979). As the Nam Co Lake is a large water body with a mean depth of more than 50 m (Wang et al. 2009), offline simulated lake fluxes compare reasonably well to observations (Gerken et al. 2012).

2.1 Field measurements

In this work, we conduct 2D simulations of a cross section through the Nam Co basin (Fig. 1b) by using realistic topography, in order to gain a better understanding on the physical processes involved in the generation of mesoscale circulations and convection. We apply the interactive surface model shown to work in Gerken et al. (2012) and make use of data collected during a field campaign conducted between 26 June and 9 August 2009 by the University of Bayreuth in cooperation with the Institute of Tibetan Plateau Research, Chinese Academy of Sciences (Biermann et al. 2013). In this period, eddy covariance and standard atmospheric measurements were carried out at two locations close to the lake, but, due to logistical reasons (power supply), not close to the mountains. The measurements of both eddy covariance stations were post-processed using the TK2/3 software package (Mauder and Foken 2004, 2011), applying all necessary flux corrections and post-processing steps for turbulence measurements as recommended by Foken et al. (2012) and Rebmann et al. (2012). On the vast majority of days, a lake breeze developed, which could be observed at the Nam Co research station (30°46.44' N; 90°57.72' E), located about 300 m from the shoreline of a small lake next to the Nam Co Lake at around 1000 hours Beijing Standard Time (BST). It should be noted that local solar time is approximately 2 h earlier than BST. Lake breezes developed frequently between 0900 and 1200 hours BST (Biermann et al. 2013). When the system was not observed, it was most likely due to closed cloud cover and lack of terrestrial surface heating or due to synoptic scale offshore winds. While measured turbulent surface fluxes were similar on 5 and 6 August, a lake breeze failed to develop in the morning

Table 1 Mean cross-shore wind component measured at the Nam Co Lake 3 m above the ground on 5 and 6 August 2009. The averaging interval is 30 min centred around the given time. Positive values indicate offshore flow

	Time (in hours BST)				
	0815	0915	1115	1145	1215
	[m s ⁻¹]				
5 August 2009	2.3	1.5	-1.1	-1.5	-1.6
6 August 2009	6.1	6.1	5.3	3.9	3.7

of 6 August, when the offshore component of the measured surface wind exceeded 6 m s⁻¹. On 5 August in contrast, the initial offshore wind component of 2.3 m s⁻¹ at 0815 hours changes to an onshore wind of 1.6 m s⁻¹ at 1215 (Table 1). The change in direction occurred around 1045 hours, indicating the lake-breeze onset. Starting from approximately 1200 hours BST, deep convection was frequently observed over the mountains during the field campaign.

2.2 Simulation setup

ATHAM is run in Cartesian 2D mode, with the horizontal coordinate oriented perpendicular to the lake-land boundary and Nyenchen Thanglha mountain chain, which is situated approx. 10 km south of the Nam Co Lake. Both the lake shore and the mountains are almost parallel to each other and extend over more than 100 km. In the absence of large-scale forcings, the circulation in the basin is primarily driven by a lake breeze and a thermal mountain circulation. Hence, a 2D cross section is capable of reproducing the system's most important dynamical features. We chose a cut across the eastern part of the lake, passing through the Nam Co Lake research station and a comparatively low section of the Nyenchen Thanglha mountain chain. The main reasons are the availability of observations and the fact that 2D simulations have a tendency to overestimate the influence of topography. The domain size is 150 km with a constant grid spacing of 200 m resolving the central 80 km, which includes the lake and the mountains to the south and north of the lake, as indicated in Fig. 1b). Outside the basin, horizontal grid stretching is applied to achieve a resolution of approx. 1,300 m near the lateral boundaries and giving a total number of grid points of $n_x = 486$. The lateral boundary conditions are cyclic, but hydrometeors and water vapour exceeding the

Table 2 Description of the soil and surface parameters determined for the Nam Co Lake (N 30°46.50'; E 90°57.61') in summer 2009

Parameter	
Coordinates	
Soil	Sandy-loamy
Porosity	0.63
Field capacity	0.184
Wilting point	0.115
Heat capacity (c_p) [J m ⁻³ K ⁻¹]	2.5×10^6
Thermal Conductivity [W m ⁻¹ K ⁻¹]	0.53
Surface albedo (α)	0.2
Surface emissivity (ϵ)	0.97
Vegetated fraction	0.9
LAI [m ² m ⁻²]	0.9
Vegetation height [m]	0.07

initial moisture profile are removed at the lateral boundaries, without adding a density perturbation. We use 150 layers, starting at 25 m of vertical resolution for the first 30 layers, then stretching to a maximum vertical resolution of approx. 300 m at the model top 15 km above ground level (a.g.l.). The model topography is taken from the ASTER-DEM with a 90-m resolution and was smoothed with a 2-km moving window in order to remove large vertical cliffs and single grid-point depressions. Additionally, the topography outside the Nam Co basin is set to the lake level, and turbulent surface fluxes are gradually reduced to zero near the lateral boundary. This is justified as our area of interest is within the Nam Co Lake basin. The simulation is integrated from 0600 hours BST (approx. 1.25 h before sunrise) to 1800 hours BST. We acknowledge that 2D simulations have a simplified wind field, where clouds can only move along one horizontal direction. Consequently, the surface may experience artificially high shading, which can lead to a potential underestimation of turbulent latent (Q_E) and sensible heat fluxes (Q_H), as soon as large clouds are present. Hence, we limit our analysis to the time before and immediately after the triggering of deep convection.

2.2.1 Test cases

We selected as a base case for this work 6 August 2009, a radiation day at the centre of the basin, with sudden triggering of deep convection in the afternoon as seen by the MODIS satellites (Fig. 1c and d). The soil model is initialised in a similar way as that of the previous study (Gerken et al. 2012), when surface fluxes were already modelled, assuming homogeneous soil properties (Table 2). The soil model was initialised with $T_1 = 9.4$ and $T_2 = 3.7$ °C as mean layer temperatures, corresponding to a surface temperature $T_0 = 5.8$ °C for the land surface, while the lake temperature was set to

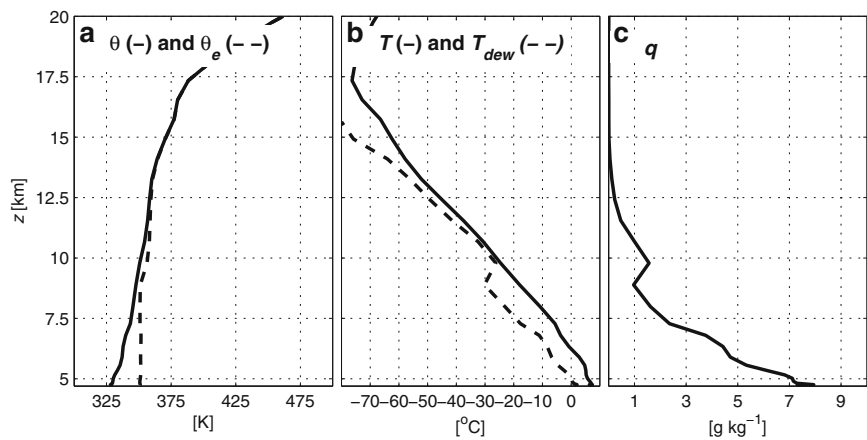
15.0 °C. A random perturbation in the surface cover of ± 5 % was added in order to account for variations of surface cover. Additionally, the initial volumetric moisture in the model’s surface layer (SM_0 , [%]) was set to $1.4 \times$ field capacity and is scaled with height according to

$$SM_0 = SM_0 - (SM_0 - SM_{PWP}) \times h/h_{max} \tag{1}$$

with SM_{PWP} as the soil moisture at permanent wilting point, h the terrain height and h_{max} as the maximum terrain height in the domain.

The atmosphere is initialised from GFS-FNL downscaled to the Nam Co basin (Maussion et al. 2011). The profile on 6 August (Fig. 2) is relatively dry for the lowermost 5 km a.g.l. with relative humidities between 60–70 % and a moist layer above, which is also seen in the 00-UTC Nagqu radiosounding (not shown, approx. 150 km to the north-east) indicating southerly upper-level winds. The equivalent potential temperature (θ_e) indicates conditional instability in the profile as is commonly encountered in summer atmospheric profiles on TP. While there is no convective available potential energy (CAPE) in the initial profile, it is easily built up by surface heating and lower tropospheric moistening. The wind coordinate in our experiments is defined with positive values for winds coming from the Nyenchen Thanglha mountains (southerly winds). For our experiment, we chose to initialize our model with constant wind speeds of $-3.0, -1.5, 0.0, +1.5, +3.0$ and $+6.0$ m s⁻¹ throughout the model domain. In line with the meteorological convention, where a flow from the south to the north is positive, we define flows from the southeast towards the northwest as positive. The flow direction is indicated in the figures used in this work. We denote the simulations by the initial wind speed (e.g. U+0.00 for the case with no initial wind). The cases were chosen to analyse the development of a lake breeze and to investigate the sensitivity of convection on changing wind speed. These wind speeds reflect a realistic

Fig. 2 Initial profile for the Nam Co Lake 6 August 2009 at 0600 hours BST used in the model simulations. Derived from GFS-FNL with WRF according to Maussion et al. (2011). **a** Potential (θ) and equivalent potential temperature (θ_e). **b** Temperature (T) and dew-point temperature (T_{dew}). **c** Mixing ratio (q)



low level flow, with $U+6.00$, being close to the observed wind velocity on 6 August, but are comparatively weak for the upper atmosphere. Nevertheless, this allows for the forcing of the surface model with a realistic wind, while not having to deal with impacts of wind shear that are not the object of this study and are poorly represented in 2D simulations (i.e. Kirshbaum and Durran 2004). In order to drive the coupled surface model, specifically for the case of no initial wind, a cross-directional wind component of 1 m s^{-1} was added to all simulations, which is only seen by the surface model. It should be noted that the wind speed is not continuously forced in the simulations so that topography and surface friction lead to an equilibrium wind speed that differs from the initialised flow speed.

Even though the cases $U+6.00$ and $U+3.00$ correspond roughly to measured surface conditions on 5 and 6 August 2009, these sensitivity simulations are not intended to

reproduce the atmospheric processes as they took place in the Nam Co basin on a specific day, as this could only be achieved with a 3D simulation that takes into account a full realistic topography and synoptic forcing. Instead, we investigate the interactions between the lake, topography and atmosphere to investigate the triggering of convection under different wind conditions, in order to develop a better process understanding.

3 Results

3.1 Development of a lake-breeze system

A fundamental basis for the examination of convection triggering in the Nam Co Lake basin is the question whether ATHAM is capable producing realistic lake-breeze

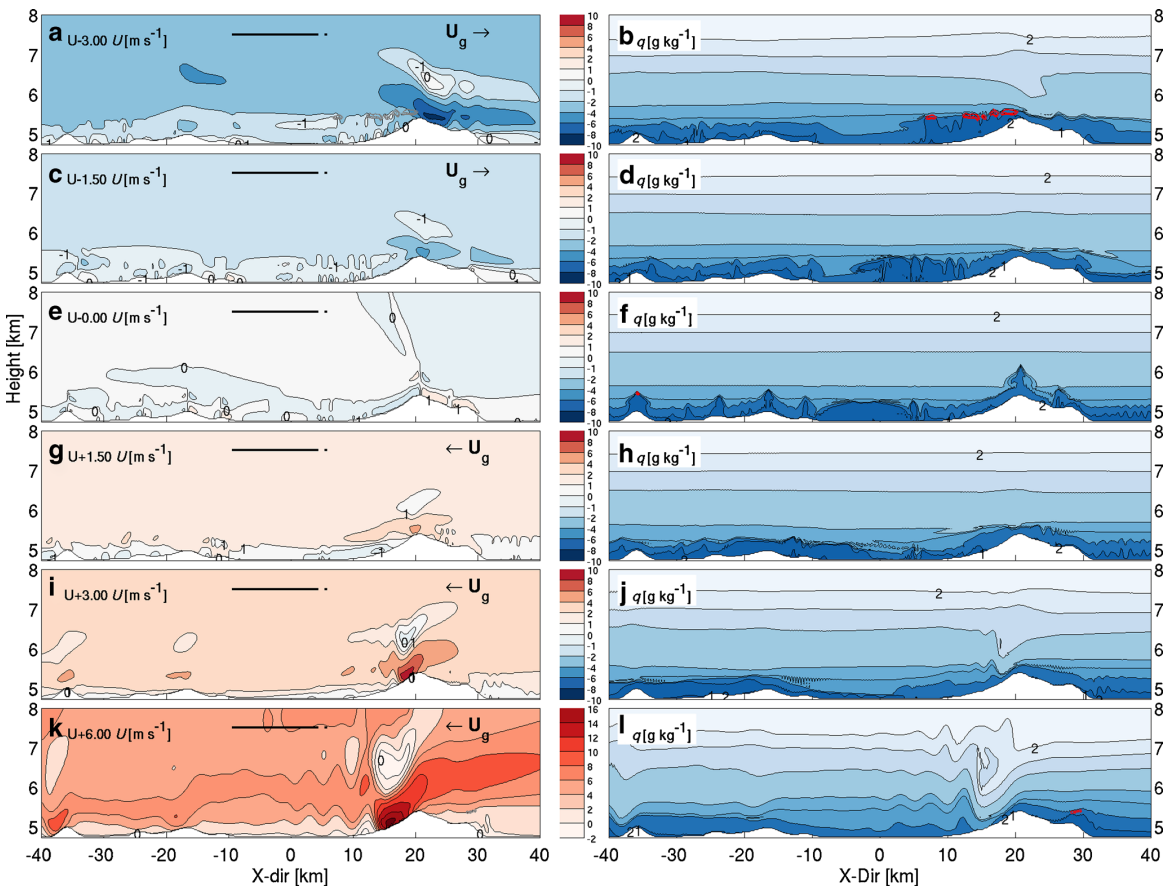


Fig. 3 Horizontal wind speed in the Nam Co Lake basin at 1100 hours BST for model runs with initial wind speeds of -6.00 , -3.00 , -1.50 , 0.00 , 1.50 and 3.00 m s^{-1} (left column). A positive wind speed indicates southeasterly winds and flow from left to right in the panel. The

black line shows the position of the lake. Right column: Corresponding water vapour mixing ratio (q , in gram per kilogram) with contour interval of 1 g kg^{-1} . The grey and red contour lines overlaid indicate the position and extent of clouds

circulations. Figures 3 and 4 display the horizontal wind speed at 1100 and 1200 hours BST. According to theory, a symmetrical and pronounced lake breeze should develop in the simulation without background wind, but due to asymmetric topography, we expect some deviations. Additionally, we expect interaction of the lake breeze with the topography. Depending on the slope angle, a mountain can either act as an obstacle to flow (Ookouchi et al. 1978) or can contribute to the lake-breeze development as it may reinforce the thermal circulation (i.e. Miao et al. 2003). With a cross section of the Nam Co Lake in the order of 10 km used in this study, there is little found in the literature about lake-breeze behaviour of “small” lakes and how their thermal circulation system interacts with the background wind. For onshore geostrophic winds (U_g), a landward shift of the lake breeze is expected. The reverse effect is expected for offshore flow. Additionally, the timing of sea breezes is affected. For oceanic settings, sea breezes with offshore $U_g > 4-8 \text{ m s}^{-1}$ are expected to stall at the land-lake

boundary. For onshore $U_g > 3-5 \text{ m s}^{-1}$, sea breezes become indistinguishable from the background flow. For lakes, these values are thought to be smaller (Crosman and Horel 2010). In our simulation setup, the thermal circulation forced by the Nyenchen Thanglha mountains on the southeast shore and the lake breeze seem to create a single mesoscale circulation system for the case $U+0.00$. Strong winds delay the formation of a lake-breeze front, or it may not be detectable in a stronger offshore background wind (Crosman and Horel 2010). As we expect from both theory and observation at the Nam Co lake, there is no lake breeze developing for the case $U+6.00$ (Fig. 4k and l). In contrast, a lake breeze is clearly visible by 1200 hours BST in the simulations $U+3.00$ and $U+1.50$ (Fig. 4g-j) on the southeastern shore of the lake, while the lake breeze is standing out less against the background flow on the northwest shore. The reverse is true for the simulations with $U < 0 \text{ m s}^{-1}$ (Fig. 4a-d). In accordance with theory, the lake breeze front penetrates less onto the lake shore in stronger winds. As the lake-breeze regime

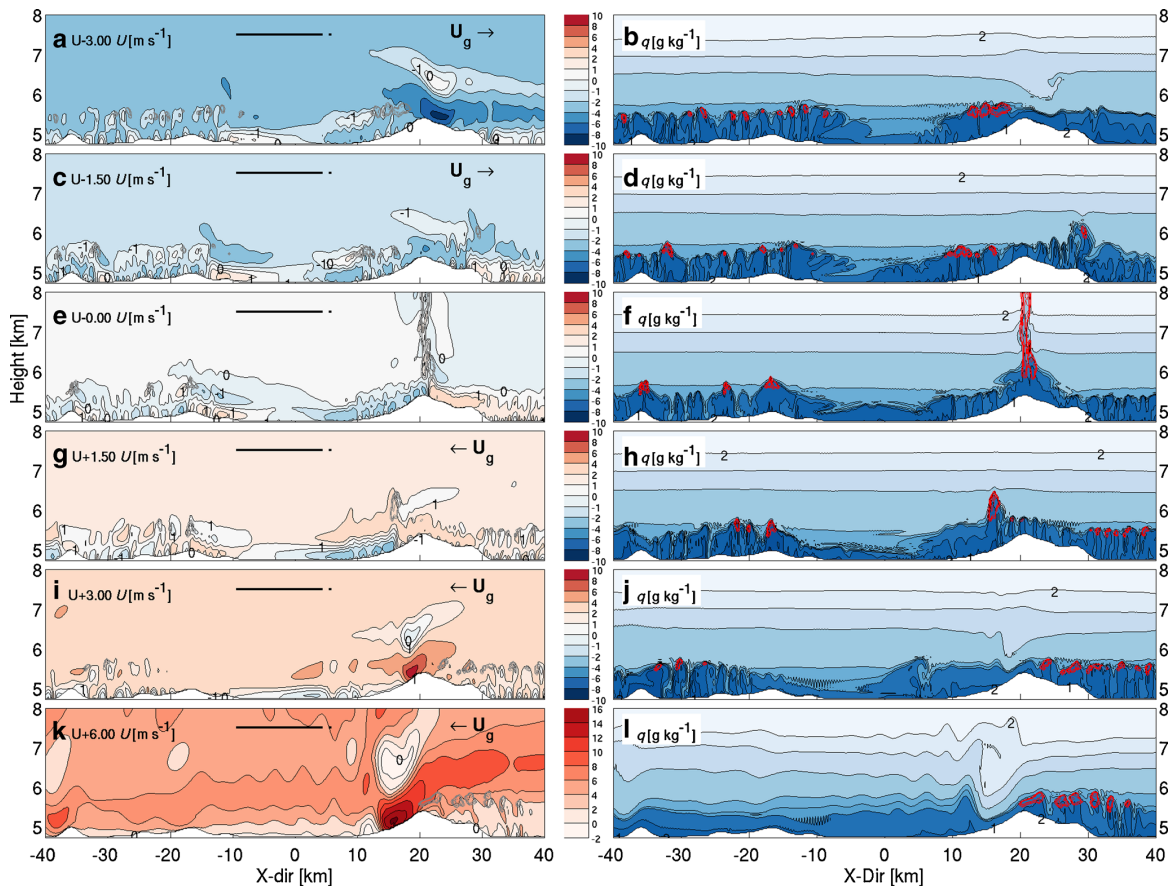


Fig. 4 As Fig. 3, but for 1200 hours BST

usually develops between 0900 and 1200 hours BST, we conclude that our simulations are capable of reproducing the characteristic lake-breeze development at the Nam Co Lake, with wind speeds differences in the order of a few metres per second as expected.

3.2 Convection development

From late morning onwards, clouds begin to form in the Nam Co basin. In our simulations, clouds are defined as grid cells in which the total content of condensed ice and water exceeds $q_t > 10^{-3} \text{ g kg}^{-1}$. After sunrise and with a growing boundary layer, shallow clouds start to appear in the model domain. These clouds grow over time and eventually lead to the triggering of deep convection and precipitation. Figure 5 displays the domain averaged q_t in the Nam Co basin. A deep convective regime is reached in all simulations. As expected, stronger and earlier convection develops in the scenarios with weaker initial winds. For these, there is little turbulent and advective transport or dispersion of

heat, and there is no wind shear to prevent the triggering of convection. As a consequence, developing local vertical instabilities are readily released. Additionally, there is reduced entrainment of dry air into thermals due to lack of turbulence. For low wind speeds, there is a relatively fast transition between shallow and deep convection as characterised by a relatively short time interval between the onset of shallow cumulus (t_{cl}), activation time of cumulus clouds (t_*) and the time when the cloud top height reaches the 13-km level (t_{13} ; Table 3). For simulations U±3.00 and U+6.00, this takes substantially longer. The transitions for all cases occur between 1140 and 1230 hours, except for U+6.00, where the definition of t_* is not applicable due to a stationary cloud over the large mountain (Fig. 5e). The transition time t_* is defined as the time when the centre of cloud mass (Z_c) starts to ascend at an increasing speed (Wu et al. 2009).

$$Z_c = \frac{\int \int q_t z dx dz}{\int \int q_t dx dz}, \quad (2)$$

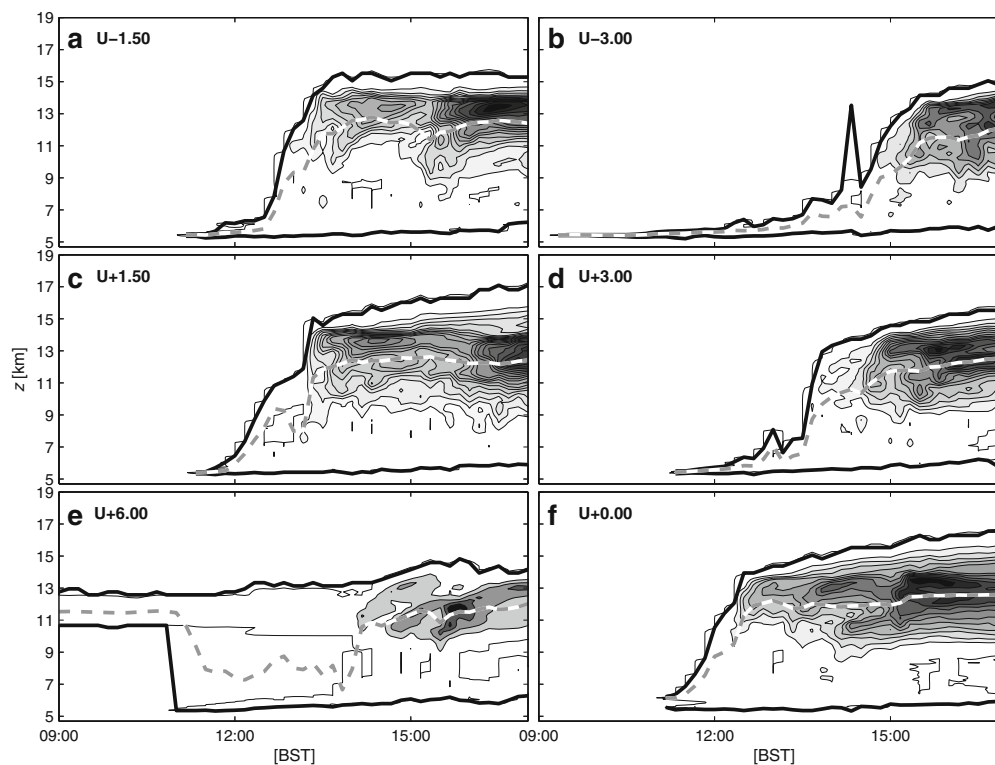


Fig. 5 Development of convection at the Nam Co Lake for model runs with initial wind of 1.50, 3.00, -1.50, -3.00 and 0.00 m s^{-1} (a–e respectively): Contours correspond to mean cloud particle concentrations in the Nam Co Lake basin. Each contour level corresponds

to 0.1 g m^{-3} . The *dashed line* indicates the height of the centre of cloud mass (Z_c), and *black lines* indicate cloud top and cloud bottom heights

Table 3 Timing of convection in hours BST

Run	t_{cl}	t_*	t_{13}
U-3.00	0920	1140	1420
U-1.50	1110	1140	1320
U+0.00	1110	1150	1230
U+1.50	1120	1200	1320
U+3.00	1120	1250	1400
U+6.00	1140	N/A	N/A

t_{cl} is the time when first boundary layer clouds appear in the model; t_* corresponds to the triggering of moist convection after Wu et al. (2009); and t_{13} is the time when convection reaches 13 km a.s.l. t_* for U-6.00 was not calculated due to the occurrence of a high cloud over the mountain chain, rendering the calculation of the centre of the cloud mass Z_c unapplicable

with z as the vertical coordinate and $dx dz$ as the area element to be integrated over. Z_c is assumed to initially grow at a constant rate so that a linear regression is fitted through Z_c for the first 30 min after clouds appear in the simulations. t_* is defined as the time when the Z_c exceeds a band around the regression (Z_{cr}). Wu et al. (2009) have proposed $Z_c > 1.15Z_{cr}$, which proved to be a robust measure and is also applied in this work. t_* practically marks a change in the regime of cloud development: Clouds that form from the mixing of air into the boundary layer become buoyant as free convection starts. The main reason for the virtually non-existing transition time in case U+0.00 is that the initial cloud forms at the top of the heated mountain and grow immediately into the level of free convection. However, for all other simulations, t_* corresponds to the first visible change in the slope (Fig. 5). The fast transition from shallow to deep convection is caused by the conditional instability of our initial atmospheric profile. It should be noted here that both Wu et al. (2009) and Kirshbaum (2011) use profiles with idealised stability, while our profile is derived from GFS analysis data, which was downscaled with WRF to reflect local conditions. It is characteristic for the atmosphere above the TP to be conditionally unstable (as indicated by vertically constant values of θ_e), and we can indeed see from observations at Nam Co that convective systems develop rapidly (Fig. 1c and d). Additionally, Wu et al. (2009) and Kirshbaum (2011) use a uniform surface initialisation with prescribed fluxes and, in the case of Wu et al. (2009), no initial wind. Calculation of CAPE (Emanuel 1994) reveals that even though there is virtually no CAPE in the initial profile, it is rapidly built up for all cases by both surface warming and boundary-layer moistening. There is little difference in absolute CAPE values between the runs, but a general tendency to generate CAPE exceeding $1,000 \text{ J kg}^{-1}$ until solar noon and a subsequent release of CAPE in the afternoon. While CAPE

behaves similarly over areas classified as mountains and the basin, CAPE values over the water build up much slower, remain lower and show hardly any tendency to be released within the time frame of this investigation. This provides first evidence for the role of land cover and topography. The mechanism of convection triggering and the role of topography will be discussed in Section 3.4. The height of Z_c reaches approx. 12 km in all cases, which corresponds to the level of neutral buoyancy. It should be highlighted that triggering of deep convection may occur too early in the model as the downscaled atmospheric profiles do not contain inversion layers that need to be overcome as would potentially be the case in directly measured profiles. As there are no directly measured radiosonde profiles available for the summer of 2009 at Nam Co, we have decided to limit the scope of this investigation to the influence of the background wind.

3.3 Modelled turbulent surface fluxes

We compare the surface fluxes generated by ATHAM with fluxes measured by eddy covariance (EC). ATHAM's surface model is fully coupled and produces fluxes through bulk transfer relationships, which take into account wind speed, temperature and moisture gradients between the surface and the air above, atmospheric stability, clouds and the net radiation. Each grid cell is treated independently. EC measurements are direct, high-frequency measurements of an atmospheric scalar and the vertical wind speed from which a vertical flux can be calculated (i.e. Foken (2008b)). While the horizontal grid resolution corresponds roughly to the footprint of the eddy covariance measurements, they are not directly comparable as surface models will close the surface energy balance by distributing the available net radiation (R_{net}) between Q_E , Q_H and the ground heat flux Q_G . During the campaign, an energy balance closure for the EC measurements of about 70 %, R_{net} was observed by Biermann et al. (2013). This is due to the inherently unclosed energy balance of EC measurements (i.e. Foken 2008a and Foken et al. 2011). Particularly under the influence of stationary secondary circulations, like sea breezes, a substantial amount of energy is exchanged without being measured by EC. Therefore, before comparing measured and modelled fluxes, EC fluxes are corrected according to the Bowen ratio (Twine et al. 2000).

The behaviour of the simulated fluxes in all cases is initially very similar and corresponds to the warming of the surface as part of the diurnal cycle. Due to the high soil moisture, we encounter Bowen ratios of approximately 1/2. Since the model is initialised with nearly homogeneous surface conditions, there is little spatial variation of turbulent fluxes as long as clouds remain absent. After sunrise, Q_E and Q_H rise in a sinusoidal manner. From 1200 hours

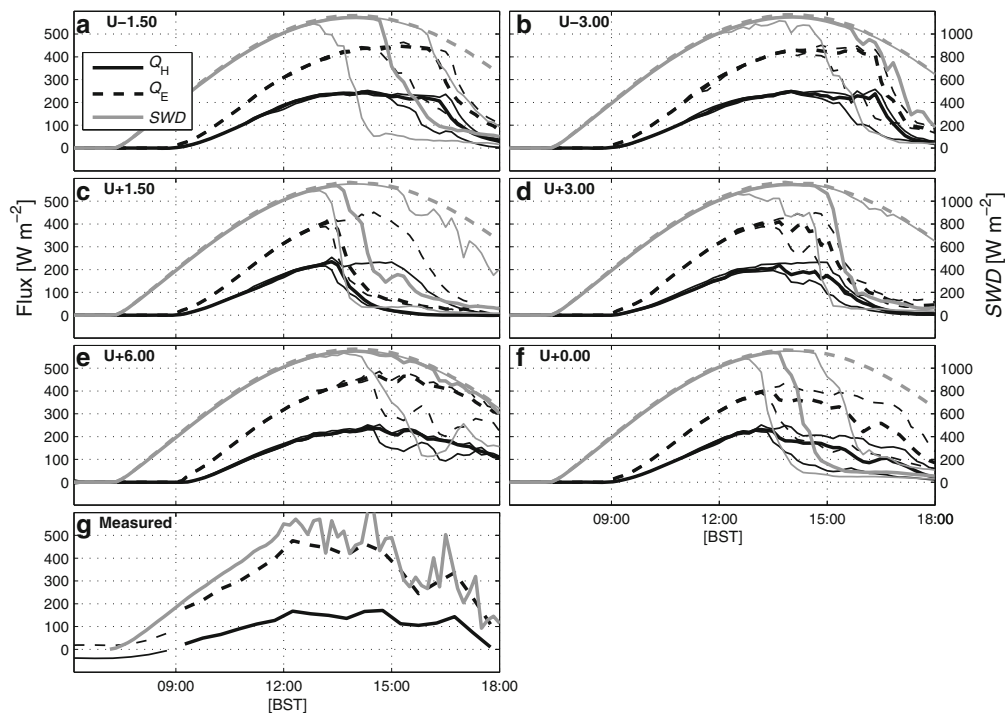


Fig. 6 Development of turbulent surface fluxes in the Nam Co Lake basin for model runs with initial wind of 1.50, 3.00, -1.50, -3.00 and 0.00 ms^{-1} (a–f respectively) (Q_H , line; Q_E , dashed line; downwelling shortwave radiation (SWD), grey line). Thick black lines correspond to median flux over land. Thin lines are upper and lower

quartiles of fluxes. The dashed grey line is clear sky SWD. g Measured turbulent fluxes near the Nam Co research station. Thin lines correspond to directly measured EC fluxes on 6 August 2009. Thick lines are energy balance-corrected fluxes according to Twine et al. (2000)

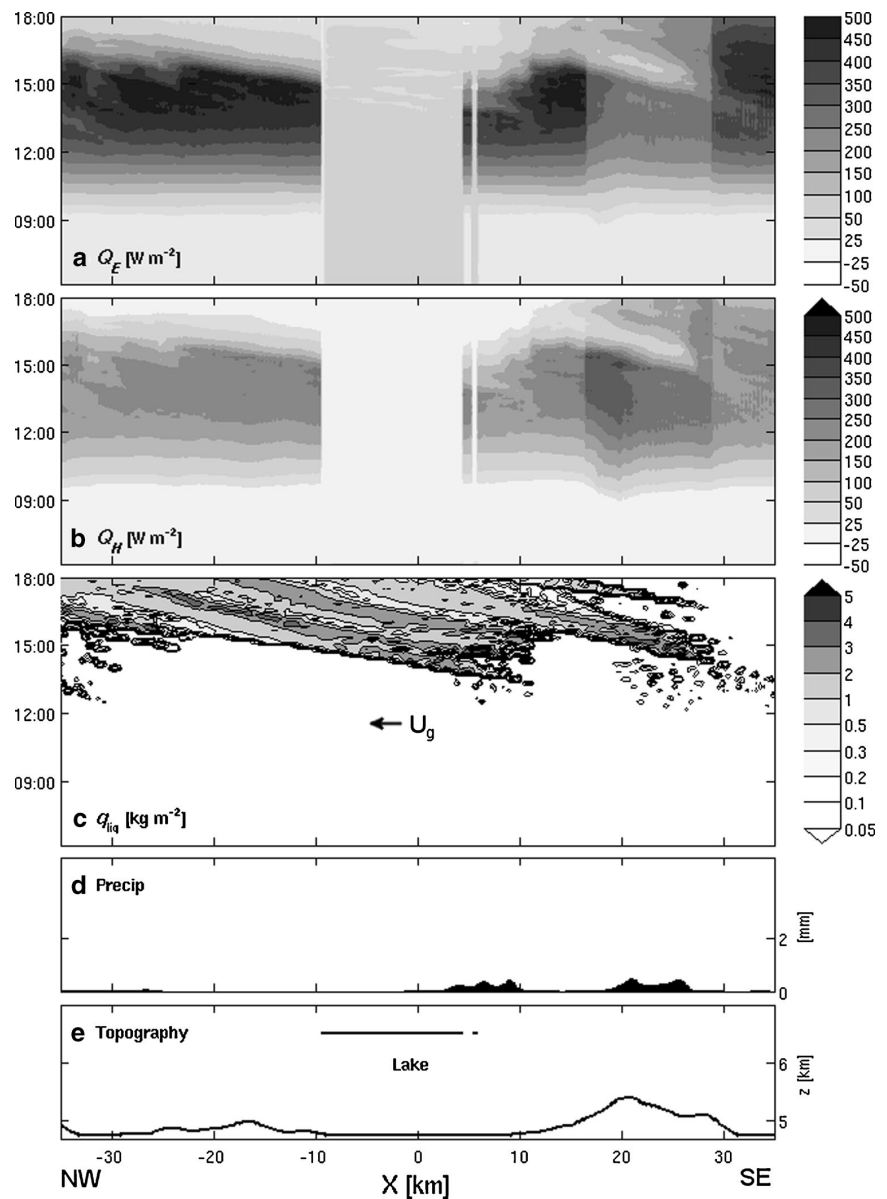
BST, the occurrence of clouds begins to reduce the downwelling shortwave radiation, which is first seen in a drop in the lower quartile and then in the median radiative flux. As a consequence, turbulent fluxes drop and have a larger spatial variation. Figure 6a–f display the median turbulent fluxes and downwelling shortwave radiation within the area of analysis for the six model runs. Figure 6g shows the measured data from two EC complexes. While the magnitudes of simulated and measured fluxes closely resembles each other, modelled fluxes lag behind measurements in the order of 1 h, which is most likely due to the formulation of the surface model, containing a 10-cm-thick soil layer with an extrapolated surface temperature. In reality, skin temperatures react almost instantaneously to changes in energy input, while both our model and integrated EC measurements react more slowly. As boundary layer clouds and later deep convection develop, the spatial variability of surface fluxes increases. In the measured data, this is represented in a higher temporal variability of R_{net} . Triggering of deep convection leads to a strong decrease in the median downwelling shortwave radiation, followed by a decrease in turbulent fluxes. Due to the 2D nature of our simulations,

we limited our analysis to the time before the simulation becomes dominated by clouds, which happens between 1400 and 1600 hours BST in all cases. It should be noted that the flux development of the case $U-3.00 \text{ m s}^{-1}$ (Fig. 6b) is most similar to the measured fluxes and agrees reasonably well. A likely reason for this is the fact that the comparatively high wind speeds dissipate enough energy to delay the triggering of convection to a realistic time. $U+6.00$, which corresponds to the observed initial wind speed, has too high fluxes in the afternoon, because too few clouds are produced that reduce solar radiation input. The observed time lag in the surface model, which is already described by Gerken et al. (2012), may be the cause of a relatively late, yet still reasonable, development of lake-breeze system in our simulations.

3.4 Triggering of deep convection

Starting from the initial hypothesis that deep convection is triggered by the interaction of locally generated mesoscale circulations, we analyse the interaction of the background flow with the lake breeze and the mountains found in the

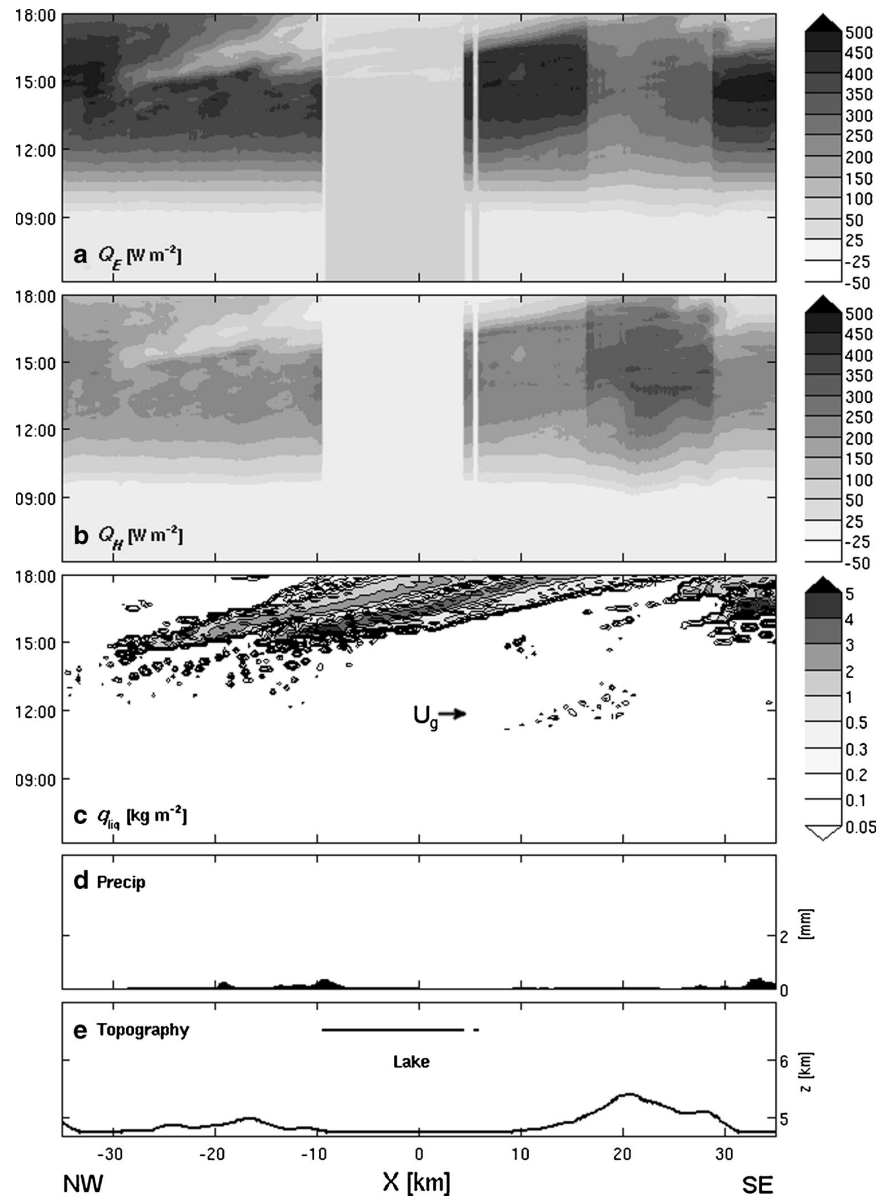
Fig. 7 Hovmøller plot of time (BST) versus horizontal extent of the Nam Co Lake basin for case U+3.00: **a** Q_E and **b** Q_H , in watt per square metre. **c** Total cloud liquid water path q_{liq} , in gram per square kilogram. **d** Total accumulated precipitation (in millimetre). **e** Topographic height z and the extent of the lake



domain. The role of the atmospheric vertical profiles is beyond the scope of this work, but strong conditionally instability (i.e. Yanai et al. 1992) as encountered in the profile used in this work is a general feature of the atmosphere on TP during the summer monsoon. Figures 7 and 8 display the spatial development of surface fluxes and the development of clouds for the cases U+3.00 and U-3.00. Both the lake and the mountains are visible from the change in surface fluxes. Later in the day, the reaction of

Q_E and Q_H to reduced shortwave radiation can be seen. The diagonal cloud patterns in the c panel of both figures show the movement of clouds with the background wind. The first clouds tend to form over land and upwind of topography. In addition to the boundary-layer clouds that form at the top of local updrafts, some clouds form on the windward side of topography, where air is forced upward. From Fig. 7, it becomes apparent that clouds are organised and form along bands. Before the development of

Fig. 8 As Fig. 7, but for case U-3.00



deep convection, which occurs in both simulations around 1500 hours and manifests itself in a large cloud liquid water path (q_{liq}) and dark colours in the plot, there is a period from about 1200 hours onwards, when clouds form and dissolve. This starts with a sequence of boundary layer clouds, which become larger over time, and then finally, deep convection is triggered. These clouds do not seem to be generated randomly but, as the diagonal pattern indicates, are linked by the “successive thermal mechanism”

(Kirshbaum 2011). After thermals have become activated ($t > t_*$), they penetrate into dryer layers of the atmosphere, entrain dry air and thus dissolve. As thermals are organised and only occupy a small area of the domain, this corresponds to a selective moistening, which is translated with the background wind. Consequently, thermals entering premoistened areas are less subject to mixing with dry air and thus retain their buoyancy. This leads to preferential cloud development downwind of the precursor

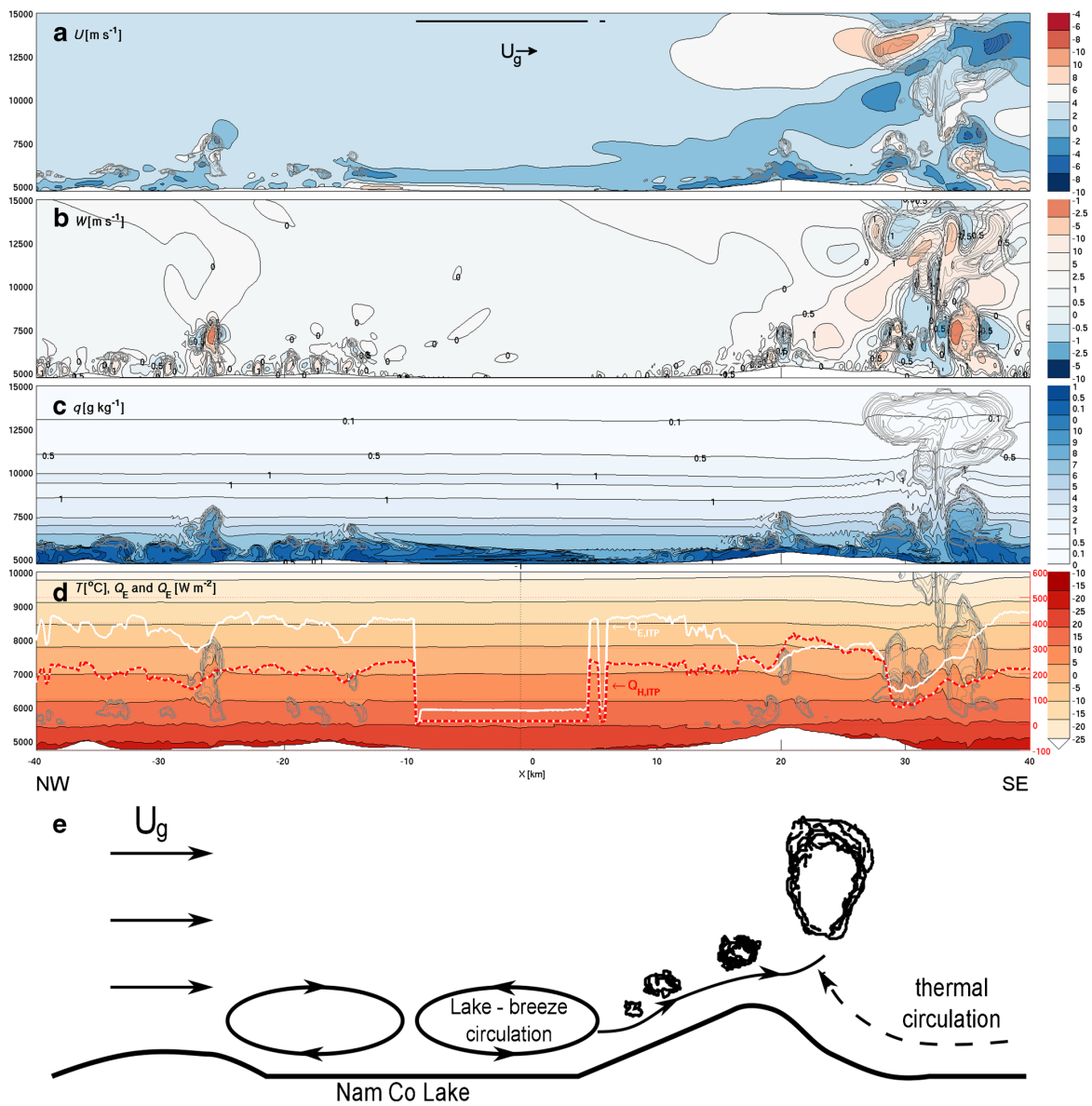


Fig. 9 Modelled **a** U , in metre per second; **b** W , in metre per second; **c** q , in gram per kilogram; and **d** T (in degrees Celsius) in the Nam Co Lake basin for case U-1.50 at 1330 hours BST. Grey contours indicate clouds. The red and white lines indicate Q_H and Q_E with

the arrows indicating the magnitude of the measured EC fluxes. The position of the lake is indicated by the black line. Plot e is a sketch of the mechanism

thermals. Since we have chosen a lake basin, with topography to the sides, some of the triggered convection is immediately transported out of the area of analysis. This is especially true for case U-3.00, where deep convection is frequently triggered by the Nyenchen Thanglha. It should also be noted that the relatively slow wind speeds in the upper troposphere reduce wind shear, the entrainment of dry air and the dispersal of moisture, but also lead to a

reduction in surface fluxes and thermal activity later in the day.

3.5 Influence of background wind speed and direction on convection triggering

As discussed in Section 3.1, the development of the lake-breeze circulation depends on the background wind. The

occurrence of boundary-layer clouds within the lake basin depends on the wind direction and, therefore, on the result of the interaction between U_g and the sea breeze. Downslope winds lead to adiabatic warming and hence inhibit cloud formation and growth by reducing relative humidity. Air masses ascending on slopes have the opposite effect. This explains why the cases U-3.00 and U-1.50 have an earlier onset of boundary-layer clouds: As the mountain range located on the southeastern shore is higher than

the mountains in the northwest, more clouds are generated there when moist air is forced upward. During the constant growth phase of the boundary layer clouds, characterised by simultaneous increase in cloud top and cloud bottom heights, convective triggering occurs when saturated air masses reach the level of free convection, which develops around 2 km a.g.l., which can be reached by boundary layer growth. We present here two examples of convection triggering, which we suggest to be

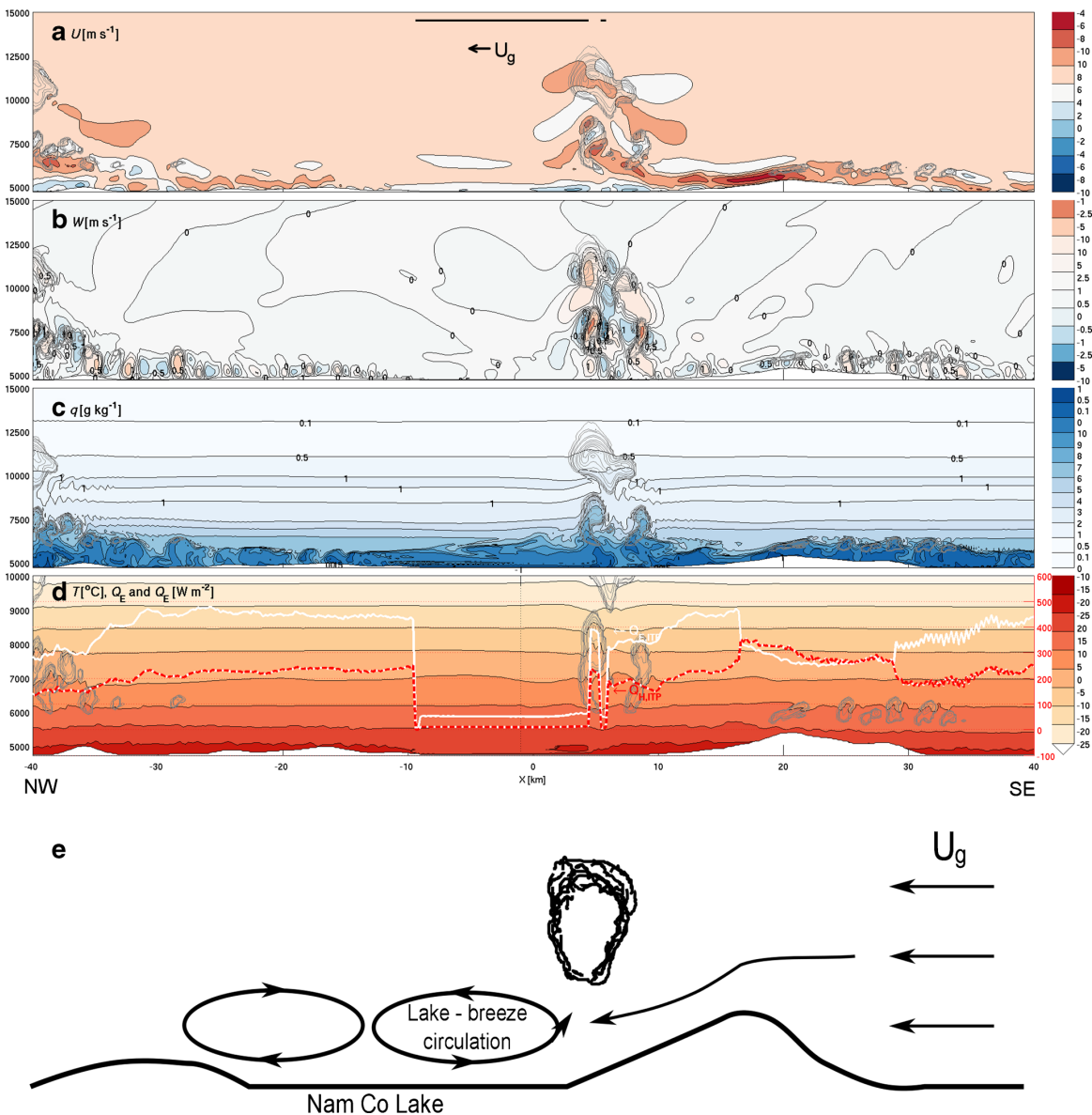


Fig. 10 As Fig. 9, but for case U+3.00 and at 1350 hours BST

representative for the triggering of convection in Nam Co region in general. Figure 9 shows the case $U-1.50$. Here, the background wind and the thermal circulation have both the same sign and transport moist air towards the southeast and over the mountain chain. With the mountain as a trigger, thermals are repeatedly triggered in similar locations, leading to a sequence of convective clouds downstream of the mountain. In the second case ($U+3.00$; Fig. 10), the lake-breeze circulation penetrates into the basin and displaces the warm and moist basin air upwards. This is most pronounced during offshore winds, when the lake-breeze front collides with the background wind. Consequently, convective thermals and eventually deep convection are triggered. In general, frontal collision and the resulting convergence seems to be an important mechanism. Yang et al. (2004) described the triggering of secondary convection in Tibetan valleys as gust fronts generated by convective downdrafts causing renewed triggering of convection within the basin. Similarly, Reeves and Lin (2007) and Miglietta and Rotunno (2009) have studied the propagation of convective systems in mountain flows with respect to the Froude number for highly idealised modelling setups. For low flow speeds ($U < 10\text{m s}^{-1}$), the system was found to be in a blocked state, with a density current travelling against the flow causing precipitation upstream of the topography. These and previous works (Chu and Lin 2000; Chen and Lin 2005) highlight the importance of cold pool

formation for blocked flows. Low wind speeds are associated with strong cold pools, while at higher wind speeds, the advection of heat reduces the strength of the cold pool. In this work, the lake breeze and the heated mountain both contribute to the development of a thermal circulation, so that near surface wind speeds are larger than the initialised U_g . Additionally, surface heating through sensible heat fluxes reduces cold pool development, and Fig. 9 does not show the development of a strong cold pool. Despite these differences, we see evidence for similar processes during the later stages of our simulations, where we indeed find the development of a cold pool, as soon as cloud cover results in a decrease of surface heating (not shown).

3.6 Moisture transport and the water cycle

The Nam Co Lake basin is located at the northern fringe of the area influenced by monsoonal circulations during the summer. While the monsoon supplies some water to the area, local recycling of water and the contribution of surface evapotranspiration to the water cycle may be important. For the following analysis, we define two control volumes as seen in the sketch of Fig. 11e): control volume A corresponds to the boundary layer and lower troposphere in the Nam Co Lake basin and extends to 3 km a.g.l., and control volume B is located above A and extends up to 10 km a.g.l. We estimate the transport of moisture, defined as the

Fig. 11 Instantaneous moisture flux f_q (in kilogram per metre per second) for the Nam Co Lake basin. **a** and **c** Moisture transport into control volume A (as indicated in panel **e**) of this figure, representing the Nam Co basin up to 3 km a.g.l.: evapotranspiration (blue line), net horizontal flux (black line), net vertical flux (dashed line) and resulting total flux (grey). The precipitation flux is not displayed as it is of negligible magnitude. **b** and **d** Transport into the mid-tropospheric control volume B with the same horizontal extent and from 3 to 10 km vertical extent. **e** Schematic drawing of the control volumes

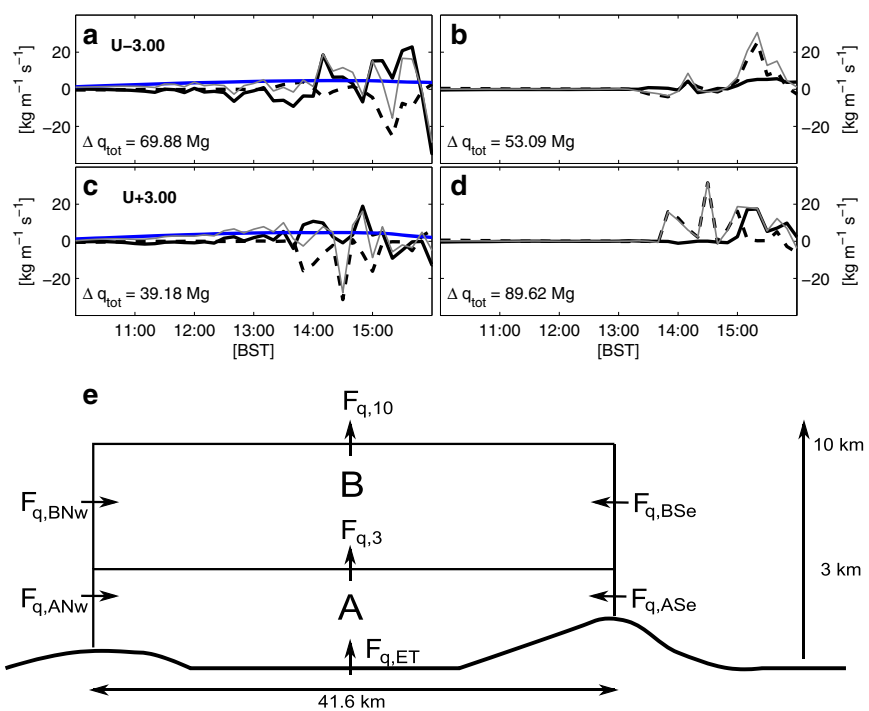


Table 4 Total integrated moisture flux (f_q) into the Nam Co Lake basin between 0600 and 1600 hours BST

Case	Volume A				Volume B				$\Delta q_{\text{tot},A}$ [Mg]	$\Delta q_{\text{tot},B}$ [Mg]
	$F_{q,ANw}$ [Mg]	$F_{q,ASe}$	$F_{q,ET}$	$F_{q,P}$	$F_{q,3}$ [Mg]	$F_{q,10}$	$F_{q,BNw}$	$F_{q,BSe}$		
U-3.00	825.27	-805.21	86.47	-1.30	-35.35	-0.02	207.30	-189.53	69.88	53.09
U-1.50	385.19	-413.81	85.67	-0.56	-11.83	-0.02	123.07	-103.34	44.66	31.54
U+0.00	-10.65	-15.96	66.32	-1.94	-24.77	-2.10	7.14	18.96	12.99	48.77
U+1.50	-403.60	451.99	73.94	-4.17	-198.10	-1.93	-93.39	109.66	20.06	112.44
U+3.00	-786.45	798.74	85.35	-1.89	-56.56	-0.11	-193.87	225.05	39.18	89.62
U+6.00	-1,613.71	1,593.66	90.70	-0.49	-45.27	-0.05	-405.13	353.97	24.89	-5.94

The control volumes denoted with subscripts *A* and *B* are indicated in Fig. 11e. The subscripts Nw and Se are for the northwest and southeast boundaries, respectively; positive fluxes across the lateral boundaries indicate flux into the volume; ET and P are the evapotranspiration and precipitation flux; 3 and 10 indicate the vertical boundaries of the control volumes, with a negative sign for upward flux; Δq_{tot} is the total net moisture flux for a volume

sum of all water species, across the boundaries of the control volumes as well as evapotranspiration and precipitation as sources and sinks, in order to develop a better understanding on the importance of the Nam Co Lake basin for the regional water cycle. The left column of Fig. 11 shows the instantaneous moisture flux for control volume A, while the right column displays the same for volume B for simulations U-3.00 and U+3.00. The full integrated moisture budget for all simulations is given in Table 4. We find a moistening of the boundary layer and the lower troposphere and a net export of moisture to the mid-troposphere in all cases. The vertical moisture transport from volume A to B is organised into a small number of distinctive events, corresponding to individual convective events carrying water into the mid-troposphere. Evapotranspiration, in contrast, is a small continuous flux into the Nam Co basin that integrated over the day ($F_{q,ET}$) which became relatively large and was, in most cases, approximately twice as large as the flux from volume A to B ($F_{q,3}$). $F_{q,3}$ varied from 0.14 $F_{q,ET}$ for U+1.50 to 2.67 $F_{q,ET}$ for U-1.50. The transport of moisture above 10 km is negligible in terms of the water balance of the Nam Co basin. In general, we found that the Nam Co Lake basin served as a significant source of moisture to the upper troposphere, where it becomes subject to both transport away from the Nam Co Lake and to local recycling through precipitation. Unfortunately, the integration time of our study does not allow us to trace the fate of this moisture during the night, which needs to be done in longer simulations over a larger domain. This study did also not take into account temporal or spatial variation in surface moisture. We started our simulations with a comparatively high surface moisture throughout the domain as the 6 August 2009 was after a period of rain. As a result, simulated and measured Q_E of the land were much larger than the flux from the lake. It is very likely that the importance

of the lake as a regional source of moisture becomes more important during drier periods, with large surface heating, such as the pre-monsoon season. As the triggering of moist convection is catalysed by topography, most of the precipitation is also formed over the mountains. Consequently and as many studies show, precipitation is higher over and, in the case of deep convection, on the leeward side of mountains. The Nam Co Lake basin is surrounded by mountain chains, and the predominant wind direction is from the northwest, so that we expect precipitation triggered by the Nyenchen Thanglha mountains to occur mainly over the mountain range itself and outside of the basin. Precipitation triggered by the northern mountains likely occurs over the northwest shore or the lake itself. This is also seen in the simulations, where little rain falls over the lake or in close proximity to the shore.

4 Conclusions

This work investigates the development of a lake-breeze system at the Nam Co Lake and its interaction with topography and background wind through an idealised modelling study, which did not consider large-scale forcings. We have demonstrated in this setting that 2D simulations conducted with ATHAM are able to reproduce the system's most important dynamical features, such as the development of a lake breeze and the transition from shallow boundary-layer clouds to moist convection, reasonably well. While we do acknowledge the limitations of this approach like an unrealistic wind field or overestimation of updraft strength, we think that a better understanding on the system can still be gained from these investigations. Modelled surface fluxes are of realistic magnitude and lead to a realistic timing of the lake breeze providing a triggering mechanism for

convection, which is in turn dependent on wind direction and speed. Stronger winds postpone the triggering of convection. An important factor governing boundary-layer cloud development in the basin is adiabatic warming or cooling as air is transported over topography. This is dependent on wind direction. The interaction or collision of the lake-breeze front with winds coming from the mountain, either as U_g or gust fronts, leads to convergence in the model and subsequently triggering of convection. Additionally, the heated mountains act as a trigger for convection as they represent a heated elevated surface transporting air parcels to the level of free convection. It should be noted though that the effect of albedo change through snow and ice is not considered in this study. This potentially limits the warming effect. Precipitation in the lake basin is mainly generated above the mountains. Therefore, stations that are located in the valley have a dry bias and are not representative for the region. This effect is exacerbated by subsidence in the basin caused by the lake. In our future work, we will look at the importance of the vertical atmospheric profiles of temperature and moisture and especially stability and smoothness of profiles. Another area of future investigations will also be at the influence of the surface configuration, such as soil moisture or land use, on turbulent surface fluxes and convection development.

Acknowledgments This research was funded by the German Research Foundation (DFG) Priority Programme 1372 “Tibetan Plateau: Formation, Climate, Ecosystems” as part of the Atmosphere–Ecology–Glaciology–Cluster (TiP-AEG): FO 226/18-1,2. The work described in this publication has been supported by the European Commission (Call FP7-ENV-2007-1 grant no. 212921) as part of the CEOP-AEGIS project (<http://www.ceop-aegis.org/>) coordinated by the University of Strasbourg. The authors wish to acknowledge Esri ArcGIS, the Microsoft Corporation, Harris Corp. and Earthstar Geographics LLC for the provision of map data of the Nam Co Lake. The landcover map was produced by Sophie Biskop and Jan Kropacek within the framework of DFG-TiP. MODIS images were provided through AERONET, and we thank the MODIS team for their work. GFS-FNL data were produced by the National Center for Environmental Prediction.

References

- Antonelli M, Rotunno R (2007) Large-eddy simulation of the onset of the sea breeze. *J Atmos Sci* 64(12):4445–4457. doi:10.1175/2007JAS2261.1
- Banta RM (1990) The role of mountain flows in making clouds. In: Blumen W (ed) Atmospheric processes over complex terrain, no. 23 in meteorological monographs. American Meteorological Society, Boston, pp 229–283
- Banta RM, Barker Schaaf C (1987) Thunderstorm genesis zones in the Colorado Rocky Mountains as determined by traceback of geosynchronous satellite images. *Mon Weather Rev* 115(2):463–476. doi:10.1175/1520-0493(1987)115<0463:TGZITC>2.0.CO;2
- Biermann T, Babel W, Ma W, Chen X, Thiem E, Ma Y, Foken T (2013) Turbulent flux observations and modelling over a shallow lake and a wet grassland in the Nam Co basin, Tibetan Plateau. *Theor Appl Climatol*. doi:10.1007/s00704-013-0953-6
- Chen SH, Lin YL (2005) Effects of moist froude number and CAPE on a conditionally unstable flow over a mesoscale mountain ridge. *J Atmos Sci* 62(2):331–350. doi:10.1175/JAS-3380.1
- Chu CM, Lin YL (2000) Effects of orography on the generation and propagation of mesoscale convective systems in a two-dimensional conditionally unstable flow. *J Atmos Sci* 57(23):3817–3837. doi:10.1175/1520-0469(2001)057<3817:EOOOTG>2.0.CO;2
- Crosman ET, Horel JD (2010) Sea and lake breezes: a review of numerical studies. *Bound-Layer Meteorol* 137(1):1–29. doi:10.1007/s10546-010-9517-9
- Cui X, Graf HF (2009) Recent land cover changes on the Tibetan Plateau: a review. *Clim Change* 94(1):47–61. doi:10.1007/s10584-009-9556-8
- Cui X, Graf HF, Langmann B, Chen W, Huang R (2006) Climate impacts of anthropogenic land use changes on the Tibetan Plateau. *Glob Plan Change* 54(1–2):33–56. doi:10.1016/j.gloplacha.2005.07.006
- Cui X, Graf HF, Langmann B, Chen W, Huang R (2007a) Hydrological impacts of deforestation on the Southeast Tibetan Plateau. *Earth Interact* 11(15):1–18. doi:10.1175/EI223.1
- Cui X, Langmann B, Graf HF (2007b) Summer monsoonal rainfall simulation on the Tibetan Plateau with a regional climate model using a one-way double-nesting system. *SOLA* 3:49–52
- Emanuel KA (1994) Atmospheric convection. Oxford University Press, New York
- Fairall CW, Bradley EF, Godfrey JS, Wick GA, Edson JB, Young GS (1996a) Cool-skin and warm-layer effects on sea surface temperature. *J Geophys Res* 101(C1):1295–1308
- Fairall CW, Bradley EF, Rogers DP, Edson JB, Young GS (1996b) Bulk parameterization of air-sea fluxes for Tropical Ocean-Global Atmosphere Coupled-Ocean Atmosphere Response Experiment. *J Geophys Res* 101(C2):3747–3764
- Foken T (2008a) The energy balance closure problem: an overview. *Ecol Appl* 18:1351–1367
- Foken T (2008b) Micrometeorology. Springer, Heidelberg
- Foken T, Aubinet M, Finnigan JJ, Leclerc MY, Mauder M, Paw UKT (2011) Results of a panel discussion about the energy balance closure correction for trace gases. *Bull Am Meteorol Soc* 92(4):ES13–ES18. doi:10.1175/2011BAMS3130.1
- Foken T, Leuning R, Oncley SR, Mauder M, Aubinet M (2012) Corrections and data quality control. In: Aubinet M, Vesala T, Papale D (eds) Eddy covariance: a practical guide to measurement and data analysis. Springer, Dordrecht, pp 85–131. doi:10.1007/978-94-007-2351-1_4
- Friend AD, Kiang NY (2005) Land surface model development for the GISS GCM: effects of improved canopy physiology on simulated climate. *J Clim* 18(15):2883–2902. doi:10.1175/JCLI3425.1
- Friend AD, Stevens AK, Knox RG, Cannell MGR (1997) A process-based, terrestrial biosphere model of ecosystem dynamics (Hybrid v3.0). *Ecol Model* 95(2–3):249–287. doi:10.1016/S0304-3800(96)00034-8
- Gao Y, Tang M, Luo S, Shen Z, Li C (1981) Some aspects of recent research on the Qinghai-Xizang Plateau meteorology. *Bull Am Meteorol Soc* 62(1):31–35. doi:10.1175/1520-0477(1981)062<0031:SAORRO>2.0.CO;2
- Gerken T, Babel W, Hoffmann A, Biermann T, Herzog M, Friend AD, Li M, Ma Y, Foken T, Graf HF (2012) Turbulent flux modelling with a simple 2-layer soil model and extrapolated surface temperature applied at Nam Co Lake basin on the Tibetan Plateau. *Hydrol Earth Syst Sci* 16(4):1095–1110. doi:10.5194/hess-16-1095-2012

- Gochis DJ, Jimenez A, Watts CJ, Garatuza-Payan J, Shuttleworth WJ (2004) Analysis of 2002 and 2003 warm-season precipitation from the North American Monsoon Experiment Event Rain Gauge Network. *Mon Weather Rev* 132(12):2938–2953. doi:10.1175/MWR2838.1
- Graf HF, Herzog M, Oberhuber JM, Textor C (1999) Effect of environmental conditions on volcanic plume rise. *J Geophys Res* 104(D20):24,309–24,320. doi:10.1029/1999JD900498
- Guo H, Penner J, Herzog M (2004) Comparison of the vertical velocity used to calculate the cloud droplet number concentration in a cloud-resolving and a global climate model. In: Carrothers D (ed) Fourteenth ARM science team meeting proceedings. Department of Energy, Boston, pp 1–6
- Herzog M, Graf HF, Textor C, Oberhuber JM (1998) The effect of phase changes of water on the development of volcanic plumes. *J Volcanol Geotherm Res* 87(1–4):55–74. doi:10.1016/S0377-0273(98)00100-0
- Herzog M, Oberhuber JM, Graf HF (2003) A prognostic turbulence scheme for the nonhydrostatic plume model ATHAM. *J Atmos Sci* 60(22):2783–2796. doi:10.1175/1520-0469(2003)060<2783:APTSFT>2.0.CO;2
- Immerzeel WW, van Beek LPH, Bierkens MFP (2010) Climate change will affect the Asian water towers. *Science* 328(5984):1382–1385. doi:10.1126/science.1183188
- Kirshbaum DJ (2011) Cloud-resolving simulations of deep convection over a heated mountain. *J Atmos Sci* 68(2):361–378. doi:10.1175/2010JAS3642.1
- Kirshbaum DJ, Durran DR (2004) Factors governing cellular convection in orographic precipitation. *J Atmos Sci* 61(6):682–698. doi:10.1175/1520-0469(2004)061<0682:FGCCIO>2.0.CO;2
- Kurita N, Yamada H (2008) The role of local moisture recycling evaluated using stable isotope data from over the middle of the Tibetan Plateau during the monsoon season. *J Hydrometeorol* 9(4):760–775. doi:10.1175/2007JHM945.1
- Kurosaki Y, Kimura F (2002) Relationship between topography and daytime cloud activity around Tibetan Plateau. *J Meteorol Soc Jpn* 80(6):1339–1355
- Kuwagata T, Kondo J, Sumioka M (1994) Thermal effect of the sea breeze on the structure of the boundary layer and the heat budget over land. *Bound-Layer Meteorol* 67(1–2):119–144. doi:10.1007/BF00705510
- Kuwagata T, Numaguti A, Endo N (2001) Diurnal variation of water vapor over the central Tibetan Plateau during summer. *J Meteorol Soc Jpn* 79(1B):401–418. doi:10.2151/jmsj.79.401
- Langmann B, Herzog M, Graf HF (1998) Radiative forcing of climate by sulfate aerosols as determined by a regional circulation chemistry transport model. *Atmos Environ* 32(16):2757–2768. doi:10.1016/S1352-2310(98)00028-4
- Liu WT, Katsaros KB, Businger JA (1979) Bulk parameterization of air-sea exchanges of heat and water vapor including the molecular constraints at the interface. *J Atmos Sci* 36(9):1722–1735. doi:10.1175/1520-0469(1979)036<1722:BPOASE>2.0.CO;2
- Ma L, Zhang T, Li Q, Frauenfeld OW, Qin D (2008) Evaluation of ERA-40, NCEP-1, and NCEP-2 reanalysis air temperatures with ground-based measurements in China. *J Geophys Res* 113(D15):115. doi:10.1029/2007JD009549
- Ma Y, Wang Y, Wu R, Hu Z, Yang K, Li M, Ma W, Zhong L, Sun F, Chen X et al (2009) Recent advances on the study of atmosphere-land interaction observations on the Tibetan Plateau. *Hydrol Earth Syst Sci* 13(7):1103–1111. doi:10.5194/hess-13-1103-2009
- Mauder M, Foken T (2004) Documentation and instruction manual of the eddy covariance software package TK2. *Arbeitsergebnisse* 26, University of Bayreuth, Bayreuth. <http://opus.ub.uni-bayreuth.de/opus4-ubbayreuth/frontdoor/index/index/docId/639>
- Mauder M, Foken T (2011) Documentation and instruction manual of the eddy covariance software package TK3. *Arbeitsergebnisse* 46, University of Bayreuth, Bayreuth. <http://opus.ub.uni-bayreuth.de/opus4-ubbayreuth/frontdoor/index/index/docId/681>
- Maussion F, Scherer D, Finkelnburg R, Richters J, Yang W, Yao T (2011) WRF simulation of a precipitation event over the Tibetan Plateau, China — an assessment using remote sensing and ground observations. *Hydrol Earth Syst Sci* 15(6):1795–1817
- Miao JF, Kroon LJM, Vila-Guerau de Arellano J, Holtslag AAM (2003) Impacts of topography and land degradation on the sea breeze over eastern Spain. *Meteorol Atmos Phys* 84(3–4):157–170. doi:10.1007/s00703-002-0579-1
- Miglietta MM, Rotunno R (2009) Numerical simulations of conditionally unstable flows over a mountain ridge. *J Atmos Sci* 66(7):1865–1885. doi:10.1175/2009JAS2902.1
- Miller STK, Keim BD, Talbot RW, Mao H (2003) Sea breeze: structure, forecasting and impacts. *Rev Geophys* 41(3):1011. doi:10.1029/2003RG000124
- Mlawer EJ, Taubman SJ, Brown PD, Iacono MJ, Clough SA (1997) Radiative transfer for inhomogeneous atmospheres: RRTM, a validated correlated-k model for the longwave. *J Geophys Res* 102(D14):16,663–16,682
- Oberhuber JM, Herzog M, Graf HF, Schwanke K (1998) Volcanic plume simulation on large scales. *J Volcanol Geotherm Res* 87(1–4):29–53. doi:10.1016/S0377-0273(98)00099-7
- Ookouchi Y, Uryu M, Sawada R (1978) A numerical study on the effects of a mountain on the land and sea breezes. *J Meteorol Soc Jpn* 56:368–386
- Petch JC (2004) The predictability of deep convection in cloud-resolving simulations over land. *QJR Meteorol Soc* 130(604):3173–3187. doi:10.1256/qj.03.107
- Petch JC (2006) Sensitivity studies of developing convection in a cloud-resolving model. *QJR Meteorol Soc* 132(615):345–358. doi:10.1256/qj.05.71
- Rampanelli G, Zardi D, Rotunno R (2004) Mechanisms of up-valley winds. *J Atmos Sci* 61(24):3097–3111. doi:10.1175/JAS-3354.1
- Rebmann C, Kolle O, Heinesch B, Queck R, Ibrom A, Aubinet M (2012) Data acquisition and flux calculations. In: Aubinet M, Vesala T, Papale D (eds) *Eddy covariance: a practical guide to measurement and data analysis*. Springer, Dordrecht, pp 59–83. doi:10.1007/978-94-007-2351-1_3
- Reeves HD, Lin YL (2007) The effects of a mountain on the propagation of a preexisting convective system for blocked and unblocked flow regimes. *J Atmos Sci* 64(7):2401–2421. doi:10.1175/JAS3959.1
- Tanaka K, Tamagawa I, Ishikawa H, Ma Y, Hu Z (2003) Surface energy budget and closure of the eastern Tibetan Plateau during the GAME-Tibet IOP 1998. *J Hydrometeorol* 283(1–4):169–183. doi:10.1016/S0022-1694(03)00243-9
- Taniguchi K, Koike T (2008) Seasonal variation of cloud activity and atmospheric profiles over the eastern part of the Tibetan Plateau. *J Geophys Res* 113(D10):104. doi:10.1029/2007JD009321
- Tian L, Masson-Delmotte V, Stievenard M, Yao T, Jouzel J (2001a) Tibetan Plateau summer monsoon northward extent revealed by measurements of water stable isotopes. *J Geophys Res* 106(D22):28,081–28,088.
- Tian L, Yao T, Numaguti A, Sun W (2001b) Stable isotope variations in monsoon precipitation on the Tibetan Plateau. *J Meteorol Soc Jpn* 79(5):959–966. doi:10.2151/jmsj.79.959

- Trentmann J, Luderer G, Winterrath T, Fromm MD, Servranckx R, Textor C, Herzog M, Graf HF, Andreae MO (2006) Modeling of biomass smoke injection into the lower stratosphere by a large forest fire (Part I): reference simulation. *Atmos Chem Phys* 6(12):5247–5260
- Twine TE, Kustas WP, Norman JM, Cook DR, Houser PR, Meyers TP, Prueger JH, Starks PJ, Wesely ML (2000) Correcting eddy-covariance flux underestimates over a grassland. *Agric Forest Meteorol* 103(3):279–300. doi:[10.1016/S0168-1923\(00\)00123-4](https://doi.org/10.1016/S0168-1923(00)00123-4)
- Wang J, Zhu L, Daut G, Ju J, Lin X, Wang Y, Zhen X (2009) Investigation of bathymetry and water quality of Lake Nam Co, the largest lake on the central Tibetan Plateau, China. *Limnology* 10(2):149–158. doi:[10.1007/s10201-009-0266-8](https://doi.org/10.1007/s10201-009-0266-8)
- Wu CM, Stevens B, Arakawa A (2009) What controls the transition from shallow to deep convection. *J Atmos Sci* 66(6):1793–1806. doi:[10.1175/2008JAS2945.1](https://doi.org/10.1175/2008JAS2945.1)
- Xu ZX, Gong TL, Li JY (2008) Decadal trend of climate in the Tibetan Plateau—regional temperature and precipitation. *Hydrol Process* 22(16):3056–3065. doi:[10.1002/hyp.6892](https://doi.org/10.1002/hyp.6892)
- Yanai M, Li C, Song Z (1992) Seasonal heating of the Tibetan Plateau and its effects on the evolution of the Asian summer monsoon. *J Meteorol Soc Jpn* 70(1B):319–351
- Yang K, Koike T, Fujii H, Tamura T, Xu X, Bian L, Zhou M (2004) The daytime evolution of the atmospheric boundary layer and convection over the Tibetan Plateau: observations and simulations. *J Meteorol Soc Jpn* 82(6):1777–1792. doi:[10.2151/jmsj.82.1777](https://doi.org/10.2151/jmsj.82.1777)
- Yang K, Ye B, Zhou D, Wu B, Foken T, Qin J, Zhou Z (2011) Response of hydrological cycle to recent climate changes in the tibetan plateau. *Clim Change* 109(3–4):517–534. doi:[10.1007/s10584-011-0099-4](https://doi.org/10.1007/s10584-011-0099-4)
- Yatagai A (2001) Estimation of precipitable water and relative humidity over the Tibetan Plateau from GMS-5 water vapor channel data. *J Meteorol Soc Jpn* 79(1B):589–598
- Yin ZY, Zhang X, Liu X, Colella M, Chen X (2008) An assessment of the biases of satellite rainfall estimates over the Tibetan Plateau and correction methods based on topographic analysis. *J Hydrometeorol* 9(3):301–326. doi:[10.1175/2007JHM903.1](https://doi.org/10.1175/2007JHM903.1)

D. Babel et al. (2014)

Babel, W., Biermann, T., Coners, H., Falge, E., Seeber, E., Ingrisch, J., Schleuß, P.-M., Gerken, T., Leonbacher, J., Leipold, T., Willinghöfer, S., Schützenmeister, K., Shibistova, O., Becker, L., Hafner, S., Spielvogel, S., Li, X., Xu, X., Sun, Y., Zhang, L., Yang, Y., Ma, Y., Wesche, K., Graf, H.-F., Leuschner, C., Guggenberger, G., Kuzyakov, Y., Miehe, G., and Foken, T.: Pasture degradation modifies the water and carbon cycles of the Tibetan highlands, *Biogeosciences*, 11, 6633-6656, doi:10.5194/bg-11-6633-2014, 2014.

Biogeosciences, 11, 6633–6656, 2014
www.biogeosciences.net/11/6633/2014/
doi:10.5194/bg-11-6633-2014
© Author(s) 2014. CC Attribution 3.0 License.



Pasture degradation modifies the water and carbon cycles of the Tibetan highlands

W. Babel^{1,17}, T. Biermann^{1,*}, H. Coners², E. Falge^{1,*}, E. Seeber³, J. Ingrisch^{4,***}, P.-M. Schleuß⁴, T. Gerken^{1,5,****}, J. Leonbacher¹, T. Leipold¹, S. Willinghöfer², K. Schützenmeister⁶, O. Shibistova^{7,8}, L. Becker⁷, S. Hafner⁴, S. Spielvogel^{4,6}, X. Li⁹, X. Xu^{4,10}, Y. Sun^{4,10}, L. Zhang¹¹, Y. Yang¹², Y. Ma¹¹, K. Wesche^{3,13}, H.-F. Graf⁵, C. Leuschner², G. Guggenberger⁷, Y. Kuzyakov^{4,14,15}, G. Miehe¹⁶, and T. Foken^{1,17}

¹University of Bayreuth, Department of Micrometeorology, Bayreuth, Germany

²University of Göttingen, Department of Plant Ecology and Ecosystem Research, Göttingen, Germany

³Senckenberg Museum Görlitz, Department of Botany, Görlitz, Germany

⁴University of Göttingen, Department of Soil Sciences of Temperate Ecosystems, Göttingen, Germany

⁵University of Cambridge, Department of Geography, Centre for Atmospheric Science, Cambridge, UK

⁶University of Koblenz-Landau, Institute of Integrated Environmental Sciences, Koblenz, Germany

⁷Leibniz Universität Hannover, Institute for Soil Science, Hanover, Germany

⁸V. N. Sukachev Institute of Forest, Krasnoyarsk, Russia

⁹School of Life Sciences, Lanzhou University, Lanzhou, China

¹⁰Chinese Academy of Sciences, Institute of Geographical Sciences and Natural Resources Research, Beijing, China

¹¹Chinese Academy of Sciences, Institute of Tibetan Plateau Research, Key Laboratory of Tibetan Environment Changes and Land Surface, Processes, Beijing, China

¹²Chinese Academy of Sciences, Institute of Tibetan Plateau Research, Laboratory of Alpine Ecology and Biodiversity Focuses, Processes, Beijing, China

¹³German Centre for Integrative Biodiversity Research (iDiv) Halle–Jena–Leipzig, Germany

¹⁴University of Göttingen, Department of Agricultural Soil Science, Göttingen, Germany

¹⁵Institute of Environmental Sciences, Kazan Federal University, Kazan, Russia

¹⁶University of Marburg, Faculty of Geography, Marburg, Germany

¹⁷Member of Bayreuth Center of Ecology and Ecosystem Research, Bayreuth, Germany

* now at: Lund University, Centre for Environmental and Climate Research, Lund, Sweden

** now at: Thünen Institute of Climate-Smart Agriculture, Braunschweig, Germany

*** now at: University of Innsbruck Institute of Ecology Research, Innsbruck, Austria

**** now at: The Pennsylvania State University, Department of Meteorology, University Park, PA, USA

Correspondence to: T. Foken (thomas.foken@uni-bayreuth.de)

Received: 21 May 2014 – Published in Biogeosciences Discuss.: 12 June 2014

Revised: 29 October 2014 – Accepted: 30 October 2014 – Published: 2 December 2014

Abstract. The Tibetan Plateau has a significant role with regard to atmospheric circulation and the monsoon in particular. Changes between a closed plant cover and open bare soil are one of the striking effects of land use degradation observed with unsustainable range management or climate change, but experiments investigating changes of surface properties and processes together with atmospheric feedbacks are rare and have not been undertaken in the world's

two largest alpine ecosystems, the alpine steppe and the *Kobresia pygmaea* pastures of the Tibetan Plateau. We connected measurements of micro-lysimeter, chamber, ¹³C labelling, and eddy covariance and combined the observations with land surface and atmospheric models, adapted to the highland conditions. This allowed us to analyse how three degradation stages affect the water and carbon cycle of pastures on the landscape scale within the core region of the

Published by Copernicus Publications on behalf of the European Geosciences Union.

Kobresia pygmaea ecosystem. The study revealed that increasing degradation of the *Kobresia* turf affects carbon allocation and strongly reduces the carbon uptake, compromising the function of *Kobresia* pastures as a carbon sink. Pasture degradation leads to a shift from transpiration to evaporation while a change in the sum of evapotranspiration over a longer period cannot be confirmed. The results show an earlier onset of convection and cloud generation, likely triggered by a shift in evapotranspiration timing when dominated by evaporation. Consequently, precipitation starts earlier and clouds decrease the incoming solar radiation. In summary, the changes in surface properties by pasture degradation found on the highland have a significant influence on larger scales.

1 Introduction

Alpine ecosystems are considered as being highly vulnerable to the impacts of climate and land use change. This is especially the case for two of the world's highest and largest alpine ecosystems: the *Kobresia pygmaea* pastures covering 450 000 km² in the southeast and the alpine steppe covering 600 000 km² in the northwest of the Tibetan Plateau. The *Kobresia pygmaea* pastures typically form a closed grazing lawn of about 2 cm in height with up to 98 % cover of *Kobresia pygmaea*, as main constituent of a felty turf (Kaiser et al., 2008; Mieke et al., 2008b). The alpine steppe is a central Asian short grass steppe with alpine cushions and a plant cover declining from 40 % in the east to 10 % in the west (Mieke et al., 2011). Both ecosystems are linked by an ecotone of 200 km in width over 2000 km length (Fig. 1).

Obvious features of degradation in the *Kobresia* pastures and their ecotone are controversially discussed as being caused by either natural abiotic and biotic processes or human impacts (Zhou et al., 2005). The most widespread pattern are mosaics of: (i) closed *Kobresia* grazing lawns (later named as intact root Mat, IM); (ii) root turf that is only sparsely vegetated by *Kobresia pygmaea* but sealed with Cyanophyceae (later named as partly degraded root Mat, DM); and (iii) open loess and gravels that are sparsely colonised by cushions, rosettes and small grasses of the alpine steppe (later named as bare soil, BS).

Assessments of pasture degradation have been either based on biotic parameters such as decreasing vegetation cover, species diversity, productivity and forage quality, or alternatively on abiotic factors including nutrient loss, soil compaction and ongoing soil erosion (Harris, 2010). A definition of degradation stages was given by Liu et al. (2003, in Chinese) and later on used by Zhou et al. (2005). According to a study by Niu (1999), 30 % of the *Kobresia* grassland is degraded at various levels. Holzner and Kriebbaum (2000) reported that about 30 % is in optimal condition, about 30 % shows characteristics of overgrazing where regeneration seems to be possible after improved utilisation

and about 40 % shows recent or ancient complete degradation. Here, we regard bare silty soil as the final degradation stage of a former *Kobresia* pasture with its intact root turf. Loss of *Kobresia* cover goes along with a decrease of palatable species and thus pasture quality.

The general lack of data on the alpine ecology of *Kobresia* pastures is in strong contrast to the relevance of this ecosystem. However, it is important not only to gain more knowledge on single aspects of the *Kobresia* pasture, but especially on ecological functions of the ecosystem. Therefore, modelling of the effects of degradation on atmospheric processes as well as more general analysis of interactions is necessary (Cui and Graf, 2009). Only when this challenge has been met can the effect be investigated in climate models, both for the past, but mainly for a future climate. The model simulations of Cui et al. (2006) clearly demonstrate that anthropogenic land use change on the Tibetan Plateau has far reaching implications for the Indian and East Asian summer monsoons. In order to correctly reproduce the hydrological regime on the plateau, a spatial resolution of the order of 10 km is required (Cui et al., 2007b). This resolution is typical for state-of-the-art weather forecast models, but is by far not reached by any climate model simulation. This lack of scale compatibility can to some degree be compensated by sophisticated treatment of surface energy fluxes and their impact on convective clouds. Therefore, there is an urgent need to identify the parameters and factors influencing the pastures and to quantify energy and matter fluxes.

In order to model fluxes over *Kobresia* and degraded areas, it is necessary to identify those model parameters which change significantly due to any degradation present. Three factors could reflect these problems:

- Missing vegetation: the difference is considered in the simulation through the fraction of vegetated areas and the respective parameter differences between bare soil evaporation and grassland evapotranspiration, as well as assimilation and respiration.
- Different soil properties: due to the missing *Kobresia* turf, soil properties of the upper layer might be changed: less living and dead organic material lead to poor isolation and switch from hydrophobic to more hydrophilic properties, thus leading to higher infiltration capacity and higher soil hydraulic conductivity.
- The available energy changes mostly due to albedo differences and outgoing long-wave radiation. Furthermore, the direct solar irradiation is much larger than diffuse radiation compared to other regions of the world.

We expect that degradation of vegetation and soil surface at the plot scale leads to changes of water and carbon fluxes, as well as carbon stocks, at the ecosystem level, with consequences for the whole Tibetan Plateau. The aim of this study was to analyse and model for the first time the water

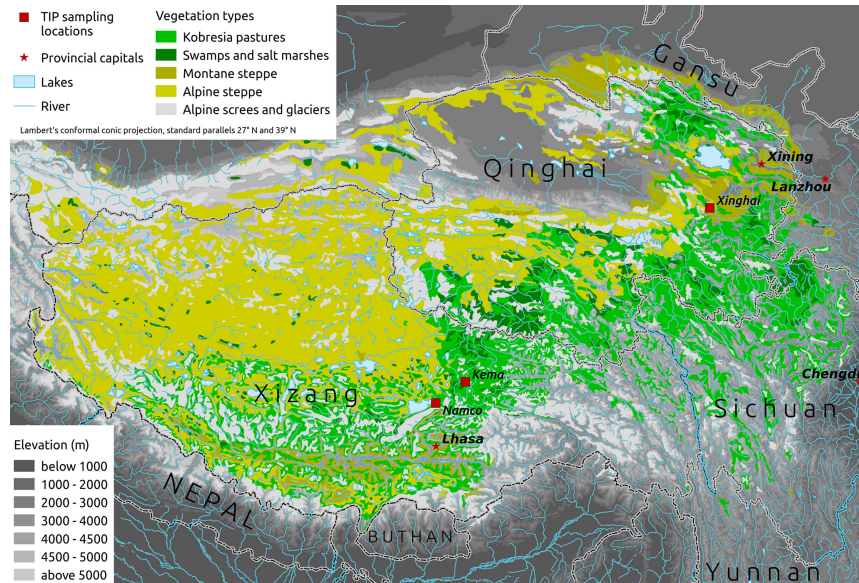


Figure 1. *Kobresia pygmaea* pastures (in green) dominate the southeastern quarter of the Tibetan highlands, whereas the alpine steppe covers the arid northwestern highlands. The experimental sites Xinghai and Kema are in montane and alpine *Kobresia* pastures, whereas the Nam Co site is situated in the ecotone towards alpine steppe (modified after Miehe et al., 2008b).

and carbon fluxes in the above-mentioned three types of surface patterns of *Kobresia* pastures on the Tibetan Plateau. We combine the benefits of observing water and carbon fluxes at the plot scale, using micro-lysimeter, chamber-based gas exchange measurements and ^{13}C labelling studies, and also simultaneously at the ecosystem scale with eddy-covariance measurements. Our model studies are focused on land surface models, where the description of plant and soil parameters is more explicitly parameterised than in larger-scale models. They bridge between the plot and the ecosystem scale and simulate the influence of increasing degradation on water and carbon fluxes, which ultimately leads to changes of cloud cover and precipitation. Explicitly simulating the impact of changes in vegetation on turbulent surface fluxes (Gerken et al., 2012), local to regional circulation (Gerken et al., 2014) and variability in the evolution of convective clouds and rainfall due to different tropospheric vertical profiles (Gerken et al., 2013) allows for the assessment of the sensitivity of the energetic and hydrological regimes on the Tibetan Plateau. Such model simulations on the local scale serve as an important tool for the interpretation of larger scale simulations and sensitivity studies. The current study provides a link between degradation studies (Harris, 2010) and remote sensing and modelling for the whole Tibetan Plateau (Ma et al., 2011, 2014; Maussion et al., 2014; Shi and Liang,

2014) and climate studies (Cui et al., 2006, 2007a; Yang et al., 2011; Yang et al., 2014).

2 Material and methods

2.1 Study sites

For the present study, measurements were taken at three study sites on the Tibetan Plateau. Details are given in Table 1. For the experimental activities at the sites see Sect. 2.5.

Xinghai: The experimental site is located in Qinghai province in the northeastern Tibetan Plateau, approximately 200 km southwest of Xining, and about 15 km south of Xinghai city. The montane grassland has developed on a loess-covered (1.2 m) terrace of the Huang He River. The grassland is used as a winter pasture for yaks and sheep for 6–7 months of the year (Miehe et al., 2008b; Unteregelsbacher et al., 2012). About 20 % of the pasture at the experiment site is completely covered with blue-green algae and crustose lichens.

Kema: The “*Kobresia pygmaea* Research Station Kema”, established in 2007, is located in the core area of alpine *Kobresia pygmaea* pasture. All measurements were established either within or in the close surroundings of an area of 100 m

Table 1. Characteristics of the three study sites.

	Xinghai	Kema	Nam Co	
Coordinates	35°32' N, 99°51' E	31°16' N, 92°06' E	30°46' N, 90°58' E	
Altitude a.s.l.	3440 m	4410 m	4730 m	
Soil (IUSS-ISRIC-FAO, 2006)	Haplic Kastanozems	Stagnic (mollic) Cambisol	Stagnic Cambisols and Arenosol	
Pasture type	Montane <i>Kobresia-Stipa</i> winter pastures	Alpine <i>Kobresia pygmaea</i> pastures	Alpine steppe pastures with mosaic <i>Kobresia</i> turfs	
Source for soil and plant types	Kaiser et al. (2008), Mieke et al. (2008a), Unteregelsbacher et al. (2012), and Hafner et al. (2012)	This study, Kaiser et al. (2008), Mieke et al. (2011), and Biermann et al. (2011, 2013)	Kaiser et al. (2008), and Mieke et al. (2014)	
Climate period	1971–2000	1971–2000	1971–2000	1971–2000
Climate station	Xinghai 3323 m.a.s.l., 35°35' N, 99°59' E	Naqu 4507 m.a.s.l., 31°29' N, 92°04' E	Baingoin 4700 m.a.s.l., 31°23' N, 90°01' E	Damxung 4200 m.a.s.l., 30°29' N, 91°06' E
Annual precipitation*	353 mm	430 mm	322 mm	460 mm
Mean annual temperature	1.4 °C	−1.2 °C	−0.8 °C	1.7 °C
Mean Jul temperature	12.3 °C	9.0 °C	8.7 °C	10.9 °C
Source for climate data	http://cdc.cma.gov.cn/			

* Due to the East Asian monsoon, almost all of the precipitation falls in the summer months from May to Sep, most frequently in the form of torrential rain during afternoon thunderstorms.

Table 2. Criteria for a differentiation of main degradation classes at Kema site and survey results.

Stage	Intact root Mat (IM)	Degraded root Mat (DM)	Bare soil (BS)
Dominant plant species	<i>Kobresia pygmaea</i>	<i>Kobresia pygmaea</i> , Lichens, Algae	Annuals, e.g. <i>Axyris prostrata</i>
Root mat layer	Yes	Yes	No
Proportion of total surface area (% , $n = 2618$)*	65	16	19
Mean vegetation cover within the respective stage (%)*	88 ± 6 (SD)	26 ± 10 (SD)	12 ± 8 (SD)
Maximal vegetation cover (%)*	99	65	35
Minimal vegetation cover (%)*	72	5	0
Level difference to BS (cm, $n = 60$)	9.4 ± 2.0 (SD)	8.5 ± 2.0 (SD)	–

* $n = 100$ for IM, DM, BS; considered are only “higher graduated plants” (grasses, herbs).

by 250 m, fenced in 2009, on a pasture where grazing was restricted to a few months during winter and spring. The growing season strongly depends on the availability of water, and usually starts at the end of May with the onset of the monsoon and ends with longer frosts by the end of August or September. *Kobresia pygmaea* has an average vegetation grazed height of 1–2 cm (Mieke et al., 2008b) and forms a very tough felty root turf of living and dead *Kobresia* roots, leaf bases and soil organic matter (Kaiser et al., 2008). It is

designated as *Kobresia* root mat throughout this study and attains a thickness of 14 cm.

The site is covered with *Kobresia pygmaea* (Cyperaceae), accompanied by other monocotyledons (*Carex ivanoviae*, *Carex* spp., *Festuca* spec., *Kobresia pusilla*, *Poa* spp., *Stipa purpurea*) and to a minor degree by perennial herbs. For more details on the species diversity see Biermann et al. (2011, 2013).

Nam Co: The “Nam Co Monitoring and Research Station for Multisphere Interactions” (NAMORS) of the Institute of

Table 3. Instrumentation of Kema site in 2010 (6 June–2 August) and 2012 (11 July–10 September, AWS: automatic weather station).

	Complex 1 <i>Kobresia</i> pasture, 2010	Complex 2* <i>Kobresia</i> pasture, 2010	Complex 3 bare soil 2010	AWS 2012	Radiation and soil complex 2012
Wind velocity and wind direction	2.21 m, CSAT3 (Campbell Sci. Ltd.)	2.20 m, CSAT3 (Campbell Sci. Ltd.)	–	2.0 m, WindSonic 1 (Gill)	–
CO ₂ and H ₂ O concentration	2.16 m, LI-7500 (LI-COR Biosciences)	2.19 m, LI-7500 (LI-COR Biosciences)	–	–	–
Air temperature and humidity	2.20 m, HMP 45 (Vaisala)	2.20 m, HMP 45 (Vaisala)	–	2.0 m, CS 215 (Campbell Scientific Ltd.)	–
Ambient pressure	–	Inside Logger Box (Vaisala)	–	–	–
Solar radiation	1.90 m, CNR1 (Kipp & Zonen)	1.88 m; CNR1 (Kipp & Zonen)	–	2.0 m, Pyranometer SP 110 (Apogee), NR Lite (Kipp & Zonen), LI 190 SB (LI-COR)	2.0 m; CNR1 (Kipp & Zonen)
Precipitation	–	1.0 m, Tipping bucket	–	0.5 m, Tipping Bucket (Young)	–
Soil moisture	–0.15, Imko-TDR	–0.1, –0.2, Imko-TDR	–0.15, Imko-TDR	–0.05, –0.125, –0.25, Campbell CS 616	–0.1, –0.2, Imko-TDR
Soil water potential	–	–	–	–0.05, –0.125, –0.25, Campbell 257-L	–
Soil temperature	–0.025, –0.075, –0.125, Pt 100	–0.025, –0.075, –0.125, –0.2, Pt 100	–0.025, –0.075, –0.125, Pt 100	–0.025, –0.075, –0.125, –0.25, Pt 100	–0.025, –0.075, –0.125, –0.175, Pt 100
Soil heat flux	–0.15, HP3	–0.15, HP3	–0.15, HP3	–	–0.2, HP3, Hukseflux

* This complex was used due to the higher data availability. There was no difference between the two instruments.

TibetanPlateauResearch of the Chinese Academy of Science (Ma et al., 2008) is located within an intramontane basin, 1 km SE of Lake Nam Co and in approximately 10 km distance NNW of the foot of the Nyainqentanglha mountain range. The zonal vegetation comprises mosaics of *Kobresia* turfs and open alpine steppe; water surplus sites have degraded Cyperaceae swamps (Mügler et al., 2010; Wei et al., 2012; Miehe et al., 2014).

2.2 Classification of the degradation classes at Kema site

At the Kema site a patchy structure of different degradation stages exists, which were classified according to the following classes (Fig. 2): intact root Mat (IM), degraded root Mat (DM) and bare soil (BS).

Intact root Mat (IM)

Although this degradation class is named as IM in this study, according to the definition of Miehe et al. (2008b) it is already degraded. Closed *Kobresia* mats are normally characterized as 90–98 % cover of *Kobresia pygmaea*, and additionally occurring biennial rosette species (Miehe et al., 2008b), which is not the case at Kema site. Nevertheless, soil is covered completely with the characteristic root turf of these Cyperaceae communities and a fairly closed cover of vegetation can be observed.

Degraded root Mat (DM)

For the DM class, not only is the spatial cover of *Kobresia pygmaea* much lower (less than 26 %), but also the proportion of crusts compared to IM is much higher; the root turf is still present. Crusts were formed by Cyanophyceae (blue algae, Miehe et al., 2008b; Unteregelsbacher et al., 2012) and were a characteristic property of this classification.



Figure 2. The three defined vegetation classes: (a) intact root Mat (IM); (b) degraded root Mat (DM); and (c) bare soil (BS).

Bare soil (BS)

In contrast to IM and DM, this surface class is missing the dense root turf and *Kobresia pygmaea* completely, resulting in a height step change. Most of the surface is unvegetated, nevertheless annual and perennial plants still occur, e.g. *Lancea tibetica* and *Saussurea stoliczkae*, described as endemic biennial rosettes and endemic plants with rhizomes, adapted to soil movement and the occurrence of trampling (Miehe et al., 2011).

These classes co-exist on scales which are too small to be resolved by the eddy-covariance method. Therefore we conducted a field survey within the eddy-covariance footprint to estimate their spatial abundance (Table 2). The degradation classes were recorded at a defined area of 5 cm × 5 cm over a regular grid according to the step point method (Evans and Love, 1957), yielding a total of 2618 observations. The proportion of total surface area is then calculated from the frequency of a given class vs. the total number of sampling points. With a *Kobresia pygmaea* cover of approximately 65 %, an area of 16 % crust-covered turf as well as 19 % bare soil spots, the main study site is considered to be a typical alpine *Kobresia pygmaea* pasture with a low to medium degradation state (Table 2).

2.3 Measuring methods

2.3.1 Micrometeorological measurements

The measurements of the water and carbon fluxes with the eddy-covariance (EC) method were conducted at the Nam Co site in 2009 and at the Kema site in 2010. The EC towers were equipped with CSAT3 sonic anemometers (Campbell Sci. Inc.) and LI-7500 (LI-COR Biosciences) gas analysers. The complete instrumentation, including radiation and soil sensors, is given in Tables 3 and 4; for more details see Zhou et al. (2011) and Biermann et al. (2011, 2013).

Turbulent fluxes were calculated and quality controlled based on micrometeorological standards (Aubinet et al., 2012) through the application of the software package TK2/TK3 developed at the University of Bayreuth (Mauder and Foken, 2004, 2011). This includes all necessary data correction and data quality tools (Foken et al., 2012a), was ap-

proved by comparison with other commonly used software packages (Mauder et al., 2008; Fratini and Mauder, 2014), and calculated fluxes match up-to-date micrometeorological standards (Foken et al., 2012a; Rebmann et al., 2012). It also offers a quality flagging system evaluating stationarity and development of turbulence (Foken and Wichura, 1996; Foken et al., 2004). Furthermore, a footprint analysis was performed (Göckede et al., 2004, 2006), which showed that the footprint area was within the classified land use type. This finding is in agreement with the results obtained by Zhou et al. (2011) for the Nam Co site.

For the interpretation of the results, the so-called unclosure of the surface energy balance (Foken, 2008) with eddy-covariance data must be taken into account, especially when comparing eddy-covariance measurements with models that close the energy balance, like SEWAB (Kracher et al., 2009), or when comparing evapotranspiration sums with micro-lysimeter measurements. For the Nam Co site Zhou et al. (2011) found that only 70 % of the available energy (net radiation minus ground heat flux) contributes to the sensible and latent heat flux, which is similar to the findings of other authors for the Tibetan Plateau (Tanaka et al., 2001; Yang et al., 2004). For the Nam Co 2009 data set we found a closure of 80 %, while both eddy-covariance measurements in Kema 2010 showed a closure of 73 %. Following recent experimental studies, we assume that the missing energy is to a large extent part of the sensible heat flux (Foken et al., 2011; Charuchittipan et al., 2014), which was also postulated from a model study (Ingwersen et al., 2011). We thus corrected the turbulent fluxes for the missing energy according to the percentage of sensible and latent heat flux contributing to the buoyancy flux according to Charuchittipan et al. (2014), Eqns 21–23 therein. This correction method attributes most of the residual to the sensible heat flux depending on the Bowen ratio (see Charuchittipan et al., 2014, Fig. 8 therein). For the measured range of Bowen ratios from 0.12 (5 % quantile) to 3.3 (95 % quantile), 37 to 2 % of the available energy was moved to the latent heat flux. For Kema in 2010, this is equal to an addition of 5 W m⁻² missing energy to the latent heat flux on average. In contrast, eddy-covariance-derived net ecosystem exchange (NEE) fluxes were not corrected (Foken et al., 2012a).

Table 4. Instrumentation of NamCo site in 2009 (25 June–8 August, only relevant instruments are shown).

Device	Type/manufacturer	Height
Ultrasonic anemometer	CSAT3 (Campbell Scientific Ltd.)	3.1 m
Gas analyser	LI-7500 (LI-COR Biosciences)	3.1 m
Temperature–humidity sensor	HMP 45 (Vaisala)	3.1 m
Net radiometer	CM3 & CG3 (Kipp&Zonen)	1.5 m
Rain gauge	Tipping bucket	1 m
Soil moisture	Imko-TDR	−0.1, −0.2, −0.4, −0.8, −1.60
Soil temperature	Pt100	−0.2, −0.4, −0.8, −1.60
Logger	CR5000 (Campbell Scientific Ltd.)	

2.3.2 Soil hydrological measurements

In order to directly assess hydrological properties of the different degradation stages we used small weighing micro-lysimeters as a well-established tool to monitor evapotranspiration, infiltration and volumetric soil water content (Wieser et al., 2008; van den Bergh et al., 2013). As it was necessary to allow for quick installation with minimum disturbance, we developed a technique based on near-natural monoliths extracted in transparent plexiglass tubes (diameter 15 cm, length 30 cm). The monoliths were visually examined for intactness of the soil structure and artificial water pathways along the sidewall and then reinserted in their natural place inside a protecting outer tube (inner diameter 15 cm).

A general problem with soil monoliths is the disruption of the flow paths to the lower soil horizons leading to artificially high water saturation in the lower part of the monolith (Ben-Gal and Shani, 2002; Gee et al., 2009). This was prevented by applying a constant suction with 10 hPa of a hanging water column maintained by a spread bundle of 20 glass wicks (2 mm diameter) leading through the bottom plate into a 10 cm long downward pipe (15 mm diameter). Drained water was collected in a 200 ml PE bottle.

Micro-lysimeters were set up in June 2010 on four subplots inside the fenced area of the Kema site at a distance of 20 to 50 m from the eddy-covariance station. On each subplot one micro-lysimeter was installed in IM and one in BS at a maximum distance of 1 m. All micro-lysimeters were weighed every 2 to 10 days with a precision hanging balance from 23 June to 5 September 2010 and from 2 June to 5 September 2012. Soil cores (3.3 cm diameter, 30 cm depth) were taken near every micro-lysimeter on 29 June 2010. The soil samples were weighed fresh and after drying in the laboratory at Lhasa. By relating the given water content to the weight of the corresponding micro-lysimeter at that date, we were able to calculate volumetric soil water content for each micro-lysimeter over the whole measuring period. Further details about the micro-lysimeter technique and set-up are given by Biermann et al. (2013).

2.3.3 Soil gas exchange measurements

In 2012, CO₂ flux measurements were conducted with an automatic chamber system from LI-COR Biosciences (Lincoln, NE, USA). This LI-COR long-term chamber system contains a LI-8100 Infrared Gas Analyser (LI-COR Lincoln, NE, USA), is linked with an automated multiplexing system (LI-8150) and two automated chambers, one opaque and the other transparent for R_{eco} and net ecosystem exchange (NEE), respectively. The chambers are equipped with a fully automatically rotating arm that moves the chamber 180° away from the collar and therefore ensures undisturbed patterns of precipitation, temperature and radiation. Furthermore, by moving the chamber in-between measurements the soil and vegetation itself experiences less disturbance. The applied LI-COR chambers were compared during a separate experiment against eddy-covariance measurements by Riederer et al. (2014). Besides differences – mainly under stable atmospheric stratification – the comparison was satisfactory in daytime.

The three surface types IM, DM and BS were investigated with respect to their CO₂ fluxes between 30 July and 26 August 2012 at Kema. The CO₂-flux measurements of the three treatments were conducted consecutively. Therefore, the long-term chambers were moved to a patch representing the surface of interest. Measurements were conducted for 5 to 9 days before rotating to another location, starting from IM (30 July–7 August), continuing at BS (7–15 August), DM (15–21 August) and ending again at IM (21–26 August).

Intact root Mat has been measured twice during the observation period to provide information about possible changes in the magnitude of CO₂ fluxes, due to changing meteorological parameters. The two measurements will be denoted as IM period 1 and IM period 4. Note that during the measurement of IM period 4, other collars than during IM period 1 have been investigated. Nevertheless, the patches selected for the collar installation consisted of the same plant community, and showed the same soil characteristics. Because of lack of time the other two surfaces BS and DM were only measured once, but for as long as possible to gather sufficient information on diurnal cycles for these treatments.

2.3.4 ^{13}C labelling

$^{13}\text{CO}_2$ pulse labelling experiments were used to trace allocation of assimilated C in the shoot–root–soil system in a montane *Kobresia pygmaea* pasture 2009 in Xinghai (Hafner et al., 2012) and in alpine *Kobresia pygmaea* pasture 2010 in Kema (Ingrisch et al., 2014). Plots ($0.6 \times 0.6 \text{ m}^2$) with plants were labelled with ^{13}C -enriched CO_2 in transparent chambers over 4 h at the periods of maximal *Kobresia* growth in summer. Afterwards, ^{13}C was traced in the plant–soil system over a period of 2 months with increasing sampling intervals (10 times).

Aboveground biomass was clipped and belowground pools were sampled with a soil core (0–5 cm, 5–15 cm and in Xinghai additionally in 15–30 cm). After drying and sieving (2 mm), two belowground pools were separated into soil and roots. As the only means of obtaining measurements of soil CO_2 efflux and its $\delta^{13}\text{C}$ in a remote location, the static alkali absorption method with installation of NaOH traps was used (Lundegardh, 1921; Singh and Gupta, 1977; Hafner et al., 2012). Natural ^{13}C abundance in the pools of plant–soil systems, including CO_2 efflux, was sampled with a similar procedure on unlabelled spots. Total carbon and nitrogen content and $\delta^{13}\text{C}$ of the samples were analysed with an Isotope-Ratio Mass Spectrometer. All details of the $^{13}\text{CO}_2$ pulse labelling experiments were described in Hafner et al. (2012) and Ingrisch et al. (2014). All data from ^{13}C labelling experiments are presented as means \pm standard errors. The significance of differences was analysed by ANOVA at $\alpha = 0.05$.

2.4 Soil–vegetation–atmosphere transfer models

We conducted model experiments in order to estimate the impact of the defined degradation classes on water and carbon fluxes, including feedback on atmospheric circulation. Therefore three 1-D soil–vegetation–atmosphere transfer models were utilised to examine evapotranspiration (Sect. 2.4.1), carbon fluxes (Sect. 2.4.2), and surface feedbacks (Sect. 2.4.3). While the first two models were driven by measured standard meteorological forcing data, the latter is fully coupled to the atmosphere, which allows for feedbacks of land surface exchange to the atmosphere.

2.4.1 Evapotranspiration – the SEWAB model

To model the sensible and latent heat flux (evapotranspiration) the 1-D soil–vegetation–atmosphere transfer scheme SEWAB (Surface Energy and Water Balance model) was applied (Mengelkamp et al., 1999, 2001). The soil temperature distribution is solved by the diffusion equation and vertical movement of soil water is described by the Richards equation (Richards, 1931). Relationships between soil moisture characteristics are given by Clapp and Hornberger (1978). Atmospheric exchange is given by bulk approaches, taking into account aerodynamic and thermal roughness lengths with re-

spect to atmospheric stability (Louis, 1979). The latent heat flux is split up into vegetated surface flux and bare soil evaporation. The flux from vegetation is composed of wet foliage evaporation and transpiration of dry leaves. For the latter, the stomata resistance is constrained by minimum resistance and stress factors in a Jarvis-type scheme (Noilhan and Planton, 1989). In contrast to many other SVAT models, SEWAB parameterises all energy balance components separately and closes the energy balance by an iteration for the surface temperature using Brent's method.

2.4.2 Carbon dioxide exchange – the SVAT-CN

The model SVAT-CN (Reichstein, 2001; Falge et al., 2005) simulates CO_2 and H_2O gas exchange of vegetation and soil. It consists of a 1-D canopy model (Caldwell et al., 1986; Tenhunen et al., 1995), a 1-D soil physical model of water and heat fluxes (Moldrup et al., 1989, 1991), and a model of root water uptake (Reichstein, 2001). The model has been further developed with respect to soil gas emissions of CO_2 and N_2O from forest, grassland, and fallow (Reth et al., 2005a, b, c). In combination with a 3-D model, it has been used to simulate vertical profiles of latent heat exchange and successfully compared to vertical profiles of latent heat exchange in a spruce forest canopy (Staudt et al., 2011; Foken et al., 2012b). Plant canopy and soil are represented by several horizontally homogeneous layers, for which microclimate and gas exchange is computed. The soil module simulates unsaturated water flow according to Richards equation (Richards, 1931) parameterised with van Genuchten (1980) soil hydraulic parameters. C_3 photosynthesis is modelled using the basic formulation described by Farquhar et al. (1980). Stomatal conductance is linked linearly to assimilation and environmental controls via the Ball–Berry equation (Ball et al., 1987). The slope of this equation (gfac) is modelled depending on soil matrix potential (Ψ) in the main root layer.

2.4.3 2-D atmospheric model – ATHAM

For estimation of surface feedbacks the Hybrid vegetation dynamics and biosphere model (Friend et al., 1997; Friend and Kiang, 2005) was utilised, which is coupled to the cloud-resolving Active Tracer High-resolution Atmospheric Model (ATHAM, Oberhuber et al., 1998; Herzog et al., 2003). In a separate work (Gerken et al., 2012), the SEWAB model compared well with Hybrid. The fully coupled system was successful in simulating surface–atmosphere interactions, mesoscale circulations and convective evolution in the Nam Co basin (Gerken et al., 2013, 2014). In a coupled simulation, surface fluxes of energy and moisture interact with the flow field. At the same time, wind speed as well as clouds, which modify the surface radiation balance, provide a feedback to the surface and modify turbulent fluxes. Such simulations can produce a complex system of interactions.

Table 5. Experimental setup during the different experiments, with the corresponding measuring technique and the degree of degradation, (intact root Mat: IM, degraded root Mat: DM, bare soil: BS, alpine steppe: AS).

Experiment	Eddy-covariance H ₂ O-, CO ₂ flux	Micro-lysimeter H ₂ O flux	Chamber CO ₂ - flux LI-8100, (R _{eco} , NEE)	¹³ C pulse labelling, ¹³ C chasing
Plot area	10 ² –10 ⁵ m ² (footprint)	0.018 m ²	0.031 m ²	0.6 m ²
Xinghai 2009				IM, DM
Nam Co 2009	AS			
Kema 2010	65 % IM, 16 % DM, 19 % BS	IM, BS		IM, DM
Kema 2012		IM, BS	IM ^a , DM ^b , BS ^c	

^a From 30 July to 7 August and from 21 to 26 August

^b From 7 to 15 August

^c From 15 to 21 August

Table 6. Overview of model scenarios conducted with SEWAB and SVAT-CN for Kema site, periods 2010 and 2012 and Nam Co 2009. The numbers for vegetation fraction and the tile approach have been derived by the classification survey described in Sect. 2.2.

Simulation	Proportion of total surface area	Vegetation cover	Model parameter
S _{AS}	100 % Alpine steppe	0.6	Nam Co AS
S _{IM}	100 % IM	0.88	Kema RM
S _{DM}	100 % DM	0.26	Kema RM
S _{BS}	100 % BS	0.12	Kema BS
S _{RefEC}	Tile approach: $S_{\text{RefEC}} = 0.65 \cdot S_{\text{IM}} + 0.16$ $\cdot S_{\text{DM}} + 0.19 \cdot S_{\text{BS}}$		

2.4.4 Problems of land surface modelling on the Tibetan Plateau

Land surface modelling of energy and carbon dioxide exchange faces specific problems on the Tibetan Plateau. Most influential is the strong diurnal cycle of the surface temperature, observed in dry conditions over bare soil or very low vegetation, leading to overestimation of surface sensible heat flux (Yang et al., 2009; Hong et al., 2010) caused by too high turbulent diffusion coefficients. Land surface models usually parameterise these coefficients by a fixed fraction between the roughness length of momentum and heat, however, Yang et al. (2003) and Ma et al. (2002) observed a diurnal variation of the thermal roughness length on the Tibetan Plateau. As another special feature, land surface models tend to underestimate bare soil evaporation in semiarid areas (e.g. Agam et al., 2004; Balsamo et al., 2011).

Especially the *Kobresia* mats are characterised by changing fractions of vegetation cover and partly missing root mats, exposing almost bare soil with properties different from the turf below the *Kobresia*. From investigations of soil vertical heterogeneity by Yang et al. (2005) it can be concluded that such variations will significantly influence the exchange processes, posing a challenge for land surface mod-

elling. The models have therefore been adapted to these conditions and specific parameter sets have been elaborated from field measurements for Nam Co and Kema (Gerken et al., 2012; Biermann et al., 2014), see Appendix A for more details.

2.5 Experimental and modelling concept

Experimental investigations on the Tibetan Plateau are not comparable with typical meteorological and ecological experiments. Not only do the high altitude and the remoteness of the area impose limitations, but also unforeseeable administrative regulations challenge the organisation of experiments with different groups and large equipment. It was initially planned to investigate small degraded plots with chambers and micro-lysimeters and to use a larger plot, in the size of the eddy-covariance footprint, as a reference area to investigate the daily fluctuations of the evaporation and carbon dioxide flux. Due to customs and permit problems, this was unfortunately only partly possible at Kema site in 2010, and not at all during the main chamber experiment in 2012.

Therefore, model-specific parameters were investigated in 2012 and the models were adapted to the specific Tibetan conditions with the chamber data. These model versions were then tested with the eddy-covariance data in 2010 at the Kema site with nearly intact *Kobresia* cover. Forced with measured atmospheric conditions, these simulations are used to examine the differences among degradation classes in carbon and water exchange between surface and atmosphere. The ¹³C labelling studies enabled us to relate the differences in carbon exchange to the specific vegetation and soil compartments. Finally, a surface scheme coupled with a meso-scale atmospheric model served to estimate feedbacks of surface forcing on the atmosphere. A summary of the experimental setup according to measurement technique is given in Table 5.

In accordance with this concept, we adapted both SEWAB and SVAT-CN to the Kema site using the vegetation and soil parameters elaborated in 2012, and chamber measurements

Table 7. Comparison of the models SEWAB and SVAT-CN against eddy-covariance and chamber measurements, using the squared Pearson correlation coefficient r^2 , as well as slope and offset of the linear regression; n is the number of observations

Experiment	Comparison	Class	Variable	Unit	r^2	Slope	Offset	n
Nam Co 2009	EC vs. SEWAB	AS	30 min ET ^a	mm d ⁻¹	0.74	1.10	-0.50	572
	EC vs. SVAT-CN	AS	Median NEE ^b	g C m ⁻² d ⁻¹	0.90	1.15	-0.15	124
Kema 2010	EC vs. SEWAB	RefEC	30 min ET	mm d ⁻¹	0.72	1.03	-0.28	577
	EC vs. SVAT-CN	RefEC	Median NEE	g C m ⁻² d ⁻¹	0.81	0.99	-0.02	124
Kema 2012	Chamber vs. SVAT-CN	IM ^c	30 min NEE	g C m ⁻² d ⁻¹	0.86	0.80	-0.89	537
		DM	30 min NEE	g C m ⁻² d ⁻¹	0.74	0.85	-0.24	363
		BS	30 min NEE	g C m ⁻² d ⁻¹	0.48	1.77	-0.38	195

^a ET at Nam Co 2009 is already published by Biermann et al. (2014), offset recalculated in mm d⁻¹

^b Hourly medians from an ensemble diurnal cycle over the entire period

^c Both period 1 and period 4

from 2012 for calibration. Two parameter sets were established: one for surfaces with root mat (Kema RM: IM and DM differ only in vegetation fraction), and one for BS conditions (Kema BS). Simulations with in situ measured atmospheric forcing data were performed specifically for each of the degradation classes S_{IM} , S_{DM} and S_{BS} according to the definition in Table 2. These model runs serve to expand the chamber data beyond their measurement period, and we are now able to compare the class-specific fluxes over a 46-day period (12 July to 26 August 2012).

Furthermore, we compared the adapted model versions with eddy-covariance data from 2010 using the respective forcing data measured in situ in 2010. The eddy-covariance measurements integrate the fluxes from a source area ranging 50–200 m around the instrument (for detailed footprint analysis see Biermann et al., 2011, 2013), and therefore represent H₂O and CO₂ fluxes from IM, DM and BS according to their proportion of total surface area in Table 2. In order to ensure comparability, we reproduce this composition with the simulations as well using the tile approach (S_{RefEC}). An overview of model scenarios conducted at the Kema site is given in Table 6.

The differences in flux simulations among the degradation stages were controlled by the variation of the vegetation fraction and soil properties. A consistent parameter set for several experiments and multiple target variables (evapotranspiration, net/gross ecosystem exchange, ecosystem respiration) is a necessary pre-condition to ensure that the model physics implemented reflect these changes in a realistic manner. Therefore we abstained from optimising the parameter space, but used parameter estimates from field and laboratory measurements as far as possible (Appendix A), and inevitable calibration has been done for SVAT-CN by scaling the leaf area index with a single factor as well as a complete set of leaf physiology parameters.

For the investigation of the impact of surface degradation on the atmosphere, it was decided to run a relatively

simple numerical experiment prescribing a symmetric, two-dimensional Tibetan valley with 150 km width, and surrounded by Gaussian hills with 1000 m altitude. A sounding taken at Nam Co on 17 July 2012 was used as the initial profile. The setup is comparable to Gerken et al. (2013, 2014). A total of four cases were chosen for this preliminary analysis. A dry scenario with initial soil moisture of 0.5 × field capacity and a wet scenario with soil moisture at field capacity, as might be the case during the monsoon season, were used. For both surface states, simulations were performed with a vegetation cover of 25 and 75 % corresponding to a degraded and intact soil-mat scenario.

The study is limited by conceptual restrictions, which are mainly due to the scale problem in the different compartments (Foken et al., 2012b, see Appendix of this paper) and the working conditions in remote and high altitudes. Only one more-or-less uniform type of degradation has been investigated within the footprint area of the eddy-covariance measurements (Göckede et al., 2006) of 50–200 m extent, which is, in the case of this study, an almost non-degraded *Kobresia* pasture. The other types could only be found on much smaller plots, and had no significant influence on the whole footprint area, even when the non-linear influence of the different land-cover areas on the fluxes of the larger area is considered (Möllders, 2012). However, the investigation of degraded stages could only be done with small-scale measurements, such as those obtained with chambers and micro-lysimeters.

3 Results and discussion

We used separate experiments in 2009 (Nam Co) and 2010 (Kema) to validate models against eddy-covariance data (Sect. 3.1). These models were compared in 2012 against micro-lysimeters (Sect. 3.2) and against chambers (Sect. 3.3). The specific results – in the sense of our research questions – are given in Sects. 3.4–3.6.

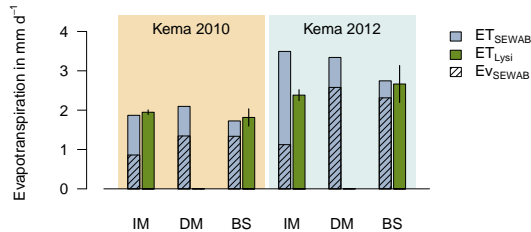


Figure 3. Evapotranspiration (ET) derived with SEWAB and with micro-lysimeter measurements at Kema in 2010 (33 days: 23 June–25 July) and Kema in 2012 (40 days: 16 July–24 August) for intact root mat (IM), degraded root Mat (DM) and bare soil (BS). Hatched bars denote the simulated evaporation (Ev) as part of the total simulated ET, the remainder is transpiration. Black lines on top of the bars for the micro-lysimeter illustrate standard deviations ($n = 4$).

3.1 Comparison of eddy-covariance flux measurements with modelled fluxes

In order to test the performance of evapotranspiration (ET) with SEWAB and net ecosystem exchange (NEE) with SVAT-CN, we compared the model results for Kema with the eddy-covariance measurements from 2010 (Sect. 2.5). The results show that SEWAB simulations represent the half-hourly measured turbulent fluxes at Kema generally well (Table 7, see scatter plots and diurnal cycles in the Appendix, Figs. B1–B5). Model performance at Nam Co for the measurements in 2009 was very similar, as well as the magnitude of the fluxes (Table 7, from Biermann et al., 2014). Measured hourly medians (from an ensemble diurnal cycle over the entire period) of NEE at Kema ranged between -2.8 and $1.5 \text{ g C m}^{-2} \text{ d}^{-1}$ over the course of the day, whereas modelled medians reached a minimum -3.0 and a maximum of $1.7 \text{ g C m}^{-2} \text{ d}^{-1}$. Although the model overestimated the CO_2 uptake, especially in the midday hours, the correlation between hourly medians of model output and measured NEE was generally realistic (Table 7). Compared to Kema data, mean diurnal patterns of measured and modelled NEE at Nam Co site showed smaller fluxes and less variation. Measured hourly medians of NEE ranged between -2.3 and $1.0 \text{ g C m}^{-2} \text{ d}^{-1}$ over the course of the day, and modelled medians between -2.7 and $1.0 \text{ g C m}^{-2} \text{ d}^{-1}$ (Table 7).

3.2 Class-specific comparison of evapotranspiration with micro-lysimeter measurements and SEWAB simulations

Daily evapotranspiration (ET) of the *Kobresia pygmaea* ecosystem was about 2 mm d^{-1} during dry periods and increased to 6 mm d^{-1} after sufficient precipitation (not shown). This was confirmed with small weighable micro-lysimeters giving a direct measure of ET from small soil

columns over several days and SEWAB simulations. For a 33-day period at Kema 2010, ET for both micro-lysimeter and simulations varied around 1.9 mm d^{-1} , reflecting drier conditions, while in 2012 the micro-lysimeter showed a maximum ET of 2.7 mm d^{-1} at BS, and the simulations 3.5 mm d^{-1} at IM (Fig. 3). In both periods, the lysimeter measurements do not differ significantly between IM and BS (two-sided Wilcoxon rank sum test, $n = 4$). The model results support this finding in general, as they are within the 95% confidence interval ($1.96 \times$ standard error) of the lysimeter measurements in three cases; however they differ significantly from the lysimeter measurements for IM in 2012. The model results suggest that even for dense vegetation cover (IM), a considerable part of ET stems from evaporation. At DM and BS, transpiration of the small above-ground part of *Kobresia* is lower, but it is compensated by evaporation. Therefore, the water balance is mainly driven by physical factors, i.e. atmospheric evaporative demand and soil water content.

3.3 Class-specific comparison of carbon fluxes with chamber measurements and SVAT-CN simulations

During the Kema 2012 campaign, the carbon fluxes for different degradation levels were investigated with chamber-based gas exchange measurements. Parallel measurements could not be established due to instrumental limitations, therefore the SVAT-CN model is utilised to compare the degradation classes over the whole period. In order to adapt SVAT-CN to the chamber measurements, the parameters of leaf physiology and soil respiration have been set to values that accommodate the different vegetation types and cover of the plots (Appendix A, Table A2).

Daily sums of ecosystem respiration (R_{eco}) over IM were overestimated by the model during period 1, but underestimated during the second setup over IM (period 4); see Fig. 4. This might be attributable to a difference in leaf area index (LAI) between the rings for period 1 and period 4, as they differed in biomass content at the end of the measurement campaign (Ring P1, NEE chamber: 3.1 g and P4, NEE chamber: 4.5 g). The model has been adapted to both periods with one parameter set in order to reflect average conditions. Overall, the model predicted a mean R_{eco} of $2.37 \text{ g C m}^{-2} \text{ d}^{-1}$ for IM, whereas the mean of the chamber data yielded $2.31 \text{ g C m}^{-2} \text{ d}^{-1}$. For the chamber setup over bare soil (BS, period 2), R_{eco} were, on average, represented well by the model (on average $0.77 \text{ g C m}^{-2} \text{ s}^{-1}$) as compared to the data average of $0.81 \text{ g C m}^{-2} \text{ d}^{-1}$. Similarly, for DM (period 3) modelled ($1.81 \text{ g C m}^{-2} \text{ d}^{-1}$) and measured ($1.69 \text{ g C m}^{-2} \text{ d}^{-1}$) average R_{eco} compared well. Analogous patterns were found for daily sums of gross ecosystem exchange ($\text{GEE} = \text{NEE} - R_{\text{eco}}$): under- and overestimations of the daily sums characterised the setups over IM (period 1 and 4), but were compensated to some extent when analysing period 1 and 4 together (modelled

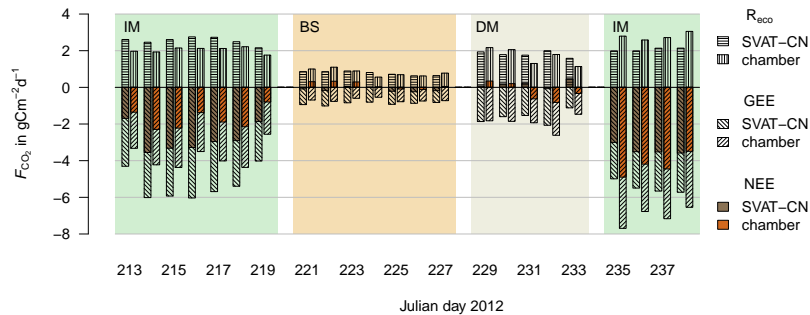


Figure 4. Comparison of measured and modelled daily carbon exchange sums from 31 July to 25 August 2012 at Kema. Hatched bars denote the simulated gross ecosystem exchange (GEE) and ecosystem respiration (R_{eco}), the sum is the net ecosystem exchange (NEE, coloured bars). The four periods represent different stages of vegetation degradation (see Table 2). Leaf physiology and soil respiration was parameterised for best representation of the gas exchange chamber data over the entire time period (see Sect. 2.5.2). Missing dates indicate days when chambers were set up or relocated to another treatment.

average GEE $-5.39 \text{ gC m}^{-2} \text{ d}^{-1}$, measured average GEE $-4.96 \text{ gC m}^{-2} \text{ d}^{-1}$. Average modelled GEE over BS with $-0.89 \text{ gC m}^{-2} \text{ d}^{-1}$ compared well to measured GEE for period 2 ($-0.69 \text{ gC m}^{-2} \text{ d}^{-1}$). Over DM, the average modelled GEE was $-1.64 \text{ gC m}^{-2} \text{ d}^{-1}$, and measured GEE showed an average of $-1.94 \text{ gC m}^{-2} \text{ d}^{-1}$. The model performance with respect to 30 min NEE is shown in Table 7, scatter plots of the regression are given in a supplement.

The mean carbon fluxes derived from SVAT-CN simulations for the different degradation classes over the vegetation period are shown in Fig. 5. A noticeable carbon uptake of $-2.89 \text{ gC m}^{-2} \text{ d}^{-1}$ for IM reduces to -0.09 for BS and even shifts to a weak release of 0.2 at DM. This is mainly related to a drop in GEE by 83 % for BS and 64 % for DM, compared to IM (100 %). While R_{eco} for BS is reduced by 66 %, it only reduces by 12 % for DM, leading to the small net release already mentioned.

Cumulative NEE was calculated applying the four different model setups previously described: IM; DM and BS stages of *Kobresia* pastures at Kema; and alpine steppe (AS) ecosystem at Nam Co (Fig. 6). The simulation period ranged from the period 12 July to 26 August 2012. For this period, only the IM stage showed significant carbon uptake of -133 gC m^{-2} . DM and BS ecosystems were more or less carbon neutral (-4 gC m^{-2} uptake at BS, and 9 gC m^{-2} release at DM). The model for AS resulted in a carbon loss of 24 gC m^{-2} for the investigated period.

3.4 Distribution of the assimilated carbon in *Kobresia* pastures and the soil

The results from two $^{13}\text{CO}_2$ pulse labelling experiments at Xinghai 2009 (Hafner et al., 2012) and Kema 2010 (Ingrisch et al., 2014) show the distribution of assimilated carbon (C) in a montane and alpine *Kobresia* pasture (Fig. 7). The study in Xinghai showed that C translocation was different on plots

where vegetation had changed from Cyperaceae to Poaceae dominance, induced by grazing cessation. Less assimilated C was stored in belowground pools. The study in Kema showed that roots within the turf layer act as the main sink for recently assimilated C (65 %) and as the most dynamic part of the ecosystem in terms of C turnover. This is also the main difference between the experiments on the two sites as in the case of the alpine pasture (Kema) more C was allocated belowground than in montane pasture, where such a turf layer does not exist. However, as the experiments were conducted under different conditions and in consecutive years, a comparison of absolute values is not possible as the determined C fraction varies also throughout the growing season (Swinnen et al., 1994; Kuzyakov and Domanski, 2000).

At Kema, the $^{13}\text{CO}_2$ labelling was furthermore coupled with eddy-covariance measurements to determine the absolute values of the carbon distribution in the plants, roots and the soil following a method developed by Riederer (2014): The relative C distribution within the various pools of the ecosystem, at the end of the allocation period (i.e. when the ^{13}C fixing reaches a steady state, in our case 15 days after the labelling) was multiplied with a nearly steady-state daily carbon uptake measured with the eddy-covariance method. Besides the determination of absolute values, the continuous observation of the exchange regime with the EC confirms that the pulse labelling was conducted under atmospheric conditions similar to those of the whole allocation period. This leads to more representativeness of the result of the $^{13}\text{CO}_2$ labelling experiment, which could not be repeated due to the short vegetation period and restricted access to this remote area. Please note that repetitions have been carried out, leading to standard errors as depicted in Fig. 7.

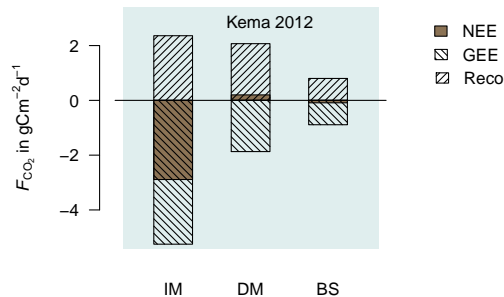


Figure 5. Simulated carbon fluxes at Kema in 2012 (46 days: 12 July to 26 August 2012) for IM, DM, and BS. Hatched bars denote the simulated GEE and R_{eco} , the sum is the NEE (brown bar).

3.5 Influence of plant cover on convection and precipitation

For investigating the influence of degradation on the development of convection and precipitation, the ATHAM model was applied for 25 % (V25) and 75 % (V75) plant cover at the Nam Co basin, with each of these in a dry and a wet scenario. From Fig. 8 it becomes immediately apparent that wet surface conditions are associated with higher deposited precipitation. At the same time, near-surface relative humidities are higher (not shown). For both the dry and wet cases an earlier cloud and convection development is observed for the less vegetated surface: simulations produce higher cloud cover and more convection from 10:00 local mean time (LMT) onward. At Nam Co we observed the frequent development of locally generated convective systems at similar hours in the field. Thus clouds block more incoming solar radiation between 10:00 and 14:00 LMT, the time with the potentially highest short-wave radiation forcing, for the less vegetated system compared to the intact vegetation scenario. Consequently, simulated surface temperatures were higher for the V75 scenario, leading to higher surface fluxes and a stronger simulated convection development over the day as a whole. A potential albedo effect can be excluded since the observed albedo of the vegetated surface is similar to that of the bare surface and surface temperatures remain virtually identical until convection develops.

The mechanism for this process is presumably that the vegetation cover reduces bare soil evaporation. At the same time, higher surface temperatures due to higher radiation input result in both larger sensible and latent heat fluxes in the afternoon hours, while the plant cover is able to access water that is not available for surface evaporation.

This hypothesis obviously needs to be investigated more thoroughly with field observations and simulations, but the findings indicate that changes in surface conditions can affect convective dynamics and local weather. This preliminary in-

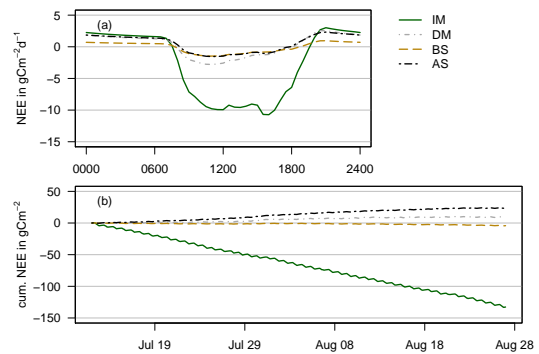


Figure 6. Model results of net ecosystem exchange (NEE) over 46 days of July and August 2012 at Kema. (a): mean diurnal cycle, and (b): cumulative NEE. The four lines represent different stages of vegetation degradation (IM, DM, BS, and AS).

vestigation of vegetation–atmosphere feedbacks did not take into account any spatial patterns in surface degradation that may result in larger patches with different surface conditions that may then affect circulation. However, such circulation effects are typically found in modelling studies using patch sizes with length scales that are several times the boundary-layer height.

3.6 Simulation of different degradation states

The results for the different degradation states allow the simulation of the NEE and evapotranspiration for a gradual change from IM to BS using a tile approach of the fluxes (Avissar and Pielke, 1989). Such a tile approach is exemplarily shown for different percentages of the ecosystem types IM and BS for a 46 days period in July and August 2012 at Kema site, with simulated NEE (Fig. 9a) and evapotranspiration (Fig. 9b). As expected from the cumulative carbon gains for S_{IM} and S_{BS} shown in Fig. 5, S_{IM} developed the largest carbon sink over the investigated summer period, whereas S_{BS} is nearly carbon neutral in summer and a source for longer periods. The intermediate stages showed decreasing average carbon uptake with increasing amount of bare soil. Diurnal variability is largest for 100 % S_{IM} and smallest for 100 % S_{BS} in the ecosystem, as indicated by the interquartile ranges in the box plot.

Evapotranspiration decreases from S_{IM} to S_{BS} in this model degradation experiment (Fig. 9b), but this reduction is small compared to the overall day-to-day variability and is not supported by the lysimeter measurements (Fig. 3). Therefore a change in mean ET due to degradation cannot be confirmed in this study. The day-to-day variability, however, increases from S_{IM} to S_{BS} . This is connected to a larger variability of simulated soil moisture in the uppermost layer, as the turf layer retains more water due to its higher field

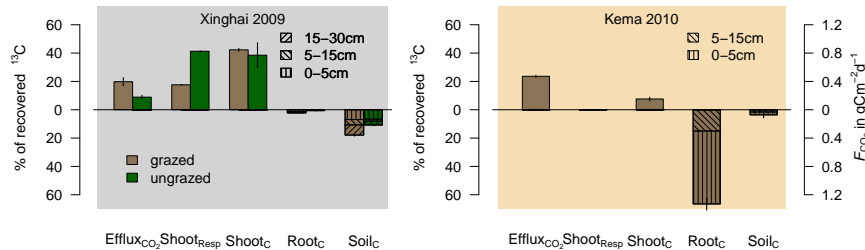


Figure 7. ^{13}C partitioning and distribution of recently allocated C within the various pools, namely CO_2 efflux, shoot respiration, shoots, roots and soil for Xinghai site (grazed and ungrazed) in 2009 and Kema site (IM) in 2010, determined at the end of a 29 day and 15 day allocation period, respectively. Vertical lines in the bars denote standard errors ($n = 3$ for Xinghai 2009 and $n = 8$ for Kema 2010). Total fluxes of C in $\text{g C m}^{-2} \text{d}^{-1}$ to the different C pools at Kema site are based on the combination of eddy-covariance measurements and labelling. Shoot respiration is not measured, but determined as difference between the ^{13}C recovery at the first sampling and the sampling at the end of the allocation period. First sampling in Xinghai was 1 day after the labelling and in Kema at the labelling day. Figure modified after Hafner et al. (2012) and Ingrisch et al. (2014).

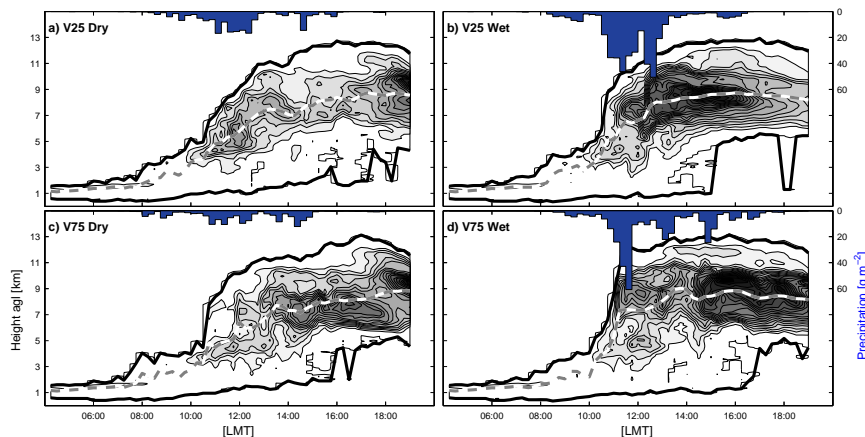


Figure 8. Simulated convection development and deposited precipitation (blue bars) for a symmetric Tibetan Valley with 150 km width. The black lines indicate cloud base and cloud top in kilometres above ground level; the dashed line shows the centre of the cloud mass and the contours give the mean cloud water and ice concentration integrated over the model domain. V25 and V75 refer to 25 % and 75 % vegetation cover, while wet and dry indicate initial soil moisture corresponding to 1.0 and $0.5 \times$ field capacity, respectively. Times are given in local mean time (LMT), which is two hours before Beijing standard time (CST).

capacity and lower soil hydraulic conductivity, and the roots can extract water for transpiration from lower soil layers as well.

4 Conclusions

Increasing degradation of the *Kobresia pygmaea* turf significantly reduces the carbon uptake and the function of *Kobresia* pastures as a carbon sink, while the influence on the evapotranspiration is less dominant. However, the shift from transpiration to evaporation was found to have a significant influence on the starting time of convection and cloud and pre-

cipitation generation: convection above a degraded surface occurs before noon instead of after noon. Due to the dominant direct solar radiation on the Tibetan Plateau, the early-generated cloud cover reduces the energy input and therefore the surface temperatures. Therefore the degradation state of the *Kobresia* pastures has a significant influence on the water and carbon cycle and, in consequence, on the climate system. Due to the relevance of the Tibetan Plateau on the global circulation changes, the surface properties on the highland have influences on larger scales. These changes in the water and carbon cycle are furthermore influenced by global warming

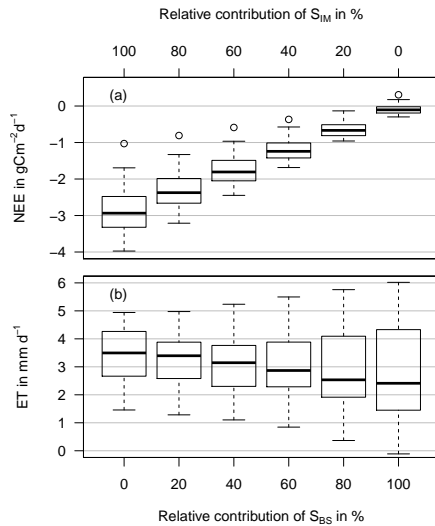


Figure 9. Modelled daily net ecosystem exchange (top, NEE) and modelled daily evapotranspiration (bottom, ET) for 46 days (12 July to 26 August 2012) at Kema (varying combination of S_{IM} and S_{BS}): box plot with median, 25 % and 75 % quartiles; bars represent quartiles ± 1.5 times interquartile range.

and an extended growing season (Che et al., 2014; Shen et al., 2014; Zhang et al., 2014).

Plot scale experiments are a promising mechanistic tool for investigating processes that are relevant for larger scales. Since all results showed a high correlation between modelled and experimental data, a combination is possible with a tile approach with flux averaging to realise model studies that consider gradual degradation schemata. The consequent combination of plot scale, ecosystem scale and landscape scale shows the importance of the integration of experimental and modelling approaches.

The palaeo-environmental reconstruction (Miehe et al., 2014) as well as the simulations of the present study suggest that the present grazing lawns of *Kobresia pygmaea* are a synanthropic ecosystem that developed through long-lasting selective free-range grazing of livestock. This traditional and obviously sustainable rangeland management would be the best way to conserve and possibly increase the carbon stocks in the turf and its functions. Otherwise, an overgrazing connected with erosion would destroy the carbon sink. Considering the large area, even the loss of this small sink would have an influence on the climate relevant carbon balance of China.

From our investigation we propose the need for the following additional research:

- Extension of this integrated experimental-modelling research scheme to the full annual cycle. This cannot be done by a single campaign but is possible within the Third Pole initiative (Yao et al., 2012). The modelling studies of this paper make such investigations realistic.
- The results obtained so far on just these three sites should be extended to an increased number of experimental sites, supported by appropriate remote sensing tools, in order to regionalise degradation patterns and related processes. The methodical and data basis is available for this (Ma et al., 2008, 2011, 2014; Yang et al., 2013)
- Investigation of the processes along elevation gradients, with special reference to functional dependences. Therefore biological data (Miehe et al., 2014) as well as atmospheric data (Ma et al., 2008) should be combined.
- The use of remote sensing cloud cover studies to evaluate simulations of cloud generation and precipitation depending on surface structures. This should be combined with high resolution WRF modelling studies, which are already available for the Tibetan Plateau (Mausson et al., 2014).

Appendix A: Model adaption to the Tibetan Plateau

A1 Adaption of SEWAB

Considering the specific problems on the Tibetan Plateau, three changes have been implemented in SEWAB. Those are a variable thermal roughness length (Yang et al., 2008), soil thermal conductivity calculation (Yang et al., 2005) and the parameterisation of bare soil evaporation (Mihailovic et al., 1993). These changes have been already applied and evaluated at the alpine steppe site Nam Co using the same data set (Gerken et al., 2012; Biermann et al., 2014).

Furthermore, all relevant model parameters have been adapted to the site-specific conditions (see Table A1). The parameters for the alpine steppe site Nam Co have been used as published in Biermann et al. (2014), which were inferred from field and laboratory measurements. Specific parameters for the Kema site have been elaborated as follows: albedo has been estimated from radiation measurements individually for the 2010 and 2012 data set. The fraction of vegetated area has been surveyed (Sect. 2.2), root depth is assessed from soil profiles (Biermann et al., 2011, 2013) and the roughness length for momentum is estimated from eddy-covariance friction velocity under neutral conditions. The LAI for the vegetated area has been calculated from a biomass survey (September 2012, $n = 5$) and subsequent scans of leaf surface using WinSeedle. Maximum stomatal conductance has been elaborated by gas exchange measurements with *Kobresia pygmaea* in Göttingen (see Appendix B2), which has been translated to minimum stomatal resistance.

Soil properties have been estimated from measurements separately for conditions with root mat (RM: IM and DM) and without root mat (BS). As SEWAB accepts only one soil parameter set for the whole soil column, the properties of the uppermost 5 cm have been used. The bulk density has been surveyed in 2012 for soil layers of 5 cm thickness, down to 30 cm for RM and 14 cm for BS ($n = 4$ plots \times 4 replicates = 16 for each layer). Average soil organic carbon content of the turf layer was 9 %, measured by dry combustion (Vario EL, Elementar, Hanau), corresponding to approximately 18 % organic matter, which is in agreement with previous analyses by Kaiser et al. (2008). This amount has been distributed to three layers of 5 cm according to the relative content of root mass in each layer, sampled in 2010 ($n = 4$ plots \times 3 replicates = 12 for each layer). From bulk density and mass fraction of organic matter the porosity in 0–5 cm depth is estimated with $0.593 \text{ m}^3 \text{ m}^{-3}$, assuming densities of 2.65 g m^{-3} for mineral content and 1.2 g m^{-3} for organic content. The soil heat capacity of solid matter is combined from $2.1 \times 10^6 \text{ J m}^{-3} \text{ K}^{-1}$ for mineral content and $2.5 \times 10^6 \text{ J m}^{-3} \text{ K}^{-1}$ for organic matter according to Hillel (1980). Thermal conductivities for dry soil and at saturation, needed for the conductivity calculation (Yang et al., 2005), have been investigated for a similar turf layer (Chen et al., 2012: Anduo site for RM, BJ site for BS). Further, we de-

rived saturated hydraulic conductivities of $1.9 \times 10^{-5} \text{ m s}^{-1}$ and $4.6 \times 10^{-5} \text{ m s}^{-1}$ as mean values for RM and BS, respectively, using infiltrometer measurements from 2010 (Biermann et al., 2011, 2013). An in situ soil water retention curve was established from tensiometer and TDR profile measurements in 2012, reflecting the properties of RM in the first 15 cm and the properties of BS in 25 cm depth. From this data the matrix potential at saturation Ψ_{sat} and the exponent b for the relationship by Clapp and Hornberger (1978) is estimated via linear regression of the logarithmic form: $\log(\Psi_{\Theta}) = \log(\Psi_{\text{sat}}) + b \cdot \log(\frac{\Theta}{\Theta_{\text{sat}}})$. Further, the soil water content at field capacity and wilting point has been derived from this relationship assuming pF values ($= \log(\Psi_{\Theta})$) of $2.5 \log(\text{hPa})$ and $4.5 \log(\text{hPa})$ for Θ_{FC} and Θ_{WP} , respectively.

A2 Adaption of SVAT-CN

Species parameterisation of the leaf model for *Kobresia pygmaea*:

Measurements of in situ CO_2 and H_2O leaf gas exchange in response to temperature, radiation, CO_2 mixing ratio, and relative humidity were made using a portable gas exchange system (WALZ GFS3000, Walz, Effeltrich/Germany). Single factor dependencies of leaf gas exchange to light, temperature, CO_2 mixing ratio, and relative humidity, were performed for copiously watered *Kobresia pygmaea* plants from greenhouse experiments at the University of Göttingen. The respective plant individuals have been collected in 2012 at the Kema site with underlying soil monoliths, and regrown/recovered in Göttingen. The measurement setup was situated in a greenhouse chamber regulated to 15°C . GFS3000 gas exchange measurements were performed at six different temperatures (7.5, 10, 15, 20, 25, and 30°C) inside the cuvette and a series of different relative humidities of the inlet air, ranging between 20 and 65 %, matching meteorological conditions found at the field site during the intensive campaign in 2010. As high humidity inside the chamber system leads to problems with water condensation in the tubes, the conditions were restricted to relative humidity up to 65 %. Data have been analysed using the physiology-based leaf gas exchange model (Farquhar et al., 1980; Ball et al., 1987) to derive estimates for those parameters that describe the carboxylase kinetics, electron transport, respiration and stomatal function. We used a non-linear least trimmed squares regression tool (Reth et al., 2005c), that minimises the sum of squared residuals excluding the largest 5 % of residuals, assumed to indicate data contamination or data-model inconsistencies. Sets of parameter values for *Kobresia pygmaea* (Appendix, Table A2) were obtained as the basis for calculating canopy flux rates at the different field sites.

Table A1. Relevant parameters to describe the surface characteristic in SEWAB and SVAT-CN. Kema represents two parameter sets: (i) root mat (RM) for IM and DM; and (ii) BS.

Parameter	Unit	Description	SEWAB			SVAT-CN		
			Kema RM	Kema BS	NamC AS	Kema RM	Kema BS	NamC AS
a	–	Albedo	0.18 ^a 0.16 ^b	0.18 ^a 0.148 ^b	0.196	0.18 ^a 0.16 ^b	0.18 ^a 0.148 ^b	0.196
ε	–	Emissivity	0.97	0.97	0.97	0.97	0.97	0.97
f_{veg}	–	Fraction of vegetated area	0.88 (IM) 0.26 (DM)	0.12	0.6	0.88 (IM) 0.26 (DM)	0.12	0.6
LAI	–	Leaf area index	1.0	1.0	1.0	0.5 ^a 1.0 ^b	0.5 ^a 1.0 ^b	1.0
z_r	m	Root depth	0.5	0.3	0.3	0.4	0.4	0.4
h_c	m	Canopy height	0.03	0.03	0.15	0.03	0.03	0.15
z_{om}	m	Roughness length	0.003	0.003	0.005	0.003	0.003	0.005
$R_{s, min}$	$s m^{-1}$		72	72	60	c	c	c
$R_{s, max}$	$s m^{-1}$		2500	2500	2500	c	c	c
$\lambda_{s, dry}$	$W m^{-1} K^{-1}$	Thermal conductivity, dry soil	0.15	0.15	0.15	c	c	c
	$W m^{-1} K^{-1}$	Thermal conductivity at saturation	0.8	1.3	1.3	c	c	c
$C_G \cdot \rho_G$	$10^6 J m^{-3} K^{-1}$	Soil heat capacity (solid matter)	2.34	2.1	2.1	2.4	2.4	2.4
Θ_{sat}	$m^3 m^{-3}$	Porosity	0.533	0.533	0.396	0.593 ^d 0.533 ^c	0.533	0.396
Ψ_{sat}	m	Matrix potential at saturation	–0.074	–0.022	–0.51	c	c	c
K_{sat}	$10^{-5} m s^{-1}$	Saturated hydraulic conductivity	1.90	4.60	2.02	1.90	4.60	2.02
Θ_{FC}	$m^3 m^{-3}$	Volumetric water content at field capacity	0.252	0.201	0.210	c	c	c
Θ_{WP}	$m^3 m^{-3}$	Volumetric water content at wilting point	0.088	0.087	0.060	c	c	c
b	–	Exponent ^f	4.38	5.54	3.61	c	c	c
θ_r	$m^3 m^{-3}$	Soil residual water content ^g	c	c	c	0.025 ^d 0.05 ^e	0.05	0.025
α	m^{-1}	Scale parameter ^g	c	c	c	0.006 ^d 0.003 ^e	0.003	0.0466
n	–	Shape parameter ^g	c	c	c	1.17 ^d 1.27 ^e	1.27	1.443

^a From measurements in 2010; ^b from measurements in 2012; ^c parameter not available due to different parameterisation; ^d organic layer (0–15 cm depth); ^e mineral layer (15+ cm depth); ^f exponent b for relationships after Clapp and Hornberger (1978); ^g parameter according to van Genuchten (1980).

Parameterisation of soil retention curve:

In SVAT-CN the relationship between soil matrix potential Ψ (or better water suction, in units of m) and soil water content θ ($m^3 m^{-3}$) is described by a retention curve after van Genuchten (1980)

$$\Psi(\theta) = \frac{1}{\alpha} \cdot \left[\left(\frac{\theta - \theta_r}{\theta_s - \theta_r} \right)^{-\frac{1}{m}} - 1 \right]^{\frac{1}{n}}, \quad (A1)$$

where θ is soil water content ($m^3 m^{-3}$), θ_r soil residual water content ($m^3 m^{-3}$), θ_s soil saturated water content ($m^3 m^{-3}$), α a scale parameter (m^{-1}), and n and m shape parameters, with $m = 1 - 1/n$. Site-specific data of measured retention curves (soil moisture and soil water potential from AWS, Table 3) have been used to parameterise θ_r , α , and n (Appendix, Table A1) by non-linear least square regression.

Parameterisation of soil respiration:

Soil respiration (R_s , $\mu mol m^{-2} s^{-1}$) is modelled as a function of modelled soil temperature T_s (K) and soil water content θ

($m^3 m^{-3}$) in 10 cm depth as follows:

$$R_s = R_{norm} \cdot e^{\left(\frac{E_0}{T_{ref} - T_0} \cdot \frac{1}{T_s - T_0} \right)} \cdot \max \left(0.01, \frac{\theta - \theta_0}{(\theta_{half} - \theta_0) + (\theta - \theta_0)} \right) \quad (A2)$$

where R_{norm} is the base rate at optimum soil water content and reference temperature ($\mu mol m^{-2} s^{-1}$); E_0 an activation energy parameter ($^{\circ}C$) that determines temperature sensitivity; T_{ref} reference temperature ($^{\circ}C$); T_0 ($-46.02^{\circ}C$, a regression parameter from Lloyd and Taylor, 1994), θ the soil water content where the rate is reduced to zero ($m^3 m^{-3}$), and θ_{half} the soil water content where the rate is reduced by half ($m^3 m^{-3}$).

The original formulation in SVAT-CN was changed to accommodate the much higher soil organic content in the *Kobresia* ecosystems. T_{ref} and E_0 were adapted to match soil respiration data measured with gas exchange chambers. For Kema a T_{ref} of $16^{\circ}C$ for the “*Kobresia*”, and $24^{\circ}C$ for the “bare soil” plots, were used. At Nam Co T_{ref} was set to $16^{\circ}C$. For all sites an E_0 of $500^{\circ}C$ was employed. R_{norm} was $2.3 \mu mol m^{-2} s^{-1}$. At all sites only weak dependences on soil

Table A2. Parameters applied to describe leaf physiology of *Kobresia pygmaea*. For detailed explanation of the leaf model and use of the parameters see Falge (1997) and Falge et al. (2003). The equations are also available in Wohlfahrt et al. (1998). Output of the model is on a projected leaf area basis.

Description	Parameter	Value original	Value Kema	Value NamCo	Unit
Dark respiration	$F(R_d)$	1.51	2.42	1.51	$\mu\text{mol m}^{-2} \text{s}^{-1}$
	$E_a(R_d)$	72 561			J mol^{-1}
Electron transport capacity	$c(P_{\text{ml}})$	61.93	99.1	28.0	$\mu\text{mol m}^{-2} \text{s}^{-1}$
	$\Delta H_a(P_{\text{ml}})$	50 224			J mol^{-1}
	$\Delta H_d(P_{\text{ml}})$	200 000			J mol^{-1}
	$\Delta S(P_{\text{ml}})$	436.8			$\text{J K}^{-1} \text{mol}^{-1}$
Carboxylase capacity	$c(V_{c_{\text{max}}})$	53.4	85.4	32.5	$\mu\text{mol m}^{-2} \text{s}^{-1}$
	$\Delta H_a(V_{c_{\text{max}}})$	41 953			J mol^{-1}
	$\Delta H_d(V_{c_{\text{max}}})$	200 000			J mol^{-1}
	$\Delta S(V_{c_{\text{max}}})$	206.1			$\text{J K}^{-1} \text{mol}^{-1}$
Carboxylase kinetics	$f(K_c)$	299.469			$\mu\text{mol mol}^{-1}$
	$E_a(K_c)$	65 000			J mol^{-1}
	$f(K_o)$	159.597			mmol mol^{-1}
	$E_a(K_o)$	36 000			J mol^{-1}
	$f(\tau)$	2339.53			–
	$E_a(\tau)$	–28 990			J mol^{-1}
Light use efficiency	α	0.0332	0.0332	0.0111	$(\text{mol CO}_2) (\text{mol photons})^{-1}$
Stomatal conductance	g_{min}	18.7			$\text{mmol m}^{-2} \text{s}^{-1}$
	$g_{\text{fac}0}$	21			–

For the Kema site, the respective formulation was adapted to: $g_{\text{fac}} = \max(15, g_{\text{fac}0} \times 10^{(0.025 \cdot \Psi)})$, Ψ in MPa, simulated in 10 cm depth.

water content were implemented, with θ set to θ_t of the retention parameterisations, and θ_{half} set to $0.035 \text{ m}^3 \text{ m}^{-3}$.

Parameterisation of leaf gas exchange:

Species-specific parameters (Table A2) for the physiology-based leaf gas exchange model have been derived from CO_2 and H_2O leaf gas exchange measurements in the greenhouse (see “Species-specific parameterisation of the leaf model for *Kobresia pygmaea*” in this section). For the simulation of the Kema campaign in 2012, at first the original parameters of Table A2 were used for the vegetated area of the different degradation states of “*Kobresia*” (IM and DM) and “bare soil” plots, but underestimated the measured chamber gas exchange data. Consequently, three scaling parameters $c(P_{\text{ml}})$, $c(V_{c_{\text{max}}})$, and $F(R_d)$ were increased to 160 % of the original values (Appendix, Table A2) for better comparison with measured data. The same parameters were used for the Kema 2010 campaign. The slope of the linear equation, which links stomatal conductance to assimilation and environmental controls, is modelled depending on soil matrix potential (Ψ) in the main root layer: $g_{\text{fac}} = \max(15, g_{\text{fac}0} \times 10^{(0.025 \cdot \Psi)})$, Ψ in

MPa, simulated in 10 cm depth. For the campaign in 2010 – a year with drought stress effects, the respective formulation was adapted to $g_{\text{fac}} = \max(5, g_{\text{fac}0} \times 10^{(0.1 \cdot \Psi)})$.

For the Nam Co site, which is characterised by a vegetation composition of alpine steppe species different from the *Kobresia* pastures, no specific leaf gas exchange parameters are available. As a first attempt, leaf parameter sets of *Kobresia* were applied, but these overestimated measured eddy-covariance fluxes. Consecutive reduction of scaling parameters (Appendix, Table A2) yielded a better representation of the measured eddy-covariance fluxes.

Appendix B: Model evaluation

B1 Evapotranspiration: EC – SEWAB

In order to test the performance of simulations of evapotranspiration with SEWAB, we compared the model results for Kema with the eddy-covariance measurements from 2010. Therefore the simulations for IM, DM and BS have been aggregated as weighted sums according to the eddy-covariance footprint (S_{RefEC} , see Table 6) and the measurements have been corrected according to the energy balance closure gap (Sect. 2.3.1). The results show that SEWAB simulations represent the measured evapotranspiration well (Fig. B1). Similarly, the simulations generally capture the diurnal cycle of evapotranspiration (Fig. B2), with median fluxes of approximately 6.5 mm d^{-1} at noon, and a large day-to-day variation caused by variable moisture conditions within the observation period in 2010. The simulations slightly overestimate daytime fluxes and underestimate night-time fluxes, the overall bias with high quality flux data (flag 1–3 out of a scheme ranging from 1–9, Foken et al., 2004) is -0.13 mm d^{-1} .

B2 Carbon flux: EC – SVAT-CN

Kema 2010:

For best representation of the eddy-covariance data footprint, model results (S_{RefEC} , Table 6) are calculated as weighed sums of IM, DM and BS according to the proportion of total surface area in Table 2. Due to drier conditions in 2010, the vegetation was partially considered to be photosynthetically inactive, therefore the LAI of vegetated area has been reduced from 1 to 0.5. Mean diurnal patterns of both, measured and modelled net ecosystem exchange showed CO_2 release during night, and uptake during daytime hours, with a pronounced peak in the late morning hours, and a smaller peak in the late afternoon (Fig. B3). However, measured hourly medians of net ecosystem exchange ranged between -2.8 and $1.5 \text{ g C m}^{-2} \text{ d}^{-1}$ over the course of the day, whereas modelled medians reached a minimum of -3.0 and a maximum of $1.7 \text{ g C m}^{-2} \text{ d}^{-1}$. Although the model overestimated the CO_2 uptake, especially in the midday hours, the comparison between hourly medians of model output and measured NEE (Fig. B4, left) showed that the simulations were generally realistic.

Nam Co 2009 (AS):

Compared to Kema data, mean diurnal patterns of measured and modelled net ecosystem exchange showed much smaller variation within a given hour (smaller interquartile ranges), and lower CO_2 release during night, and lower uptake during daytime hours (lower diurnal amplitudes, see Fig. B5). As leaf physiological parameters were adapted to match measurements and model results, the ranges of both measured and modelled medians showed a better overlap: mea-

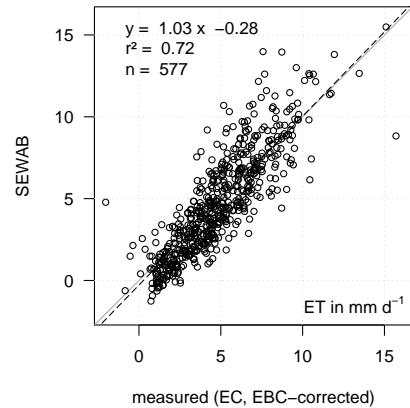


Figure B1. Scatter plot of measured vs. SEWAB modelled S_{RefEC} evapotranspiration (ET) over 61 days of 2010 (3 June to 2 August) at Kema. Measured and modelled values are restricted to high data quality (flag 1–3 out of a scheme ranging from 1 to 9, Foken et al., 2004). Measured EC data is corrected according to the surface energy imbalance with the buoyancy flux correction.

sured hourly medians of net ecosystem exchange ranged between -2.3 and $1.0 \text{ g C m}^{-2} \text{ d}^{-1}$ over the course of the day, and modelled medians between -2.7 and $1.0 \text{ g C m}^{-2} \text{ d}^{-1}$. The wide range of measured NEE from $-6 \text{ g C m}^{-2} \text{ d}^{-1}$ to $1 \text{ g C m}^{-2} \text{ d}^{-1}$ at mid-day results from variable moisture conditions during the monsoon season and is consistent with chamber-based observations at a similar spot near Nam Co station (Hu et al., 2013).

At Nam Co the model overestimated the CO_2 uptake especially in the afternoon hours, indicating a larger influence of soil respiration than currently represented by the model. Simulated soil respiration depends on simulated driving variables (soil temperature and moisture) and parameters. The latter have not been measured at Nam Co directly; instead the values from the Kema field site have been employed, eventually introducing the observed bias. Nevertheless, the correlation with r^2 of 0.90 between hourly medians of modelled and measured NEE (Fig. B4, right) was better than at Kema.

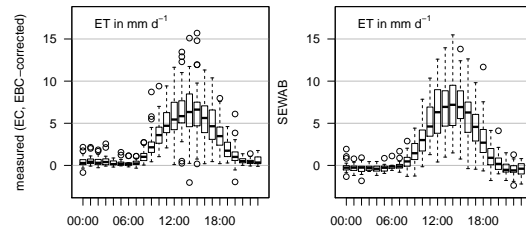


Figure B2. Mean diel course of measured and energy balance corrected evapotranspiration ET (left panel) and SEWAB modelled ET (tile approach according to the EC footprint: S_{RefEC} , right panel) over 61 days during 2010 (3 June to 2 August) at Kema: box plot with median, 25 % and 75 % quartiles; bars represent quartiles ± 1.5 times interquartile range, dots are outliers. Measured and modelled values are restricted to high flux data quality (flag 1–3). Measured data is corrected according to the surface energy imbalance with the buoyancy flux correction.

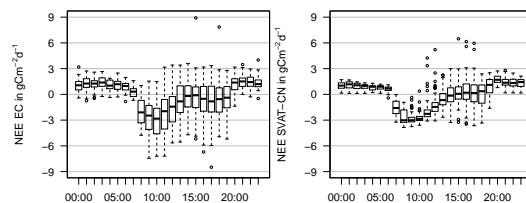


Figure B3. Mean diel course of measured (left panel) and modelled (tile approach according to the EC footprint: S_{RefEC} , right panel) net ecosystem exchange (NEE) over 61 days of 2010 (3 June to 2 August) at Kema: box plot with median, 25 % and 75 % quartiles; bars represent quartiles ± 1.5 times interquartile range, dots are outliers. Measured and modelled values are restricted to high data quality (flag 1–3 out of a scheme ranging from 1 to 9, Foken et al., 2004).

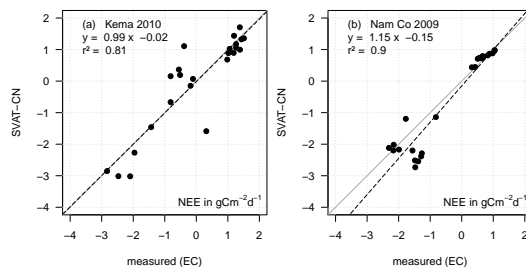


Figure B4. Comparison of hourly medians (see Fig. D3) of measured and modelled net ecosystem exchange for the 2010 campaign at Kema (left panel) and 2009 campaign at Nam Co (right panel). The regression line (dashed, black) is shown as well as the 1 : 1 line (solid, grey).

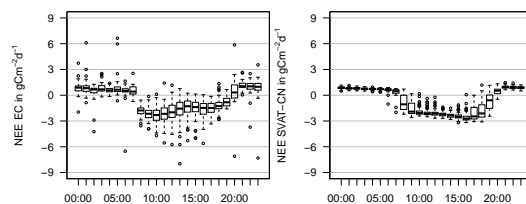


Figure B5. Mean diel course of measured (left panel) and modelled (right panel) net ecosystem exchange (NEE) over 44 days during 2009 (26 June to 8 August) at Nam Co: box plot with median, 25 and 75 % quartiles; bars represent quartiles ± 1.5 times interquartile range, dots are outliers. Measured and modelled values are restricted to high data quality (flag 1–3 out of a scheme ranging from 1 to 9, Foken et al., 2004). Model parameters for leaf physiology and soil respiration were adapted for best representation of eddy-covariance data (see Sect. 3.2.1).

The Supplement related to this article is available online at doi:10.5194/bg-11-6633-2014-supplement.

Acknowledgements. The project was funded within the DFG (German Science Foundation) priority programme 1372 “Tibetan Plateau – Formation – Climate – Ecosystems (TIP)” with the contracts FO 226/18-1,2; GU 406/22-1,2; KU 1184/14-1,2; LE 762/12-1,2; MI 338/7-1,2; WE 2601/4-1,2. Special thanks for the additional funding of the modelling study with the contract AP 34/32-3. The Chinese scientists in the Institute of Tibetan Plateau Research, the Chinese Academy of Sciences were supported by the Chinese National Key Programme for Developing Basic Sciences with the contract 2010CB951701 and the National Natural Science Foundation of China with the contracts 91337212 and 41275010. The research station at Kema was supported by the Volkswagen foundation, in cooperation with the Marburg University and the Tibet University Lhasa, now managed by the Institute of Tibetan Plateau Research, (CAS) as “*Naqu Ecological and Environmental Observation and Research Station*”. All the authors are very grateful to the staff of the research stations at Kema and Nam Co for their support. Furthermore, we thank LI-COR Biosciences for the lending of the chamber system and for their support. This publication is funded by the DFG and the University of Bayreuth in the funding programme Open Access Publishing.

Edited by: P. Stoy

References

- Agam, N., Berliner, P. R., Zangvil, A., and Ben-Dor, E.: Soil water evaporation during the dry season in an arid zone, *J. Geophys. Res.*, 109, D16103, doi:10.1029/2004JD004802, 2004.
- Aubinet, M., Vesala, T., and Papale, D.: *Eddy Covariance: a Practical Guide to Measurement and Data Analysis*, Springer, Dordrecht, Heidelberg, London, New York, 438 pp., 2012.
- Avissar, R. and Pielke, R. A.: A parametrization of heterogeneous land surface for atmospheric numerical models and its impact on regional meteorology, *Mon. Weather Rev.*, 117, 2113–2136, 1989.
- Ball, J. T., Woodrow, I. E., and Berry, J. A.: A model predicting stomatal conductance and its contribution to the control of photosynthesis under different environmental conditions, in: *Progress in Photosynthesis Research, Proceedings of the VII International Photosynthesis Congress*, edited by: Bingsins, I., 221–224, 1987.
- Balsamo, G., Boussetta, S., Dutra, E., Beljaars, A., Viterbo, P., and van den Hurk, B.: Evolution of land surface processes in the IFS, *ECMWF Newsletter*, 127, 17–22, 2011.
- Ben-Gal, A. and Shani, U.: A highly conductive drainage extension to control the lower boundary condition of lysimeters, *Plant Soil*, 239, 9–17, doi:10.1023/A:1014942024573, 2002.
- Biermann, T., Leipold, T., Babel, W., Becker, L., Coners, H., Foken, T., Guggenberger, G., He, S., Ingrisich, J., Kuzyakov, Y., Leuschner, C., Miehe, G., Richards, K., Seeber, E., and Wesche, K.: Tibet Plateau Atmosphere–Ecology–Glaciology Cluster, Joint *Kobresia* Ecosystem Experiment: Documentation of the first Intensive Observation Period Summer 2010 in Kema, Tibet, *Arbeitsergebn.*, Univ. Bayreuth, Abt. Mikrometeorol., ISSN 1614-8916, 44, 105 pp., <http://epub.uni-bayreuth.de/356/>, 2011.
- Biermann, T., Seeber, E., Schleuß, P., Willinghöfer, S., Leonbacher, J., Schützenmeister, K., Steingraber, L., Babel, W., Coners, H., Foken, T., Guggenberger, G., Kuzyakov, Y., Leuschner, C., Miehe, G., and Wesche, K.: Tibet Plateau Atmosphere–Ecology–Glaciology Cluster Joint *Kobresia* Ecosystem Experiment: Documentation of the second Intensive Observation Period, Summer 2012 in KEMA, Tibet, *Arbeitsergebn.*, Univ. Bayreuth, Abt. Mikrometeorol., ISSN 1614-8916, 54, 52 pp., <http://epub.uni-bayreuth.de/145/>, 2013.
- Biermann, T., Babel, W., Ma, W., Chen, X., Thiem, E., Ma, Y., and Foken, T.: Turbulent flux observations and modelling over a shallow lake and a wet grassland in the Nam Co basin, Tibetan Plateau, *Theor. Appl. Climatol.*, 116, 301–316, 2014.
- Caldwell, M. M., Meister, H. P., Tenhunen, J. D., and Lange, O. L.: Canopy structure, light microclimate and leaf gas exchange of *Quercus coccifera* L. in a Portuguese macchia: measurements in different canopy layers and simulations with a canopy model, *Trees*, 1, 25–41, 1986.
- Charuchittipan, D., Babel, W., Mauder, M., Leps, J.-P., and Foken, T.: Extension of the averaging time of the eddy-covariance measurement and its effect on the energy balance closure *Bound.-Lay. Meteorol.*, 152, 303–327, 2014.
- Che, M., Chen, B., Innes, J. L., Wang, G., Dou, X., Zhou, T., Zhang, H., Yan, J., Xu, G., and Zhao, H.: Spatial and temporal variations in the end date of the vegetation growing season throughout the Qinghai–Tibetan Plateau from 1982 to 2011, *Agr. Forest Meteorol.*, 189/190, 81–90, 2014.
- Chen, Y., Yang, K., Tang, W., Qin, J., and Zhao, L.: Parameterizing soil organic carbon’s impacts on soil porosity and thermal parameters for Eastern Tibet grasslands, *Sci. China Ser. D*, 55, 1001–1011, 2012.
- Clapp, R. B. and Hornberger, G. M.: Empirical equations for some soil hydraulic properties, *Water Resour. Res.*, 14, 601–604, 1978.
- Cui, X. F. and Graf, H.-F.: Recent land cover changes on the Tibetan Plateau: a review, *Clim. Change*, 94, 47–61, 2009.
- Cui, X. F., Graf, H.-F., Langmann, B., Chen, W., and Huang, R.-H.: Climate impacts of anthropogenic land use changes on the Tibetan Plateau, *Global Planet. Change*, 54, 33–56, doi:10.1016/j.gloplacha.2005.07.006, 2006.
- Cui, X. F., Graf, H.-F., Langmann, B., Chen, W., and Huang, R.-H.: Hydrological impacts of deforestation at the Southeast Tibetan Plateau, *Earth Interact.*, 11, 1–18, 2007a.
- Cui, X. F., Langmann, B., and Graf, H.-F.: Summer Monsoonal Rainfall Simulation on the Tibetan Plateau with a Regional Climate Model Using a One-way Double-nesting System, *SOLA*, 3, 49–52, 2007b.
- Evans, R. A. and Love, R. M.: The step-point method of sampling – a practical tool in range research, *J. Range Manage.*, 10, 208–212, 1957.
- Falge, E.: Die Modellierung der Kronendachtranspiration von Fichtenbeständen (*Picea abies* (L.) Karst., *Bayreuther Forum Ökologie*, 48, 215 pp., 1997.
- Falge, E., Tenhunen, J., Aubinet, M., Bernhofer, C., Clement, R., Granier, A., Kowalski, A., Moors, E., Pilegaard, K., Rannik, Ü., and Rebmann, C.: A model-based study of carbon fluxes at ten

- European forest sites, in: Fluxes of Carbon, Water and Energy of European Forests, Ecological Studies Series 163, edited by: Valentini, R., Springer, Berlin, Heidelberg, 151–177, 2003.
- Falge, E., Reth, S., Brüggemann, N., Butterbach-Bahl, K., Goldberg, V., Oltchev, A., Schaaf, S., Spindler, G., Stiller, B., Queck, R., Köstner, B., and Bernhofer, C.: Comparison of surface energy exchange models with eddy flux data in forest and grassland ecosystems of Germany, *Ecol. Model.*, 188, 174–216, 2005.
- Farquhar, G. D., von Caemmerer, S., and Berry, J. A.: A biochemical of photosynthetic CO₂ assimilation in leaves of C₃ species, *Planta*, 149, 78–90, 1980.
- Foken, T.: The energy balance closure problem – an overview, *Ecol. Appl.*, 18, 1351–1367, 2008.
- Foken, T. and Wichura, B.: Tools for quality assessment of surface-based flux measurements, *Agr. Forest Meteorol.*, 78, 83–105, 1996.
- Foken, T., Göckede, M., Mauder, M., Mahrt, L., Amiro, B. D., and Munger, J. W.: Post-field data quality control, in: Handbook of Micrometeorology: a Guide for Surface Flux Measurement and Analysis, edited by: Lee, X., Massman, W. J., and Law, B., Kluwer, Dordrecht, 181–208, 2004.
- Foken, T., Aubinet, M., Finnigan, J., Leclerc, M. Y., Mauder, M., and Paw U, K. T.: Results of a panel discussion about the energy balance closure correction for trace gases, *B. Am. Meteorol. Soc.*, 92, ES13–ES18, 2011.
- Foken, T., Leuning, R., Oncley, S. P., Mauder, M., and Aubinet, M.: Corrections and data quality in: Eddy Covariance: a Practical Guide to Measurement and Data Analysis, edited by: Aubinet, M., Vesala, T., and Papale, D., Springer, Dordrecht, Heidelberg, London, New York, 85–131, 2012a.
- Foken, T., Meixner, F. X., Falge, E., Zetzsch, C., Serafimovich, A., Bargsten, A., Behrendt, T., Biermann, T., Breuninger, C., Dix, S., Gerken, T., Hunner, M., Lehmann-Pape, L., Hens, K., Jocher, G., Kesselmeier, J., Liérs, J., Mayer, J.-C., Moravek, A., Plake, D., Riederer, M., Rütz, F., Scheibe, M., Siebicke, L., Sörgel, M., Staudt, K., Trebs, I., Tsokankunku, A., Welling, M., Wolff, V., and Zhu, Z.: Coupling processes and exchange of energy and reactive and non-reactive trace gases at a forest site – results of the EGER experiment, *Atmos. Chem. Phys.*, 12, 1923–1950, doi:10.5194/acp-12-1923-2012, 2012b.
- Fratini, G. and Mauder, M.: Towards a consistent eddy-covariance processing: an intercomparison of EddyPro and TK3, *Atmos. Meas. Tech.*, 7, 2273–2281, doi:10.5194/amt-7-2273-2014, 2014.
- Friend, A. D. and Kiang, N. Y.: Land surface model development for the GISS GCM: effects of improved canopy physiology on simulated climate, *J. Climate*, 18, 2883–2902, 2005.
- Friend, A. D., Stevens, A. K., Knox, R. G., and Cannell, M. G. R.: A process-based, terrestrial biosphere model of ecosystem dynamics (Hybrid v3.0), *Ecol. Model.*, 95, 249–287, 1997.
- Gee, G. W., Newman, B. D., Green, S. R., Meissner, R., Rupp, H., Zhang, Z. F., Keller, J. M., Waugh, W. J., van der Velde, M., and Salazar, J.: Passive wick fluxmeters: design considerations and field applications, *Water Resour. Res.*, 45, W04420, doi:10.1029/2008WR007088, 2009.
- Gerken, T., Babel, W., Hoffmann, A., Biermann, T., Herzog, M., Friend, A. D., Li, M., Ma, Y., Foken, T., and Graf, H.-F.: Turbulent flux modelling with a simple 2-layer soil model and extrapolated surface temperature applied at Nam Co Lake basin on the Tibetan Plateau, *Hydrol. Earth Syst. Sci.*, 16, 1095–1110, doi:10.5194/hess-16-1095-2012, 2012.
- Gerken, T., Babel, W., Sun, F., Herzog, M., Ma, Y., Foken, T., and Graf, H.-F.: Uncertainty in atmospheric profiles and its impact on modeled convection development at Nam Co Lake, Tibetan Plateau, *J. Geophys. Res.-Atmos.*, 118, 12317–12331, doi:10.1002/2013JD020647, 2013.
- Gerken, T., Biermann, T., Babel, W., Herzog, M., Ma, Y., Foken, T., and Graf, H.-F.: A modelling investigation into lake-breeze development and convection triggering in the Nam Co Lake basin, Tibetan Plateau, *Theor. Appl. Climatol.*, 117, 149–167, 2014.
- Göckede, M., Rebmann, C., and Foken, T.: A combination of quality assessment tools for eddy covariance measurements with footprint modelling for the characterisation of complex sites, *Agr. Forest Meteorol.*, 127, 175–188, 2004.
- Göckede, M., Markkanen, T., Hasager, C. B., and Foken, T.: Update of a footprint-based approach for the characterisation of complex measuring sites, *Bound.-Lay. Meteorol.*, 118, 635–655, 2006.
- Hafner, S., Unteregelsbacher, S., Seeber, E., Lena, B., Xu, X., Li, X., Guggenberger, G., Miede, G., and Kuzyakov, Y.: Effect of grazing on carbon stocks and assimilate partitioning in a Tibetan montane pasture revealed by ¹³C₂ pulse labeling, *Glob. Change Biol.*, 18, 528–538, 2012.
- Harris, R. B.: Rangeland degradation on the Qinghai-Tibetan plateau: A review of the evidence of its magnitude and causes, *J. Arid Environ.*, 74, 1–12, 2010.
- Herzog, M., Oberhuber, J. M., and Graf, H. F.: A prognostic turbulence scheme for the nonhydrostatic plume model ATHAM, *J. Atmos. Sci.*, 60, 2783–2796, 2003.
- Hillel, D.: Applications of Soil Physics, Academic Press, New York, 385 pp., 1980.
- Holzner, W. and Kriechbaum, M.: Pastures in South and Central Tibet (China), I. Methods for a rapid assessment of pasture conditions, *Bodenkultur*, 51, 259–266, 2000.
- Hong, J., Kim, J., Ishikawa, H., and Ma, Y.: Surface layer similarity in the nocturnal boundary layer: the application of Hilbert–Huang transform, *Biogeosciences*, 7, 1271–1278, doi:10.5194/bg-7-1271-2010, 2010.
- Hu, J., Hopping, K. A., Bump, J. K., Kang, S., and Klein, J. A.: Climate change and water use partitioning by different plant functional groups in a grassland on the Tibetan Plateau, *PLOS ONE*, 8, e75503, doi:10.1371/journal.pone.0075503, 2013.
- Ingrisch, J., Biermann, T., Seeber, E., Leipold, T., Li, M., Ma, Y., Xu, X., Miede, G., Guggenberger, G., Foken, T., and Kuzyakov, Y.: Carbon pools and fluxes in a Tibetan alpine *Kobresia pygmaea* pasture partitioned by coupled eddy-covariance measurements and ¹³C₂ pulse labeling, *Sci. Total Environ.*, in print, 2014.
- Ingwersen, J., Steffens, K., Högy, P., Warrach-Sagi, K., Zhunusbayeva, D., Poltoradnev, M., Gäbler, R., Wizemann, H.-D., Fangmeier, A., Wulfmeyer, V., and Streck, T.: Comparison of Noah simulations with eddy covariance and soil water measurements at a winter wheat stand, *Agr. Forest Meteorol.*, 151, 345–355, 2011.
- IUSS-ISRIC-FAO: World Reference Base for Soil Resources: a Framework for International Classification, Correlation and Communication, 2nd edn., World soil resources reports, 103,

- Food and Agriculture Organization of the United Nations, Rome, 128 pp., 2006.
- Kaiser, K., Mieke, G., Barthelmes, A., Ehrmann, O., Scharf, A., Schult, M., Schlütz, F., Adamczyk, S., and Frenzel, B.: Turf-bearing topsoils on the central Tibetan Plateau, China: pedology, botany, geochronology, *Catena*, 73, 300–311, 2008.
- Kracher, D., Mengelkamp, H.-T., and Foken, T.: The residual of the energy balance closure and its influence on the results of three SVAT models, *Meteorol. Z.*, 18, 647–661, 2009.
- Kuzyakov, Y. and Domanski, G.: Carbon input by plants into the soil, review, *J. Plant Nutr. Soil Sc.*, 163, 421–431, 2000.
- Liu, W., Wang, X., Zhou, L., and Zhou, H.: Studies on destruction, prevention and control of Plateau Pikas in *Kobresia pygmaea* meadow, *Acta Theriol. Sin.*, 23, 214–219, 2003 (in Chinese with English abstract).
- Lloyd, J. and Taylor, J. A.: On the temperature dependence of soil respiration, *Funct. Ecol.*, 8, 315–323, 1994.
- Louis, J. F.: A parametric model of vertical fluxes in the atmosphere, *Bound.-Lay. Meteorol.*, 17, 187–202, 1979.
- Lundegardh, H.: Ecological studies in the assimilation of certain forest plants and shore plants, *Svensk Botaniska Tidskrift*, 15, 46–94, 1921.
- Ma, Y., Tsukamoto, O., Wang, J., Ishikawa, H., and Tamagawa, I.: Analysis of aerodynamic and thermodynamic parameters on the grassy marshland surface of Tibetan Plateau, *Prog. Nat. Sci.*, 12, 36–40, 2002.
- Ma, Y., Kang, S., Zhu, L., Xu, B., Tian, L., and Yao, T.: Roof of the world: Tibetan observation and research platform, *B. Am. Meteorol. Soc.*, 89, 1487–1492, 2008.
- Ma, Y., Zhong, L., Wang, B., Ma, W., Chen, X., and Li, M.: Determination of land surface heat fluxes over heterogeneous landscape of the Tibetan Plateau by using the MODIS and in situ data, *Atmos. Chem. Phys.*, 11, 10461–10469, 2011, <http://www.atmos-chem-phys.net/11/10461/2011/>.
- Ma, Y., Han, C., Zhong, L., Wang, B., Zhu, Z., Wang, Y., Zhang, L., Meng, C., Xu, C., and Amatya, P.: Using MODIS and AVHRR data to determine regional surface heating field and heat flux distributions over the heterogeneous landscape of the Tibetan Plateau, *Theor. Appl. Climatol.*, 117, 643–652, 2014.
- Mauder, M. and Foken, T.: Documentation and Instruction Manual of the Eddy Covariance Software Package TK2, *Arbeitsergebn.*, Univ. Bayreuth, Abt. Mikrometeorol., 26, 42 pp., <http://epub.uni-bayreuth.de/884/>, 2004.
- Mauder, M. and Foken, T.: Documentation and Instruction Manual of the Eddy Covariance Software Package TK3, *Arbeitsergebn.*, Univ. Bayreuth, Abt. Mikrometeorol., 46, 58 pp., <http://epub.uni-bayreuth.de/342/>, 2011.
- Mauder, M., Foken, T., Clement, R., Elbers, J. A., Eugster, W., Grünwald, T., Heusinkveld, B., and Kolle, O.: Quality control of CarboEurope flux data – Part 2: Inter-comparison of eddy-covariance software, *Biogeosciences*, 5, 451–462, doi:10.5194/bg-5-451-2008, 2008.
- Maussion, F., Scherer, D., Mölg, T., Collier, E., Curio, J., and Finkelnburg, R.: Precipitation Seasonality and Variability over the Tibetan Plateau as Resolved by the High Asia Reanalysis, *J. Climate*, 27, 1910–1927, 2014.
- Mengelkamp, H.-T., Warrach, K., and Raschke, E.: SEWAB a parameterization of the surface energy and water balance for atmospheric and hydrologic models, *Adv. Water Res.*, 23, 165–175, 1999.
- Mengelkamp, H. T., Kiely, G., and Warrach, K.: Evaluation of the hydrological components added to an atmospheric land-surface scheme, *Theor. Appl. Climatol.*, 69, 199–212, 2001.
- Mieke, G., Kaiser, K., Co, S., and Liu, J.: Geo-ecological transect studies in northeast Tibet (Qinghai, China) reveal human-made mid-Holocene environmental changes in the upper Yellow River catchment changing forest to grassland, *Erdkunde*, 62, 187–199, 2008a.
- Mieke, G., Mieke, S., Kaiser, K., Liu, J. Q., and Zhao, X. Q.: Status and dynamics of *Kobresia pygmaea* ecosystem on the Tibetan plateau, *Ambio*, 37, 272–279, 2008b.
- Mieke, G., Mieke, S., Bach, K., Nölling, J., Hanspach, J., Reudenbach, C., Kaiser, K., Wesche, K., Mosbrugger, V., Yang, Y. P., and Ma, Y. M.: Plant communities of central Tibetan pastures in the Alpine Steppe/*Kobresia pygmaea* ecotone, *J. Arid Environ.*, 75, 711–723, 2011.
- Mieke, G., Mieke, S., Böhner, J., Kaiser, K., Hensen, I., Madsen, D., Liu, J., and Opgenoorth, L.: How old is the human footprint in the world's largest alpine ecosystem? A review of multiproxy records from the Tibetan Plateau from the ecologists' viewpoint, *Quaternary Sci. Rev.*, 86, 190–209, 2014.
- Mihailovic, D. T., Pielke, R. A., Rajkovic, B., Lee, T. J., and Jetric, M.: A resistance representation of schemes for evaporation from bare and partly plant-covered surfaces for use in atmospheric models, *J. Appl. Meteorol.*, 32, 1038–1054, 1993.
- Mölders, N.: Land-Use and Land-Cover Changes, Impact on Climate and Air Quality, Springer, Dordrecht, Heidelberg, London, New York, 189 pp., 2012.
- Moldrup, P., Rolston, D. E., and Hansen, A. A.: Rapid and numerically stable simulation of one dimensional, transient water flow in unsaturated, layered soils, *Soil Sci.*, 148, 219–226, 1989.
- Moldrup, P., Rolston, D. E., Hansen, A. A., and Yamaguchi, T.: A simple, mechanistic model for soil resistance to plant water uptake, *Soil Sci.*, 151, 87–93, 1991.
- Mügler, I., Gleixner, G., Günther, F., Mäusbacher, R., Daut, G., Schütt, B., Berking, J., Schwab, A., Schwark, L., Xu, B., Yao, T., Zhu, L., and Yi, C.: A multi-proxy approach to reconstruct hydrological changes and Holocene climate development of Nam Co, Central Tibet, *J. Paleolimnol.*, 43, 625–648, 2010.
- Niu, Y.: The study of environment in the Plateau of Qin-Tibet, *Progr. Geogra.*, 18, 163–171, 1999 (in Chinese with English abstract).
- Noilhan, J. and Planton, S.: A Simple parameterization of land surface processes for meteorological models, *Mon. Weather Rev.*, 117, 536–549, 1989.
- Oberhuber, J. M., Herzog, M., Graf, H. F., and Schwanke, K.: Volcanic plume simulation on large scales, *J. Volcanol. Geoth. Res.*, 87, 29–53, 1998.
- Rebmann, C., Kolle, O., Heinesch, B., Queck, R., Ibrom, A., and Aubinet, M.: Data acquisition and flux calculations, in: *Eddy Covariance: A Practical Guide to Measurement and Data Analysis*, edited by: Aubinet, M., Vesala, T., and Papale, D., Springer, Dordrecht, Heidelberg, London, New York, 59–83, 2012.
- Reichstein, M.: Drought Effects on Ecosystem Carbon Anwater Exchange in Three Mediterranean Forest Ecosystems – a Combined Top-Down and Bottom-Up Analysis, *Bayreuther Forum Ökologie*, 89, 1–150, 2001.

- Reth, S., Göckede, M., and Falge, E.: CO₂ efflux from agricultural soils in Eastern Germany – comparison of a closed chamber system with eddy covariance measurements, *Theor. Appl. Climatol.*, 80, 105–120, 2005a.
- Reth, S., Hentschel, K., Drösler, M., and Falge, E.: DenNit – experimental analysis and modelling of soil N₂O efflux in response on changes of soil water content, soil temperature, soil pH, nutrient availability and the time after rain event, *Plant Soil*, 272, 349–363, 2005b.
- Reth, S., Reichstein, M., and Falge, E.: The effect of soil water content, soil temperature, soil pH-value and the root mass on soil CO₂ efflux – a modified model, *Plant Soil*, 268, 21–33, 2005c.
- Richards, L. A.: Capillary conductivity of liquids in porous mediums, *Physics*, 1, 318–333, 1931.
- Riederer, M.: Carbon fluxes of an extensive meadow and attempts for flux partitioning, Ph.D. thesis, University of Bayreuth, 167 pp., 2014.
- Riederer, M., Serafimovich, A., and Foken, T.: Net ecosystem CO₂ exchange measurements by the closed chamber method and the eddy covariance technique and their dependence on atmospheric conditions, *Atmos. Meas. Tech.*, 7, 1057–1064, doi:10.5194/amt-7-1057-2014, 2014.
- Shen, M., Zhang, G., Cong, N., Wang, S., Kong, W., and Piao, S.: Increasing altitudinal gradient of spring vegetation phenology during the last decade on the Qinghai–Tibetan Plateau, *Agr. Forest Meteorol.*, 189–190, 71–80, 2014.
- Shi, Q., and Liang, S.: Surface-sensible and latent heat fluxes over the Tibetan Plateau from ground measurements, reanalysis, and satellite data, *Atmos. Chem. Phys.*, 14, 5659–5677, doi:10.5194/acp-14-5659-2014, 2014.
- Singh, J. and Gupta, S.: Plant decomposition and soil respiration in terrestrial ecosystems, *Bot. Rev.*, 43, 449–528, 1977.
- Staudt, K., Serafimovich, A., Siebicke, L., Pyles, R. D., and Falge, E.: Vertical structure of evapotranspiration at a forest site (a case study), *Agr. Forest Meteorol.*, 151, 709–729, 2011.
- Swinnen, J., Vanveen, J. A., and Merckx, R.: C-14 Pulse labeling of field-grown spring wheat – an evaluation of its use in rhizosphere carbon budget estimations, *Soil Biol. Biochem.*, 26, 161–170, 1994.
- Tanaka, K., Ishikawa, H., Hayashi, T., Tamagawa, I., and Ma, Y.: Surface energy budget at Amdo on the Tibetan Plateau using GAME/Tibet IOP98 data, *J. Meteorol. Soc. Jpn.*, 79, 505–517, 2001.
- Tenhunen, J. D., Siegwolf, R. A., and Oberbauer, S. F.: Effects of phenology, physiology, and gradients in community composition, structure, and microclimate on tundra ecosystem CO₂ exchange., in: *Ecophysiology of Photosynthesis*, edited by: Schulze, E.-D. and Caldwell, M. M., Springer, Berlin, Heidelberg, New York, 431–460, 1995.
- Unteregelsbacher, S., Hafner, S., Guggenberger, G., Miehe, G., Xu, X., Liu, J., and Kuzyakov, Y.: Response of long-, medium- and short-term processes of the carbon budget to overgrazing-induced crusts in the Tibetan Plateau, *Biogeochemistry*, 111, 187–201, 2012.
- van den Bergh, T., Inauen, N., Hiltbrunner, E., and Körner, C.: Climate and plant cover co-determine the elevational reduction in evapotranspiration in the Swiss Alps, *J. Hydrol.*, 500, 75–83, 2013.
- van Genuchten, M. T.: A closed-form equation for predicting the hydraulic conductivity of unsaturated soils, *Soil Sci. Soc. Am. J.*, 44, 892–898, 1980.
- Wei, D., Ri, X., Wang, Y., Wang, Y., Liu, Y., and Yao, T.: Responses of CO₂, CH₄ and N₂O fluxes to livestock enclosure in an alpine steppe on the Tibetan Plateau, China, *Plant Soil*, 359, 45–55, doi:10.1007/s11104-011-1105-3, 2012.
- Wieser, G., Hammerle, A., and Wohlfahrt, G.: The water balance of grassland ecosystems in the Austrian Alps, *Arct. Antarct. Alp. Res.*, 40, 439–445, 2008.
- Wohlfahrt, G., Bahn, M., Horak, I., Tappeiner, U., and Cernusca, A.: A nitrogen sensitive model of leaf carbon dioxide and water vapour gas exchange: application to 13 key species from differently managed mountain grassland ecosystems, *Ecol. Model.*, 113, 179–199, 1998.
- Yao, T., Thompson, L. G., Mosbrugger, V., Zhang, F., Ma, Y., Luo, T., Xu, B., Yang, X., Joswiak, D. R., Wang, W., Joswiak, M. E., Devkota, L. P., Tayal, S., Jilani, R., and Fayziev, R.: Third Pole Environment (TPE), *Environ. Dev.*, 3, 52–64, 2012.
- Yang, K., Koike, T., and Yang, D.: Surface flux parameterization in the Tibetan Plateau, *Bound.-Lay. Meteorol.*, 116, 245–262, 2003.
- Yang, K., Koike, T., Fuji, H., Tamura, T., Xu, X., Bian, L., and Zhou, M.: The daytime evolution of the atmospheric boundary layer and convection over the Tibetan Plateau: observations and simulations, *J. Meteorol. Soc. Jpn.*, 82, 1777–1792, 2004.
- Yang, K., Koike, T., Ye, B., and Bastidas, L.: Inverse analysis of the role of soil vertical heterogeneity in controlling surface soil state and energy partition, *J. Geophys. Res.*, 110, D08101, doi:10.1029/2004JD005500, 2005.
- Yang, K., Koike, T., Ishikawa, H., Kim, J., Li, X., Liu, H., Liu, S., Ma, Y., and Wang, J.: Turbulent flux transfer over bare-soil surfaces: characteristics and parameterization, *J. Appl. Meteorol. Clim.*, 47, 276–290, 2008.
- Yang, K., Chen, Y.-Y., and Qin, J.: Some practical notes on the land surface modeling in the Tibetan Plateau, *Hydrol. Earth Syst. Sci.*, 13, 687–701, doi:10.5194/hess-13-687-2009, 2009.
- Yang, K., Ye, B., Zhou, D., Wu, B., Foken, T., Qin, J., and Zhou, Z.: Response of hydrological cycle to recent climate changes in the Tibetan Plateau, *Clim. Change*, 109, 517–534, 2011.
- Yang, K., Qin, J., Zhao, L., Chen, Y., Tang, W., Lazhu, M. H., Chen, Z., Lv, N., Ding, B., Wu, H., and Lin, C.: A Multiscale Soil Moisture and Freeze–Thaw Monitoring Network on the Third Pole, *B. Am. Meteorol. Soc.*, 94, 1907–1916, 2013.
- Yang, K., Wu, H., Qin, J., Lin, C., Tang, W., and Chen, Y.: Recent climate changes over the Tibetan Plateau and their impacts on energy and water cycle: A review, *Global Planet. Change*, 112, 79–91, 2014.
- Zhang, D., Xu, W., Li, J., Cai, Z., and An, D.: Frost-free season lengthening and its potential cause in the Tibetan Plateau from 1960 to 2010, *Theor. Appl. Climatol.*, 115, 441–450, 2014.
- Zhou, D., Eigenmann, R., Babel, W., Foken, T., and Ma, Y.: Study of near-ground free convection conditions at Nam Co station on the Tibetan Plateau, *Theor. Appl. Climatol.*, 105, 217–228, 2011.
- Zhou, H., Zhao, X., Tang, Y., Gu, S., and Zhou, L.: Alpine grassland degradation and its control in the source region of the Yangtze and Yellow Rivers, China, *Grassland Sci.*, 51, 191–203, 2005.

E. Ingrisch et al. (2015)

Ingrisch, J., Biermann, T., Seeber, E., Leipold T., Li, M., Ma, Y., Xu, X., Mieke, G., Guggenberger, G., Foken, T., Kuzyakov Y.: Carbon pools and fluxes in a Tibetan alpine *Kobresia pygmaea* pasture partitioned by coupled eddy-covariance measurements and $^{13}\text{CO}_2$ pulse labeling, *Science of The Total Environment*, 505, 1213–1224, doi:10.1016/j.scitotenv.2014.10.082, 2015. ¹

Supplementary data:

Ingrisch, J., Biermann, T., Seeber, E., Leipold T., Li, M., Ma, Y., Xu, X., Mieke, G., Guggenberger, G., Foken, T., Kuzyakov Y.: Carbon pools and fluxes measured during a field campaign conducted in 2010 on the Tibetan Plateau at Kema. Dataset 833208, PANGAEA, doi:10.1594/PANGAEA.833208, 2014.

¹published with kind permission of (C) Elsevier



Contents lists available at ScienceDirect

Science of the Total Environment

journal homepage: www.elsevier.com/locate/scitotenv



Carbon pools and fluxes in a Tibetan alpine *Kobresia pygmaea* pasture partitioned by coupled eddy-covariance measurements and ^{13}C pulse labeling



Johannes Ingrisch ^{a,*}, Tobias Biermann ^{b,2,3}, Elke Seeber ^c, Thomas Leipold ^{b,4}, Maoshan Li ^d, Yaoming Ma ^e, Xingliang Xu ^f, Georg Mieke ^g, Georg Guggenberger ^h, Thomas Foken ^{b,i}, Yakov Kuzyakov ^{j,k,l}

^a Department of Agroecosystem Research, University of Bayreuth, Bayreuth, Germany

^b Dept. of Micrometeorology, University of Bayreuth, Bayreuth, Germany

^c Senckenberg Museum of Natural History, Görlitz, Germany

^d Cold and Arid Regions Environment and Engineering Research Institute, Chinese Academy of Sciences, Lanzhou, China

^e Key Laboratory of Tibetan Environment Changes and Land Surface Processes, Institute of Tibetan Plateau Research, Chinese Academy of Sciences, Beijing, China

^f Institute of Geographical Sciences and Natural Resources Research, Chinese Academy of Sciences, Beijing, China

^g Faculty of Geography, Philipps University Marburg, Marburg, Germany

^h Institute of Soil Science, Leibniz University Hannover, Hannover, Germany

ⁱ Member of Bayreuth Center of Ecology and Ecosystem Research (BayCEER), Germany

^j Dept. of Soil Science of Temperate Ecosystems, Georg-August University Göttingen, Göttingen, Germany

^k Dept. of Agricultural Soil Science, Georg-August University of Göttingen, Göttingen, Germany

^l Institute of Environmental Sciences, Kazan Federal University, Kazan, Russia

HIGHLIGHTS

- We lack understanding of the carbon cycling of Tibetan alpine pastures.
- We measured the turnover of recent assimilates within plant soil atmosphere system.
- Absolute fluxes were assessed by coupling eddy-covariance and CO_2 pulse labeling.
- We identify the root turf as the major part for carbon turnover in this ecosystem.
- Grazing cessation didn't affect carbon allocation and fluxes in one growing season.

ARTICLE INFO

Article history:

Received 23 July 2014

Received in revised form 21 October 2014

Accepted 22 October 2014

Editor: J.P. Bennett

Keywords:

Alpine grassland

Carbon cycle

Land use changes

Grazing

Tibetan-Plateau

ABSTRACT

The Tibetan highlands host the largest alpine grassland ecosystems worldwide, bearing soils that store substantial stocks of carbon (C) that are very sensitive to land use changes. This study focuses on the cycling of photoassimilated C within a *Kobresia pygmaea* pasture, the dominating ecosystems on the Tibetan highlands. We investigated short-term effects of grazing cessation and the role of the characteristic *Kobresia* root turf on C fluxes and belowground C turnover. By combining eddy-covariance measurements with ^{13}C pulse labeling we applied a powerful new approach to measure absolute fluxes of assimilates within and between various pools of the plant-soil-atmosphere system. The roots and soil each store roughly 50% of the overall C in the system (76 Mg C ha^{-1}), with only a minor contribution from shoots, which is also expressed in the root:shoot ratio of 90. During June and July the pasture acted as a weak C sink with a strong uptake of approximately $2 \text{ g C m}^{-2} \text{ d}^{-1}$ in the first half of July. The root turf was the main compartment for the turnover of photoassimilates, with a subset of highly dynamic roots (mean residence time 20 days), and plays a key role for the C cycling and C storage in this ecosystem. The short-term grazing cessation only affected aboveground biomass but not ecosystem scale C exchange or assimilate allocation into roots and soil.

© 2014 Elsevier B.V. All rights reserved.

* Corresponding author at: University of Innsbruck, Ecophysiology and Ecosystem Processes, Institute of Ecology, Sternwartestrasse 15, A-6020 Innsbruck, Austria. Tel.: +43 512 507 51634; fax: +43 512 507 51699.

E-mail address: johannes.ingrisc@uibk.ac.at (J. Ingrisch).

¹ Now at: Institute of Ecology, University of Innsbruck, Innsbruck, Austria.

² These authors contributed equally to this work.

³ Now at: Centre for Environmental and Climate Research, Lund University, Lund, Sweden.

⁴ Now at: Dept. of Plant Ecology, University of Bayreuth, Bayreuth, Germany.

<http://dx.doi.org/10.1016/j.scitotenv.2014.10.082>
0048-9697/© 2014 Elsevier B.V. All rights reserved.

1. Introduction

Soils of grassland ecosystems store large amounts of carbon (C) (Scurlock and Hall, 1998) and their C sequestration potential has attracted a lot of attention in recent years (IPCC, 2013). In alpine environments the sensitivity of grasslands to external influences is very pronounced (e.g. Fang et al., 2010a; Lin et al., 2011; Ni, 2002; Wohlfahrt et al., 2008). This is especially the case for the *Kobresia* pastoral ecosystem of the Tibetan highlands (Atlas of Tibet Plateau, 1990; Miede et al., 2008a,b; Chen et al., 2013, 2014; Sun and Zheng, 1998), which is among the ecosystems most sensitive to climate change and anthropogenic activities (Cui and Graf, 2009; Miede et al., 2011; Qiu, 2008; Yang et al., 2014).

Although the Tibetan Plateau only accounts for approximately 1.0% of the global terrestrial land area (Fang et al., 2010b), the C stored in its soil makes up 2.5% of the global soil C storage (Wang et al., 2002). It is therefore important to understand and to quantify the C budget as well as to estimate C fluxes and identify their drivers in these remote highland pastures with in situ studies (Hafner et al., 2012; Wang et al., 2007; Wu et al., 2010).

The Tibetan highlands in general are mainly above the tree line at about 3800 m a.s.l. in the north and above 4800 m a.s.l. in the south-east (Miede et al., 2007) and are thus characterized by alpine steppe and *Kobresia pygmaea* dominated pastures (Wang et al., 2006). *K. pygmaea*, a cyperaceae, extends approximately 450,000 km² along an altitudinal range of nearly 3000 m a.s.l., between the montane belt (around 3000 m in the northeast and around 4000 m in the eastern and southern declivity to nearly 6000 m (Miede et al., 2008b)). It grows no more than a few centimeters tall while developing a very extensive rooting system. These roots form a very dense felty turf layer, consisting of roots, root remains, amorphous humus and minerogenic matter which covers and protects the soil from wind and water erosion as well as trampling damage by large herbivores (Kaiser, 2004; Miede et al., 2011).

It is assumed that the major driver for the vegetation composition and structure of this *K. pygmaea* ecosystem is grazing by herbivores, namely traditional pastoral livestock and small mammals (Miede et al., 2008b; Wu et al., 2009). Therefore, the state of the *K. pygmaea* ecosystem is strongly dependent on the grazing practices and livestock husbandry by the local Tibetan population (Miede et al., 2014). These human activities have changed dramatically since the 1950s, for reasons including increasing livestock numbers, concentration of grazing close to settlements and fencing due to sedentarization programs (Du et al., 2004; Goldstein and Beall, 1991; Harris, 2010; Lu et al., 2009; Sheehy et al., 2006). As a reaction to overgrazing and subsequent degradation, rangeland policies of recent years included the regulation of livestock numbers and the implementation of grazing exclosures (Han et al., 2008). However, the effects of altered grazing intensity on C budgets of the alpine pastures in the highlands are not sufficiently understood yet (Gao et al., 2007). Grazing is considered to be one of the key factors for C budget and turnover of *K. pygmaea* pastures. It indirectly affects C allocation in the ecosystem by controlling species composition and functional diversity of the vegetation on the time scale of years (Cao et al., 2004; Gao et al., 2007; Klein et al., 2004; Miede et al., 2008a,b; Wei et al., 2012; Wu et al., 2009; Zhao and Zhou, 1999). Grazing has been shown to have positive effects on the overall C storage of the *Kobresia* ecosystem (Gao et al., 2007; Hafner et al., 2012; Shi et al., 2013). The crucial role of the turf layer within this ecosystem is emphasized by the findings of Hafner et al. (2012). They report that the change from a Cyperaceae to Poaceae dominated montane grassland in the northeastern highlands (3400 m a.s.l.), induced by cessation of grazing, had the greatest effect within the turf layer, with a decrease of C fluxes and lower plant-derived C stocks within the upper layer of the soil. Since all mentioned studies have been conducted in already established grazing exclosures, no short-term effects of grazing cessation on the *Kobresia* pastures have been investigated yet, although direct

physiological effects on the C allocation of plants have been observed on short time scales as well in other ecosystems (Bardgett and Wardle, 2003; Holland et al., 1996; Schmitt et al., 2013).

Two of the most commonly used methods in C studies are turbulent flux measurements with the eddy covariance (EC) method (Aubinet et al., 2012) and pulse labeling with ¹³C or ¹⁴C enriched CO₂ (see reviews by Kuzyakov and Domanski (2000) and Kuzyakov (2001)). EC measurements are a micrometeorological approach used to estimate C net ecosystem exchange (NEE) on the ecosystem scale (Baldocchi, 2003; Wohlfahrt et al., 2012). They provide absolute values for the C exchange with a high resolution and over a long time for a detailed overview of the exchange between the ecosystem and the atmosphere (Foken, 2008a). Only few studies with EC have been conducted on the Tibetan Plateau e.g. by Kato et al. (2004, 2006) and Zhao et al. (2005) in the northeast of the Plateau and by Fu et al. (2009) in the southern highlands. ¹³CO₂ pulse labeling enables tracking of the allocation of assimilated C to the various C pools within the plant–soil system. Assimilates are used for metabolism by shoots, roots and rhizosphere microorganisms or become incorporated into soil organic matter. Thus, their distribution affects how long the assimilated C will remain in the ecosystem before returning to the atmosphere by root and microbial respiration (Carbone and Trumbore, 2007). Above- and below-ground C budgets and C allocation within the plant–soil-system of the Tibetan Plateau estimated by ¹³CO₂ labeling have been presented by Wu et al. (2010), Hafner et al. (2012) and Unteregelsbacher et al. (2011), but only from the northeast part of the Plateau in about 3000 m a.s.l.

Furthermore, each of the two methods, EC measurements and CO₂ pulse labeling, has its shortcomings. EC measurements do not reveal C fluxes within single compartments of the ecosystem (Leclerc and Foken, 2014). ¹³CO₂ pulse labeling only provides a relative distribution of assimilates, yet mass units and absolute fluxes are important in in situ studies related to C balance and turnover (Kuzyakov and Domanski, 2000). To close this gap, we apply a new approach proposed by Riederer (2014). We couple the relative distribution of photoassimilates, derived from a ¹³CO₂ pulse labeling experiment, with the ecosystem C uptake, derived from EC measurements. Thereby, we can determine the absolute fluxes of assimilates into the different plant and soil compartments of the ecosystem.

We chose our study site taking into account the general lack of in situ measurements of C cycling, especially in the core distribution of the *K. pygmaea* ecosystem at high altitudes (>4000 m a.s.l.). We consequently coupled EC measurements and ¹³CO₂ labeling to characterize the C allocation and turnover and to understand the role of the turf layer in terms of C storage and cycling. Furthermore, we investigated if grazing cessation affects C fluxes and stocks of alpine *K. pygmaea* pastures already within the first growing season after cessation. We expect that short-term effects of grazing cessation would quickly express in the allocation of recent assimilates and later on in above- and belowground C stocks.

2. Material and methods

2.1. Study site

Our study site is located on the Tibetan Plateau at 4410 m a.s.l. adjacent to the village Kema and the “*Naqu Ecological and Environmental Observation and Research Station*” (92°06' E, 31°16' N; established in 2007 as “*K. pygmaea Research Station Kema*” by the Marburg University and the Tibet University Lhasa with support of the Volkswagen foundation and since 2011 operated by the Institute of Tibetan Plateau Research, Chinese Academy of Sciences, Beijing).

The site itself is a typical alpine *Kobresia* pasture on a gentle slope, covered with *K. pygmaea* (Cyperaceae), accompanied by other graminoids (*Carex* spp., *Festuca* spp., *Kobresia pusilla*, *Poa* spp., *Stipa purpurea*) and to a minor degree by small rosette plants and cushion

plants. Thus, the site is representing one of the most common and important vegetation types on this ecosystem (Miehe et al., 2008b). The average vegetation height at the grazed plots of less than 2 cm is typical for the golf course-like *Kobresia* mats (Miehe et al., 2008b), and the characteristic turf layer has an approximate thickness of 7 cm overlying soils classified as stagnic Cambisols (humic, eutric) (Table 1, IUSS-ISRIC-FAO, 2006). The specific turf mats of *K. pygmaea* grasslands are designated as Afe horizons according to Kaiser et al. (2007) and Kaiser et al. (2008) throughout this study. Most of the pasture (65%) is covered by dense vegetation and an intact turf layer. 16% of the surface is covered by turf patches with crusts of lichens and algae, and only few grass bunches and cushion plants or rosettes turf (Unteregelsbacher et al., 2011). The remaining 19% of the surface is bare soil, with only few plants occurring and the characteristic turf layer missing. The distribution of the surfaces was surveyed in 2012 (Biermann et al., 2013). Grazing with a stocking rate of about 2.5 yaks per hectare is restricted to one month in winter or spring due to a governmental pasture health program started in 2006.

The nearest weather station of the Chinese weather service in Naqu (4507 m a.s.l.) recorded for the period 1971–2000 an annual precipitation of 430 mm as well as a mean maximum temperature for the warmest month of 15.6 °C and an annual average temperature of −0.9 °C (<http://www.weather.com.cn>). Precipitation falls mainly as rain during the summer months from May to August, but heavy snow events can occur in winter and spring. In contrast to the typical pattern, the spring and summer month in 2010 were comparably dry with only 40 mm of precipitation recorded at the study site in July.

2.2. Grazing treatments

At the research site a pasture area of 100 × 250 m was fenced in 2009, excluding grazing livestock such as yak, sheep and goat. In addition, four subplots (15 × 15 m) were established inside the livestock enclosure to additionally exclude the only surviving wild herbivore, an endemic small soil-dwelling mammal, the Plateau Pika (*Ochotona curzoniae*).

All three grazing treatments were investigated within the labeling experiment: normal grazing (G), a partial enclosure, with exclusion of livestock but allowing for grazing by Pikas (P) and ungrazed plots (U), with exclusion of livestock and pikas. EC measurements were only possible over G and P, but not over U, because maintaining an enclosure of pikas of the size necessary for EC measurements was not possible. Thus, effects of livestock grazing correspond to the difference between G and P, whereas the combined grazing effects of livestock and pikas are reflected by the difference between U and G.

During the experimental period from June to August 2010 the pasture was stocked with 2.5 yaks per hectare additionally to the governmental management, which is within the range of stocking rates applied in the Naqu prefecture (from 0.1 to 3.4 yaks per hectare; Wei and Chen (2001)) However, most of this stocking is beyond the carrying capacity and thus pastures in this region are overgrazed (Wei and Chen, 2001).

Table 1

Horizons and texture of the stagnic Cambisol (humic, eutric) according to WRB (IUSS-ISRIC-FAO, 2006). The turf mat is designated as Afe following Kaiser et al. (2008) (Suffix fe from felty according to Kaiser (2004)).

Horizon	Depth [cm]	Texture	Description
Afe	0–7	Ls2	Felty <i>Kobresia pygmaea</i> turf mats consisting of woody roots
Ah1	7–15	Ls3	<i>K. pygmaea</i> turf mats with decreasing root density and woody roots
Ah2	15–23	Ls3	Accumulation of organic carbon in mineral soil
Sg-Bw	23–49	Tl	Redoximorphic features, carbonate content 0.003%
Ck	>49		Diffuse CaCO ₃

2.3. Eddy-covariance measurements

2.3.1. Data acquisition

Turbulent atmospheric fluxes, additional energy balance components and meteorological parameters were measured from 8 June to 2 August 2010, inside (EC-P) and outside (EC-G) the livestock enclosure. Eddy-covariance fluxes were determined with an ultrasonic anemometer (CSAT3, Campbell Sci. Inc.) and an open path infrared gas analyzer (IRGA, LicOR 7500, LicOR Bioscience Inc.). Further energy balance components were estimated with a net radiometer (CNR1, Kipp & Zonen) and soil temperature profiles beneath bare soil, grazed and ungrazed *Kobresia* mats. Meteorological reference data was also measured on site (HMP45, & PTB210, Vaisala; rain gauge, Ott). Detailed setup information is given in Table A1 or by Biermann and Leipold (2011).

2.3.2. Post processing

The turbulent fluxes, averaged for 30 min, were calculated from the high frequency raw data with the well-tested software package TK3 (Department of Micrometeorology, University of Bayreuth; Mauder and Foken, 2011). Furthermore a footprint analysis was performed to ensure representativeness of the measurements (Göckede et al., 2006). It showed that the source areas for both eddy-covariance stations were dominated by *K. pygmaea* mats. Furthermore, towers were separated far enough so that the measurements can be considered to be independent from each other and can be attributed to either G or P. This analysis also ensures the comparability between the ¹³CO₂ pulse labeling experiment and the EC measurements, as recommended in Reth et al. (2005). Since heterogeneity within the roughness or thermal properties of the underlying surface might result in large-scale turbulent structures not measured with EC, gaps can be found in the energy balance closure (EBC) (Foken, 2008b). Investigation of the EBC for the 2010 experiment at Kema showed that 73% of the energy balance is closed for observations from EC-G and EC-P. The here presented NEE measurements are not corrected for this missing energy in the turbulent exchange as it is not applicable (Foken et al., 2011) while it is a standard procedure for the latent and sensible heat flux. Due to malfunction of the measurement devices or the above-mentioned quality assessment and consequent rejection of data with poor quality, gaps are found within the time series of turbulent fluxes and C exchange measurements. To ensure a continuous time series of NEE, which is necessary for the estimation of C budgets, the data gaps were filled with a widely used technique as described in Ruppert et al. (2007) and Appendix A3.

2.4. ¹³CO₂ pulse labeling

2.4.1. Experimental setup and sampling

The ¹³CO₂ pulse labeling was conducted on the 1st of July 2010 (for details on selection of this date see 3.1) with four replicates of each of the three treatments (G, P, U), grouped in four blocks (in detail described in Biermann and Leipold (2011)). The labeling procedure itself is presented in detail in Appendix B1 and by Hafner et al. (2012).

The ¹³C was chased in the plant–soil–atmosphere system over a period of two months with increasing sampling intervals (0, 1, 4, 8, 15, 23, 29, 36, 48 and 64 days after the labeling). The first sampling (0) was conducted immediately after the labeling. The following pools were sampled: plant shoots, roots and soil organic matter in two layers (0–5 cm and 5–15 cm) and soil CO₂ efflux. Shoots were sampled by clipping and belowground pools were sampled with a soil corer. Total belowground CO₂ efflux and its δ¹³C signature were measured with the static alkali absorption method (Hafner et al., 2012; Lundegardh, 1921; Singh and Gupta, 1977). We are aware that this method is often described as inaccurate for the determination of the soil CO₂ efflux. However, it has been shown that this method can give reasonable

estimates for sufficiently long deployment times (Rochette and Hutchinson, 2005). It was the only means at this remote location of obtaining measurements of soil CO₂ efflux and its isotopic signature. The sampling is described in detail in Appendix B2.

2.4.2. Data analysis

To investigate the C distribution in the ecosystem and to compare C sequestration in the grazing treatments, C stocks (Mg C ha⁻¹) of the plant and soil pools were calculated on the basis of the pool mass and the C content determined by the IRMS (Appendices B2, B3).

The distribution of photoassimilates in the system is calculated based on the enrichment of ¹³C in each sample achieved by the ¹³CO₂ pulse labeling. Briefly, this enrichment can be calculated as a product of the increment of ¹³C (¹³C_{t atom%excess}) and the amount of C in the corresponding pool at a specific time after the labeling. For an inter-comparison between different plots all amounts of recovered ¹³C in a pool at a given sampling time are expressed as percentage of the reference recovery. The reference recovery is defined for each plot, as the sum of all excess ¹³C recovered in shoots, roots and soil organic carbon (SOC) at the first sampling, directly after opening the labeling chamber. The details of the calculation are given in Hafner et al. (2012) and Appendix B3. The figures and tables present means and standard errors of the mean (SEM).

Soil respiration measurements were distorted by the admixture of atmospheric CO₂ in the traps, which became apparent from a shifting towards higher values of the δ¹³C signature of the non-enriched reference measurements of soil respiration. Therefore, Keeling Plots (Keeling, 1961) were used to account for this admixture and to obtain the natural abundance isotope signature of the soil CO₂ efflux.

2.5. Coupling of eddy-covariance flux measurements and ¹³CO₂ labeling

The ¹³CO₂ pulse labeling reveals the relative fraction of recently assimilated C that is transported into various pools of the plant–soil system after a given time. The EC technique measures absolute values of C fluxes on ecosystem scale. By coupling these two techniques, we assume that the fraction of recovered ¹³C in a specific pool after a defined allocation period represents the ratio between the flux into this pool and the overall assimilation. Therefore, we use the following equation, adapted from Riederer (2014) to estimate absolute fluxes into the different pools within the ecosystem for the defined allocation period:

$$F(C)_i = R(^{13}C)_i * \overline{GPP}_{daily} \quad (1)$$

with $F(C)_i$ being the absolute flux into a specific pool i , $R(^{13}C)_i$ the fraction of recovered ¹³C within pool i at the end of the defined allocation period and \overline{GPP}_{daily} being the mean daily assimilation estimated with EC during the allocation period.

Although this approach is simple, it is essential that meteorological conditions and assimilation on ecosystem scale don't vary strongly since this would affect the transport of C within the plant–soil system, needs to be stable throughout the allocation period of the ¹³C. Furthermore, it is difficult to estimate the length of this allocation period, which should not be confused with the end of the chase period. However, this period is critical for the interpretation of the distribution of the assimilated tracer (Wang et al., 2007). Allocation of ¹³C to various pools in the plant–soil system is considered to be complete when the metabolic plant components are depleted of ¹³C (Saggar et al., 1997). This point is difficult to identify, but numerous studies report that allocation is finished within 3–4 weeks (Hafner et al., 2012; Keith et al., 1986; Riederer, 2014; Swinnen et al., 1994; Wu et al., 2010).

3. Results

3.1. Carbon exchange on ecosystem scale

The observed matter and energy fluxes observed by the EC stations as well as temperature, humidity and precipitation measurements for the period 9 June to 2 August (Fig. 1) enable us to characterize the overall exchange conditions between the *K. pygmaea* ecosystem and the atmosphere. In general, the dynamics of the C fluxes measured at both EC stations were very similar. When averaged over the whole period, the NEE resembled a weak sink for both stations (Table 2). However, the observations can be divided into three periods with different characteristics. At the beginning of the observation period, the NEE did not show a clear daily cycle with mainly respiration and only weak assimilation. Starting from 24 June assimilation increased which resulted in a negative NEE during the day, leading to the decline of the cumulated NEE after this date. This can be explained by onset of rain, rise in soil water content and a rise in air temperature in June. For a period that lasted until 24 July fluxes showed a constant behavior. After 24 July till the end of the EC measurements the NEE was again characterized by a weaker assimilation during overall drier conditions. This was also apparent in the ratio between the sensible and latent heat flux, the Bowen ratio, for these periods, which was greater than one, since the sensible heat flux dominated over the latent heat flux (data not shown). Based on the in situ calculated fluxes and the so gained knowledge about the C dynamic, the start of the ¹³CO₂ pulse labeling experiment was scheduled on 1 July.

A comparison of the measured NEE fluxes from the two stations using the geometric mean regression (Dunn, 2004) – the method of choice to account for random errors in both time series – shows only a 3% difference. This small difference in mean NEE measurements on ecosystem scale cannot be considered as relevant and, additionally, cannot be attributed to any differences in grazing. Rather, existing differences between individual half-hour values of the two EC stations were related to differences in the distribution of vegetation and bare soil within the actual footprint of these flux estimates, or free convection events which were not captured with the EC measurements. This also propagated into the cumulated and mean daily fluxes (Fig. 1) and explained the small divergence within the dynamics of the fluxes from the two sites.

3.2. Carbon distribution within the ecosystem

Averaged over all grazing treatments, the total C stored aboveground and in the upper 15 cm of the soil made up 76.1 ± 1.6 Mg C ha⁻¹. The aboveground biomass had only a very marginal contribution (~0.6%) to the overall C stocks whereas equal C amounts (ca. 50%) were stored in roots and soil organic carbon (SOC) of the upper 15 cm (Fig. 2a). The mean root:shoot (R:S) ratio was 90.

The grazing treatment had a significant effect on the C stocks of the shoots ($F_{2,59} = 4.81$, $p_{adj} = 0.046$). The post-hoc test revealed that the shoot C of the livestock enclosure (P) was significantly lower than that of the ungrazed (U) treatment (difference 0.11 ± 0.03 Mg ha⁻¹, $z = -3.096$, $p_{adj} = 0.03$). The grazing treatment had no effect on belowground C stocks or the R:S ratio.

3.3. Dynamics of assimilate allocation

Tracing the distribution of ¹³C in the plant–soil–atmosphere system over the course of the chase period allowed assessment of the dynamics of allocation of recent assimilates. In general, the grazing treatments did not reveal any difference in the recovery of ¹³C in the C pools. The total uptake of ¹³C during the labeling was not differing between treatments. On average, the total ¹³C recovered right after the labeling was 0.54 ± 0.02 g ¹³C m⁻². Additionally, the overall tracer dynamics in the different investigated pools were very similar between the treatments. The data was therefore pooled for further analysis to increase sample size.

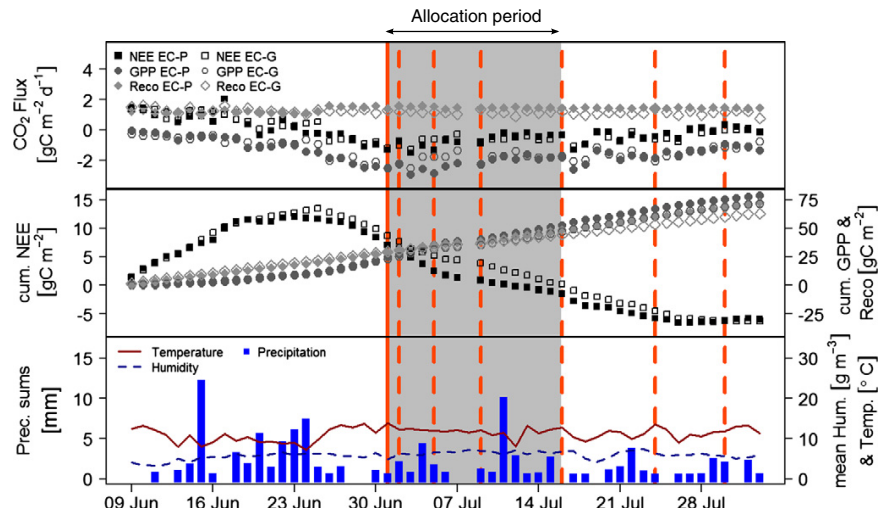


Fig. 1. CO₂ fluxes from 9 June to 2 August 2010 including the EC measured Net ecosystem exchange (NEE, black square) as well as the partitioned fluxes; gross primary production (GPP, dark grey circle) and total ecosystem respiration (Reco, light grey diamond). Closed symbols represent the partially grazed site EC-P and open symbols represent the grazed site EC-G. The upper panel shows daily mean values and the middle panel shows the cumulated C-fluxes. Additionally, the lower panel shows sums of daily precipitation (blue bars), mean daily temperature (dark red line) and humidity (dark blue dashed line) characterizing the weather conditions for the duration of the labeling experiment. The ¹³C labeling event on 1 July is marked by the vertical red line; ¹³C sampling dates are indicated by vertical dashed red lines, the estimated allocation period by the grey shaded area.

In all pools, ¹³C was significantly enriched after the labeling compared to its natural abundance, except for the SOC 5–15 cm. In this pool the ¹³C_{atexcess} was solely significantly different from zero for the first two samplings and days 36 and 64 after the labeling.

The percentage of recovered ¹³C in the shoots decreased rapidly within the first days after the labeling and stabilized below 10% of recovered ¹³C after 4 days (Fig. 3a). Afterwards the ¹³C recovery in the shoots did not change significantly anymore.

The ¹³C recovery in the CO₂ efflux from soil reflects root respiration and the belowground mineralization of recent assimilates. The highest rate of ¹³C efflux in the belowground CO₂ efflux was detected within the first 24 h after the labeling (Fig. 3b). Afterwards, the contribution of ¹³C to the CO₂ efflux declined rapidly. The decline can be described by the sum of two exponential functions. This provides turnover rates for two metabolic stages, one for root respiration and a rapid use of rhizodeposits by microorganisms (TR₁ = 0.66 ± 0.08 days⁻¹) and a second, slower, stage of utilization of transformation products and dying roots (TR₂ = 0.05 ± 0.02 days⁻¹). This corresponds to mean residence times (MRT) of 1.5 days (MRT₁) and 20 days (MRT₂). Due to the uniform behavior of the efflux from the three grazing treatments it can be stated that, on average, 36.8 ± 1.4% of recovered ¹³C was released as belowground CO₂ efflux during two months.

The majority of the ¹³C (58%) was already allocated belowground at the first sampling immediately after the labeling (day 0, roughly 4 h after the start of the ¹³CO₂ labeling), which reflected a fast allocation

of assimilates to belowground pools. Most assimilates were recovered in roots of the layer 0–5 cm (Fig. 4a). Recovered ¹³C peaked 15 days after the labeling and declined during the second half of the chase period between several sampling steps. The ¹³C dynamic in the SOC of both layers was very low. In the soil of the upper layer, ¹³C incorporation increased during the chase period (Fig. 4c). This increase of ¹³C in SOC corresponded to the ¹³C decline in the roots (Fig. 4a, b), reflecting their transformation to SOC. No clear trend could be obtained for the soil of 5–15 cm (Fig. 4d), because the mean ¹³C enrichment was not significantly higher than in the unlabeled soil at several sampling times.

3.4. Absolute fluxes within the *K. pygmaea* ecosystem

Absolute C fluxes within the plant–soil–atmosphere continuum were calculated according to Eq. (1) using the relative distribution of ¹³C at the end of the allocation period and the mean daily GPP of this period derived from a partitioning of the NEE measured with EC. The end of the allocation period is defined as the time when ¹³C in the roots of the top layer reached a maximum, in our case 15 days after the labeling (Fig. 4a). The C fluxes estimated with the EC showed a fairly strong and constant assimilation during this period. Weather conditions were also quite stable with no relevant changes in temperature or available moisture between the days (Fig. 1). The relative distribution of assimilates as well as the resulting absolute fluxes derived from the coupling, are presented for each pool in Fig. 2b. It is clearly visible that most of the

Table 2

Mean daily CO₂ fluxes and standard errors measured at the EC Stations P and G, estimated for the whole period and the main vegetation period in July as well as the allocation period and the labeling day of the CO₂ labeling experiment.

Station	Flux [gC m ⁻² d ⁻¹]	Observation period 8 Jun–2 Aug 10	Constant flux period 24 Jun–24 Jul 10	Allocation period 1 Jul–16 Jul 10	Labeling day 1 Jul 10
EC-P	NEE	-0.12 ± 0.09	-0.66 ± 0.01	-0.71 ± 0.10	-1.24
	GPP	-1.51 ± 0.10	-2.1 ± 0.01	-2.18 ± 0.10	-2.52
	Reco	1.38 ± 0.02	1.48 ± 0.00	1.47 ± 0.02	1.32
EC-G	NEE	-0.12 ± 0.09	-0.65 ± 0.01	-0.68 ± 0.08	-1.22
	GPP	-1.37 ± 0.08	-1.84 ± 0.01	-1.87 ± 0.10	-2.53
	Reco	1.19 ± 0.02	1.15 ± 0.00	1.16 ± 0.03	1.30
Mean both	NEE	-0.12 ± 0.09	-0.65 ± 0.01	-0.69 ± 0.09	-1.23
	GPP	-1.44 ± 0.09	-1.97 ± 0.01	-2.02 ± 0.10	-2.53
	Reco	1.28 ± 0.02	1.32 ± 0.00	1.32 ± 0.03	1.31

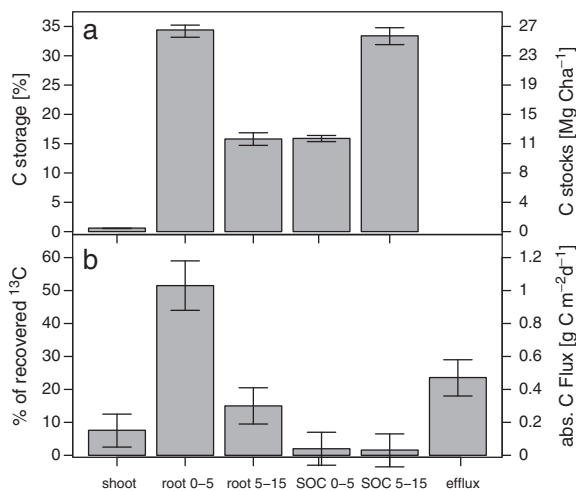


Fig. 1. (a) Relative distribution and absolute C stocks within the different compartments of the system. (b) Partitioning of assimilates (as % of recovered ¹³C) at the end of the allocation period (15 days after the labeling) and the corresponding mean daily fluxes of C into the different C pools, based on the combination of eddy covariance measurement and pulse labeling.

assimilates were recovered within the roots of the first 5 cm resulting in an absolute flux of recent assimilates of $1.04 \text{ g C m}^{-2} \text{ d}^{-1}$ into this pool during this period of the growing season. The belowground CO_2 efflux represented the second largest flux with $0.48 \text{ g C m}^{-2} \text{ d}^{-1}$ while the flux of recent assimilates into aboveground biomass only accounted for $0.15 \text{ g C m}^{-2} \text{ d}^{-1}$.

4. Discussion

4.1. Grazing effects on C fluxes and C budget

One of the aims of our study was to test whether grazing cessation already affected C fluxes and stocks of the alpine *K. pygmaea* ecosystem within the first growing season after grazing cessation. Therefore, we

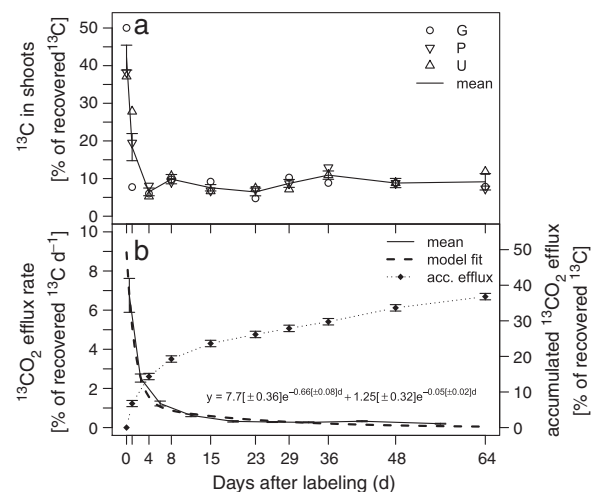


Fig. 3. (a) Dynamic of ¹³C (\pm SEM) in the shoots, (b) mean ¹³CO₂ efflux-rates (\pm SEM) from soil with a fitted biexponential model and accumulated amount of ¹³CO₂ efflux (\pm SEM) during the chase period. The model fit is given by the formula. Open symbols indicate mean values of the different grazing treatments.

investigated ecosystem C fluxes, C allocation in the plant–soil–system and C stocks of this ecosystem in a grazing experiment. As grazing has been shown to affect belowground C allocation on a short time scale for several grassland species (Bardgett et al., 1998; Holland et al., 1996; Kuzyakov et al., 2002; Paterson and Sim, 2000; Schmitt et al., 2013) we expected that short-term effects of grazing would quickly express in the allocation of recent assimilates.

However, only the aboveground C stocks were affected by grazing cessation. It is intuitive that aboveground grazing affects the aboveground biomass. However, it is remarkable, that neither the allocation of recent assimilates nor the NEE on ecosystem scale were affected. This suggests that grazing cessation did not influence the C cycling, at least during the first half of the first growing season after grazing cessation. The very large R:S ratio of our study site (R:S = 90) is even higher than in other studies conducted in the alpine pastures of the Tibetan Plateau (52, Fan et al. (2008; 35.7), Yang et al. (2009)). It is conceivable that the high belowground biomass enables *K. pygmaea* to buffer aboveground effects of grazing in terms of C cycling, thus making the ecosystem resistant against short-term changes in the grazing regime. This emphasizes the importance of belowground plant compartments in this ecosystem and the need to increase knowledge of belowground C cycling of this extraordinary grassland ecosystem.

The lowest aboveground biomass was not found in the full grazing treatment (G), but in the livestock enclosure (P), where only small mammals – mainly pika – were grazing. We assume that pikas were attracted by the fenced area, due to fewer disturbances by livestock and herders, which increases overall pika density. This might actually have resulted in an overall higher grazing pressure on the livestock enclosure. We cannot verify this, because we lack data of pika density on the study site during the season of our experiment. But high pika density has been shown to negatively affect aboveground biomass (Liu et al., 2013). Additionally, pikas can graze vegetation completely down to the turf surface due to their smaller body size and more suitable teeth (Retzer, 2007).

We found no effects of grazing cessation on belowground C stocks. After several years of grazing enclosure Hafner et al. (2012) observed a decrease of belowground C stocks in a *Kobresia humilis* grassland (~3000 m a.s.l.) in the northeastern highlands. However, due to the large size of the belowground C stocks and the low productivity of these alpine ecosystems, such changes in the C stocks can rather be expected to be a long-term effect of grazing on the scale of years.

Unfortunately, we were not able to conduct EC measurements over the whole growing season due to logistical restrictions. Therefore, we were not able to test, if the grazing treatments started to affect ecosystem C exchange later in the growing season. Additionally, it was not possible to measure C fluxes on the ungrazed site (U) with EC, because maintaining a suitable area free of pikas is not feasible. Thus, the influence of the pika grazing on ecosystem scale remains uninvestigated in this study.

4.2. Distribution of C within *K. pygmaea* pastures

In the following section we discuss the C distribution within the plant–soil–atmosphere continuum of an alpine *K. pygmaea* pasture ecosystem for the main vegetation period in summer 2010. We present the relative distribution of C within the compartments of the ecosystem revealed by a ¹³CO₂ pulse labeling experiment. Furthermore, we are able to present absolute estimates of these fluxes through the relatively new combination of labeling results and EC flux measurements (Riederer, 2014). For the better introduction of the new approach, we will start out with general remarks and explanations. Absolute fluxes were estimated by the pooled data from the ¹³CO₂ pulse labeling experiment and a mean daily GPP value was estimated from both EC measurements for the allocation period. Due to lack of differences between the grazing treatments, the discussion will be grazing-independent.

Partitioning patterns of assimilates can vary greatly depending on the climatic conditions (Meharg and Killham, 1989; Palta and Gregory, 1997)

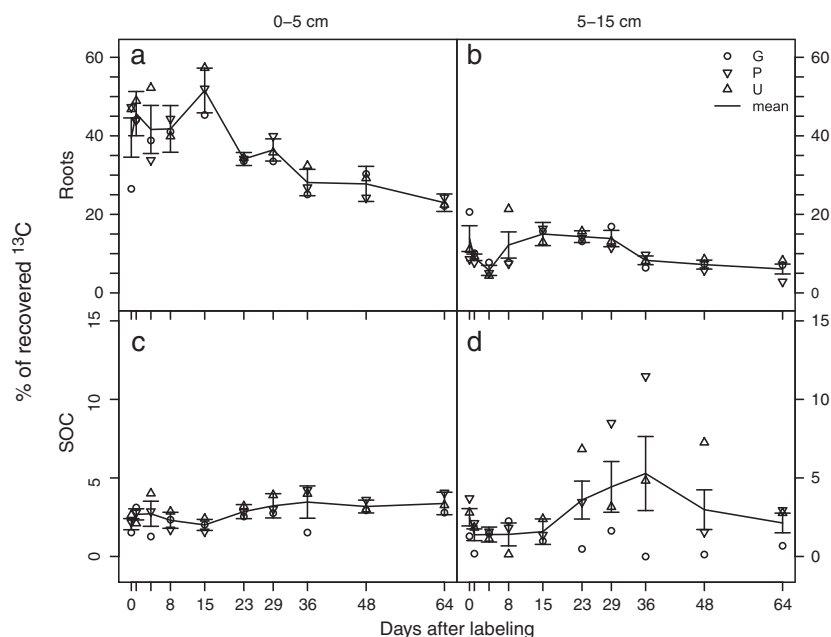


Fig. 4. Dynamic of recovered ^{13}C in roots and SOC in the two soil layers (\pm SEM, solid line) in (a) roots 0–5 cm (b) roots 5–15 cm, (c) SOM 0–5 cm, (d) SOM 5–15 cm). Open symbols indicate mean values of the different grazing treatments.

and change over the course of the growing season (Swinnen et al., 1994). This usually makes it impossible to extrapolate the partitioning of a single ^{13}C pulse labeling to the whole growth period (Kuzuyakov and Domanski, 2000; Swinnen et al., 1994). Therefore, extrapolating partitioning patterns and fluxes over a longer period needs to be done with caution. The EC measurements provide a valuable constraint to judge whether C fluxes undergo strong changes within the allocation period. The labeling experiment was conducted in a period with a strong assimilation signal and overall constant fluxes (Fig. 1), which was only possible to identify through the simultaneous EC measurements and represents a great advantage of the new coupling approach. We therefore considered partitioning from the labeling experiment to be representative for the whole allocation period, since EC data showed constant C fluxes and comparable weather conditions (Fig. 1).

During the two months experiment the alpine *K. pygmaea* pasture acted as a weak C sink with a mean NEE of $-0.1 \text{ g C m}^{-2} \text{ d}^{-1}$. The estimated mean ecosystem assimilation of $1.36 \pm 0.09 \text{ g C m}^{-2} \text{ d}^{-1}$ is in good agreement with values from another study over alpine *Kobresia* pastures in about 4000 m a.s.l. (Fu et al., 2009). However, it is roughly $1\text{--}2 \text{ g C m}^{-2} \text{ d}^{-1}$ smaller than the values from studies over montane *K. humilis* pastures at altitudes lower than 4000 m a.s.l. (e.g. Hirota et al., 2009; Kato et al., 2004, 2006; Zhao et al., 2006).

In the investigated alpine *K. pygmaea* ecosystem, the majority of assimilated C was allocated into belowground pools (Fig. 2b). This was reflected in the rapid decline of recovered ^{13}C in the shoots during the first days after labeling (Fig. 3). Leake et al. (2006) report ^{13}C losses in shoots of 32–70% in upland grassland within one day. Wu et al. (2010) observed a decline of fixed C in the shoots of 36.7% within 24 h after the labeling in a secondary *K. humilis* pasture (3250 m a.s.l.) in the northeastern highlands on the QTP. The slower decline of ^{13}C in shoots of a *Kobresia* pasture shown by Hafner et al. (2012) is associated with their definition of the reference recovery and differences in the vegetation itself. In contrast to our study, they relate the recovered ^{13}C to the amount of ^{13}C found one day after the labeling.

The shoot respiration, however, was of minor importance for the decline due to the small aboveground biomass and the high R:S ratio of the

Kobresia ecosystem. The photoassimilates remaining in the shoots were likely incorporated into structural shoot tissue. However, this remains speculative, because we do not have compound specific measurements of ^{13}C incorporation.

The total ^{13}C recovered belowground and in soil CO_2 efflux after 15 days accounts for 93.7% of recovered ^{13}C . According to the EC fluxes it corresponds to $1.87 \text{ g C m}^{-2} \text{ d}^{-1}$. This is more than the 59% reported for *K. humilis* pasture (Wu et al., 2010) and the observed 40% for a *Kobresia* pasture (Hafner et al., 2012). This emphasizes the importance of belowground C allocation and cycling in these alpine *K. pygmaea* pastures. In our study, 23.6% of the $^{13}\text{CO}_2$ allocated belowground was recovered in CO_2 efflux from soil (root exudates and root-derived CO_2), which is in good accordance with values reviewed by Kuzuyakov and Domanski (2000). The roots acted as the largest sink of ^{13}C in the system (Fig. 2). This high incorporation of assimilates can be related to the very large rooting system maintained by the perennial plant *K. pygmaea* as adaptation to trampling and grazing (Miehe et al., 2008b).

The high ^{13}C recovery in roots and the low recovery in SOC are in contrast to the results observed for a montane *Kobresia* pastures in Qinghai by Hafner et al. (2012), who report only minor ^{13}C allocation into roots, but already very high amounts in the SOC one day after the labeling. Their ^{13}C pulse labeling was conducted later in the growing season. They argue that the rooting system was already developed and assimilates were invested mainly aboveground in vegetative and generative organs and shoot tissue and belowground into root exudation. In our study assimilates were mainly invested into the build-up of roots, leading to a longer turnover time of this C to become SOC. This might not only be an effect of the growing season, but could additionally be a response of the plant to the relatively dry growing season. However, we lack data from other years to estimate effects of this dry season.

In general, belowground pools have the largest contribution to C turnover within *K. pygmaea* pastures. The roots within the turf layer acted as the greatest sink for recently assimilated C, which is in good agreement with Fan et al. (2008) who found the highest C density in

the uppermost centimeter of alpine soils on the southeastern highlands. For the allocation period of the ^{13}C labeling experiment, which was also the period with the greatest C uptake during the observation period, this sums up to 28 g C m^{-2} . The further fate of these assimilates, e.g. their turnover in the roots or a possible incorporation into SOC, is of major importance to understand the role of recent assimilates for the overall C sequestration within this ecosystem.

4.3. Rapid turnover of assimilates in the root turf

Tracing ^{13}C of the pulse labeling in the soil CO_2 efflux gives valuable information about belowground metabolism and turnover of recent assimilates (Unteregelsbacher et al., 2011). By following the ^{13}C incorporation in roots and SOC we gain an overall picture of the role of the root turf for the fate and turnover of assimilates in this ecosystem.

During the first days after the labeling the recovery of tracer in soil CO_2 efflux was high, which was associated with root and rhizomicrobial respiration of assimilates. Its MRT of 1.5 days is well in accordance with (Kuzyakov, 2006), who reports that in grasses a maximum of 1–2 days is necessary for most of the C allocated to root respiration to return to the atmosphere as CO_2 .

After approximately two weeks, the amount of tracer recovered in roots peaked (Fig. 4a,b). In contrast to other pulse labeling studies on the northeastern highlands of the Tibetan Plateau (Hafner et al., 2012; Wu et al., 2010), the long chase period and the high number of replicates after pooling the grazing treatments allows us to follow tracer dynamics precisely over a time scale of several weeks. The decline after two weeks was accompanied by a simultaneous slight but steady $^{13}\text{CO}_2$ efflux from soil (Fig. 3). This might partly be caused by metabolic turnover of assimilates from storage pools. Lehmeier et al. (2008) showed that stores play a central role for respiratory C metabolism, but also that these stores are quite short lived. Additionally, we also observed an increase in the recovery of ^{13}C in SOC (Fig. 4c). This suggests that labeled root material, i.e., roots that had been built up by recent assimilates, started to be decomposed, which contributed to soil CO_2 efflux, and partly transformed to soil organic matter. The mean residence time of recently assimilated C in these *Kobresia* roots is approximately 20 days, as described by the slower decay rate of the biexponential decline fitted to the CO_2 efflux rate (Fig. 3b). Thus, a subset of roots in the root turf, probably fine roots, had a rapid turnover, as it has also been reported by Wu et al. (2011) for a *K. humilis* pasture of the northeastern highlands and others for forest and grassland ecosystems (Gill et al., 2002; Hendrick and Pregitzer, 1993). Roots that become lignified have a much longer lifespan, which we can't estimate with our two months study.

The decomposition of fine roots partially leads to a stabilization of root C in SOC due to the chemical recalcitrance of root compounds (Rasse et al., 2005), however, this will be of minor importance for these fine roots, which are poor in lignin and suberin. The two other mechanisms important in temperate ecosystems (physico-chemical protection through interaction with minerals and physical protection from decomposition by aggregation) are of minor importance in *Kobresia* ecosystems. Interaction with minerals is hardly possible because most of the Ah horizon consists of dead roots, and the minerals are mainly quartz crystals of a medium and large silt size without any relevant sorption places. The further common mechanism—protection by aggregation, is also of minor importance because the aggregate structure is not well presented in these soils. Therefore, C stabilization mechanisms (cold temperatures and short period of microbial activity) in soils under *Kobresia* root mats may be different from that under temperate grasslands.

5. Conclusions

By combining two commonly used methods, pulse labeling and EC, we present a new and more powerful approach to understand C cycling in the plant–soil–atmosphere system compared to singular plot- or ecosystem scale approaches. It enabled us to estimate absolute C fluxes into

various pools of the *K. pygmaea* pastures and to identify C dynamics on various spatial scales.

Within the first growing season after grazing cessation we observed effects on aboveground C stocks of the alpine *K. pygmaea* pasture, whereas recent C fluxes were not influenced. This was shown for the partitioning and turnover of recently assimilated C on plot scale as well as the overall C budget at ecosystem scale by combining $^{13}\text{CO}_2$ pulse labeling with eddy-covariance flux measurements. We conclude that the high belowground biomass, expressed in the very large R:S ratio of 90, enables *K. pygmaea* to buffer aboveground effects of short term changes in the grazing regime.

The *K. pygmaea* root turf makes up roughly 50% of the overall C stocks. However, besides its huge size in terms of relative as well as absolute C storage, it is a highly dynamic component of the C cycle in this ecosystem. A more detailed investigation of C fluxes identified the root turf as major sink for recent assimilates. Our study showed that a subset of roots is highly dynamic, with a mean residence time of 20 days. Carbon input into the soil is controlled by root turnover and not rhizodeposition.

Overall, we conclude that the living roots of the turf layer represent the most active part in terms of C cycling and play a key role in the turnover of recent assimilates. As the turf stores a very high amount of C its destruction through environmental or anthropogenic factors, e.g. overgrazing-induced degradation or changes of vegetation could lead to a great release of CO_2 to the atmosphere.

This unique ecosystem requires further studies on the role of grazing, especially on longer time scales, for C stabilization and a more in-depth understanding of the development, age and structure of the turf layer as well as its protective role for the ecosystem. This knowledge is necessary in order to evaluate and mitigate the effects of climate and land use change on the Tibetan Plateau.

Acknowledgments

Supplementary data is available at <http://doi.org/10.1594/PANGAEA.833208>. This work was supported by the German Research Council (DFG) DFG Fo 226/18-1.2, DFG KU 1184/14, MI 338/7-2; WE 2601/4-2;(SPP1372) within the Priority Program 1372 “Tibetan Plateau: Formation, Climate, Ecosystems” (TiP). Access to the “*Naqu Ecological and Environmental Observation and Research Station*” was granted by the Tibet University, Lhasa and the Institute of Tibetan Plateau Research (ITP), Chinese Academy of Sciences. Furthermore, the authors would like to thank everybody who participated in the collection of the data on the Tibetan plateau. We also are thankful to the Centre for Stable Isotope Research and Analysis (KOSI) of Göttingen University and the Laboratory of Isotope Biogeochemistry of the Bayreuth Center of Ecology and Environmental Research (BayCEER) for the $\delta^{13}\text{C}$ analysis.

Table A1
Setup specification for the eddy covariance stations, EC-P and EC-G.

Measured quantity	EC-station	Device	Height [m]
Wind components	P and G	CSAT3 (Campbell Sci., Inc.)	2.20
CO_2 and H_2O Concentration	P and G	LICOR 7500 (LI-COR Biosciences)	2.20
Reference temperature and humidity	P and G	HMP45 (Vaisalla)	2.20
Precipitation	P	Tipping rain gauge	1.00
Radiation components	P and G	CNR1 (Kipp & Zonen)	2.00
Soil temperature “ <i>Kobresia</i> mat”	P and G	Pt100	−0.025, −0.075, −0.125 (−0.200 only at P)
Soil water content “ <i>Kobresia</i> mat”	P and G	TDR probes (IMKO)	P: −0.10, −0.20 G: −0.15
Soil temperature “bare soil”	Only P	Pt100	−0.025, −0.075, −0.125
Soil water content “bare soil”	Only P	TDR probes (IMKO)	−0.15

Appendix A. Eddy covariance

A1. Instrumentation EC stations

Table A1 lists the devices used at the two stations EC-P and EC-G. It describes the measured quantity, manufacturer and measurement height.

A3. Post processing of turbulent fluxes

The internationally compared software TK3 (Mauder et al., 2008) includes all necessary data correction and provides tools for the quality control of data. Therefore, calculated fluxes match up-to-date micrometeorological standards (Foken et al., 2012; Rebmann et al., 2012). Wind data was rotated according to the planar-fit rotation method considering terrain effects on the measurements (Wilczak et al., 2001). Quality of the derived fluxes is indicated with a quality-flagging scheme after Foken and Wichura (1996), accounting for development of turbulence as well as stationarity. It enables to be distinguish between data of high quality (flag 1–3), intermediate quality (flag 4–6) and poor quality (flag 7–9) (Foken et al., 2004).

The utilized footprint analysis is based on a Lagrangian stochastic forward model, providing a two dimensional representation of the contributions of source areas (Rannik et al., 2000). Nevertheless, it needs to be considered that, depending on the wind direction, the distribution of IM, DM and BS within the footprint for single half-hour values might differ from the overall distribution within the research area.

A3. Gap filling and partitioning of turbulent C fluxes

Gap filling of NEE measurements and also the partitioning of this flux in C uptake and respiration is a common procedure (e.g. Desai et al., (2008); Falge et al., (2002); Lasslop et al., (2010); Reichstein et al., (2012)). Therefore, gross primary production (GPP) was estimated with a light response function following Michaelis and Menten (1913) using in situ solar radiation measurements. This technique also enables estimation of the C uptake of the *Kobresia* pastures from the measured NEE. The approach is described in Ruppert et al. (2007) follows Falge et al. (2001):

$$GPP = \frac{aRgNEE_{sat,day}}{aRg + NEE_{sat,day}} + R_{eco,day} \quad (A1)$$

with a the initial slope of the function, the global radiation Rg , the saturated NEE rate $NEE_{sat,day}$ and the respiration rate during daytime $R_{eco,day}$.

Ecosystem respiration (R_{eco}) is parameterized from in situ measured night-time NEE and temperature measurements following Lloyd and Taylor (1994) as used in Falge et al. (2001):

$$R_{eco} = R_{eco10} e^{E_0 \left[\left(\frac{1}{283.15 - T_0} \right) - \left(\frac{1}{T - T_0} \right) \right]} \quad (A2)$$

with R_{eco10} being the respiration rate at 10 °C and E_0 the sensitivity of the respiratory fluxes at a constant T_0 .

The fitting of the parameters for GPP and R_{eco} was done with high quality data (flag 1–3) for two periods due to the strong differences in the diurnal cycle. Respiratory fluxes dominated within the first period and no daily cycle existed from 9 to 23 June, while assimilation became more dominant leading to a daily cycle in the second period from 24 June to 8 August. The NEE time series selected for intermediate data quality was gap-filled with estimated values, where missing values due to instrument failure or rejection of data due to inappropriate data quality made this necessary. The time series of GPP and R_{eco} are

entirely made up of parameterized values originating from the measured NEE.

Appendix B. ¹³CO₂ pulse labeling

B1. Labeling procedure

Chambers of the size 60 cm × 60 cm × 10 cm were erected with transparent plastic foil. The chambers were carefully sealed by burying the foil in the soil and additionally sealing with wet soil. Prior to the closing, a vial with 2 g of ¹³C enriched (99 atom-%) Na₂CO₃ dissolved in water was placed inside each chamber. The label was released into the chamber atmosphere by injecting an excess of 5 M sulphuric acid with a syringe into the vial. To facilitate a uniform distribution of the tracer inside the chamber, the chambers were agitated from time to time. The labeling started at noon; chambers were opened after 4 h of labeling.

B2. Sampling procedure

Plant shoots were cut from a small circular area (diameter 6.5 cm). Belowground samples (soil and roots) were taken with a soil corer (diameter 2.6 cm) from two layers (0–5 cm and 5–15 cm), which contain the vast majority of roots and soil organic matter. Except for the first sampling, all samples from each compartment were taken as mixed samples of two soil cores from each plot. The samples were dried at 50 °C and belowground samples were separated into roots and soil afterwards. All samples were weighed and homogenized in a ball mill prior to further analysis. To make sure that the soil samples were free of carbonates, they were decalcified with hydrochloric acid (HCl).

Total belowground CO₂ efflux and its ^{δ13}C signature were measured as follows. CO₂ originating from the soil was captured in a sodium hydroxide solution (NaOH). After clipping of the shoots an opaque aluminum chambers, with a diameter of 6.5 cm, was placed on the bare soil. A graduated beaker with a defined amount of 1 M NaOH was placed inside the chamber. The NaOH captures the CO₂ flowing out from the soil into the chamber. Clipping of the shoots is necessary to avoid the additional CO₂ originating from shoot respiration. The beakers were changed on the sampling days, and thus measured the cumulative CO₂ efflux in the periods between the sampling days. The amount of NaOH was adjusted between 20 to 30 ml according to the length of these trapping periods to ensure that NaOH was not neutralized. The amount of CO₂ captured in the NaOH in the measurement periods was quantified by titration against 0.1 M HCl to the color change of phenolphthalein (pH = 8.2). To determine the ^{δ13}C signature of the CO₂ efflux, 2 M SrCl₂ was added to precipitate the carbonate captured in the NaOH as SrCO₃. The precipitation was neutralized by repeated addition of purified water and dried afterwards.

The natural abundance of ¹³C in the different plant and soil pools, as well as of the soil CO₂ was measured by doing the identical sampling and analysis procedure on unlabeled spots at the field site. Carbon content and the ^{δ13}C signature of enriched and non-enriched (reference) samples were determined by an isotope ratio mass spectrometer coupled with an elemental analyzer at the laboratory of Isotope Biogeochemistry, Bayreuth Center of Ecology and Environmental Research (BayCEER) (IRMS: Delta Plus, Thermo Fisher Scientific, Bremen Germany; EA: NC 2500, CE Instruments, Milano, Italy) and at the Centre for Stable Isotope Research and Analysis, University of Göttingen (IRMS: Delta C, Finnigan MAT, Bremen, Germany; EA: NA1108, Fisons-Instruments, Rodano, Milano, Italy). With the exception of the samples from the first sampling, a subset of three replicates per treatment and sampling day were analyzed.

B3. Calculations

The belowground C stocks were calculated for both layers (0–5 cm, 5–15 cm):

$$C(\text{Mg ha}^{-1}) = z \cdot \rho \cdot C \quad (\text{B1})$$

where z (cm) is the thickness of each layer, ρ (g cm^{-3}) is the bulk density and C (%) is the C content.

The soil CO_2 efflux rate ($\text{mol C m}^{-2} \text{d}^{-1}$) was calculated by:

$$\text{CO}_2 \text{ efflux} = \frac{m(C)}{A \Delta t} \quad (\text{B2})$$

where $m(C)$ represents the amount of C absorbed in the trap, A is the area of the soil under the chamber and Δt is the length of the trapping period.

The enrichment of ^{13}C ($^{13}\text{C}_{\text{atom}\% \text{ excess}}$, % of total C atoms) in each sample achieved by the pulse labeling is calculated by subtracting the amount of ^{13}C in the natural abundance samples ($^{13}\text{C}_{\text{atom}\% \text{ of NA}}$, % of total C atoms) from the amount of ^{13}C in the sample ($^{13}\text{C}_{\text{atom}\% \text{ of sample}}$, % of total C atoms):

$$^{13}\text{C}_{\text{atom}\% \text{ excess}} = ^{13}\text{C}_{\text{atom}\% \text{ of sample}} - ^{13}\text{C}_{\text{atom}\% \text{ of NA}} \quad (\text{B3})$$

The amount of ^{13}C in the C pools at a specific time t after the labeling ($^{13}\text{C}_t$, g m^{-2}) is the product of the increment of ^{13}C at that time ($^{13}\text{C}_{\text{atom}\% \text{ excess}}$) and the amount of C in the corresponding pool (C_{pool} , g m^{-2}) and can be calculated as such:

$$^{13}\text{C}_t = \frac{^{13}\text{C}_{\text{atom}\% \text{ excess}}}{100} \cdot C_{\text{pool}} \quad (\text{B4})$$

To make the ^{13}C incorporation into the investigated pools comparable between the plots, the amounts of ^{13}C in a pool at time t ($^{13}\text{C}_t$) are expressed in percentage of the reference recovery at day 0 ($^{13}\text{C}_{\text{rec}}$) of the corresponding plot:

$$^{13}\text{C}_{\text{rec}} = \frac{^{13}\text{C}_t}{^{13}\text{C}_{\text{rec}}} \cdot 100\% \quad (\text{B5})$$

The reference recovery $^{13}\text{C}_{\text{rec}}$ is defined as the total amount of $^{13}\text{C}_{\text{atom}\% \text{ excess}}$ found in all investigated plant and soil C pools at the first sampling (day 0), directly after opening the labeling chamber. A time delay of 12 h was assumed between the clipping and the complete stop of metabolic processes by drying. These ^{13}C losses during the drying of soil and plant samples were corrected.

The statistical analysis was done in R 2.10.1 (R Development Core Team, 2009). To test for treatment effects in the five investigated pools we used linear mixed effect models (R-package nlme, Pinheiro et al., 2011) with 'Treatment' (U, P, G) as fixed effect and 'Block' (1–4) and 'sampling date' as random effects. To account for the multiple testing of the treatment effect in the five C pools p -values were adjusted according to Holm's procedure ($n = 5$). In case of a significant treatment effect within a C pool ($p_{\text{adj}} < 0.05$) we used a post-hoc Tukey test (R-package multcomp, Hothorn et al., (2008), p -adjustment by Holm's procedure), to test which treatments show differences in the respective pool. A non-parametric Mann–Whitney–U test was applied to evaluate differences between the grazing treatments in ^{13}C partitioning at every sampling step of the chase period. Differences in the percentage of recovered ^{13}C between time-steps were tested with the non-parametric Wilcoxon matched pair test (significance level $p = 0.05$).

References

Atlas of Tibet Plateau. Edited by the Institute of Geography, Beijing: Chinese Academy of Sciences; 1990 [237 pp. (in Chinese)].

- Aubinet M, Vesala T, Papale D, editors. Eddy covariance. Dordrecht: Springer; 2012. [438 pp.].
- Baldocchi D. Assessing the eddy covariance technique for evaluating carbon dioxide exchange rates of ecosystems: past, present and future. Glob Chang Biol 2003;9(4): 479–92. <http://dx.doi.org/10.1046/j.1365-2486.2003.00629.x>.
- Bardgett RD, Wardle DA. Herbivore-mediated linkages between aboveground and below-ground communities. Ecology 2003;84(9):2258–68. <http://dx.doi.org/10.1890/02-0274>.
- Bardgett RD, Wardle DA, Yeates GW. Linking above-ground and below-ground interactions: how plant responses to foliar herbivory influence soil organisms. Soil Biol Biochem 1998;30(14):1867–78. [http://dx.doi.org/10.1016/S0038-0717\(98\)00069-8](http://dx.doi.org/10.1016/S0038-0717(98)00069-8).
- Biermann T, Leipold T. Tibet Plateau atmosphere-ecology-glaciology cluster joint Kobresia Ecosystem experiment: documentation of the first Intensive Observation Period Summer 2010 in Kema, Tibet, Arbeitsergebn. Bayreuth: Univ. Bayreuth Abt. Mikrometeorol; 2011 [ISSN 1614-89166, 44, 107 pp.].
- Biermann T, Seeber E, Schleuß P, Willinghöfer S, Leonbacher J, Schützenmeister K, et al. Tibet Plateau atmosphere-ecology-glaciology cluster joint Kobresia ecosystem experiment: documentation of the second Intensive Observation Period, Summer 2012 in KEMA, Tibet, Arbeitsergebn. Bayreuth: Univ. Bayreuth Abt. Mikrometeorol; 2013 [ISSN 1614-89166, 54, 54 pp.].
- Cao G-M, Tang Y, Mo WH, Wang YA, Li YN, Zhao X. Grazing intensity alters soil respiration in an alpine meadow on the Tibetan plateau. Soil Biol Biochem 2004;36(2):237–43. <http://dx.doi.org/10.1016/j.soilbio.2003.09.010>.
- Carbone MS, Trumbore SE. Contribution of new photosynthetic assimilates to respiration by perennial grasses and shrubs: residence times and allocation patterns. New Phytol 2007;176(1):124–35. <http://dx.doi.org/10.1111/j.1469-8137.2007.02153.x>.
- Chen H, Zhu Q, Peng C, Wu N, Wang Y, Fang X, et al. The impacts of climate change and human activities on biogeochemical cycles on the Qinghai–Tibetan Plateau. Glob Chang Biol 2013;19(10):2940–55. <http://dx.doi.org/10.1111/gcb.12277>.
- Chen B, Zhang X, Tao J, Wu J, Wang J, Shi P, et al. The impact of climate change and anthropogenic activities on alpine grassland over the Qinghai–Tibet Plateau. Agr Forest Meteorol 2014;189–190:11–8. <http://dx.doi.org/10.1016/j.agrformet.2014.01.002>.
- Cui X, Graf H-F. Recent land cover changes on the Tibetan Plateau: a review. Clim Change 2009;94(1–2):47–61. <http://dx.doi.org/10.1007/s10584-009-9556-8>.
- Desai AR, Richardson AD, Moffat AM, Kattge J, Hollinger DY, Barr AG, et al. Cross-site evaluation of eddy covariance GPP and RE decomposition techniques. Agr Forest Meteorol 2008;148(6–7):821–38. <http://dx.doi.org/10.1016/j.agrformet.2007.11.012>.
- Du M, Kawashima S, Yonemura S, Zhang X, Chen S. Mutual influence between human activities and climate change in the Tibetan Plateau during recent years. Hum Dimens Nat Proc Environ Chang 2004;41(3–4):241–9. <http://dx.doi.org/10.1016/j.gloplacha.2004.01.010>.
- Dunn G. Statistical evaluation of measurement errors. Design and analysis of reliability studies. 2nd ed. London: Arnold; 2004. p. 220.
- Falge E, Baldocchi D, Olson R, Anthoni P, Aubinet M, Bernhofer C, et al. Gap filling strategies for defensible annual sums of net ecosystem exchange. Agr Forest Meteorol 2001;107(1):43–69. [http://dx.doi.org/10.1016/S0168-1923\(00\)00225-2](http://dx.doi.org/10.1016/S0168-1923(00)00225-2).
- Falge E, Baldocchi D, Tenhunen J, Aubinet M, Bakwin P, Berbigier P, et al. Seasonality of ecosystem respiration and gross primary production as derived from FLUXNET measurements. Agr Forest Meteorol 2002;113(1–4):53–74. [http://dx.doi.org/10.1016/S0168-1923\(02\)00102-8](http://dx.doi.org/10.1016/S0168-1923(02)00102-8).
- Fan J, Zhong H, Harris W, Yu G, Wang S, Hu Z, et al. Carbon storage in the grasslands of China based on field measurements of above- and below-ground biomass. Clim Change 2008;86(3–4):375–96. <http://dx.doi.org/10.1007/s10584-007-9316-6>.
- Fang J, Yang Y, Ma W, Mohammad A, Shen H. Ecosystem carbon stocks and their changes in China's grasslands. Sci China Life Sci 2010a;53(7):757–65. <http://dx.doi.org/10.1007/s11427-010-4029-x>.
- Fang J, Tang Y, Son Y. Why are East Asian ecosystems important for carbon cycle research? Sci China Life Sci 2010b;53(7):753–6. <http://dx.doi.org/10.1007/s11427-010-4032-2>.
- Foken T. Micrometeorology. Berlin: Springer; 2008a. p. 306.
- Foken T. The energy balance closure problem: an overview. Ecol Appl 2008b;18(6): 1351–67. <http://dx.doi.org/10.1890/06-0922.1>.
- Foken T, Wichura B. Tools for quality assessment of surface-based flux measurements. Agr Forest Meteorol 1996;78(1–2):83–105. [http://dx.doi.org/10.1016/0168-1923\(95\)02248-1](http://dx.doi.org/10.1016/0168-1923(95)02248-1).
- Foken T, Göckede M, Mauder M, Mahrt L, Amiro B, Munger W. Post-field data quality control. In: Lee X, Massman WJ, Law BE, editors. Handbook of micrometeorology. A guide for surface flux measurement and analysis. Dordrecht: Kluwer Academic Publishers; 2004. p. 181–208.
- Foken T, Aubinet M, Finnigan JJ, Leclerc MY, Mauder M, Paw U KT. Results of a panel discussion about the energy balance closure correction for trace gases. Bull Am Meteorol Soc 2011;92(4):ES13. <http://dx.doi.org/10.1175/2011BAMS3130.1>.
- Foken T, Aubinet M, Leuning R. The eddy covariance method. In: Aubinet M, Vesala T, Papale D, editors. Eddy covariance. Dordrecht: Springer; 2012. p. 1–19.
- Fu Y, Zheng Z, Yu G, Hu Z, Sun X, Shi P, et al. Environmental influences on carbon dioxide fluxes over three grassland ecosystems in China. Biogeosciences 2009;6(12): 2879–93. <http://dx.doi.org/10.5194/bg-6-2879-2009>.
- Gao YLP, Wu N, Chen H, Wang G. Grazing intensity impacts on carbon sequestration in an alpine meadow on the eastern Tibetan Plateau. Res J Agric Biol Sci 2007(3):642–7.
- Gill RA, Burke IC, Lauenroth WK, Milchunas DG. Longevity and turnover of roots in the shortgrass steppe: influence of diameter and depth. Plant Ecol 2002;159:241–51. <http://dx.doi.org/10.1023/A:1015529507670>.

- Göckede M, Markkanen T, Hasager C, Foken T. Update of a footprint-based approach for the characterisation of complex measurement sites. *Bound-Layer Meteorol* 2006; 118(3):635–55. <http://dx.doi.org/10.1007/s10546-005-6435-3>.
- Goldstein MC, Beall CM. Change and continuity in Nomadic Pastoralism on the Western Tibetan Plateau. *Nomadic Peoples* 1991;28:105–22.
- Hafner S, Unteregelsbacher S, Seeber E, Lena B, Xu X, Li X, et al. Effect of grazing on carbon stocks and assimilate partitioning in a Tibetan montane pasture revealed by ^{13}C pulse labeling. *Glob Chang Biol* 2012;18(2):528–38. <http://dx.doi.org/10.1111/j.1365-2486.2011.02557.x>.
- Han JG, Zhang YJ, Wang CJ, Bai WM, Wang YR, Han GD, et al. Rangeland degradation and restoration management in China. *Rangel J* 2008;30(2):233–9. <http://dx.doi.org/10.1071/RJ08009>.
- Harris RB. Rangeland degradation on the Qinghai–Tibetan plateau: a review of the evidence of its magnitude and causes. *J Arid Environ* 2010;74(1):1–12. <http://dx.doi.org/10.1016/j.jaridenv.2009.06.014>.
- Hendrick RL, Pregitzer KS. Patterns of fine root mortality in two sugar maple forests. *Nature* 1993;361(6407):59–61. <http://dx.doi.org/10.1038/361059a0>.
- Hirota M, Zhang P, Gu S, Du M, Shimono A, Shen H, et al. Altitudinal variation of ecosystem CO_2 fluxes in an alpine grassland from 3600 to 4200 m. *J Plant Ecol* 2009;2(4):197–205. <http://dx.doi.org/10.1093/jpe/rtp024>.
- Holland JN, Cheng W, Crossley DA. Herbivore-induced changes in plant carbon allocation: assessment of below-ground C fluxes using carbon-14. *Oecologia* 1996;107:87–94. <http://dx.doi.org/10.1007/BF00582238>.
- Hothorn T, Bretz F, Westfall P. Simultaneous inference in general parametric models. *Biom J* 2008;50(3):346–63. <http://dx.doi.org/10.1002/bimj.200810425>.
- IPCC. Climate change 2013: the physical science basis. Contribution of working group I to the fifth assessment report of the intergovernmental panel on climate change. Cambridge, United Kingdom and New York, NY, USA: Cambridge University Press; 2013. p. 1535.
- IUSS-ISRIC-FAO. World reference base for soil resources. A framework for international classification, correlation and communication. World soil resources reports. 2nd ed. Rome: Food and Agriculture Organization of the United Nations; 2006. p. 128.
- Kaiser K. Pedogeomorphological transect studies in Tibet: Implications for landscape history and present-day dynamics. *Prace Geograficzne* 2004(200):147–65.
- Kaiser K, Schoch WH, Miehle G. Holocene paleosols and colluvial sediments in Northeast Tibet (Qinghai Province, China): properties, dating and paleoenvironmental implications. *Catena* 2007;69(2):91–102. <http://dx.doi.org/10.1016/j.catena.2006.04.028>.
- Kaiser K, Miehle G, Barthelme A, Ehrmann O, Scharf A, Schlütz F, et al. Turf-bearing topsoils on the Central Tibetan Plateau, China: Pedology, Botany, Geochronology. *Catena* 2008;73(3):300–11. <http://dx.doi.org/10.1016/j.catena.2007.12.001>.
- Kato T, Tang Y, Gu S, Cui X, Hirota M, Du M, et al. Carbon dioxide exchange between the atmosphere and an alpine meadow ecosystem on the Qinghai–Tibetan Plateau, China. *Agr Forest Meteorol* 2004;124(1–2):121–34. <http://dx.doi.org/10.1016/j.agrformet.2003.12.008>.
- Kato T, Tang Y, Gu S, Hirota M, Du M, Li Y, et al. Temperature and biomass influences on interannual changes in CO_2 exchange in an alpine meadow on the Qinghai–Tibetan Plateau. *Glob Chang Biol* 2006;12(7):1285–98. <http://dx.doi.org/10.1111/j.1365-2486.2006.01153.x>.
- Keeling CD. The concentration and isotopic abundances of carbon dioxide in rural and marine air. *Geochim Cosmochim Acta* 1961;24(3–4):277–98. [http://dx.doi.org/10.1016/0016-7037\(61\)90023-0](http://dx.doi.org/10.1016/0016-7037(61)90023-0).
- Keith H, Oades JM, Martin JK. Input of carbon to soil from wheat plants. *Soil Biol Biochem* 1986;18(4):445–9. [http://dx.doi.org/10.1016/0038-0717\(86\)90051-9](http://dx.doi.org/10.1016/0038-0717(86)90051-9).
- Klein JA, Harte J, Zhao X. Experimental warming causes large and rapid species loss, dampened by simulated grazing, on the Tibetan Plateau. *Ecol Lett* 2004;7(12):1170–9. <http://dx.doi.org/10.1111/j.1461-0248.2004.00677.x>.
- Kuzyakov Y. Tracer studies of carbon translocation by plants from the atmosphere into the soil (a review). *Eurasian Soil Sci* 2001;34(1):28–42.
- Kuzyakov Y, Domanski G. Carbon input by plants into the soil. *Review J Plant Nutr Soil Sci* 2000;163(4):421–31. [http://dx.doi.org/10.1002/1522-2624\(200008\)163:4<421::AID-JPLN421>3.0.CO;2-R](http://dx.doi.org/10.1002/1522-2624(200008)163:4<421::AID-JPLN421>3.0.CO;2-R).
- Kuzyakov Y, Biryukova OV, Kuznetsova TV, Molter K, Kandeler E, Stahr K. Carbon partitioning in plant and soil, carbon dioxide fluxes and enzyme activities as affected by cutting ryegrass. *Biol Fertil Soils* 2002;35(5):348–58. <http://dx.doi.org/10.1007/s00374-002-0480-6>.
- Kuzyakov Y. Sources of CO_2 efflux from soil and review of partitioning methods. *Soil Biol. Biochem* 2006;38(3):425–48. <http://dx.doi.org/10.1016/j.soilbio.2005.08.020>.
- Lasslop G, Reichstein M, Papale D, Richardson AD, Arneth A, Barr AG, et al. Separation of net ecosystem exchange into assimilation and respiration using a light response curve approach: critical issues and global evaluation. *Glob Chang Biol* 2010;16(1):187–208. <http://dx.doi.org/10.1111/j.1365-2486.2009.02041.x>.
- Leake JR, Ostle N, Rangel-Castro I, Johnson D. Carbon fluxes from plants through soil organisms determined by field ^{13}C pulse-labeling in an upland grassland. *Appl Soil Ecol* 2006;33(2):152–75. <http://dx.doi.org/10.1016/j.apsoil.2006.03.001>.
- Leclerc M, Foken T. Footprints in micrometeorology and ecology. Springer; 2014.
- Lehmeier C, Lattanzi F, Schäufele R, Wild M, Schnyder H. Root and shoot respiration of perennial ryegrass are supplied by the same substrate pools: assessment by dynamic ^{13}C labeling and compartmental analysis of tracer kinetics. *Plant Physiol* 2008;148:1148–58. <http://dx.doi.org/10.1104/pp.108.127324>.
- Lin X, Zhang Z, Wang S, Hu Y, Xu G, Luo C, et al. Response of ecosystem respiration to warming and grazing during the growing seasons in the alpine meadow on the Tibetan plateau. *Agr Forest Meteorol* 2011;151(7):792–802. <http://dx.doi.org/10.1016/j.agrformet.2011.01.009>.
- Liu Y, Fan J, Harris W, Shao Q, Zhou Y, Wang N, et al. Effects of plateau pika (*Ochotona curzoniae*) on net ecosystem carbon exchange of grassland in the Three Rivers Headwaters region, Qinghai–Tibet, China. *Plant Soil* 2013;366:491–504. <http://dx.doi.org/10.1007/s11104-012-1442-x>.
- Lloyd J, Taylor J. On the temperature dependence of soil respiration. *Funct Ecol* 1994;4(8):315–23. <http://dx.doi.org/10.2307/2389824>.
- Lu T, Wu N, Luo P. Sedentarization of Tibetan Nomads. *Conserv Biol* 2009;23(5):1074. <http://dx.doi.org/10.1111/j.1523-1739.2009.01312.x>.
- Lundegårdh H. Ecological studies in the assimilation of certain forest plants and shore plants. *Sven Bot Tidskr* 1921;15:46–94.
- Mauder M, Foken T. Documentation and instruction manual of the eddy-covariance software package TK3, Arbeitsergebn. Bayreuth: Univ. Bayreuth Abt. Mikrometeorol; 2011 [ISSN 1614-89166, 46, 60 pp.].
- Mauder M, Foken T, Clement R, Elbers JA, Eugster W, Grünwald T, et al. Quality control of CarboEurope flux data—part 2: inter-comparison of eddy-covariance software. *Biogeosciences* 2008;5(2):451–62. <http://dx.doi.org/10.5194/bg-5-451-2008>.
- Meharg A, Killham K. Distribution of assimilated carbon within the plant and rhizosphere of *Lolium perenne*: influence of temperature. *Soil Biol Biochem* 1989;21(4):487–9. [http://dx.doi.org/10.1016/0038-0717\(89\)90119-3](http://dx.doi.org/10.1016/0038-0717(89)90119-3).
- Michaelis L, Menten ML. Die Kinetik der Invertinwirkung, kinetics of the invertin reaction. *Biochem Z* 1913;49:333–69.
- Miehle G, Miehle S, Vogel J, Co S, La D. Highest treeline in the Northern Hemisphere found in Southern Tibet. *Mt Res Dev* 2007;27(2):169–73. <http://dx.doi.org/10.1659/mrd.0792>.
- Miehle G, Kaiser K, Co S, Zhao X, Liu J. Geo-ecological transect studies in northeast Tibet (Qinghai, China) reveal human-made mid-holocene environmental changes in the upper yellow river catchment changing forest to grassland. *erdkunde* 2008a;62(3):187–99. <http://dx.doi.org/10.3112/erdkunde.2008.03.01>.
- Miehle G, Miehle S, Kaiser K, Liu J, Zhao X. Status and dynamics of *Kobresia pygmaea* ecosystem on the Tibetan plateau. *Ambio* 2008b;37(4):272–9. [http://dx.doi.org/10.1579/0044-7447\(2008\)37\[272:SADOTK\]2.0.CO;2](http://dx.doi.org/10.1579/0044-7447(2008)37[272:SADOTK]2.0.CO;2).
- Miehle G, Miehle S, Bach K, Nölling J, Hanspach J, Reudenbach C, et al. Plant communities of central Tibetan pastures in the Alpine Steppe/*Kobresia pygmaea* ecotone. *J Arid Environ* 2011;75(8):711–23. <http://dx.doi.org/10.1016/j.jaridenv.2011.03.001>.
- Miehle G, Miehle S, Böhner J, Kaiser K, Hensen I, Madsen D, et al. How old is the human footprint in the world's largest alpine ecosystem? A review of multiproxy records from the Tibetan Plateau from the ecologists' viewpoint. *Quat Sci Rev* 2014;86:190–209. <http://dx.doi.org/10.1016/j.quascirev.2013.12.004>.
- Ni J. Carbon storage in grasslands of China. *J Arid Environ* 2002;50(2):205–18. <http://dx.doi.org/10.1006/jare.2001.0902>.
- Palta JA, Gregory PJ. Drought affects the fluxes of carbon to roots and soil in ^{13}C pulse-labelled plants of wheat. *Soil Biol Biochem* 1997;29(9–10):1395–403. [http://dx.doi.org/10.1016/S0038-0717\(97\)00050-3](http://dx.doi.org/10.1016/S0038-0717(97)00050-3).
- Paterson E, Sim A. Effect of nitrogen supply and defoliation on loss of organic compounds from roots of *Festuca rubra*. *J Exp Bot* 2000;51(349):1449–57. <http://dx.doi.org/10.1093/jexbot/51.349.1449>.
- Pinheiro J, Bates D, DebRoy S, Sarkar D, R Development Core Team. nlme: linear and non-linear mixed effects models; 2011.
- Qiu J. China: the third pole. *Nature* 2008;454(7203):393–6. <http://dx.doi.org/10.1038/454393a>.
- R Development Core Team. R: a language and environment for statistical computing. Vienna, Austria. available at <http://www.R-project.org>, 2009.
- Rannik Ü, Aubinet M, Kurbanmuradov O, Sabelfeld KK, Markkanen T, Vesala T. Footprint analysis for measurements over a heterogeneous forest. *Bound-Layer Meteorol* 2000; 97(1):137–66. <http://dx.doi.org/10.1023/A:1002702810929>.
- Rasse D, Rumpel C, Dignac M-F. Is soil carbon mostly root carbon? Mechanisms for a specific stabilisation. *Plant Soil* 2005;269:341–56. <http://dx.doi.org/10.1007/s11104-004-0907-y>.
- Rebmann C, Kölle O, Heinesch B, Queck R, Ibram A, Aubinet M. Data acquisition and flux calculations. In: Aubinet M, Vesala T, Papale D, editors. Eddy covariance. Dordrecht: Springer; 2012. p. 59–83.
- Reichstein M, Stoy PC, Desai AR, Lasslop G, Richardson AD. Partitioning of net fluxes. In: Aubinet M, Vesala T, Papale D, editors. Eddy covariance. Dordrecht: Springer; 2012. p. 263–89.
- Reth S, Göckede M, Falge E. CO_2 efflux from agricultural soils in Eastern Germany—comparison of a closed chamber system with eddy covariance measurements. *Theor Appl Climatol* 2005;80(2–4):105–20. <http://dx.doi.org/10.1007/s00704-004-0094-z>.
- Retzer V. Forage competition between livestock and Mongolian Pika (*Ochotona pallasi*) in Southern Mongolian mountain steppes. *J Basic Appl Ecol* 2007;8(2):147–57. <http://dx.doi.org/10.1016/j.baec.2006.05.002>.
- Riederer M. Carbon fluxes of an extensive meadow and attempts for flux partitioning (Dissertation) Bayreuth: University of Bayreuth, 2014.
- Rochette P, Hutchinson GL. Measurement of soil respiration in situ: chamber techniques. In: Hatfield JL, Baker JM, Viney MK, editors. Micrometeorology in agricultural systems. AgronomyMadison, Wisconsin: American Society of Agronomy, Crop Science Society of America, and Soil Science Society of America; 2005. p. 247–86.
- Ruppert J, Mauder M, Thomas C, Lüers J. Innovative gap-filling strategy for annual sums of CO_2 net ecosystem exchange. *Agr Forest Meteorol* 2007;138:5–18. <http://dx.doi.org/10.1016/j.agrformet.2006.03.003>.
- Saggar S, Hedley C, Mackay AD. Partitioning and translocation of photosynthetically fixed ^{14}C in grazed hill pastures. *Biol Fertil Soils* 1997;25:152–8. <http://dx.doi.org/10.1007/s003740050296>.
- Schmitt A, Pausch J, Kuzyakov Y. Effect of clipping and shading on C allocation and fluxes in soil under ryegrass and alfalfa estimated by ^{14}C labeling. *Appl Soil Ecol* 2013;64:228–36. <http://dx.doi.org/10.1016/j.apsoil.2012.12.015>.
- Scurlock JM, Hall DO. The global carbon sink: a grassland perspective. *Glob Chang Biol* 1998;4(2):229–33. <http://dx.doi.org/10.1046/j.1365-2486.1998.00151.x>.
- Sheehy DP, Miller D, Johanson DA. Transformation of traditional pastoral livestock systems on the Tibetan steppe. *Sécheresse* 2006;17(1–2):142–51.

- Shi X-M, Li XG, Li CT, Zhao Y, Shang ZH, Ma Q. Grazing exclusion decreases soil organic C storage at an alpine grassland of the Qinghai-Tibetan Plateau. *Ecol Eng* 2013;57:183–7. <http://dx.doi.org/10.1016/j.ecoleng.2013.04.032>.
- Singh J, Gupta S. Plant decomposition and soil respiration in terrestrial ecosystems. *Bot Rev* 1977;43:449–528. <http://dx.doi.org/10.1007/BF02860844>.
- Sun H, Zheng D. Formation, evolution and development of Qinghai-Xizang (Tibetan) Plateau. Guangdong: Guangdong Science & Technology Press; 1998.
- Swinnen J, Vanveen JA, Merckx R. C-14 pulse labeling of field-grown spring wheat—an evaluation of its use in rhizosphere carbon budget estimations. *Soil Biol Biochem* 1994;26(2):161–70. [http://dx.doi.org/10.1016/0038-0717\(94\)90159-7](http://dx.doi.org/10.1016/0038-0717(94)90159-7).
- Unteregelsbacher S, Hafner S, Guggenberger G, Miehe G, Xu X, Liu J, et al. Response of long-, medium- and short-term processes of the carbon budget to overgrazing-induced crusts in the Tibetan Plateau. *Biogeochemistry* 2011. <http://dx.doi.org/10.1007/s10533-011-9632-9>.
- Wang G, Qian J, Cheng G, Lai Y. Soil organic carbon pool of grassland soils on the Qinghai-Tibetan Plateau and its global implication. *Sci Total Environ* 2002;291(1–3):207–17.
- Wang W, Wang Q, Wang H. The effect of land management on plant community composition, species diversity, and productivity of alpine *Kobresia* steppe meadow. *Ecol Res* 2006;21(2):181–7. <http://dx.doi.org/10.1007/s11284-005-0108-z>.
- Wang Z, Li L-H, Han X-G, Li Z, Chen Q-S. Dynamics and allocation of recently photo-assimilated carbon in an Inner Mongolia temperate steppe. *Environ Exp Bot* 2007;59(1):1–10. <http://dx.doi.org/10.1016/j.envexpbot.2005.09.011>.
- Wei Y, Chen Q. Grassland classification and evaluation of grazing capacity in Naqu Prefecture, Tibet Autonomous Region, China. *N Z J Agric Res* 2001;44(4):253–8. <http://dx.doi.org/10.1080/00288233.2001.9513482>.
- Wei D, Ri X, Wang Y, Wang Y, Liu Y, Yao T. Responses of CO₂, CH₄ and N₂O fluxes to live-stock enclosure in an alpine steppe on the Tibetan Plateau, China. *Plant Soil* 2012;359(1–2):45–55. <http://dx.doi.org/10.1007/s11104-011-1105-3>.
- Wilczak J, Oncley SP, Stage S. Sonic anemometer tilt correction algorithms. *Bound-Layer Meteorol* 2001;99(1):127–50. <http://dx.doi.org/10.1023/A:1018966204465>.
- Wohlfahrt G, Anderson-Dunn M, Bahn M, Balzarolo M, Berninger F, Campbell C, et al. Biotic, abiotic, and management controls on the net ecosystem CO₂ exchange of European mountain grassland ecosystems. *Ecosystems* 2008;11(8):1338–51. <http://dx.doi.org/10.1007/s10021-008-9196-2>.
- Wohlfahrt G, Klumpp K, Soussana J-F. Eddy covariance measurements over grasslands. In: Aubinet M, Vesala T, Papale D, editors. *Eddy covariance*. Dordrecht: Springer; 2012. p. 333–44.
- Wu G-L, Du G-Z, Liu Z-H, Thirgood S. Effect of fencing and grazing on a *Kobresia*-dominated meadow in the Qinghai-Tibetan Plateau. *Plant Soil* 2009;319:115–26. <http://dx.doi.org/10.1007/s11104-008-9854-3>.
- Wu Y, Tan H, Deng Y, Wu J, Xu X, Wang Y, et al. Partitioning pattern of carbon flux in a *Kobresia* grassland on the Qinghai-Tibetan Plateau revealed by field ¹³C pulse-labeling. *Glob Chang Biol* 2010;16(8):2322–33. <http://dx.doi.org/10.1111/j.1365-2486.2009.02069.x>.
- Wu Y, Wu J, Deng Y, Tan H, Du Y, Gu S, et al. Comprehensive assessments of root biomass and production in a *Kobresia humilis* meadow on the Qinghai-Tibetan Plateau. *Plant Soil* 2011;338(1–2):497–510. <http://dx.doi.org/10.1007/s11104-010-0562-4>.
- Yang J, Mi R, Liu J. Variations in soil properties and their effect on subsurface biomass distribution in four alpine meadows of the hinterland of the Tibetan Plateau of China. *Environ Geol* 2009;57(8):1881–91. <http://dx.doi.org/10.1007/s00254-008-1477-8>.
- Yang K, Wu H, Qin J, Lin C, Tang W, Chen Y. Recent climate changes over the Tibetan Plateau and their impacts on energy and water cycle: a review. *Global Planet Change* 2014;112:79–91. <http://dx.doi.org/10.1016/j.gloplacha.2013.12.001>.
- Zhao X, Zhou XM. Ecological basis of Alpine meadow ecosystem management in Tibet: Haibei Alpine Meadow Ecosystem Research Station. *Ambio* 1999;28(8):642–7. (<http://www.jstor.org/stable/4314976>).
- Zhao L, Li Y, Zhao X, Xu S, Tang Y, Yu G, et al. Comparative study of the net exchange of CO₂ in 3 types of vegetation ecosystems on the Qinghai-Tibetan Plateau. *Chin Sci Bull* 2005;50(16):1767–74. <http://dx.doi.org/10.1360/04wd0316>.
- Zhao L, Li Y, Xu S, Zhou H, Gu S, Yu G, et al. Diurnal, seasonal and annual variation in net ecosystem CO₂ exchange of an alpine shrubland on Qinghai-Tibetan plateau. *Glob Chang Biol* 2006;12(10):1940–53. <http://dx.doi.org/10.1111/j.1365-2486.2006.01197.x>.

F. Biermann et al. (subm)

Biermann, T., Pfab, D., Babel, W., Li, M., Wang, B., Ma, Y., and Foken, T.: Note: Measurements of latent heat flux and humidity on the Tibetan Plateau during winter conditions, submitted to Atmos. Meas. Tech. Diss..

Manuscript prepared for Atmos. Meas. Tech. Discuss.
with version 4.1 of the L^AT_EX class copernicus_discussions.cls.
Date: 12 July 2014

Note: Measurements of latent heat flux and humidity on the Tibetan Plateau during winter conditions

Tobias Biermann^{1*}, Daniela Pfab^{1}, Wolfgang Babel¹, Maoshan Li², Binbin Wang³, Yaoming Ma³, and Thomas Foken^{1***}**

¹Department of Micrometeorology, University of Bayreuth, Bayreuth, Germany

²Cold and Arid Regions Environment and Engineering Research Institute, Chinese Academy of Sciences, Lanzhou, China

³Key Laboratory of Tibetan Environment Changes and Land Surface Processes, Institute of Tibetan Plateau Research, Chinese Academy of Sciences, Beijing, China

*now at: Centre for Environmental and Climate Research, Lund University, Lund, Sweden

**now at: Wind Cert Services, TÜV SÜD Industrie Service GmbH, Ludwig-Eckert-Str. 8, 93049 Regensburg, Germany

***Member of Bayreuth Center of Ecology and Ecosystem Research (BayCEER)

Correspondence to: Tobias Biermann
(tobias.biermann@cec.lu.se)

Abstract

Harsh weather conditions, great changes in seasonal concentrations, temperature or pressure and general low atmospheric water vapour concentrations in arid or semi arid environments pose a challenge for an accurate estimation of humidity concentrations and latent heat flux. Furthermore, necessary calibration on a regular basis usually involves a great effort due to the remoteness of these areas. Within a quality check of data measured on the Tibetan Plateau, Metzger et al. (2006) have shown a super saturation within humidity measurements with an open path infrared gas analyser (Li-7500) during winter conditions. They suggested to investigate the consequence of these findings for the latent heat flux be investigated as well. Humidity concentrations and latent heat flux were therefore estimated within this study through parallel measurements by a Krypton Hygrometer (KH20) and a Li-7500 in February 2010, showing that both devices measure the latent heat flux with great accuracy but flux estimates of the KH20 are greater by 20%. Unfortunately the cause of this divergence cannot be exactly determined nor attributed to one of the devices. It can be generally stated, however that the estimation of evaporation is still within an acceptable error range, but that improvement of long-term monitoring in areas with low water vapour concentrations is necessary. Furthermore, this comparison also showed that neither the Li-7500 nor the KH20 are capable to accurately measure absolute humidity concentrations under such conditions. All this shows the need for a good calibration strategy for stations with limited access and therefore a new mobile KH20 calibration device was tested. This test showed that a KH20 in combination with the calibration device offers an easy method to maintain the possibility checking on the latent heat flux estimates of a routine EC station equipped with a Li-7500.

1 Introduction

In those arid and semi arid areas found in high elevation, polar or desert environments where atmospheric humidity concentrations are low, measurements of water vapour content are challenging. An example of such problematic measurements is revealed within a comparative data

quality investigation of turbulent flux estimates measured at two eddy-covariance (EC) stations on the Tibetan Plateau by Metzger et al. (2006). They observed during winter a super saturation within humidity measurements derived with an open path infrared gas analyzer Li-7500 (Li-COR Bioscience Inc.). The two EC stations, namely *Qomolangma Station for Atmospheric and*
5 *Environmental Observation and Research* (Everest Station) and *Nam Co Monitoring and Research Station for Multisphere Interactions* (NAMORS), are part of the framework *Tibetan Observation and Research Platform* (TORP, Ma et al., 2008) installed by the *Institute of Tibetan Plateau Research* (ITP), *Chinese Academy of Sciences*, and are also used within the Project CEOP-AEGIS of the European Union Menenti et al. (2014, <http://www.ceop-aegis.org>). In order to gain more insight into this problem and following the suggestion by Metzger et al. (2006)
10 side-by-side measurements, of a Li-7500 and an ultra violet gas analyzer (Krypton Hygrometer KH20, Campbell Sci. Inc.) were conducted in February 2010 at NAMORS under winter conditions. The goal was to investigate whether the problem of unrealistic humidity concentration measurements with the Li-7500 would affect the estimation of the latent heat flux with the eddy-covariance method. Furthermore, a mobile calibration unit for the KH20 was utilized
15 for an in-situ calibration under field conditions directly before the inter comparison (Foken and Falke, 2012).

2 Material and Methods

2.1 Study site

20 The chosen study site NAMORS (30°46'22" N, 90°57'47" E) is located within the Nam Co Basin on the Tibetan Plateau, 220km north of Lhasa, at 4730masl.. The permanent eddy-covariance tower (3 m, Figure 1) is equipped with an open path infrared gas analyzer Li-7500 (LiCOR Bioscience Inc.), an ultrasonic anemometer (CSAT3, Campbell Sci. Inc.) and a combined humidity and temperature sensor (HMP45, Vaisala). For the side-by-side measurements
25 the setup was extended with a Krypton Hygrometer, measuring absorption through water vapour concentration with ultraviolet light (KH20, Campbell Sci. Inc.). The CSAT3 was installed fac-

ing southm, with the Li-7500 along its east and the KH20 along its west side. Further radiation components, as well as soil moisture and soil temperature, are measured at close to the EC station. All data is logged to a Cr5000 Datalogger (Campbell Sci. Inc.).

2.2 Post processing of turbulent data and quality control

5 Calculation of turbulent fluxes and aggregation to 30 min averages was done with the software package TK2, Department of Micrometeorology, University of Bayreuth (Mauder and Foken, 2004), a more recent version, TK3, has become available in the mean time (Mauder and Foken, 2011). The software is internationally compared (Mauder et al., 2008), calculated fluxes match up-to-date micrometeorological standards (Foken et al., 2012; Rebmann et al., 2012) due to
10 the data corrections included and the quality control tools. Wind data was rotated according to the planar-fit rotation method (Wilczak et al., 2001) considering terrain effects on the measurements. Data quality is assured by the implemented flagging scheme after Foken and Wichura (1996). For the comparison of absolute humidity concentrations data with intermediate quality (flag 4-6) was selected while for the comparison of the latent heat flux of the two sensors only
15 data with best quality (flags 1-3) was used and data with poor quality (flag 7-9) was rejected. The classification of the data quality follows Foken et al. (2004).

2.3 Operation, calibration and sensitivity of the KH20 and Li-7500 gas analyser

2.3.1 Li-7500

The Li-7500 is an open path infrared gas analyzer which measures water vapour and CO₂ concentration within a fixed path length of 125 mm through absorption of infrared light, within the
20 wavelengths of 4.26 and 2.59 μm and non-absorbing reference wavelengths of 3.95 and 2.40 μm . Maintenance and calibration requirements for the Li-7500 are usually quite low with the field calibration and changing of internal desiccants recommended 1-2 times a year depending on environmental conditions. The manufacturer's calibration curve itself is considered to be
25 valid for several years, and a change would be revealed during the field calibration carried out by

the user of the device, which sets a “zero” and “span” value to be used within the calculation of the concentration to account for any drift within the measurements (LI-COR, 2004). Although it is possible to set “span” and “zero” on a mounted device, it is recommended that the device to be disassembled for a calibration inside a laboratory to minimize errors and leaks especially when the drying chemicals are changed as well. Furthermore, the Li-7500 is considered to be quite resistant against contamination of the window through dust and rain (Burba, 2013). Although the above-mentioned points make the Li-7500 a reliable and easy to handle device there are some problems. A change in specification of the original design of the Li-7500 in 2002 has increased the temperature sensitivity of the H₂O measurements while solving problems arising from penetrating sunlight for CO₂ measurements. A comparison between a reference and a Li-7500 before and after being re-adjusted to the specifications prior to 2003 showed that the specifications used after 2003 introduce a greater temperature drift for low temperatures and low humidity concentration (Weisensee et al., 2003). Burba et al. (2008) introduced an additional correction term to the WPL correction (Webb et al., 1980; Leuning, 2007), accounting for a heat flux within the observation path of the Li-7500 (Grelle and Burba, 2007), however the application of this correction is controversially discussed (Wohlfahrt et al., 2008; Reverter et al., 2011; Oechel et al., 2014). In this study the additional correction is not applied since, in general, the WPL correction has more effect on CO₂ fluxes and is of minor importance for the latent heat flux (Liebethal and Foken, 2003). A study by Fratini et al. (2014) revealed that a bias in measurements of gas concentrations introduced by contamination will also propagate into the flux estimates.

2.3.2 KH20

The Krypton Hygrometer (KH20) estimates water vapour concentration in the air by measuring the absorption with ultra violet radiation emitted by krypton gas (Campbell, 1985). Main absorption by water vapour happens within the main band of 123,58nm and a the secondary band of 116,49nm. Absorption within the main band is chiefly caused by water vapour, while the influence of other gases is relatively weak. Within both bands the absorption is caused by water vapour and oxygen, which needs to be accounted for in a special correction (Tanner et al.,

1993). Due to both the strong absorption within the main wavelength and the short path length, typically 10 mm, the device is quite sensitive and therefore well-suited for the use in arid environments. Absorption by oxygen and water vapor for both absorption-bands can be calculated according to the Lambert-Beer's law (Campbell, 1985). The KH20 factory calibration procedure estimates K_w , the effective absorption coefficient of water vapour, by varying the absolute humidity while path length and oxygen level remain constant; unfortunately such procedures are somewhat impractical, if not impossible, for the use as field calibration due to a missing moisture chamber. However, field calibrations become necessary due to contamination of the windows or strong changes in environmental circumstances, or possible changes of the intensity of the UV lamps. In order to make the field calibration of the KH20 more convenient, Foken and Falke (2012) introduced a new calibration device for the KH20 which follows in principle the proposed calibration procedure for the Lyman-alpha Hygrometer allowing calibration for constant absolute humidity through varying the path length ((Buck, 1976) updated by Foken et al., 1998). A more detailed description of how to operate the calibration device and technical details can be found in Foken and Falke (2012).

The new device does not directly calibrate the coefficient for water vapour absorption, however the calibration is done with oxygen as proxy. It is therefore assumed that changes in the intensity of the Krypton lamp affect the absorption by water vapour and oxygen in the same manner. This is possible due to the higher concentration of oxygen in the atmosphere and therefore enhanced absorption. It is consequently necessary to estimate the calibration coefficients for humidity ($K_{W_{original}}$) and oxygen ($K_{O_{original}}$), parallel for a new KH20. Most conveniently, $K_{W_{original}}$ is taken from the calibration by the manufacturer and $K_{O_{original}}$ is determined right after the purchase with the mobile calibration device. Any changes in the intensity of the lamp, which will also be reflected in the change of calibration coefficient for oxygen ($K_{O_{in situ}}$), can be then scaled to the new calibration coefficient of water vapour ($K_{W_{in situ}}$).

$$K_{W_{in situ}} = K_{W_{original}} \cdot \frac{K_{O_{in situ}}}{K_{O_{original}}} \quad (1)$$

In general this KH20 calibration has an error range between 5-10% (Foken and Falke, 2012). This calibration uncertainty becomes even greater with increasing timespan between the determination of $K_{W_{original}}$ and $K_{O_{original}}$.

5 2.3.3 Application of the Li-7500 and KH20

Due to their different designs both, the Li-7500 and the KH20 sensors, have advantages and disadvantages which might affect their applicability on the TP during winter when temperatures and absolute humidity concentrations are low. Besides using either UV or IR light, the greatest difference between the two devices is the variable path length of the KH20 versus the fixed
10 path length of the Li-7500. This allows a better adjustment of the KH20 to low water vapour concentrations or for measurements of small eddies close to the ground due to the short path length. However, a change in altitude requires a recalibration of the KH20 due to its great sensitivity to changes in oxygen concentration. Furthermore, the device is sensitive to contamination through dust and rain and needs a regular maintenance. On the other hand the calibration of
15 the Li-7500 involves the use of a "zero" gas, a reference gas for CO₂ and a dew point generator for H₂O. Furthermore, the calibration is ideally carried out in a laboratory setting where temperature and pressure are kept at a constant level. In addition it needs to be considered that the manufacturer calibration is carried out under different conditions. For the LI-7500 used, the smallest calibration mass density scaled to typical ambient pressure on the TP during winter is
20 2.77g m^{-3} .

3 Results and Discussion

In order to identify a pattern within the course of a year, continuous measurements of absolute humidity with the Li-7500 and the HMP45 for 2009 and 2010 are shown in Figure 2. Also included is the maximal absolute humidity at saturation and air temperature. It is clearly visible
25 that the humidity measurements by the Li-7500 regularly exceed the threshold of the maximum absolute humidity at saturation during the winter month, while this only occurs occasionally

during the summer months. Furthermore, the effect of field calibration on 30 June 2009 is also visible in this figure. After the calibration, measurements of the Li-7500 and the HMP45 are in great accordance until air temperature starts to fall below 0°C in October. While in 2009 the absolute humidity measurements by the Li-7500 start to decrease again with the rise of the air temperature above 0°C in April and May, in 2010 such an effect is not visible. However, the calibration on July 8th, 2010 is again visible. Together with the data gap in May, this indicates a malfunction of the sensor in June 2010.

We also compared measurements of absolute humidity from the LI-7500 and the KH20 to humidity measurements by an HMP45 for 22 February, since an under or overestimation of water vapour concentrations could cause a bias in the turbulent flux estimates (Fratini et al., 2014). The comparison reveals an offset between Li-7500 and HMP45 absolute humidity measurements (Figure 3). Values of absolute humidity measured with the KH20 are forced to the HMP45 values since the device is only set up to measure the fluctuations correctly and not capable of this kind of measurement. However, even though they are in the same range as the HMP45 values, there are still differences, between both time series. Besides this differences, it is notable that the fluctuations of the two fast sensors have the same pattern throughout the day but the magnitude of the fluctuations of the KH20 and the Li-7500 differ. The range of the fluctuations measured with the KH20 is greater than those of the Li-7500.

The direct comparison of the latent heat fluxes measured with both devices during the side-by-side experiment in February 2010 in the Tibetan Plateau reveals only a little scatter between the measurements. However, fluxes measured by the KH20 are 20% greater than those measured with the Li-7500 (Figure 4), although the deviation is greatest for high latent heat fluxes above 150 W m⁻², which rarely occur. It cannot be determined whether the difference is related to either an uncertainty in the measurements by the Li-7500 or the KH20, since the Li-7500 was not specially calibrated for winter conditions and the calibration of the KH20, even though carried out in situ in the field during the experiment has an error range of up to 10%. The power spectra for both devices were plotted, and Figure 5 shows that energy follows the power law of -5/3 required for ideal conditions within the inertial subrange (Kolmogorov, 1941).

4 Conclusions

The short study on the Tibetan Plateau showed that both sensors can be considered suitable for measuring the latent heat flux on the TP even under winter condition since the measurements of both devices is small and the power spectra follows the required decline. However, used by themselves are not capable of measuring accurate absolute humidity concentrations. Furthermore, the comparison of the latent heat flux measurements with the Li-7500 and KH20 gas analysers showed that even though the fluctuations can be measured with high accuracy, a difference of 20% between the two measurements was observed, with higher fluxes detected with the KH20. Therefore the absolute estimates of the flux might be prone to an error which should not be neglected, although it needs to be kept in mind that the TP is an area with low data coverage and limited accessibility so that the long term flux estimation with the Li-7500 can be still considered as acceptable. It is nevertheless highly recommended to take great care to properly calibrate and maintain devices which are used under harsh conditions in order to minimise error and use the full range of possibilities provided by the measuring equipment. A strong control of the “span” and “zero” drift for the Li-7500 is recommended and a second field calibration during winter time might improve the measurements and furthermore frequent field calibration would allow use of the estimation of a bias for the turbulent flux as proposed by Fratini et al. (2014). Because Weisensee et al. (2003) could show that a Li-7500 with the settings prior to the sunlight correction from 2003 would be more accurate in the estimation of low absolute humidity concentrations, utilizing a device factory re calibrated for winter conditions needs to be considered. One additional winter field calibration for the Li-7500 and parallel measurements with a regular in-situ calibrated KH20 can be considered as the most practical procedure, as remote stations are not permanently staffed with trained persons for a regular calibration of the Li-7500. We are aware that our experiment on the Tibetan Plateau during winter is prone to certain shortcomings. Due mainly to the logistical problems we were not able to use recently factory calibrated devices and had to rely on the equipment at the Station which had already been exposed to the harsh conditions on the Plateau for some time. Nevertheless we see that there is a need to look into winter-time data, especially when used in larger projects

such as CEOP-AEGIS (Menenti et al., 2014), as a bias exists between the two estimated latent heat fluxes obtained with the two different devices. We therefore want to encourage everyone measuring in similar environments to not only look at the flux estimates but also look critically at absolute humidity concentrations measured with the Li-7500.

- 5 *Acknowledgements.* This work was funded by the German Research Foundation (Deutsche Forschungsgemeinschaft; DFG) Priority Programme 1372 Tibetan Plateau: Formation, Climate, Ecosystems (TiP) and CEOP-AEGIS, a Collaborative Project/Small or medium-scale focused research project Specific International Co-operation Action coordinated by the University of Strasbourg, France and funded by the European Commission under FP7 topic ENV.2007.4.1.4.2 Improving observing systems for water resource management. Furthermore, the authors would like to thank everybody who participated in the collection of the data on the Tibetan plateau and the colleagues from the ITP, in particular Zhu Zhikun, for logistical support during the field campaign. This publication is funded by the DFG and the University of Bayreuth in the funding programme Open Access Publishing.

References

- 15 Buck, A. L.: Variable-Path Lyman-Alpha Hygrometer and its Operating Characteristics, *Bull Amer Meteor Soc*, 57, 1976.
- Burba, G.: Eddy covariance method for scientific, industrial, agricultural, and regulatory applications, *A field book on measuring ecosystem gas exchange and areal emission rates*, LI-COR Biosciences, Lincoln, Nebraska, 2013.
- 20 Burba, G. G., McDERMITT, D. K., Grelle, A., ANDERSON, D. J., and XU, L.: Addressing the influence of instrument surface heat exchange on the measurements of CO₂ flux from open-path gas analyzers, *Global Change Biol*, 14, 1854–1876, doi:10.1111/j.1365-2486.2008.01606.x, <http://doi.wiley.com/10.1111/j.1365-2486.2008.01606.x>, 2008.
- Campbell, G. S. a. B. D. T.: A Krypton hygrometer for measurement of atmospheric water vapour concentrations, in: *Moisture and humidity*, 1985.
- 25 Foken, T. and Falke, H.: Technical Note: Calibration device for the krypton hygrometer KH20, *Atmos MeasTech*, 5, 1861–1867, doi:10.5194/amt-5-1861-2012, 2012.

- Foken, T. and Wichura, B.: Tools for quality assessment of surface-based flux measurements, *Agr Forest Meteorol*, 78, 83–105, doi:10.1016/0168-1923(95)02248-1, <http://www.sciencedirect.com/science/article/pii/0168192395022481>, 1996.
- Foken, T., Buck, A. L., Houghton, R. A., and Horn, R. D.: A Lyman-alpha hygrometer with variable pathlength, *J Atmos Ocean Sci*, 15, 211–214, 1998.
- 5 Foken, T., Göckede, M., Mauder, M., Mahrt, L., Amiro, B., and Munger, J.: Post-field data quality control, in: *Handbook of Micrometeorology: A Guide for Surface Flux Measurement and Analysis*, edited by Lee, X., Massman, W. J., and Law, B., vol. 29 of *Atmospheric and Oceanographic Sciences Library*, pp. 181–208, Kluwer Academic Publishers, Dordrecht, http://dx.doi.org/10.1007/1-4020-2265-4_9, 2004.
- 10 Foken, T., Leuning, R., Oncley, S. P., Mauder, M., and Aubinet, M.: Corrections and data quality, in: *Eddy Covariance: A Practical Guide to Measurement and Data Analysis*, edited by Aubinet, M., Vesala, T., and Papale, D., pp. 85–131, Springer, Dordrecht, Heidelberg, London, New York, 2012.
- Fratini, G., McDermitt, D. K., and Papale, D.: Eddy-covariance flux errors due to biases in gas concentration measurements: origins, quantification and correction, *Biogeosciences*, 11, 1037–1051, doi:10.5194/bg-11-1037-2014, <http://www.biogeosciences.net/11/1037/2014/>, 2014.
- 15 Grelle, A. and Burba, G.: Fine-wire thermometer to correct CO₂ fluxes by open-path analyzers for artificial density fluctuations, *Agr Forest Meteorol*, 147, 48–57, doi:10.1016/j.agrformet.2007.06.007, 2007.
- Kolmogorov, A. N.: Rassejanie energii pri lokalno-isotropoi turbulentnosti (Dissipation of energy in locally isotropic turbulence), *Dokl AN SSSR*, 32, 22–24, 1941.
- 20 Leuning, R.: The correct form of the Webb, Pearman and Leuning equation for eddy fluxes of trace gases in steady and non-steady state, horizontally homogeneous flows, *Boundary-Layer Meteorology*, 123, 263–267, doi:10.1007/s10546-006-9138-5, <http://link.springer.com/10.1007/s10546-006-9138-5>, 2007.
- LI-COR: Li-7500 Open Path CO₂/H₂O Analyzer Instruction Manual, Lincoln, Nebraska USA, 2004.
- 25 Liebethal, C. and Foken, T.: On the Significance of the Webb Correction to Fluxes, *Boundary-Layer Meteorology*, 109, 99–106, doi:10.1023/A:1025421903542, <http://dx.doi.org/10.1023/A%3A1025421903542>, 2003.
- Ma, Y., Kang, S., Zhu, L., Xu, B., Tian, L., and Yao, T.: ROOF OF THE WORLD: Tibetan Observation and Research Platform, *Bull Amer Meteor Soc*, 89, 1487–1492, doi:10.1175/2008bams2545.1, <http://dx.doi.org/10.1175/2008BAMS2545.1>, 2008.
- 30

- Mauder, M. and Foken, T.: Documentation and Instruction Manual of the Eddy Covariance Software Package TK2, Arbeitsergebn, Univ Bayreuth, Abt Mikrometeorol, ISSN 1614-89166, 26, 26, 42, <http://nbn-resolving.de/urn/resolver.pl?urn:nbn:de:bvb:703-opus-8000>, 2004.
- Mauder, M. and Foken, T.: Documentation and Instruction Manual of the Eddy-Covariance Software Package TK3, Arbeitsergebn, Univ Bayreuth, Abt Mikrometeorol, ISSN 1614-89166, 46, 46, 60, <http://nbn-resolving.de/urn/resolver.pl?urn:nbn:de:bvb:703-opus-8665>, 2011.
- 5 Mauder, M., Foken, T., Clement, R., Elbers, J. A., Eugster, W., Grünwald, T., Heusinkveld, B., and Kolle, O.: Quality control of CarboEurope flux data – Part 2: Inter-comparison of eddy-covariance software, *Biogeosciences*, 5, 451–462, doi:10.5194/bg-5-451-2008, <http://www.biogeosciences.net/5/451/2008/>, 2008.
- 10 Menenti, M., Colin, J., Jia, L., D’Urso, G., Foken, T., Immerzeel, W., Jha, R., Liu, Q., Liu, C., Ma, Y., Sobrino, J. A., Yan, G., Pelgrum, H., Porcu, F., Wang, J., Wang, J., Shen, X., Su, Z., and Ueno, K.: Hydro-meteorological processes on the Qinghai – Tibet Plateau observed from space, *Geophysical Research Abstracts*, 16, EGU2014–4567, 2014.
- 15 Metzger, S., Ma, Y., Markkanen, T., Göckede, M., Li, M., and Foken, T.: Quality assessment of Tibetan Plateau Eddy Covariance measurements utilizing Footprint modeling, *Adv Earth Sci*, 21, 1260–1267, http://www.bayceer.uni-bayreuth.de/mm/de/pub/pub/pub_detail.php?id_obj=42418, 2006.
- Oechel, W. C., Laskowski, C. A., Burba, G., Gioli, B., and Kalhori, A. A. M.: Annual patterns and budget of CO₂ flux in an Arctic tussock tundra ecosystem, *Journal of Geophysical Research: Biogeosciences*, 119, 323–339, doi:10.1002/2013JG002431, <http://doi.wiley.com/10.1002/2013JG002431>, 2014.
- 20 Rebmann, C., Kolle, O., Heinesch, B., Queck, R., Ibrom, A., and Aubinet, M.: Data Acquisition and Flux Calculations, in: *Eddy Covariance: A Practical Guide to Measurement and Data Analysis*, edited by Aubinet, M., Vesala, T., and Papale, D., pp. 59–83, Springer, Dordrecht, http://dx.doi.org/10.1007/978-94-007-2351-1_3, 2012.
- 25 Reverter, B., Carrara, A., Fernández, A., Gimeno, C., Sanz, M., Serrano-Ortiz, P., Sánchez-Cañete, E., Were, A., Domingo, F., Resco, V., Burba, G., and Kowalski, A.: Adjustment of annual NEE and ET for the open-path IRGA self-heating correction: Magnitude and approximation over a range of climate, *Agricultural and Forest Meteorology*, 151, 1856–1861, doi:10.1016/j.agrformet.2011.06.001, <http://linkinghub.elsevier.com/retrieve/pii/S016819231100178X>, 2011.
- 30 Tanner, B. D., E., S., and J. P., G.: Density fluctuations and use of the krypton hygrometer in surface flux measurements, in: *Management of irrigation and drainage systems: integrated perspectives*, edited by R.G. Allen, American Society of Civil Engineers, New York., 1993.

- Webb, E. K., Pearman, G. I., and Leuning, R.: Correction of flux measurements for density effects due to heat and water vapour transfer, *Quarterly Journal of the Royal Meteorological Society*, 106, 85–100, doi:10.1002/qj.49710644707, <http://doi.wiley.com/10.1002/qj.49710644707>, 1980.
- Weisensee, U., Beyrich, F., and Leps, J.-P.: Integration of humidity fluctuation sensors into the Lindenberg boundary layer measurement facilities: Experiences, problems, and future requirements, in: *Proceedings 83rd AMS Annual Meeting*, Long Beach, 2003.
- 310 Wilczak, J., Oncley, S. P., and Stage, S.: Sonic Anemometer Tilt Correction Algorithms, *Bound-Lay Meteorol*, 99, 127–150, doi:10.1023/A:1018966204465, <http://dx.doi.org/10.1023/A%3A1018966204465>, 2001.
- 315 Wohlfahrt, G., Fenstermaker, L. F., and Arnone Iii, J. A.: Large annual net ecosystem CO₂ uptake of a Mojave Desert ecosystem, *Global Change Biol*, 14, 1475–1487, doi:10.1111/j.1365-2486.2008.01593.x, 2008.



Fig. 1. Eddy-covariance station with the CSAT3, Li-7500, KH20 and HMP45 at NAMORS in February 2010.

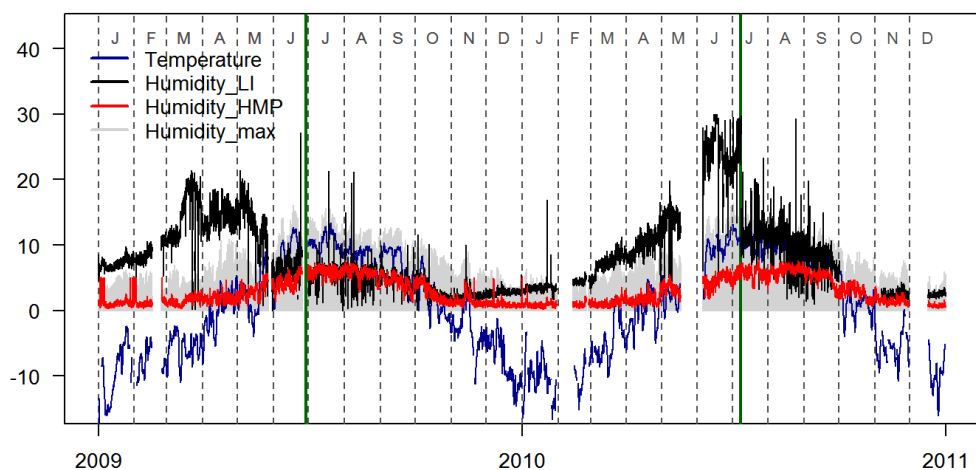


Fig. 2. Timeline of absolute humidity measurements conducted with the LiCOR 7500 (black) and the HMP 45 (red) at NAMORS from 2008 to 2011. The grey shaded area indicates the amount of water in the air when 100% relative humidity is reached; the blue line represents air temperature. Vertical green lines mark the field calibration dates for the LiCOR 7500 on 30.06.2009 and 08.07.2010.

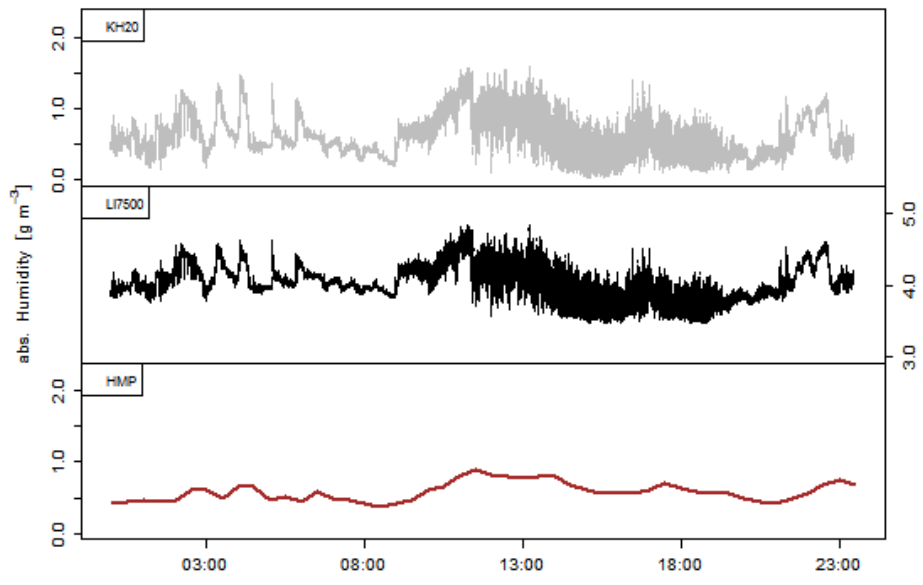


Fig. 3. Comparison of measurements conducted with the Li-7500, HMP45 and KH20 on 22 February 2010 at NAMORS. The measurements are shown with the same resolution but the observations with the Li-7500 show higher absolute values.

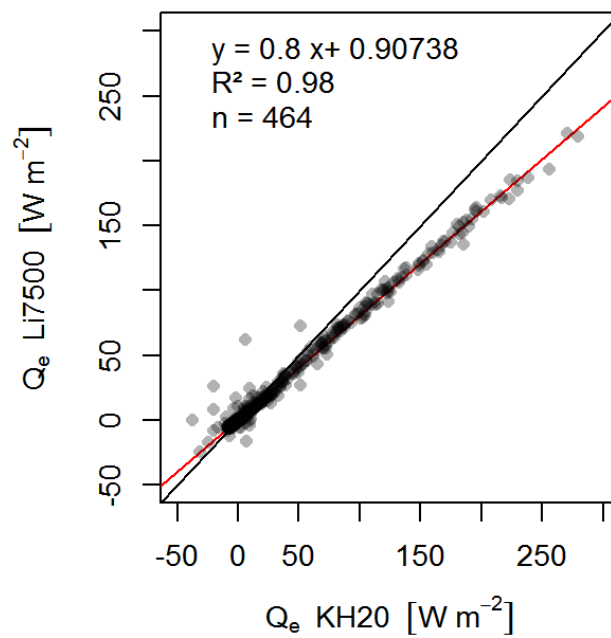


Fig. 4. Comparison of the observed latent heat flux with both gas analyzers, Li-7500 and KH20, during the side-by-side measurements in February 2010 at NAMORS.

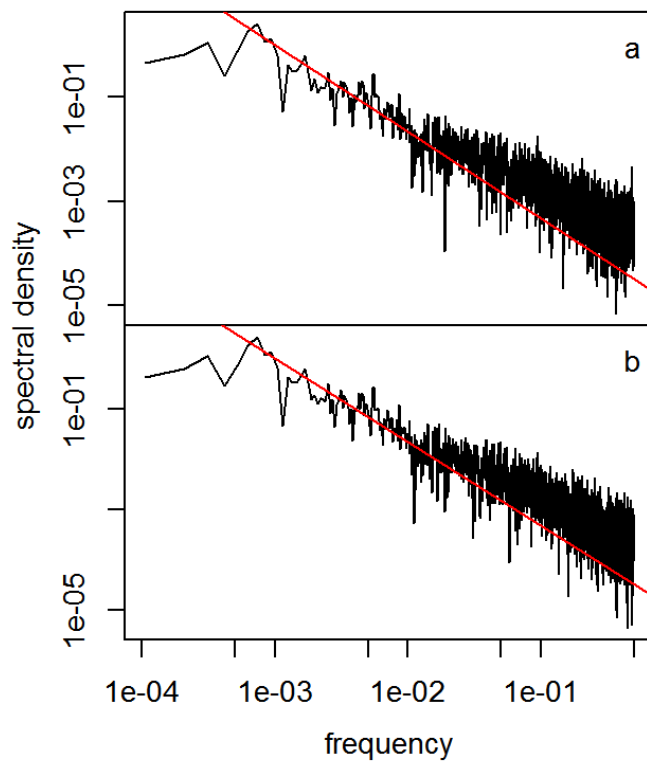


Fig. 5. Spectra of energy dissipation for the Li-7500 (a) and the KH20 (b). The red line indicates a dissipation of $-5/3$.

Versicherungen und Erklärungen

Hiermit erkläre ich, dass keine Tatsachen vorliegen, die mich nach den gesetzlichen Bestimmungen über die Führung akademischer Grade zur Führung eines Doktorgrades unwürdig erscheinen lassen.

Hiermit erkläre ich mich damit einverstanden, dass die elektronische Fassung meiner Dissertation unter Wahrung meiner Urheberrechte und des Datenschutzes einer gesonderten Überprüfung hinsichtlich der eigenständigen Anfertigung der Dissertation unterzogen werden kann.

Hiermit erkläre ich eidesstattlich, dass ich die Dissertation selbständig verfasst und keine anderen als die von mir angegebenen Quellen und Hilfsmittel benutzt habe.

Ich habe die Dissertation nicht bereits zur Erlangung eines akademischen Grades anderweitig eingereicht und habe auch nicht bereits diese oder eine gleichartige Doktorprüfung endgültig nicht bestanden.

Hiermit erkläre ich, dass ich keine Hilfe von gewerbliche Promotionsberatern bzw. -vermittlern in Anspruch genommen habe und auch künftig nicht nehmen werde.

Bayreuth, den _____

Tobias Biermann